Universidade de Aveiro
Ano 2017
Departamento de Química

JOANA FERREIRA LEAL

Foto-degradação de contaminantes como meio de remediação de águas de aquacultura.

Photo-degradation of contaminants as a way of remediation of aquaculture's water.

Universidade de Aveiro
Ano 2017

Departamento de Química

JOANA FERREIRA LEAL

Foto-degradação de contaminantes como meio de remediação de águas de aquacultura.

Photo-degradation of contaminants as a way of remediation of aquaculture's water.

Tese apresentada à Universidade de Aveiro para cumprimento dos requisitos necessários à obtenção do grau de Doutor em Química, realizada sob a orientação científica do Doutor Valdemar Inocêncio Esteves e da Doutora Maria Eduarda Bastos Henriques dos Santos, professores auxiliares do Departamento de Química da Universidade de Aveiro.

Apoio financeiro da FCT e do FSE através do POCH. Referência da bolsa: SFRH/BD/88572/2012.

À minha família. A mim e a ti, minha riqueza.

o júri

Presidente

Prof. Doutor João Manuel Nunes Torrão
Professor Catedrático da Universidade de Aveiro

Vogais

Prof. Doutor Joaquim Carlos Gomes Esteves da Silva
Professor Catedrático da Faculdade de Ciências da Universidade do Porto

Prof. Doutora Maria Conceição Branco da Silva de Mendonça Montenegro
Professora Catedrática da Faculdade de Farmácia da Universidade do Porto

Doutor Ricardo Jorge Guerra Calado
Investigador principal da Universidade de Aveiro

Prof. Doutora Marcela Alves Segundo
Professora Auxiliar da Faculdade de Farmácia da Universidade do Porto

Prof. Doutor Valdemar Inocêncio Esteves
Professor Auxiliar da Universidade de Aveiro (Orientador)

Prof. Doutora Maria Cristina Guiomar Antunes
Professora Auxiliar da Universidade de Trás-os-Montes e Alto Douro

Doutora Marta Otero Cabero
Investigadora da Universidade de León, Espanha

Agradecimentos

Alcançada esta meta, os sentimentos são muitos: alegria e felicidade, ansiedade e nostalgia, orgulho e conquista. Sou grata pela oportunidade que me foi dada e para a qual lutei. Sou grata a todos aqueles que me fizeram sorrir, que acreditaram em mim, que fizeram do otimismo deles o meu e pelos quais eu estou aqui hoje. Seria grande a lista de pessoas que, de uma forma ou de outra, contribuíram para que eu aqui chegasse, mas no fundo, elas sabem que lhes sou e serei sempre grata.

Agradeço especialmente à minha família – pai, mãe, irmã e avós – pela compreensão, paciência e apoio incondicional. Não podia deixar também de agradecer a "impaciente" paciência de duas crianças muito especiais que, mesmo sem o saberem, contribuíram muito para o meu crescimento e que, em cada abraço, me davam mais força para continuar e sorrir. Minha querida afilhada e sobrinho, correr pelo que nos faz felizes nem sempre é fácil, mas vale a pena.

Não podia deixar de agradecer à Dra. Eduarda Santos e ao Dr. Valdemar Esteves pela constante aprendizagem, incentivo e dedicação. Muito obrigado professores por acreditarem em mim. De todos estes anos fica a lição de que "nunca está tudo feito" e de que, com persistência e trabalho, tudo se consegue.

Pela disponibilidade e entusiasta colaboração durante este percurso, agradeço também à Profª. Dra. Graça P. M. S. Neves, ao Prof. Dr. António Correia, à Dra. Isabel S. Henriques, à Dra. Paula A. A. P. Marques e à Dra. Maria Teresa Caldeira. Obrigado também ao Prof. Dr. Artur Silva pelas conversas e conselhos.

Por fim, mas não menos importante, agradeço à Associação Portuguesa de Aquacultores (APA) pelo envolvimento e interesse demonstrado por este trabalho. Um obrigado especial aos responsáveis das empresas diretamente envolvidos neste projeto.

Palavras-chave Foto-degradação, BDE-209, oxitetraciclina, formalina, aquacultura, luz solar, cálcio, magnésio, rendimento quântico, fotoprodutos, atividade biológica.

Resumo

A aquacultura é uma atividade em crescente expansão em resultado do aumento do consumo de peixe e da estagnação das pescas. O aumento da densidade de produção em aquacultura potencia o aparecimento de microrganismos patogénicos, como as bactérias, obrigando a um maior controlo sanitário que é feito com desinfetantes. Em alguns casos, pode ser necessário o uso de antibióticos. Neste trabalho são estudados dois compostos químicos autorizados em aquacultura: a oxitetraciclina (antibiótico) e a formalina (desinfetante). Além dos compostos introduzidos intencionalmente, existem outros que, por via indireta, atingem estes sistemas aquáticos. Como exemplo de um contaminante indireto, o éter deca-bromodifenilo (BDE-209) foi também incluído neste estudo.

A foto-degradação com luz solar é uma das principais vias de degradação natural de contaminantes em águas superficiais e pode constituir uma via económica para o tratamento de águas contaminadas antes da sua descarga ou reutilização. Contudo, este é um processo influenciado pela matriz das águas, nomeadamente pela concentração e natureza da matéria orgânica e pelos sais.

Sob a ação direta da luz solar, o BDE-209 e a oxitetraciclina (OTC) são degradados rapidamente. Contudo, na presença de substâncias húmicas (HS), que são as principais componentes da matéria orgânica, a degradação de ambos é retardada. Enquanto o efeito de filtro da luz explica o atraso da foto-degradação da OTC, no caso do BDE-209, as interações hidrofóbicas entre o composto e as HS são a razão principal desse atraso.

Os sais e o pH das águas de aquacultura marinha favorecem a foto-degradação da OTC relativamente à água desionizada. O cálcio e o magnésio têm uma forte influência na cinética e nos produtos de foto-degradação da OTC. Importa salientar que, em todas as matrizes salinas, os produtos resultantes da foto-degradação da OTC não revelaram atividade biológica para a *E. coli, Aeromonas* sp. e *Vibrio* sp., o que é uma vantagem no que diz respeito à resistência bacteriana a este antibiótico.

A formalina (formaldeído aquoso) apenas sofre foto-degradação indireta. O TiO_2 puro e dois compósitos de TiO_2 ativos na zona visível (TiO_2–Tetra-fenilo porfirina e TiO_2–óxido de grafeno) foram testados como foto-catalisadores. A conjugação de TiO_2 com óxido de grafeno revelou-se a melhor escolha para a degradação da formalina, usando luz solar. Contudo, a metodologia proposta deverá ser otimizada com vista à sua aplicação a águas de aquacultura marinha, uma vez que a matriz destas águas reduz a eficiência do foto-catalisador.

Em suma, o trabalho desenvolvido e aqui apresentado tem grande potencialidade de aplicação, em particular no setor da aquacultura, mas também em outros sistemas aquáticos onde estes contaminantes estejam presentes.

Keywords Photo-degradation, BDE-209, oxytetracycline, formalin, aquaculture, sunlight, calcium, magnesium, quantum yield, photoproducts, biological activity.

Abstract

As result of an increase in fish consumption and fisheries stagnation, aquaculture is a growing and widespread activity. The increasing density in aquaculture production potentiates the appearance of pathogenic microorganisms, like bacteria, requiring a greater health control, achieved with disinfectants. In some cases, the use of antibiotics may be necessary. In this work, two chemical compounds approved for aquaculture are studied: oxytetracycline (antibiotic) and formalin (disinfectant). In addition to the intentionally introduced compounds, several others reach these water systems indirectly. As example of an indirect contaminant, decabromodiphenyl ether (BDE-209) was also included in this study.

The photo-degradation under sunlight is one of the main routes of natural degradation of contaminants in surface waters and may be an economic process for treatment of contaminated waters before their reuse or discharge. However, this process is influenced by water matrix, namely the nature and concentration of organic matter and salts.

Under the direct action of sunlight, BDE-209 and oxytetracycline (OTC) are rapidly degraded. However, in the presence of humic substances (HS), which are the main components of organic matter, the degradation of these two compounds is delayed. While the filter effect of light explains the delay on OTC photo-degradation, in the case of BDE-209, the hydrophobic interactions between the compound and the HS are the main reason for the delay.

Salts and pH of marine aquaculture's water favour the OTC photo-degradation relatively to deionized water. Calcium and magnesium have a strong influence on the kinetics and products of OTC photo-degradation. It should be noted that, in all saline matrices, the products resulting from OTC photo-degradation revealed no biological activity for *E. coli, Aeromonas* sp. and *Vibrio* sp., which is an advantage in what the bacterial resistance to this antibiotic is concerned.

Formalin (aqueous formaldehyde) undergoes only indirect photo-degradation. Neat TiO_2 and two visible light active TiO_2 composites (TiO_2–Tetra-phenyl porphyrin and TiO_2–Graphene oxide) were tested as photo-catalysts. The combination of TiO_2 with graphene oxide was the best choice for formalin degradation, under sunlight. However, the methodology proposed should be optimized in view of its application to marine aquaculture's waters since the matrix of these waters reduces the photo-catalyst efficiency.

In summary, the work carried out and disclosed herein has great application potential, especially in the aquaculture industry, but also in other water systems where these contaminants are present.

Abbreviations

A – Absorbance

ANOVA – Analysis of Variance

AOP – Advanced oxidation processes

AU – Arbitrary units

BDE-209 – Decabromodiphenyl ether or bis(pentabromophenyl) ether

CB – Conduction band

CDOM – Coloured or chromophore portion of dissolved organic matter

DAD – Diode array detector

DDL – 3,5-diacetyl-1,4-dihydrolutidine

DGAV – Direcção-Geral de Alimentação e Veterinária

DOC – Dissolved organic carbon

DOM – Dissolved organic matter

DRS – Diffuse reflectance spectra

DWTP – Drinking water treatment plants

E. coli – Escherichia coli

EC_{50} – Half maximal effective concentration

EEM – Excitation-emission matrix

E_{HOMO} - Energy of highest unoccupied molecular orbital

E_{LUMO} – Energy of lowest unoccupied molecular orbital

EMA – European Medicines Agency

EPA – Environmental Protection Agency (USA)

EU – European Union

FA – Fulvic acids

FAO – Food and Agriculture Organization of United Nations

FDA – Food and Drug Administration (USA)

FM – Formaldehyde

GF – Graphene

GO – Graphene oxide

ha – Hectare

HA – Humic acids

HPLC – High-performance liquid chromatography

HS – Humic substances

IC – Inorganic carbon

IUPAC – International Union of Pure and Applied Chemistry

k – Kinetic rate constant

K_H – Henry´s constant

K_{hydr} – Equilibrium constant of hydration

K_{OA} – Partition coefficient octanol-air

K_{OTC} – Binding constants to OTC

K_{ow} – Octanol-water partitioning coefficient (also described as P_{OW})

LB – Lysogeny broth

LC_{50} – Median lethal concentration

LOD – Limit of detection

MHA – Mueller Hinton agar

MIC – Minimum inhibitory concentration

NCBI – National Center for Biotechnology Information

NOM – Natural organic matter

NPOC – Non-purgeable organic carbon

OC_{part} – Particulate organic carbon

OD – Optical density

OECD – Organisation for Economic Co-operation and Development

OIE – World Organisation for Animal Health

OTC – Oxytetracycline

PBDEs – Polybrominated diphenyl ethers

PS. – Pseudomonas

PVC - Polyvinyl chloride

R^2 – Determination coefficient

RAS – Recirculating aquaculture system

RDD – Recommended daily dose

ROS – Reactive oxygen species

SEM – Scanning electron microscopy

$SUVA_{254}$ – Specific UV absorbance at 254 nm

S_λ – Light-screening effect

TC – Total carbon

TOC – Total organic carbon

TPP – 5, 10, 15, 20 - Tetra-phenyl porphyrin (also described as H2TPP)

TSS – Total suspended solids

TTC – Tetracycline

UV – Ultraviolet

UV-Vis – Ultraviolet-visible

VB – Valence band

W(λ) – Spectral photon fluence rate

WHO – World Health Organization

WWTP – Wastewater treatment plants

yr – Year

Φ – Quantum yield

Index

Index of figures

Index of tables

General contextualization

Earlier in this PhD project, a survey of the main problems in aquaculture companies was done. Information about water characteristics and potential contaminants was collected. Regarding to the problems more mentioned by aquaculture producers stand out the water quality that goes into the fish tanks (water intake) and the water quality released into environment (effluent).

Additionally, there are other specific problems that the producers would like to see solved or minimized, namely, the removal of therapeutic agents and disinfectants from water after their use. Their use poses a problem of water contamination that, in the case of antibiotics, can contributes to the dissemination of bacterial resistance. Formalin is a disinfectant frequently used in tanks cleaning and its complete removal is one of the problems more times mentioned by aquaculture producers. It reduces the amount of oxygen dissolved in water and, even at low concentrations, can be toxic.

Beyond the problems identified by aquaculture producers, there are other contaminants that are not so well known by them and are introduced through the fat accumulated in water, when the feed is not totally eaten. An example of this is the decabromodiphenyl ether (BDE-209), a very hydrophobic compound that is preferentially transported adsorbed to particulate matter.

Among the different aquaculture systems, the intensive production system, in closed or semi-closed circuits, was chosen by several reasons, among which: (1) a higher use of therapeutic agents (e.g.: antibiotics) due to increased production density that propitiates the appearance of diseases; (2) an increased use of disinfectants caused by greater need for health control; (3) the existence of specific water treatment processes, such as ozonation, to removal potential water contaminants. So, the purpose of this PhD thesis is to evaluate the potential of photo-degradation, using sunlight, as an alternative or complementary method to remove organic contaminants from the aquaculture's water circuits. With this main purpose, this thesis is organized in eight chapters, whose contents will be briefly presented below.

Chapter 1 introduces some aquaculture concepts, with emphasis on water treatment processes currently used in closed or semi-closed circuit in intensive aquaculture.

Chapter 2 describes the potential aquaculture's contaminants. It briefly presents some characteristics of an indirect contaminant of aquaculture's water – BDE-209 – and includes an extensive literature review of two direct contaminants: the antibiotic oxytetracycline (OTC) and the disinfectant formalin. This chapter is based on two review papers, one already published and the other being prepared for submission:

J. F. Leal, E. B. H. Santos, V. I. Esteves. Oxytetracycline in intensive aquaculture: water quality during and after its administration, environmental fate, toxicity and bacterial resistance. *In preparation*.

J. F. Leal, M. G. P. M. S. Neves, E. B. H. Santos and V. I. Esteves (2016). Use of formalin in intensive aquaculture: properties, application and effects on fish and water quality. *Reviews in Aquaculture*: 1-15.

Chapter 3 compiles some theoretical fundaments of photochemistry, highlighting concepts, such as direct and indirect photo-degradation. Additionally, it presents the state of art regarding to the photo-degradation studies existing in the literature for BDE-209, OTC and formalin. Some topics related to OTC and formalin photo-degradation presented in this chapter also integrate the two review articles above mentioned.

Chapter 4 discusses the effect of humic substances, as representative of dissolved organic matter, on photo-degradation of BDE-209 and OTC in synthetic aqueous solutions. It is an adaption of the followings research articles:

J.F. Leal, V.I. Esteves, E.B.H. Santos (2015). Does light-screening by humic substances completely explain their retardation effect on contaminants photo-degradation? *Journal of Environmental Chemical Engineering*, 3, 3015-3019.

J.F. Leal, V.I. Esteves, E.B.H. Santos (2013). BDE-209: Kinetic Studies and Effect of Humic Substances on Photodegradation in Water. *Environmental Science & Technology*, 47, 24, 14010-14017.

Chapter 5 describes the physical-chemical and spectroscopic characterization of natural brackish aquaculture's waters, further used to perform the photo-degradation experiments of OTC and formalin. This chapter is based on the following research article:

J.F. Leal, V.I. Esteves, E.B.H. Santos (2016). Use of sunlight to degrade oxytetracycline in marine aquaculture's water. *Environmental Pollution*, 213, 932-939.

Chapter 6 relates to the OTC photo-degradation and is subdivided into three main sub-chapters. The first sub-chapter (6A) regards the kinetics studies of OTC in aquaculture's water and the effects of pH and salinity on its photo-degradation. The second sub-chapter (6B) concerns the calcium and magnesium binding to OTC and their effects on photo-degradation kinetics and by-products formation. The third sub-chapter (6C) refers the studies of antibacterial activity performed before and after OTC photo-degradation. This chapter originates three research articles:

J.F. Leal, V.I. Esteves, E.B.H. Santos. Ca^{2+} and Mg^{2+} binding to oxytetracycline in brackish aquaculture's water: effects on photo-degradation kinetics and on by-products formation, *submitted*.

J.F. Leal, I.S. Henriques, A. Correia, E.B.H. Santos, V.I. Esteves (2017). Antibacterial activity of oxytetracycline photoproducts in marine aquaculture's water. *Environmental Pollution*, 220, 644-649.

J.F. Leal, V.I. Esteves, E.B.H. Santos (2016). Use of sunlight to degrade oxytetracycline in marine aquaculture's water. *Environmental Pollution*, 213, 932-939.

Chapter 7 presents the formalin photo-degradation, also under sunlight, using TiO_2 and visible-light active TiO_2-composites. It compares the efficiency of the different photo-catalysts on the formaldehyde degradation in synthetic aqueous solutions and in brackish aquaculture's water.

Chapter 8 highlights the key findings of this work. Furthermore, it also presents the future perspectives and the potentialities for pursuing the work.

Chapter 1: Aquaculture

Aquaculture has become the fastest growing food production sector involving aquatic species worldwide, due to the increased fish consumption and stagnation of catches. Aquaculture products already account with 50% of fish consumption in the world. This activity can be developed in fresh-, brackish- or sea-water and practiced in extensive, semi-intensive or intensive systems.

Intensive aquaculture frequently employs recirculation or re-used water systems, where a small portion of water is released into the environment, while the other part is treated and re-enters in the tanks production together with new water. The most common processes applied to water treatment are the mechanical and biological filtration, ozonation and aeration. The concern is that the conventional processes commonly used for water treatment are not always completely effective in removing of potential contaminants.

This chapter briefly describes the main concepts and features of aquaculture and shows the impact of this activity at environmental and social levels. Additionally, it describes the main processes of water treatment and indicates their advantages and potential limitations.

1.1 Concepts and values

Aquaculture is defined as rearing or culture of aquatic organisms (plants and animals) where are applied techniques to increase the production beyond the natural capacity of the environment (COM 2002). Aquaculture production has become the fastest growing food production sector involving animal species (Greenpeace 2008). Production of aquatic animals from aquaculture has expanded over the years, reaching 73.8 million tonnes in 2014 (FAO 2016). Data from the year of 2014 show that the percentages of world total production by region were 88.91 %, 4.54 %, 3.97 %, 2.32 % and 0.26 % for Asia, Americas, Europe, Africa and Oceania, respectively. Globally, China represented 61.61 % of aquaculture production. In Europe, Norway was the highest aquaculture producer in 2014 (FAO 2016).

Portugal is one of the largest consumers of fish in world (> 60 kg per capita per year, 2009 data) (FAO 2012). Despite our country have excellent natural and environmental conditions to the development of aquaculture activity, it is still poorly developed. According to 2013 data, this activity represents only 0.65 % (7874 tons of live weight) of the aquaculture production in European Union. The production in brackish and saltwater corresponds to the most of the total production – 93 %, of which 52 % relate to the production of fish (INE/DGRM 2016).

1.2 Aquaculture methods

Aquaculture may take different forms of production, and can make use of natural or artificial structures to develop its activity (EuropeanComission 2012), such as ponds or tanks, respectively. With regard to the production methods in aquaculture systems, they can be defined, at least, according to five main criteria: farming systems, farming types, groups of species, ways of fish production and ways of bivalve production (Gonçalves 2013). This information is synthetized in **figure 1**.

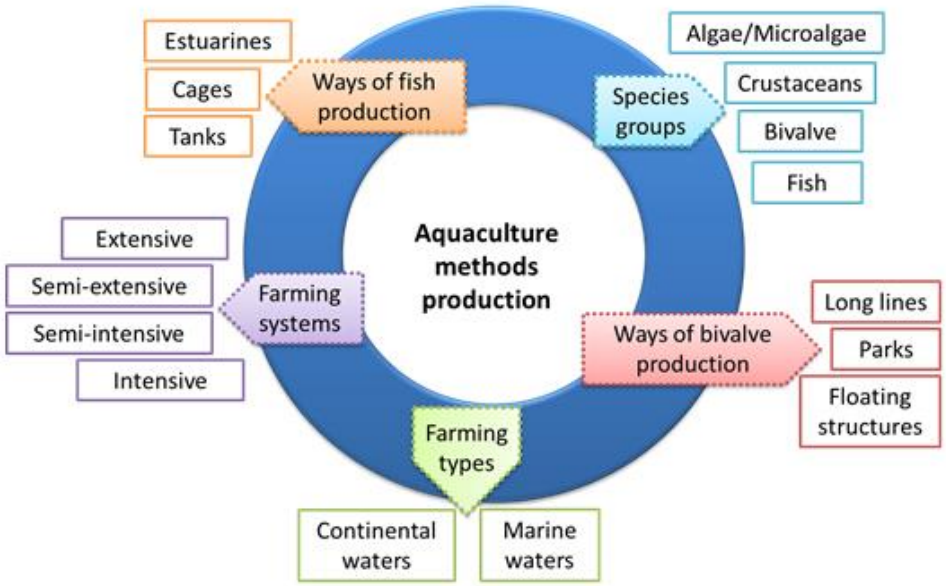

Figure 1 – Production systems in aquaculture

1.2.1 Farming systems

The main features that distinguish the production systems are the food (natural or complementary feed) and the density of production. A brief definition of the different production systems is presented below (FAO 2008).

- **Extensive aquaculture** – Production systems characterized by a low degree of control, in regards to the environmental conditions, nutrition, predators, competitors and disease agents, with low-level of technology and investment (low initial costs) and, consequently, with a low efficiency of production (up 500 kg/ha/yr). It is highly dependent on local climate and water quality and uses natural structures, such as lagoons and bays.
- **Semi-intensive aquaculture** – Culture system largely dependent on natural food, which is augmented by fertilization or complemented using supplementary feed. It is regular the use of fertilisers, aeration and water exchange, often pumped or by gravity supplied. It implies a simple monitoring of water quality and, usually, is practiced in improved ponds, some enclosures, or simple cage systems. These systems are characterized by an average production of 2–20 tonnes/ha/yr.
- **Intensive aquaculture** – System characterized by a high degree of control, high initial costs, high-level of technology and, consequently, high efficiency of

production (up to 200 tonnes/ha/yr). It tends to increase the independence of local climate and water quality and uses man-made culture systems.

1.2.2 Farming types, species produced and production ways

Aquaculture's activity can be developed in fresh-, brackish- or sea-water. In freshwater (continental water), species such as *Cyprinus carpio* (carp), *Oncorhynchus mykiss* (rainbow trout), *Anguillidae* (eel) or sturgeon can be produced in extensive or intensive systems. *Dicentrarchus labrax* (sea bass) and *Sparus aurata* (sea bream) are aquatic organisms generally produced in semi-intensive and intensive systems, in brackish water, which is a mixture of continental and marine water (EuropeanComission 2012). This activity can also be developed in tanks (fiberglass or concrete) on land supplied with sea water, or in cages – intensive production system. Marine species like *Psetta maxima* (turbot) and *Soleidae* (sole) are mainly produced in shore-based installations, while species such as *Salmo salar* (atlantic salmon), *Dicentrarchus labrax* (sea bass), *Sparus aurata* (sea bream) or *Argyrosomus regius* (meagre) can be produced in marine cages (EuropeanComission 2012).

In addition to these ways of production, a more recent and developed way has gained prominence: the offshore mariculture. It takes place in open sea and is subjected to exposure of wind and wave action. Its production is almost entirely composed by fish and shellfish (Kapetsky et al. 2013).

1.3 Environmental and social impacts

Aquaculture can reduce the dependence on natural stocks and contributes to genetic conservation of endangered species (Cole et al. 2009). It can create jobs, contribute to improvement of rural economy and food security (Hu et al. 2012). Furthermore, farmed fish provide a good and low-cost source of polyunsaturated fatty acids, which can enhance cardiovascular health in humans (Cole et al. 2009). On the other hand, the modification or destruction of natural habitats is the main negative consequence to the environment (Cao et al. 2007; Greenpeace 2008; Cole et al. 2009; Hu et al. 2012). This aspect is particularly worrying because may cause local extinction of certain plants and aquatic species (Cole et al. 2009). The wastewater and the waste of the aquaculture are other problems with negative ecological impact (Cao et al. 2007). The discharge of effluents with high concentration of organic matter and nutrients can

contribute to organic pollution and eutrophication (Hu et al. 2012), causing oxygen depletion, algae bloom and water quality deterioration (Cao et al. 2007; Cole et al. 2009). The principal wastes are solids (e.g. faeces or uneaten food), chemicals (such as stabilizers or pigments applied to construction materials) and therapeutics agents (Cao et al. 2007).

1.4 Water treatment processes in aquaculture

In semi-intensive aquaculture, there is no strict control over the water cycle. For instance, water can come from a channel of the estuary directly to the ponds of production, where it is maintained during the growth cycle of the fish. Finalized this cycle, the pond is naturally leaked and stays exposed to the natural environmental conditions. When water enters in tanks upstream and leaves downstream circulation, the system of water circulation is denominated continuous flow system – open circuit (EuropeanComission 2012).

In intensive aquaculture, the density of production and the necessary resources of water and energy are much higher than in extensive or semi-intensive aquaculture. To ensure the sustainability of intensive aquaculture and minimize its impact on the environment, recirculating aquaculture systems (RAS) are frequently adopted. These systems improve the use and management of resources, the quality of water and species and minimize the environmental impact of this activity, through the decrease of effluent volumes released into environment (Goncalves and Gagnon 2011). RAS are characterised by semi-closed circuits, where a part of water that circulates in the system is treated and reused, while the other part is released into the environment (Bostock et al. 2010; EuropeanComission 2012). This system provides the reduction of water usage, the improvement of waste management and the recycling of nutrients (Martins et al. 2010). Its application must be adjusted according to the requirements and characteristics of fish, the environmental parameters and the technology available (Bostock et al. 2010).

RAS generally include five main processes: aeration, oxygenation, solids removal, bio-filtration and ozonation (Piedrahita 2003).

a) Aeration is a mixture of air and water across the air-liquid interface (FAO 2008). This mixture can occur naturally and/or mechanically, using aerators.

b) Oxygenation is a mixture of pure oxygen and water. This process generally occurs in a gas cylinder where oxygen pressurized is diffused into the water mass to be oxygenated (FAO 2008).

c) Solids removal corresponds to mechanical filtration process of particulate matter and suspended solids.

d) Bio-filtration occurs in biological filters. These are physical structures with large surface areas containing "packing material" (generally, particles of PVC with about 1 cm of diameter and an irregular surface). Aerobic nitrifying bacteria (Branson 1993; Martins et al. 2010) are allocated in these structure and grow up. Here, sub-products of fish faeces, for instance, urea, ammonia and nitrites (NO_2^-) are progressively oxidized to nitrates (NO_3^-) (final oxidation product – **reactions 1** to **3**). Un-ionised ammonia and nitrites are highly toxic for fish, while nitrate is considered relatively "inoffensive" to fish and safe levels should be achieved with regular water changes (Keck and Blanc 2002). During the nitrification process, two main autotrophic bacteria (Eiroa et al. 2004; Fredricks 2015) are involved – the *Nitrosomonas* sp. bacteria promote the conversion of ammonia into nitrite (**reaction 2**), while *Nitrobacter* sp. are responsible for the conversion of nitrite into nitrate (**reaction 3**) (Branson 1993).

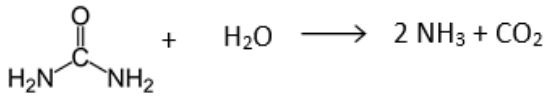

Reaction 1

$$2\ NH_3 + 3\ O_2 \longrightarrow 2\ NO_2^- + 2\ H_2O + 2H^+$$

Reaction 2

$$2\ NO_2^- + O_2 \longrightarrow 2\ NO_3^-$$

Reaction 3

e) Ozonation occurs in skimmer and promotes the oxidation and degradation of organic compounds through the formation of reactive oxygen species (ROS), namely hydroxyl radicals ($HO^{\bullet}$): **reactions 4-9** (Andreozzi et al. 1999). Residual ozone is highly toxic to fish at low concentrations and the direct treatment of the culture tank is not recommended (Goncalves and Gagnon 2011).

$$O_3 + OH^- \rightarrow O_2 + HO_2^-$$

Reaction 4

$$O_3 + HO_2^- \rightarrow HO_2^{\cdot} + O_3^{\cdot -}$$

Reaction 5

$$HO_2^{\cdot} \rightarrow H^+ + O_2^{\cdot -}$$

Reaction 6

$$O_2^{\cdot -} + O_3 \rightarrow O_2 + O_3^{\cdot -}$$ **Reaction 7**

$$O_3^{\cdot -} + H^+ \rightarrow HO_3^{\cdot}$$ **Reaction 8**

$$HO_3^{\cdot} \rightarrow OH^{\cdot} + O_2$$ **Reaction 9**

Ozonation contributes to water disinfection, eliminating most target pathogens, and improves the water quality by reduction of biochemical oxygen demand, ammonia and nitrite. As consequence of organic matter degradation, this process also decreases the turbidity, colour, odour and taste of water (FAO 2008; Goncalves and Gagnon 2011). However, this process has its limitations once it is strongly influenced by pH variations (the increase of pH promotes the beginning of ozone decomposition) and its performance is affected by temperature, presence of organic matter, suspended solids, carbonate, bicarbonate and chlorine ions (Andreozzi et al. 1999; von Gunten 2003; Barndok et al. 2012). Nevertheless, the main concern related to the use of ozone is the formation of toxic by-products, such as bromate (BrO_3^-) and bromoform ($CHBr_3$), resulting of reaction between ozone and natural constituents of seawater. For instance, the presence of bromide ion (Br^-) catalytically decomposes ozone and promotes a series of redox-reactions described by **reactions 10–12** (Goncalves and Gagnon 2011 and authors cited therein). This means that ozone concentrations applied by aquaculture producers must be reduced when this treatment is applied to marine water, which decreases its effectiveness.

$$O_3 + Br^- \rightarrow O_2 + OBr^-$$ **Reaction 10**

$$O_3 + OBr^- \rightarrow 2O_2 + Br^-$$ **Reaction 11**

$$2O_3 + OBr^- \rightarrow 2O_2 + BrO_3^-$$ **Reaction 12**

1.5 References

Andreozzi, R., V. Caprio, A. Insola and R. Marotta (1999). Advanced oxidation processes (AOP) for water purification and recovery. *Catalysis Today* **53**(1): 51-59.

Barndok, H., D. Hermosilla, L. Cortijo, C. Negro and A. Blanco (2012). Assessing the Effect of Inorganic Anions on TiO_2-Photocatalysis and Ozone Oxidation Treatment Efficiencies. *Journal of Advanced Oxidation Technologies* **15**(1): 125-132.

Bostock, J., B. McAndrew, R. Richards, K. Jauncey, T. Telfer, K. Lorenzen, D. Little, L. Ross, N. Handisyde, I. Gatward and R. Corner (2010). Aquaculture: global status and trends. *Philosophical Transactions of The Royal Society B* **365**: 2897–2912.

Branson, E. (1993). Environmental Aspects of Aquaculture. *Aquaculture for veterinarians: fish husbandry and medicine*. L. Brown, Pergamon Press**:** 447.

Cao, L., W. Wang, Y. Yang, C. Yang, Z. Yuan, S. Xiong and J. Diana (2007). Environmental impact of aquaculture and countermeasures to aquaculture pollution in China. *Environmental Science and Pollution Research* **14**(7): 452-462.

Cole, D. W., R. Cole, S. J. Gaydos, J. Gray, G. Hyland, M. L. Jacques, N. Powell-Dunford, C. Sawhney and W. W. Au (2009). Aquaculture: Environmental, toxicological, and health issues. *International Journal of Hygiene and Environmental Health* **212**(4): 369-377.

COM (2002). Communication from the Commission to the Council and the European Parliament. A Strategy for the sustainable development of European Aquaculture. Brussels, Commission of the European Communities**:** 26.

Eiroa, M., C. Kennes and M. C. Veiga (2004). Formaldehyde biodegradation and its inhibitory effect on nitrification. *Journal of Chemical Technology and Biotechnology* **79**(5): 499-504.

EuropeanComission. (2012). "Aquaculture methods." Fisheries Retrieved 21 January, 2014, from http://ec.europa.eu/fisheries/cfp/aquaculture/aquaculture_methods/index_en.htm.

FAO (2008). *Glossary of Aquaculture*. Rome, FAO Fisheries and Aquaculture

FAO (2012). *The State of World Fisheries and Aquaculture*. Rome, Food and Agriculture Organization of the United Nations

FAO (2016). *The State of World Fisheries and Aquaculture 2016. Contributing to food security and nutrition for all.* Rome, Food and Agriculture Organization of the United Nations

Fredricks, K. T. (2015). Literature Review of the Potential Effects of Formalin on Nitrogen Oxidation Efficiency of the Biofilters of Recirculating Aquaculture Systems (RAS) for Freshwater Finfish. Virginia, U.S. Geological Survey Open-File Report 2015-1097**:** 17.

Goncalves, A. A. and G. A. Gagnon (2011). Ozone Application in Recirculating Aquaculture System: An Overview. *Ozone-Science & Engineering* **33**(5): 345-367.

Gonçalves, F. (2013). Aquacultura e Pescas Oportunidades e desafios. Aquacultura e Pescas Portugal-Brasil Oportunidades de negócio. University of Aveiro, Associação Portuguesa de Aquacultores.

Greenpeace (2008). Challenging the Aquaculture Industry on Sustainability. Amsterdam, Greenpeace International**:** 24.

Hu, Z., J. W. Lee, K. Chandran, S. Kim and S. K. Khanal (2012). Nitrous Oxide (N_2O) Emission from Aquaculture: A Review. *Environmental Science & Technology* **46**(12): 6470-6480.

INE/DGRM (2016). Estatísticas da Pesca 2015. I. P. Instituto Nacional de Estatística**:** 146.

Kapetsky, J. M., J. Aguilar-Manjarrez and J. Jenness (2013). A global assesment of offshore mariculture potential from a spatial perspective. FAO Fisheries and Aquaculture Technical Paper 549. Rome, Food and Agriculture Organization of the United Nations**:** 181.

Keck, N. and G. Blanc (2002). Effects of formalin, chemotherapeutic treatments on biofilter efficiency in a marine recirculating fish farming system. *Aquatic Living Resources* **15**(6): 361-370.

Martins, C. I. M., E. H. Eding, M. C. J. Verdegem, L. T. N. Heinsbroek, O. Schneider, J. P. Blancheton, E. R. d'Orbcastel and J. A. J. Verreth (2010). New developments in recirculating aquaculture systems in Europe: A perspective on environmental sustainability. *Aquacultural Engineering* **43**(3): 83-93.

Piedrahita, R. H. (2003). Reducing the potential environmental impact of tank aquaculture effluents through intensification and recirculation. *Aquaculture* **226**(1-4): 35-44.

von Gunten, U. (2003). Ozonation of drinking water: Part I. Oxidation kinetics and product formation. *Water Research* **37**(7): 1443-1467.

Chapter 2: Water quality – potential aquaculture's contaminants [1]

Three aquaculture contaminants were considered in this work: decabromodiphenyl ether (BDE-209), oxytetracycline (OTC) and formalin.

BDE-209 is an indirect contaminant of aquaculture's water. The subchapter relating thereto (2.2) briefly describes its physical-chemical properties and explain the introduction pathways of this contaminant in aquaculture's systems.

OTC is one of the most used antibiotics in aquaculture (direct contaminant). The subchapter concerning it (2.3) covered its physical-chemical properties, interaction with ions, application to farmed fish, effects in water quality within water circuit and its environmental fate (release into environment and degradation pathways).

Formalin is one of the most used disinfectants in aquaculture (direct contaminant). The subchapter related to it (2.4) presents its physical-chemical properties and discuss about reactions/interactions that occur in intensive aquaculture and in environment. The types of treatments and its action mode are also described.

---

[1] Adapted from:

- **J.F. Leal**, E.B.H. Santos, V.I. Esteves. Oxytetracycline in intensive aquaculture: water quality during and after its administration, environmental fate, toxicity and bacterial resistance, *in preparation*.
- **J.F. Leal**, M.G.P.M.S. Neves, E.B.H. Santos, V.I. Esteves (2016). Use of formalin in intensive aquaculture: properties, application and effects on fish and water quality. *Reviews in aquaculture*, 0, 1-15.

2.1 Contextualization

There are several environmental factors affecting the production of aquatic organisms: natural and anthropogenic (or artificial). Natural environmental stress factors are difficult to control and include seasonal variations, photoperiod, temperature, salinity, dissolved oxygen, organic matter and overcrowding (Bly et al. 1997). Anthropogenic or artificial environmental stress factors are frequently chemicals (inorganic and organic) that may have three main origins: feed components, treatment agents and construction materials (Haya et al. 2001). These main sources include several groups of compounds, which are listed in **table 1** (GESAMP 1997; Boyd and Massaut 1999; Costello et al. 2001; Haya et al. 2001; Johnston and Santillo 2002; Burridge et al. 2010; A.F.S.F.C.S 2011).

Table 1 – Compounds used in aquaculture

Food components	Treatment agents	Construction materials
Fish oils	Anaesthetics	Fuels and lubricants
Probiotics	Antibiotics	Metals
Antioxidants	Disinfectants	Paints
Essential minerals	Biological (e.g.: vaccines)	Plastics
	Pesticides	
	Fertilisers	

The introduction of substances in aquaculture systems may be unintentional (indirect contamination) or intentional (direct contamination).

Substances introduced indirectly are difficult to control because they are introduced unintentionally. For example, polybrominated diphenyl ethers (PBDEs), like BDE-209, have been detected in fish and their concentrations vary with trophic level, age/size and habitat of fish (Dodder et al. 2002; Blanco et al. 2011). The main source of contamination with PBDEs seems to be the feed (fish meal and fish oil) (Blanco et al. 2011).

Substances intentionally added have different purposes, such as water quality control, tank cleaning, prevention and treatment of aquatic organisms' diseases (Piedrahita 2003; Cao et al. 2007; Hu et al. 2012; Rico et al. 2012). In this context, antibiotics and disinfectants are two of the main groups of chemicals intentionally introduced in the aquaculture production systems.

Antibiotics are natural or synthetic drugs able to kill or inhibit the growth of micro-organisms (FAO 2008). According to *The European Agency for the Evaluation of Medicinal Products* (EMA 1999), the classes of antibiotics authorized for oral use in fish in European Union (EU) are β-lactams (ampicillin and amoxicillin), tetracyclines (oxytetracycline, chlortetracycline and tetracycline), trimethoprim, sulphonamides, quinolones (flumequin and oxolinic acid), fluoroquinolones (sarafloxacin) and fenicols (florfenicol). Among these classes of antibiotics, only the active substances oxytetracycline and florfenicol, belonging to tetracycline and fenicols classes, respectively, are allowed for use in Portuguese aquaculture (DGAV 2015).

Disinfectants are agents able to destroy the infectious agents (FAO 2008) that cause diseases. There are some chemicals disinfectants that may be used in aquaculture, such as ethyl alcohol, copper sulphate, iodine, potassium permanganate, formalin, Virkon® Aquatic and hydrogen peroxide (Bowker et al. 2014; Boyd and McNevin 2014). Among them, formalin is one of the most applied in intensive aquaculture (Boyd and McNevin 2014) and its use is also allowed in Portugal (DGAV 2015).

So, from now on, this work will focus on the indirect contaminant BDE-209 and on two main direct aquaculture's contaminants, the antibiotic oxytetracycline and the disinfectant formalin.

2.2 BDE-209

2.2.1 Physical-chemical properties

The 2,2',3,3',4,4',5,5',6,6' – Decabromodiphenyl ether (**figure 2**) is known as decaBDE, BDE-209 or bis(pentabromphenyl) ether (IUPAC name) and it is the most brominated flame retardant. Its main physical-chemical properties are presented in **table 2** (EHC162 1994). Commercial BDE-209 is a mixture that contains 0.3 – 3 % of nonaBDEs and 97 – 99 % of decaBDE (EPA 2006).

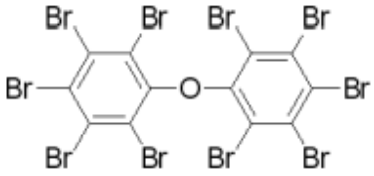

Figure 2 – Structure of BDE-209

Table 2 – Main physical-chemical properties of BDE-209

Chemical formula	$C_{12}Br_{10}O$
Relative molecular mass	959.22 g/mol
Bromine content	81-83 %
Vapour pressure (20 ºC)	$< 10^{-6}$ mmHg
Solubility in water (25 ºC)	20-30 µg/L
log K_{ow}	5.24
Melting point	290-306 ºC
Density (20 ºC)	3.25
Physical aspect and colour	Solid (powder), white

The high octanol/water partition coefficient (K_{OW}) of BDE-209 is related to its high degree of bromination and low water solubility (Vonderheide et al. 2008). Due to its properties, BDE-209 tends to accumulate in sediments and soils and is transported preferentially adsorbed onto particulate matter.

2.2.2 Indirect introduction of BDE-209 in aquaculture

BDE-209 is an additive flame retardant often incorporated into polymers (EHC192 1997). As an additive flame retardant, BDE-209 molecules are not covalently bond to the polymers and can be easily leached to the aquatic environment (EHC162 1994; Vonderheide 2009).

A large part of aquaculture feed – fish meal and fish oil – is obtained mainly from by-products of fish, where BDE-209 is preferentially bio-accumulated (due to its low water solubility). Thus, feed seems to be a main source of introduction of this contaminant in aquaculture, but other sources should not be discarded (Zitko 1999; van Leeuwen et al. 2009). Indeed, significant levels of PBDEs, including BDE-209, have been reported in European fish aquacultures (Jacobs et al. 2002; Stapleton et al. 2004; van Leeuwen et al. 2009; Blanco et al. 2011).

For instance, Blanco et al. (2011) studied the dietary uptake of PBDEs, their occurrence and profiles in aquacultured turbots (*Psetta maxima*), in Spain. BDE-209 concentrations detected in feeding stuffs ranged between 311.9 and 380.64 pg/g original weight. In the same study, BDE-209 represents percentages ranging between 6.4 and 15.1 of total PBDEs in the feed given to turbots. Van Leeuwen et al. (2009) analysed several compounds, namely PBDEs, from farmed fish samples such as salmon, trout, tilapia, pangasius and farmed shrimp. They observed median concentrations ranging between 12 pg/g wet weight for tilapia and 1164 pg/g wet weight for salmon. BDE-209 was the predominant compound in shrimp and most pangasius samples.

Despite the low solubility of BDE-209 in water, its study in aquatic environment is fully justified due to the bioaccumulation characteristics of this compound. Furthermore, the toxicity associated with long-term chronic exposure to low doses of BDE-209 in solution (from 0.959 µg/L) was demonstrated for zebrafish (vertebrate model organism) (He et al. 2011). The conclusions attained by the authors raise some concern because their results showed that chronic exposure to low levels of BDE-209 has a significant impact on overall fitness and reproduction (male gamete quantity and quality, gonad development) in parental fish. Moreover, the chronic exposure of zebrafish to BDE-209 seems to be associated to delay motor neuron development, loss of muscle fibre and slow locomotion behaviour (He et al. 2011).

2.3 Oxytetracycline

2.3.1 Physical-chemical characteristics

Oxytetracycline (**figure 3**) or 4-(Dimethylamino)-1, 4, 4a, 5, 5a, 6, 11,12a-octahydro-3, 5, 6, 10, 12, 12a - hexahydroxy -6 -methyl- 1, 11-dioxo-2-naphthacenecarboxamide (AliAbadi and MacNeil 2002) is a broad spectrum bacteriostatic antibiotic, highly active, produced by a fermentation process that involves the actinomycete *Streptomyces rimosus* (Rigos and Troisi 2005; NCBI 2016). It exists as amphoteric base compound, as the hydrochloride salt, or as a complex of quaternary ammonium salt. Oxytetracycline hydrochloride is the most common form in parenteral and water soluble animal health products (FAO n.d.). **Table 3** presents the main physical-chemical characteristics of oxytetracycline hydrochloride.

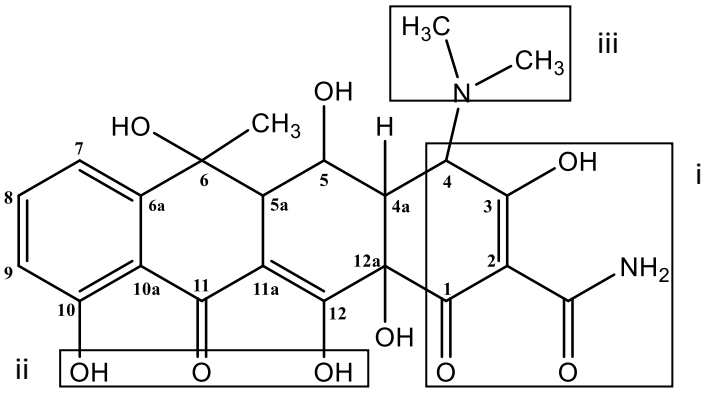

Figure 3 – Molecular structure of oxytetracycline: i – Tricarbonyl system; ii – phenolic diketone; iii – dimethylamine group.

Table 3 – Main physical and chemical properties of oxytetracycline hydrochloride

Molecular formula	$C_{22}H_{24}N_2O_9.HCl$	(NCBI 2016)
Molecular weight	496.8949 g/mol	(NCBI 2016)
Water solubility (25 ºC)	>100 g/L	(Kolodziejska et al. 2013)
Density (20 ºC)	1.634	(NCBI 2016)
Melting point	180 ºC	(ChemicalBook 2016)
Henry's law constant	3.91 x 10^{-26} atm m^3/mol	(Daghrir and Drogui 2013)
log $K_{ow\ (octanol/water)}$	-1.12	(Daghrir and Drogui 2013)
pKa values	pka_1 = 3.22; pka_2 = 7.46; pka_3 = 8.94 pka_1 = 3.3; pka_2 = 7.3; pka_3 = 9.1 pka_1 = 3.57; pka_2 = 7.49; pka_3 = 9.88	(Zhao et al. 2013) (Kulshrestha et al. 2004) (Jiao et al. 2008)
Physical aspect, colour	Solid (powder), dark	---

The pH has a strong influence on OTC structure and its properties, once it alters the protonation state of OTC and its absorbance spectrum (Boreen et al. 2004). According to Zhao et al. (2013), the light absorption of OTC exhibits a red shift to visible light (between 320 and 450 nm) with the increase of pH values. Thus, a greater amount of photons, from solar radiation, is absorbed at high pH values, promoting the direct photo-degradation. Furthermore, at pH values higher than pka_2 (> 7.3), OTC molecules (negatively charged) have a high electronic density on the ring system and tend to attract reactive species such as $HO^{\bullet}$ (Jiao et al. 2008). As one can see in **figure 4**, OTC molecules present one positive charge at low pH values (pH < pka_1 < 3.6), one negative charge at pH values higher than pka_2 (> 7.3) and two negative charges at high pH values (pH > pka_3 > 8.9). For the pH values ranging between the pka_1 and the pka_2, OTC molecules exist in neutral or zwitterion form. In this form, OTC is able to establish intermolecular interactions, forming aggregates in aqueous solution (Tongaree et al. 1999). The structural groups mainly affected by those pH variations are the tricarbonyl system (pka_1), the phenolic diketone (pka_2) and the dimethylamine group (pka_3) (see **figure 3**) (Kulshrestha et al. 2004; Zhao et al. 2013).

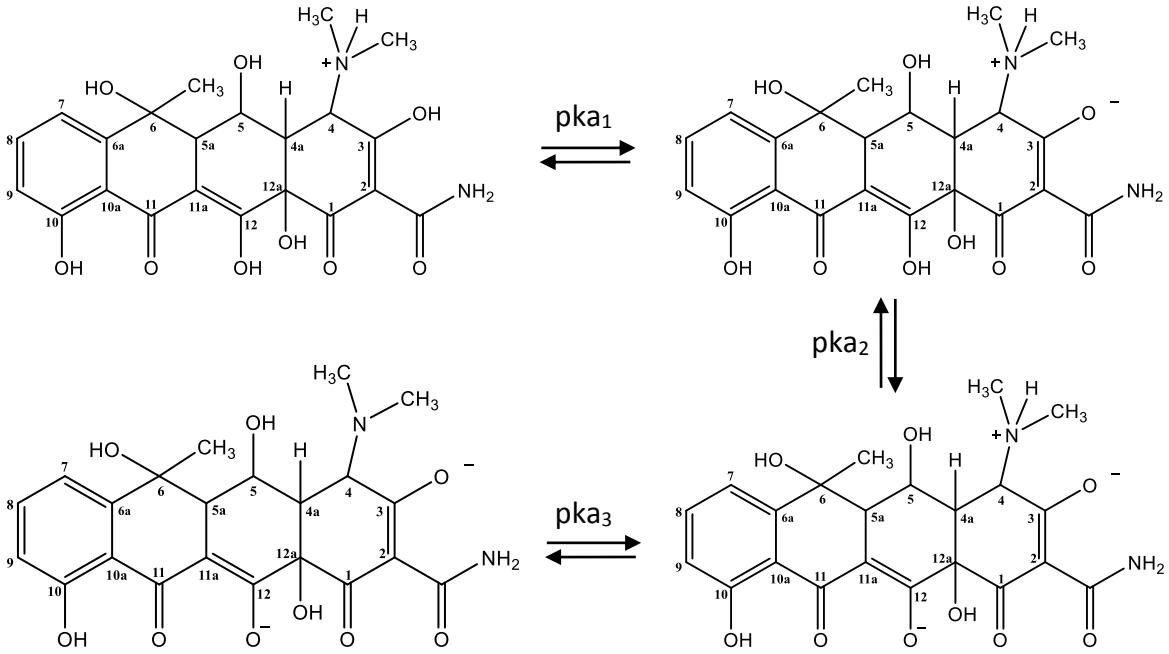

Figure 4 – Ionization states of OTC (Jiao et al. 2008)

2.3.2 Interaction with ions

In aqueous solution, OTC can form complexes with several di- and even trivalent metal ions, such as Ca^{2+}, Mg^{2+}, Zn^{2+}, Cu^{2+}, Co^{2+}, Hg^{2+}, Ni^{2+}, Fe^{3+} and Al^{3+} (Halling-Sorensen et al. 2002; Arias et al. 2007; Schmidt et al. 2007). The ability to form complexes between OTC and cations is related to the capacity of cations accept electrons. Among the cations above referred, the complexation with calcium (Ca^{2+}) and magnesium (Mg^{2+}) is more favourable because these divalent cations are considered hard electron acceptors. They present binding constants to OTC (K_{OTC}) higher than the binding constants for other cations, such as Ni^{2+}, Fe^{2+} Co^{2+} and Hg^{2+}, classified as intermediate or soft acceptors (Arias et al. 2007). Furthermore, among the cations mentioned, the concentrations of calcium and magnesium in natural aquatic systems, namely in brackish and seawater, are much higher than the concentrations of the remaining cations (Lunestad and Goksoyr 1990). However, it is worth to notice that the complexation of OTC with calcium and magnesium is not exclusive in brackish or marine water. Also in hard fresh water, where the calcium and magnesium concentrations generally range between 48-72 mg/L and 29-43 mg/L, respectively, the complexation with OTC can occur (Schmidt et al. 2007). Given the greater environmental relevance of OTC complexation with calcium and magnesium, the interaction of this antibiotic with these two metal cations will be preferably highlighted hereinafter.

The OTC complexation with calcium or magnesium is a process strongly dependent on pH (Schmidt et al. 2007), being generally favoured at high pH values, for which OTC is more deprotonated (**figure 4**). Some examples of the binding constants found in the literature are $K_{OTC–Ca} = 1.9x10^2$ and $K_{OTC–Mg} = 2.9x10^2$, at pH 8.0 (Lunestad and Goksoyr 1990) or $K_{OTC–Ca} = 55 \pm 9$ and $K_{OTC–Mg} = 66 \pm 9$, at pH 4.0–5.0 (Arias et al. 2007), revealing in the two cases a higher affinity to the formation of complex OTC–magnesium (OTC–Mg) than of complex OTC–calcium (OTC–Ca).

The stoichiometry of the OTC–Ca and OTC–Mg complexes depends on the proportion and concentration of the ligand (OTC) and cation (Schmitt and Schneider 2000; Carlotti et al. 2012; Guerra et al. 2016). According to Schmitt and Schneider (2000), the formation of complexes 1:2 occurs with a large excess of cation concentration comparatively to the ligand concentration. At the molar ratio 1:1, most of the chelates are considered insoluble in water (Dixon 2000), but at environmental relevant trace levels, those chelates may be soluble (Schmidt et al. 2007). Indeed, Tongaree et al. (1999) proposed that the formation of complexes of OTC–Mg (at pH 7.5) and OTC–Ca (at pH

ranging between 6.8-8) increase the solubility of OTC comparatively with OTC un-complexed, at respective pH values.

Regarding to the binding sites, at typical pH values of natural saltwater (around 7), the phenolic diketone group (**figure 3**) is commonly proposed as the first site of coordination, although the exact position is often questioned (Newman and Frank 1976; Schmitt and Schneider 2000). The positions C(11)–C(12) have been suggested as the major sites of complex formation (Clive 1968; Halling-Sorensen et al. 2002), being that the coordination occurs through oxygen, as revealed by spectroscopic measurements (Clive 1968). When 1:2 (OTC: cation) complexes are formed, the site N4-O3 is proposed as the most favourable binding site (Schmitt and Schneider 2000).

The OTC complexation with calcium and magnesium generally reduces the bioavailability of OTC (Lunestad and Goksoyr 1990; Halling-Sorensen et al. 2002), which may have implications on biological activity of the antibiotic (Serrano 2005) and in the metabolism of fish (Rigos and Smith 2015). Additionally, the OTC complexation with these cations has been reported as affecting the photo-degradation (Xuan et al. 2010; Chen et al. 2011) of this compound in the environment. Each of these implications will be discussed in more detail below.

2.3.3 Use of oxytetracycline in farmed fish

Oxytetracycline is mainly indicated for the treatment of fish bacterial diseases caused by *Aeromonas salmonicida* (furunculosis); *Aeromonas hydrophila* and *Aeromonas sobia* (aeromonosis); *Pseudomonas* (pseudomonosis); *Lactococcus garvieae* (lactococcosis) and *Vibrio anguillarum* (vibriosis) (AliAbadi and MacNeil 2002; Cenavisa 2016; Drugs.com 2016). The main target species in aquaculture for the treatment using OTC are salmonids (*Salmo* sp. and *Oncorhynchus* sp.), turbot (*Psetta máxima*), sea bream (*Sparus aurata*), sea bass (*Dicentrarchus labrax*), European eel (*Anguilla Anguilla*) and European carp (*Cyprinus carpio*) (Cenavisa 2016).

Doses and treatments

Doses and treatment conditions are dependent on factors, such as, nature and extension of the disease; species, age and condition of fish; and on composition and characteristics of the aqueous matrices.

With respect to treatments, there are three main ways to administrate OTC to farmed fish: through the feed (medicated feed), bath treatment and injection. Among these possible ways, the oral administration by incorporation of the antibiotic into the feed before pelleting (Schmidt et al. 2007) is the most common and is preferred because it represents a minimal risk of environmental pollution (Sekkin and Kum 2011). The bath treatment is discouraged in marine or fresh water at high pH (harder water) once OTC is able to form chelates with some divalent cations, which may decrease the effectiveness of its antibacterial action (Dixon 2000). After treatment, water should be changed.

Regarding to the conditions of OTC administration, **table 4** shows some examples of the recommended daily doses (RDD), target species fish, time period and ways of administration for this antibiotic. Based on the data collected and presented in that table, 75 mg OTC/kg of body weight is a common recommended daily dose (RDD) and 250 mg OTC/kg of body weight is the maximum RDD, administered through the feed (via oral). Considering the typical density range of intensive production, from 10 kg/m^3 to 50 kg/m^3 (Barnabé 1994), the conversion of OTC recommended daily dose (mg/kg body weight) to OTC daily concentration by unit volume was calculated and indicated in **table 5**.

Table 4 – Recommended conditions for OTC administration to farmed fish

Daily doses (mg/kg body weight)	**Time period of administration** (days)	**Target fish species**	**Way of administration**	**References**
75	4-8	n.d.	Oral	(Bishop 2005)
55	7-10	Salmonids, turbot, gilthead sea bream, sea bass, European eel, European carp	Oral	(Cenavisa 2016)
75	10	Salmonids	Oral	(Scott 1993)
75	14	Gilthead sea bream (50-70 g), European sea bass (80-100 g)	Oral	(Malvisi et al. 1996)
50-100	3-14	Salmonids	Oral	(Namdari et al. 1996)
40	n.d	European sea bass (110 g)	Intravascular	(Rigos et al. 2002)
50-125	4-10	Salmon	Oral	(Burridge et al. 2010)
100-150	10-15	n.d.	n.d.	(Romero et al. 2012)
5-60	s.d.	African catfish, carp, rainbow trout, red pacu, sockeye salmon	Intramuscular (12-25 ºC)	(Reimschuessel et al. 2005; Sekkin and Kum 2011)
5-60	s.d.	African catfish, Atlantic salmon, carp, Chinook salmon, eel, rainbow trout, red pacu, sea bass, sea bream, sharp-snout	Intravenous (8-25 ºC)	
10-100	Up to 10	Atlantic salmon, black sea bream, carp, channel catfish, eel, perch, rainbow trout, sea bass, sea bream, hybrid sea bass, flounder, walleye	Oral (7-27 ºC)	
10-100	s.d.	Arctic char, Sockeye salmon, Chinook salmon	Oral (6-11 ºC)	
75	10	Atlantic salmon	Oral (14 ºC)	Pursel (1998) in Rigos and Smith (2015)
100	10	Rainbow trout	Oral (12 ºC)	Bruun et al. (2002) in Rigos and Smith (2015)
250	4	Pacific salmon	Oral	(Schmidt et al. 2007)

n.d. – not defined; s.d. – single dose

Table 5 – Conversion of OTC recommended daily dose – RDD (mg/kg body weight) to OTC daily concentration by unit volume (mg/L).

Density of production	**RDD (mg/kg)**	**[OTC] (mg/L)**	**RDD (mg/kg)**	**[OTC] (mg/L)**
10 kg/m^3 → 0.010 kg/L	75	0.75	250	2.50
25 kg/m^3 → 0.025 kg/L		1.88		6.25
50 kg/m^3 → 0.050 kg/L		3.75		12.50

Fish metabolism

Temperature affects the absorption of OTC, increasing with the increase of water temperature (Rigos et al. 2004[a]). Additionally, the effectiveness of the treatment can be affected by the presence and quantity of sea-salts in water, as was observed for the absorption of OTC in euryhaline fish species (fish able to tolerate a wide range of salinities) (Rigos et al. 2004[a]; Rigos et al. 2004[b]; Rigos and Troisi 2005). As previously referred, the binding of OTC with divalent cations, such as Ca^{2+} and Mg^{2+} causes a significant reduction of the bioavailability of OTC in fish (Lunestad and Goksoyr 1990; Halling-Sorensen et al. 2002). Some authors reported that its bioavailability was only 1 % in seawater, which implies that the minimum inhibitory concentration (MIC) of OTC must be much higher in saltwater or hard freshwater than in soft freshwater (Rodgers and Furones 2009). The complexation occurs in water containing those cations, but may also occur in the intestinal tract of fish (Rigos and Troisi 2005; Sekkin and Kum 2011).

OTC is rapidly, but poor to moderately absorbed through the intestinal tract of fish (EMA 1995; Romero et al. 2012). It is widely distributed throughout the body and is retained particularly in liver, kidney, bones and dentine (EMA 1995). Oxytetracycline is poorly metabolized or un-metabolized, being the most part excreted via urine and faeces unchanged, this is, in its parent form (EMA 1995; Rigos and Troisi 2005; Sekkin and Kum 2011; Romero et al. 2012; Slana and Dolenc 2013).

2.3.4 Effects of OTC in water quality of recirculating/reuse circuits

Two of the treatment processes usually integrated in the water circuit (closed or semi-closed) are bio-filtration and ozonation. As previously referred in *chapter 1*, bio-filtration occurs through nitrifying bacteria, promoting the nitrification of ammonia (NH_4^+) and nitrites (NO_2^-) into nitrates (NO_3^-). Ozonation promotes the oxidation and degradation of organic compounds, whereby it is expected that ozonation degrades and removes OTC. Thus, nitrification, ozonation and their interactions with OTC will be discussed in more detail below.

Effect of OTC on nitrification

The main bacteria responsible by nitrification in bio-filters are Gram-negatives: *Nitrosomonas* sp., which promotes the conversion of ammonia into nitrite, and *Nitrobacter* sp., which converts nitrite into nitrate (Branson 1993; Klaver and Matthews

1994). As a broad-spectrum antibiotic, OTC is able to inhibit the growth of these bacteria. Halling-Sorensen (2001) reported a half maximal effective concentration (EC_{50}) of 1.7 mg/L (10 days) regarding to the growth inhibition of *Nitrosomas europaea*. Such inhibition negatively affects the conversion of ammonia (NH_4^+/NH_3) and nitrite (NO_2^-) (toxic products for fish) into nitrates (NO_3^-) (Carlucci and Pramer 1960; Klaver and Matthews 1994; Halling-Sorensen 2001; Stickney and McVey 2002; Roose-Amsaleg and Laverman 2016).

The literature data indicate that OTC inhibit primarily the action of *Nitrosomonas* sp., inhibiting consequently the following step of conversion into nitrates. Indeed, Carlucci and Pramer (1960) observed that the conversion of ammonia into nitrite was 95.7 %, 91.3 % and 5.6 %, at OTC concentrations of 1 mg/L, 10 mg/L and 100 mg/L, respectively, in seawater. Klaver and Matthews (1994) also studied the effect of OTC (12.5 – 75 mg/L) on nitrification, in a synthetic freshwater system. The conclusions obtained by them were similar to those obtained by Carlucci and Pramer (1960) in seawater, observing an inhibition of nitrification for all tested concentrations. At higher OTC concentrations, the amount of ammonia little or no decrease, but a moderate conversion of ammonia to nitrite and nitrate occurred at lower OTC concentrations. Thus, the results obtained in these studies suggest that the inhibitory effect on nitrification is higher when the OTC concentration is also higher.

Other authors, who performed their studies using nitrifying sludge, observed that nitrification was not inhibited at OTC concentrations up 100 mg/L, but an inhibition of 50 % of nitrification occurred when OTC concentration increased from 100 to 250 mg/L (Campos et al. 2001). The different results obtained by these authors can perhaps be explained by the different experimental conditions in comparison to the previous studies, namely the matrices (water vs. sludge).

Ozonation of oxytetracycline

Ozone (O_3) is a strong oxidant able to oxidize organic molecules directly or indirectly through of $HO^{\bullet}$ formation, which is a powerful and non-selective oxidant. In aqueous solution, ozone can react with organic molecules, such as OTC, mainly by direct 1,3-dipolar cycloaddition to double bonds and via *in situ* generation of hydroxyl radicals, which is favoured at high pH values (> 7) (Glaze 1987; Dalmazio et al. 2007; Li et al. 2008).

Li et al. (2008) investigated the effect of ozonation ($[O_3]$ in gas phase = 11 mg/L) on OTC degradation (100 mg/L) in ultra-pure water, at three different pH values: 3, 7 and 11.

These authors concluded that the degradation rate of OTC at pH 7 is fastest, having obtained almost 90 % of OTC decomposition after 5 minutes of ozonation.

Yalap and Balcioglu (2009) also studied the ozone oxidation process, in ultra-pure water, applied to OTC degradation ([OTC] = 46 mg/L). The authors evaluated different doses of ozone (10, 18 and 30 mg/L), at pH 7, concluding that the increase of ozone dose from 10 to 18 mg/L caused a significant increase (2.5 times) on the rate of OTC degradation. The increase of ozone dose from 18 mg/L to 30 mg/L only slightly increase the OTC degradation rate. Additionally, the authors assessed the effect of some water components (100 mg/L of each component), such as Ca^{2+}, Cl^{-} and humic acid, on the OTC ozonation (ozone dose: 1086 mg L^{-1} h^{-1}). They reported that the rate constant (k) decreased in the following order: in distilled water (k = 4.18 min^{-1}) > with Ca^{2+} (k = 1.67 min^{-1}) > with Cl^{-} (k = 1.36 min^{-1}) > humic acids (k = 1.13 min^{-1}) (Yalap and Balcioglu 2009). Thus, in addition to the concern related to the production of toxic compounds (eg.: BrO_3^{-}) caused by ozonation in saltwater (*chapter 1*), the results reported by these authors indicate that ozonation is also affected by other constituents typically present in natural water.

Thus, due to the different ozone chemistry in fresh- or saltwater (Reiser et al. 2011), the results obtained in deionised-, synthetic- or even in fresh-water cannot be simply extrapolated to marine conditions once the ozone-induced oxidants differ much in these aqueous systems. Furthermore, the ozone concentrations applied in the above referred studies are much higher than those recommended. Low applied doses from 0.5 to 1.5 mg/L have revealed to be effective to inactivate bacterial, viral and protozoan agents, with a time of contact varying between 1-10 minutes (Colt and Cryer 2000; Lekang 2007). Using ozone doses of the same order of magnitude referred to above (≈ 1 mg/L) some authors reported that the ozonation only removed 57 % of amount of OTC (43 ng/L) in a drinking water treatment plant (DWTP) (Liu et al. 2016). This result indicates that ozonation may not be a method so efficient for the degradation of OTC, even for low initial OTC concentrations.

Additionally, based on studies performed with tetracycline (TTC), which has a molecular structure very similar to OTC, ozonation does not seem to promote the removal of total organic carbon – TOC (mineralization), once that only about 5 % of TOC removal was observed after 120 minutes (Dalmazio et al. 2007). Other authors, who applied 12 mg ozone in water to degrade TTC (5 x 10^{-5} M), also observed the formation of TTC by-products (Ziolkowska et al. 2016), corroborating the inability of ozonation to mineralize, even applying higher doses of ozone.

2.3.5 Environmental fate

In recirculated or reused water systems, part of water is treated and re-enters in tanks production, while other part of water is released into environment. After reach aquatic systems, the environmental fate of a compound is strongly dependent on its molecular structure and its physical-chemical properties, such as the Henry's constant, the octanol-water partitioning constant – K_{ow}, the water solubility and the adsorption to the particulate matter (mineral or organic) (Slana and Dolenc 2013).

Henry's law constant of OTC is low (3.91 x 10^{-26} atm m^3/mol), which means that OTC molecules are weakly lost by volatilization (Daghrir and Drogui 2013). OTC has a very high mobility in water due to its high water solubility (> 100 g/L) (Kolodziejska et al. 2013) and low log K_{ow} (-1.12) (Daghrir and Drogui 2013).

As previously referred, the most part of OTC is excreted via urine and faeces in its original form (EMA 1995; Rigos and Troisi 2005; Sekkin and Kum 2011; Romero et al. 2012; Slana and Dolenc 2013). According to several authors (Schmidt et al. 2007, Romero et al. 2012, Daghrir and Drogui 2013), 70 to 80 %, or even more, of ingested OTC is excreted intact to aquatic environment, in un-metabolized form. **Figure 5** presents a schematic representation of OTC fate, since its administration to fish in aquaculture facilities, until its discharge into environment, where it may suffer several reactions explained in more detail below.

From **figure 5**, one observes that the introduction of OTC in the environment can occur through four main direct pathways: (1) freely-dissolved ionic OTC in water (chelated or/and un-chelated) or from fish urine, (2) associated to dissolved organic matter (DOM), (3) sorbed to organic and inorganic solids (e.g.: desorption from fish feed and faeces), (4) OTC-medicated feed leached from uneaten feed (Rigos and Troisi 2005; Schmidt et al. 2007). Note that even when OTC is added to water in the form of pellets (OTC-medicated feed), fragments may fall and OTC can be released into water (Lunestad et al. 1995). Then, as result of its high water solubility, it is predictable that it can be leached to groundwater (Slana and Dolenc 2013), where it can pass to the sediment/soil. The contaminated water can enter in the drinking water treatment plants (DWTPs) or wastewater treatment plants (WWTPs), where the conventional treatment methods are not designed or prepared to remove effectively these type of antibiotics, highly polar (Homem and Santos 2011; Daghrir and Drogui 2013). As consequence, the systems of water distribution remain contaminated, reaching at last the human beings.

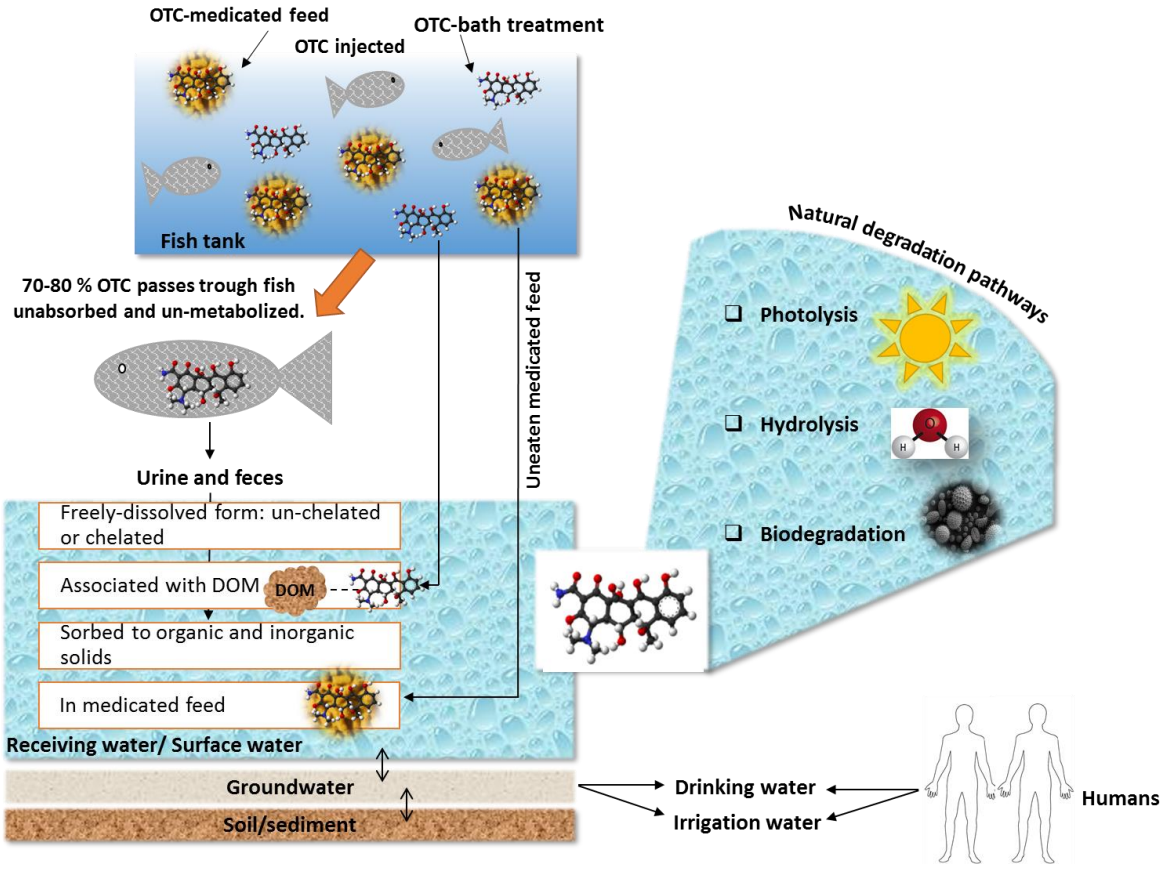

Figure 5 – Environmental fate of OTC from its administration to its release into aquatic environment, including the main natural degradation pathways.

Based on high hydrophilic character and low volatilization of OTC, a significant persistence of this compound in water (Daghrir and Drogui 2013) is predicted. For instance, OTC concentrations ranging between 9.1 and 33.3 ng/L were detected in a river located at 250 m downstream of an aquaculture system (Pereira et al. 2015). Other authors (Dietze et al. 2005) detected maximum OTC concentrations of 10 µg/L in intensive fish hatcheries, in USA. However, after reaching the aquatic environment, OTC is naturally subjected to three main degradation pathways: photolysis, hydrolysis and biodegradation.

Photolysis or photo-degradation caused by solar radiation has been pointed as the major and the most important degradation pathway of tetracycline antibiotics in shallow and transparent aquatic environment (Schmidt et al. 2007; Xuan et al. 2010; Borghi and Palma 2014). Photo-degradation can occur by two main ways: directly (absorption of radiation by the compound) and /or indirectly (photosensitization of the compound by natural water constituents, such as DOM) (Borghi and Palma 2014). However, it is worth

to notice that DOM can also have a light-screening effect, which can prevail over photosensitization effect, causing an inhibition of OTC photo-degradation. Solar photo-degradation can be affected by several factors, namely pH, composition and turbidity of water, season, latitude and own absorption spectrum of the compound (Kummerer 2009; Borghi and Palma 2014).

Hydrolysis may be an important degradation pathway of OTC in relatively deep water (Schmidt et al. 2007). It has been reported that OTC hydrolysis is affected by pH of solution (Loftin et al. 2008; Slana and Dolenc 2013). Acidic conditions (pH = 3) seem to favour the stability of OTC, while alkaline conditions (pH = 10) seem to favour its degradation (Doi and Stoskopf 2000). Indeed, Halling-Sorensen et al. (2002) refer that basic conditions promote faster OTC breakdown than neutral or acidic conditions. In addition, temperature can affect the OTC hydrolysis (Loftin et al. 2008). For example, Xuan et al. (2010) reported that the half-life of OTC decreased from 1.2×10^2 to 0.15 day with the increase of temperature from 4 ± 0.8 ◦C to 60 ± 1 ◦C. However, these extreme temperatures cannot be applied in an aquaculture system. It would be interesting to consider a shorter range of temperatures (e.g.: 10 to 20 ºC) to assess the real effect that such temperature variations would have on the degradation of OTC by hydrolysis.

Biodegradation is a breakdown of a substance catalysed by enzymes *in vitro* or *in vivo* (IUPAC 2011). It may be classified as primary, environmentally acceptable or ultimate. Primary or environmental acceptable biodegradation are similar and involve the chemical structure alteration, implying the loss of some specific properties. The dependence of the circumstances in which these substances are discharged into the environment is what distinguishes the environmental acceptable biodegradation of primary biodegradation. Ultimate biodegradation corresponds to complete breakdown of a compound by total oxidation or reduction to simple molecules, such as carbon dioxide or methane (IUPAC 2011). Some studies of OTC biodegradation have been reported in the literature (Ingerslev et al. 2001; Migliore et al. 2012; Dzomba et al. 2015; Ahumada-Rudolph et al. 2016), but the data suggest that OTC biodegradation can be slow and take several days. For instance, Ahumada-Rudoph et al. (2016) observed a decrease of 72 % to 92 % of the OTC concentration caused by biodegradation, after 21 days of treatment. For these experiments, the authors previously isolated marine fungi strains (*Trichoderma harzianum*, *Trichoderma deliquescens*, *Penicillium crustosum*, *Rhodotorula mucilaginosa* and *Talaromyces atroroseus*) from sediment samples collected in a fish farming.

2.4 Formalin

2.4.1 Physical-chemical properties

Dissolution of formaldehyde (methanal) in water attains a rapid and almost complete equilibrium with the corresponding hydrate (**reaction 13**), also known as formalin ($CH_2(OH)_2$). The equilibrium constant for this hydration (K_{hydr}) is 41 and the conversion of formaldehyde to its hydrate is 99.96 % (Carey 2000). However, in some conditions, such as high concentrations of formaldehyde hydrate and high temperatures, the dissociation of formalin is favoured (Fox et al. 1985).

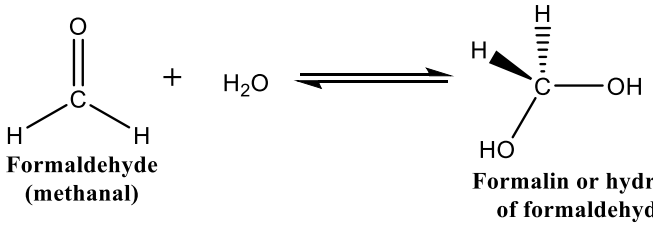

Reaction 13

So, the commercial formulation of formalin is an aqueous solution, containing usually 37–40 % (w/w) of formaldehyde. To avoid the formation of paraformaldehyde (white precipitate), formalin should be stored in the dark, at temperatures above 4 ºC (Francis-Floyd 1996; Masters 2004). Additionally, the aqueous solution of formaldehyde is stabilized with 10–15 % of methanol (w/w) in order to prevent the formation of paraformaldehyde (polyoxymethylene – $OH(CH_2O)_nH$), which is very toxic to fish (Tucker and Robinson 1990). In the commercial formulation (formalin), methanol is used to prevent the polymerization due to the formation of hemiacetal, which exists in equilibrium with the hydrated formaldehyde (**reaction 14**) (Kitchens et al. 1976). The hemiacetal formation (hemiformal in this specific case) prevents the polymerization because the hydrogen bonded to oxygen is replaced by a $–CH_3$ group (**reaction 14**), not allowing the formation of polyoxymethylene (paraformaldehyde).

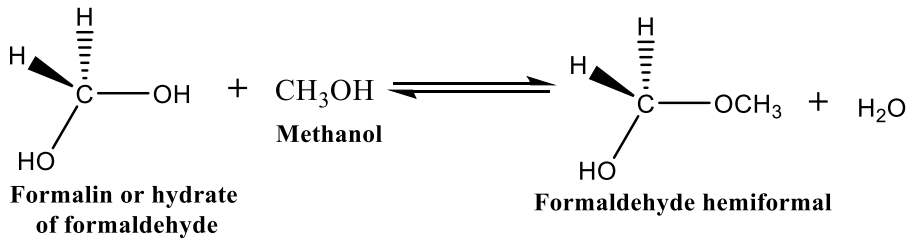

Reaction 14

Formalin presents a pH between 2.8 and 4.0 and a flash point (the lowest temperature at which it can vaporize to form an ignitable mixture in air) of 60 ºC (FDA 1995; Masters 2004). Considering a solution of formalin containing 37 % of formaldehyde and 10 % of methanol, the usual commercial formulation, its boiling point and density is 97.8 ºC and 1.089 g/mL (at 18 ºC), respectively (Kitchens et al. 1976). With respect to the use of methanol as stabilizer of formalin solution, the concern is related to the toxicity of methanol for aquatic species. Studies pointed for methanol median lethal concentrations – LC_{50} (at 96 hours) ranging between 15.4 and 29.4 mg/L to fish (Poirier et al. 1986; Kaviraj et al. 2004). LC_{50} is an indicator of acute toxicity and corresponds to the concentration able to kill fifty percent of the exposed organisms (Mayes and Barron 1991; Rand 1995). Some of the most common effects on fish resulting of methanol toxicity are the hyperactivity and convulsion, as well as respiratory distress, reduction of growth and impairment of reproductive performance (Kaviraj et al. 2004 and authors cited therein).

In the presence of atmospheric oxygen, the oxidation of formaldehyde/ formalin to formic acid can occur (**reaction 15**) (Fox et al. 1985; FDA 1995). This acid can undergo further reactions mediated by microorganisms to produce carbon dioxide and water (**reaction 16**) (FDA 1995). The oxidation process of formalin to carbon dioxide and water naturally consumes oxygen, what may constitute a serious problem in the aquaculture systems, as will be discussed next.

$$2\ H_2C{=}O + O_2 \longrightarrow 2\ HCOOH \qquad \textbf{Reaction 15}$$

$$HCOOH + 0.5\ O_2 \longrightarrow CO_2 + H_2O \qquad \textbf{Reaction 16}$$

2.4.2 Types of treatment in intensive aquaculture

Formalin is one of the most applied chemical disinfectants in intensive aquaculture (Boyd and McNevin 2014). It may be used as prophylactic measure or with therapeutic purposes and is extremely effective against most protozoan parasites (*Ichthyophthirius* spp., *Costia* spp., *Epistylis* spp., *Chilodonella* spp., *Scyphidia* sp., *Trichodina* spp.) and monogenetic trematodes (*Cleidodiscus* spp., *Gyrodactylus*_spp., *Dactylogyrus* spp.) (FDA 1995; Francis-Floyd 1996; Shao 2001).

Formalin is frequently added to water and the concentration applied for treatment should be sufficient to kill the infectious agent, without endangering the fish. However, the margin between the concentration needed to kill the infectious agent and the

concentration able to cause negative effects on fish may be small, whereby the treatment should be done very carefully and only when it is really necessary (Shepherd and Bromage 2001). For an appropriate treatment, several factors such as water flow rates, operating volume of the tank, temperature (must be the lowest) and oxygen levels should be considered and evaluated previously. The concentration applied to the treatment is also strongly dependent on the fish age and water quality. For example, a lower range of formalin concentrations should be adopted if water hardness is less than 100 mg/L of calcium carbonate and under conditions of soft un-buffered water (Shepherd and Bromage 2001). The time in which the fish is in contact with the treatment agent and the own condition of fish cannot also be negligible when choosing the concentration to be used (Francis-Floyd 1996). Nevertheless, the monitoring of fish behaviour must be ensured during all treatment. In tanks and raceways, the water supply should be turned off before treatment and a suitable amount of formalin must be added to water, ensuring equal distribution in the tank (FDA 1995).

Regarding to the treatments, two main types can be distinguished: the short-term bath and the prolonged immersion (prolonged bath) (Scott 1993; Francis-Floyd 1996). The most common dosage of formalin for the short bath treatment is up to 250 mg/L up to one hour (commonly varies between 30 and 60 minutes) (Scott 1993; Francis-Floyd 1996; Shepherd and Bromage 2001), which corresponds to the maximum concentration level used in treatment for parasite infected fish (FDA 1995). Considering a solution of formalin of 250 mg/L, containing 37 % by weight of formaldehyde gas per weight of water, the conversion of formalin concentration to formaldehyde concentration is achieved multiplying 0.37 by 250 mg/L (formalin concentration), which is equal to 92.5 mg/L (formaldehyde concentration). However, special attention should be given to some situations. For example, for salmon and trout in tanks and raceways, the concentration of 250 mg/L of formalin is only recommended for water temperatures below 10 ºC; for water temperatures above 10 ºC lower concentrations of formalin (up to 170 mg/L) are more appropriate (Masters 2004). At water temperatures above 21 ºC, the formalin concentration should not be more than 150 mg/L (Francis-Floyd 1996). In the case of the prolonged baths (long-exposure treatment), the appropriate formalin concentration frequently ranges between 15 and 25 mg/L for 12 hours (Scott 1993; Francis-Floyd 1996).

2.4.3 Formalin exposure: consequences for fish

The effects of formalin exposure for fish are strongly dependent of several factors such as the species of fish and their size/stage of life, the time of formalin exposure and its concentration, as well as, physical parameters like temperature. The toxicity increases when the exposure time and temperature also increase (Bills et al. 1993; FDA 2002). Furthermore, the toxicity of formalin to aquatic species is also affected by water chemistry, namely by factors such as pH, hardness and the presence of some natural constituents in water (Bills et al. 1977; Chinabut et al. 1988; Bills et al. 1993; Meinelt et al. 2005). For example, Meinelt et al. (2005) found a reduction of formalin toxicity in the presence of NOM (5 mg/L of dissolved organic carbon, DOC), attributing this reduction to a possible binding of formalin to specific functional groups or structures of NOM.

In literature, there are studies with controversial conclusions about the possible consequences for fish, as result of formalin/formaldehyde exposure. Some studies have reported negative effects in rainbow trout (*Oncorhynchus mykiss*) (Williams and Wooten 1981; WHO 1989; Buchmann et al. 2004), sea bream (*Sparus aurata)* and sea bass (*Dicentrarchus labrax)* (Yildiz and Ergonul 2010) and olive flounder (*Paralichthys olivaceus*) (Jung et al. 2003).

The most common negative consequences reported in the literature are the permanent damage on gills (Shepherd and Bromage 2001), in gill lamellar epithelium (Williams and Wooten 1981) and alterations on mucous cells (Buchmann et al. 2004). In addition, hypochloraemia, reduced blood pH or increase of blood-haemoglobin and plasm-protein concentrations are examples of toxic effects reported for rainbow trout and Atlantic salmon (WHO 1989 and authors cited therein).

Jung et al. (2003) performed several biochemical tests in olive flounder (*Paralichthys olivaceus*) and observed that most part of the parameters is significantly altered by the presence of formalin at different concentrations (100 – 300 mg/L). However, those evidences are only observed after three hours of formalin exposure, which corresponds to a time of treatment higher than what is recommended (1 hour). It has been also examined the effects of one hour of treatment with formalin (100 – 300 mg/L) in olive flounder (390 – 480 g), but they did not find significant changes in haematological and haemochemical values in fish.

Moreover, there are also some studies that report no significant or limited significant negative effects for fish when exposed to recommended dosages of formalin. For example, some authors evaluated the effects of repeated prophylactic formalin

treatments (167–250 mg/L) on the gill structure of juvenile salmonids (Atlantic salmon with one-year-old and rainbow trout with an average weight of 6 g). They did not obtain evidence of lamellar oedema or necrosis of lamellar epithelial cells. The significant effects that they observed were limited to the increase of mucous cells number on gill lamellae (Speare et al. 1997).

Chinabut et al. (1988) continuously exposed common carp (0.8 g) to formalin (25, 50 and 75 mg/L) for eight weeks and did not observe histological changes in gills, liver, kidney, spleen, intestine, muscle and skin. Nevertheless, in the same conditions, their results indicated a reduction of the growth of common carp fry. These authors proposed that the formalin concentrations of 25-50 mg/L should be safe for common carp unless continuously exposed for more than four weeks. However, the growth of common carp was slightly affected when the fish was exposed at 75 mg/L of formalin during more than two weeks (Chinabut et al. 1988).

Considering all these studies, it is important to stand out that the results and conclusions are always variable with the experimental conditions applied and the tests performed. One positive aspect regarding to the use of this disinfectant is that formaldehyde is very soluble in water and its bioaccumulation in aquatic organisms is not expected due to its low n-octanol/water partition coefficient ($-0.75 < \log K_{ow} < 0.35$) (WHO 1989; Liteplo et al. 2002).

2.4.4 Effect of formalin on water quality

In semi-closed aquaculture intensive systems, there are three processes particularly relevant: aeration/oxygenation, bio-filtration and ozonation. The integration of formalin in these processes may have direct effects on normal action mode of them, calling into question the quality of water and the health of fish. Besides formalin being able to interact with water treatment processes, its application in the tank may cause depression of oxygen levels, as explained above. Additionally, the aqueous effluent which is released into environment may also contain formalin and this situation is worrying because it will also affect the receiving water in the natural environment (Lalonde et al. 2015). For example, if the water containing formalin is released into small, stagnant or slow-moving water bodies, the inhibition or death of phytoplankton and zooplankton population may temporarily occur as a result of decrease of oxygen levels (FDA 1995).

Thus, to clarify the effects of use of formalin in intensive production, the different ways for formalin to affect the water quality in aquaculture systems and in aqueous natural environment are discussed below. To help to understand the discussion about this topic, **figure 6** is presented. It illustrates an example of a semi-closed circuit of intensive aquaculture. The steps of water treatment presented in that scheme are frequently the most common, but depending on water characteristics, the treatments and/or their sequence into circuit can be different between companies.

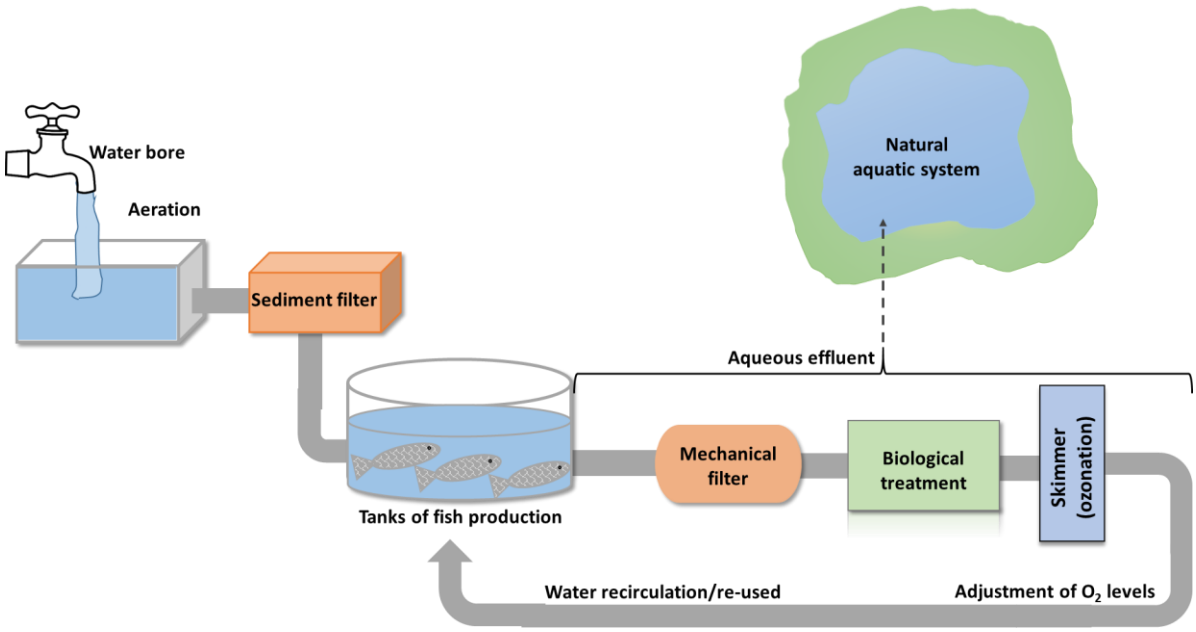

Figure 6 – Example of a semi-closed circuit of intensive aquaculture

Water quality in tanks during the treatment

As has been suggested throughout this work, during the bath treatment with formalin, a depression of dissolved oxygen concentrations can occur (Muir and Roberts 2012). Francis-Floyd (1996) suggests that by each 5 mg/L applied to aquatic environment, 1 mg/L of dissolved oxygen is removed. Assuming this extreme condition, for a bath treatment with 250 mg/L of formalin, 50 mg/L of dissolved oxygen will be removed. These data are very worrying since the oxygen solubility in water at 25°C, in equilibrium with air at atmospheric pressure, is only 8.3 mg/L in freshwater and even lower in seawater (salinity: 35 ‰) – 6.6 mg/L (Manahan 2000; Fish 2012). This should be a concern for aquaculture companies that should ensure an adequate aeration during the process

because if the rate of formalin oxidation is faster than the rate of water aeration, the oxygen levels will decrease (FDA 1995; Muir and Roberts 2012), causing stress in fish. As result of oxygen deficiency, the most frequent symptoms on fish are the difficulty in breathing at the surface and the gathering of fish at water inlets (Branson 1993). The depletion of dissolved oxygen concentrations is even more worrying in slow-moving water at higher temperatures, not only because the metabolic effect of bacteria increases with water temperature, but also because the dissolved oxygen saturation level (which corresponds to the oxygen storage capacity) and the rates of oxygen reaeration decrease with increasing water temperature (FDA 1995; Fish 2012). Formalin also contributes to the depletion of oxygen through its algaecide activity. When applied to water, it kills a portion of algae, contributing to the decrease of oxygen production through photosynthesis (Francis-Floyd 1996). However, this effect is not so relevant in intensive aquaculture, which frequently uses tanks of concrete and fiberglass protected from sunlight, but assumes greater importance in semi-intensive and extensive aquaculture, which are almost always practiced in earthen ponds exposed to sunlight.

Recirculating/re-use water

Before and during the bath treatment with formalin, water supply should be turned off (FDA 1995) and the tank closed at least during the time recommended for treatment. The oxygenation should also be guaranteed to avoid the depletion of oxygen levels. After treatment, the recirculating aquaculture system must be re-established and water containing formaldehyde may pass by the bio-filter and skimmer (where ozonation occurs). Thus, the main purpose of this topic is to understand how the processes on bio-filter are affected by the presence of formalin, as well as the mutual interaction between ozonation and formalin/formaldehyde.

a. Formalin in biological-filters

In what way formalin can disturb the normal action mode of biological filters? It can interact with processes that occur on bio-filter by three different ways:

- First of all, formalin can react with ammonia to form imines ($HN=CH_2$) (**reaction 17**); additionally, it can also react with ammonia to quantitatively form hexamethylenetetramine [$(CH_2)_6N_4$] (**reaction 18**) (Kitchens et al. 1976). It is expectable that these reactions contribute to decrease of ammonia concentrations on bio-filter. In

what concerns to the toxicity of the products formed towards aquatic organisms, the very few data available do not reveal significant toxic effects (Sigma-Aldrich 2015).

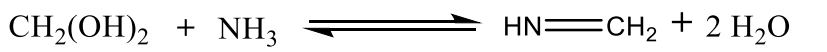

Reaction 17

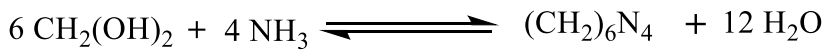

Reaction 18

- Secondly, the nitrifying bacteria involved on nitrification processes (conversion of ammonia into nitrates) are aerobic (Branson 1993; Fredricks 2015) and, as stated above, the presence of formalin promotes the depression of oxygen concentrations. This may have direct consequences on oxidation of ammonia to nitrites and of nitrites to nitrates, since these two reactions are oxygen-dependent. Some authors proposed that low dissolved oxygen concentrations strongly inhibited the oxidation of nitrite, but also reported that the dissolved oxygen concentrations (≥ 1mg/L) do not affect the ammonia oxidation (Hanaki et al. 1990; Eiroa et al. 2004).

- Finally, hydrated formaldehyde acts as bactericide and its regular use, namely under high concentration and prolonged exposure may affect the microbial community (composition) and microbial activity in the bio-filters (Keck and Blanc 2002; Pedersen et al. 2007; Pedersen et al. 2010).

Keck & Blanc (2002) suggested an inhibition of nitrite-oxidizing bacteria in the presence of formalin (dosages above 100 mg/L). These authors studied the effects of formalin bath treatments on nitrification in a semi-closed pilot scale saltwater recirculating turbot culture system. They evaluated two different situations: (first situation) 1h treatments in tank, every week, with concentrations ranging between 20 and 90 mg/L of formaldehyde and then released in the recirculating system; (second situation) the entire system was exposed to long term dynamic treatments (2, 4 and 6 hours) with a formaldehyde concentration of 60 mg/L, without stopping the recirculation of water. Their results showed that the bath treatments with formalin do not have any effect on ammonia oxidation but the efficacy of nitrite removal is much lower in treated systems than in control (untreated) ($p < 0.001$). They observed that nitrite concentrations increased after 1 hour with formaldehyde concentration equal or higher than 40 mg/L (Keck and Blanc 2002).

Eiroa et al. (2004) also reported the inhibition of the nitrification process in the presence of hydrated formaldehyde. The authors observed that nitrification was

completely inhibited at initial concentrations of formaldehyde higher than 1500 mg/L. This inhibition causes an accumulation of ammonia in the system, which is very toxic to fish. The authors also observed that, in the presence of 12.5 % of methanol (used as stabilizer in formalin solution), nitrification started to decrease at formaldehyde concentrations above 175 mg/L and the complete inhibition occurred at formaldehyde concentrations above 500 mg/L (lower concentrations than in the absence of methanol) (Eiroa et al. 2004). The limitations of this last study are the high concentrations used in the experiments that do not correspond to the concentrations used in formalin bath treatment in aquaculture systems.

Pedersen et al. (2010) used formalin (equivalent to a nominal formaldehyde concentration of 10 and 20 mg/L) to treat six pilot-scale recirculation aquaculture systems holding rainbow trout (*Oncorhynchus mykiss*) on daily or weekly basis. The authors evaluated the microbial composition of bio-filter samples and observed that the relative abundances of ammonia-oxidizing bacteria and nitrite-oxidizing bacteria were generally higher in the untreated system than in systems exposed to formalin.

The residence time of formalin in recirculating aquaculture systems and the possible disturbs resulting of its presence may vary depending on the management and design of system (Keck and Blanc 2002). The extension of effects seems to be strongly dependent on formaldehyde concentration in aqueous solution and its residence time. So, formalin degradation in bio-filters is strongly affected by the available bio-filter surface area, the microbial community abundance and by the temperature of the system (Pedersen et al. 2007).

b. Formalin and ozonation

Ozonation is also a process that contributes to water disinfection (eliminating most target pathogens) and improves the water quality by reduction of biochemical oxygen demand, ammonia and nitrite (Goncalves and Gagnon 2011). It promotes the oxidation and degradation of organic compounds by formation of reactive oxygen species which may react with the organic molecules, as is the case of formaldehyde.

Considering the reactivity of ozone and its capability to act as oxidizing agent (more powerful than oxygen present in atmosphere), it is reasonable propose that the ozonation should be turned off during the bath treatment with formalin, if the water flow is not stopped. Similarity to what happens in the presence of oxygen (**reactions 15** and **16**), the ozone molecules can oxidize formaldehyde/formalin affording carbon dioxide

and water. Thus, this reaction should be considered from two points of view: on one hand, as already referred, the ozonation process should be turned off during the bath treatment with formalin if the water flow is not stopped. In this situation, if the ozonation remains turned on, the formalin oxidation will be faster than if the ozonation was turned off. Consequently, the formalin concentration necessary for treatment will be reduced drastically before of the end of treatment time recommended. On the other hand, after the bath treatment with formalin and the restoring of water flow, the ozonation process should be activated (turned on) to eliminate faster formalin/formaldehyde from aquaculture system, minimizing the excessive exposure of the remainder system and aquatic species included in it.

Effects on aqueous effluents and environment

Formalin can reach the environment through effluent discharge after bath treatments in aquaculture systems. The effluent containing formalin may be released into natural environment with or without a specific treatment.

When the aqueous effluent containing formalin is not subject to any specific treatment before its release into environment, the reduction of formalin concentration is often achieved by dilution (WHO 1989; Masters 2004). The recommendation is that the formaldehyde concentrations released into environment do not exceed 1 mg/L (FDA 1995). Other specific limit values for formaldehyde discharge are reported in Masters (2004) and cover almost all range between 0.74 mg/L and 2.4 mg/L.

When water is discharged into a settlement tank outside and remain there for some period of time, the concentrations of formalin that are then released into the natural environment (effluent) would be smaller. In this situation, the decrease of formalin concentration occurs not only by the dilution of water containing formalin. As result of exposure to the environmental conditions in the settlement tank, natural degradation of formalin also happens, in addition to oxidation-reduction reactions described above. The degradation of formalin (hydrate of formaldehyde) by direct photolysis is not expected under normal environmental conditions because it is not a chromophore and, as such, it is not able to absorb natural light (Masters 2004). However, indirect photo-degradation may occur through reactions with reactive oxygen species formed during irradiation.

The biological degradation (biodegradation) of formalin can also occur in the aquatic environment (WHO 1989). Despite of bactericidal effect of formaldehyde, some bacteria such as *Pseudomonas (Ps.) fluorescens*, *Ps. desmolytica* and *Ps. ovalis* are able to

assimilate organic compounds with one carbon atom, like formaldehyde and formic acid, as their sole carbon source. These types of bacteria are denominated methylotrophic bacteria and are microorganisms capable to assimilate formaldehyde into bacterial cellular material according to two main pathways – through ribulose monophosphate cycle and serine pathway (Kitchens et al., 1976 and authors cited therein). A very interesting study performed by Kamata (1966) demonstrates the biodegradation of hydrated formaldehyde under natural environmental conditions. The author added in laboratory known formaldehyde concentrations (50 µg/L) to the samples of lake water (Lake Kezaki, in Japan) and observed that formaldehyde was completely decomposed in 30 hours at 20 ºC under aerobic conditions. Under anaerobic conditions at 8 ºC, its concentration "invariably remains for 3 days, and then is gradually decomposed and so completely lost over the next 3 days" (Kamata 1966). Also under anaerobic conditions, the author observed that the half-life time of formaldehyde, at 20 ºC, is twice that under aerobic conditions. To prove that the results were a consequence of biological degradation (microbiological processes), the author also performed studies in sterilized lake water and the decomposition of formaldehyde was not observed over an 8-day period.

When specific treatments to reduce or eliminate formalin from water were not applied, its half-life time in natural environmental conditions is estimated to be 36 hours (FDA 1995; Masters 2004), but there are some controversial data related to this point. The variations in the rates of formalin degradation are frequently justified by differences in chemistry and organic content of natural water and are depending on natural factors such as temperature, presence of degrading microbes and oxygen levels.

Mopper and Stahovec (1986) (cited in FDA, 1995) reported that in a nutrient-enriched seawater, the measurable loss of formaldehyde occurred after 40 hours (approximately). Additionally, other authors made experiments with initial concentration of formaldehyde of 75.6 mg/L, over a period of 20 hours, and observed no decrease in formalin concentration in distilled water (Wienbeck and Koops 1990).

Based on Henry's constant of formaldehyde (k_H = 0.02 Pa.m^3/mol) (WHO 1989), it is not expectable the volatilization of formaldehyde, under normal environmental conditions, from an aquatic environment. The adsorption on suspended solids and partition in sediments is not also expected to occur due to the low n-octanol/water partition coefficient (log K_{OW} = - 1) and high water solubility (400 mg/L) of formaldehyde (WHO 1989).

2.4.5 Formalin removal treatments

Ideally, an efficient and low-cost method to formalin treatment, without negative impacts for aquaculture system and environment should be applied. The dilution process requires large amounts of water for appropriate dilution and demonstrates not be completely efficient as treatment method (Masters 2004). In addition, three main specific treatments to reduce or eliminate formalin from aquaculture's water have been referred in the literature: aeration, biodegradation and bio-filtration.

Aeration is a physical process that may contribute to the decrease of formalin concentrations, by providing the oxygen levels necessary to promote its oxidation to carbon dioxide and water. Some authors observed that the average half-lives of formaldehyde at 25, 50, 100 and 200 mg/L of formalin were 3.4 ± 0.3 days and 2.3 ± 0.5 days in non-aerated seawater and in aerated seawater, respectively (Jung et al. 2001). This indicates that this process is not completely efficient on formaldehyde removal from water.

Biodegradation may occur naturally in aquatic environment, as referred above, or may be promoted and applied to formalin removal from water. For instance, Eiroa et al. (2004) investigated the biodegradation of formaldehyde (30 – 3890 mg/L) in batch assays, in the presence and in the absence of methanol as co-substrate. They observed higher formaldehyde biodegradation rates in the presence of methanol as co-substrate (12.5 %) than in the absence of it (the first order rate constants were 0.51 h^{-1} and 0.31 h^{-1} in the presence and in the absence of methanol, respectively).

Lastly, bio-filtration was proposed by Pedersen et al. (2010) as a possible treatment strategy for formaldehyde removal in an aquaculture system. The authors observed that regular dosages of formalin at low concentrations increased the formaldehyde removal rate up to tenfold. Considering these data, a higher frequency of the treatment with lower concentration of formalin may be preferable to a lower frequency of the treatment with higher concentration of formalin, probably due to the adaptation of bacterial community on bio-filter. The authors suggested that the microbial acclimatization may occur due to increasing specific microbial activities and/or by the number of microorganisms that use formaldehyde (Pedersen et al. 2010), since after adaptation formaldehyde can be a good substrate for microbial growth at low concentrations (Chongcharoen et al. 2005).

In addition to these processes, other methods for the detoxification and neutralization of formalin have been proposed (Masters 2004; Gearheart et al. 2006).

Masters (2004) suggests the neutralization (chemical degradation) of formalin in water, using commercial products. They are easy to administrate and neutralize formaldehyde in water for acceptable disposal. However, these products are moderately expensive and some of them require pH adjustments following treatment (Masters 2004), whereby they do not also represent an "ideal" alternative.

Gearheart et al. (2006) evaluated the potential of sodium sulphite, *Neutralex*, hydrogen peroxide without and with a ferric iron catalyst to reduce the concentration of formalin in effluents from aquaculture facilities and obtained different results for each case. On one hand, the reactions with the hydrogen peroxide without or with a ferric iron catalyst did not cause substantial reductions in formalin concentrations. One the other hand, the maximum reduction of 75 % of the initial formalin concentration was achieved using sodium sulphite – Na_2SO_3 (**reaction 19**), while the commercial product *Neutralex* completely eliminated formalin in the test solutions (Gearheart et al. 2006).

Neutralex is indicated to reduce formaldehyde concentrations to less than 10 mg/L within 24 hours in 10 % neutral buffered formalin wastes (Masters 2004; Gearheart et al. 2006). The sodium meta-bisulphite ($Na_2S_2O_5$) is the main ingredient of *Neutralex* and when it is dissolved in water originates sodium bisulphite – $NaHSO_3$ (**reaction 20**) (Irwin 2011). In turn, sodium bisulphite can react with formalin in a similar mode to sodium sulphite, originating the same type of adduct described in **reaction 19**. In addition to the necessary pH adjustments following the treatment, the products resulting of these reactions affected the survival and reproduction of an indicator organism, the water flea (*Ceriodaphnia dubia*), in chronic toxicity tests (Gearheart et al. 2006)

$$CH_2(OH)_2 + Na_2SO_3 \rightleftharpoons HOCH_2NaSO_3 + NaOH$$ **Reaction 19**

$$Na_2S_2O_5 + H_2O \rightleftharpoons 2\ NaHSO_3$$ **Reaction 20**

Apart from all these processes mentioned above and focused on formalin removal from aquaculture's water, there are others that have gained prominence in the last years by their efficient removal of formaldehyde from other contaminated aqueous systems. Those processes are recognized as advanced oxidation processes (AOPs) (e.g.: UV/H_2O_2, Photo-Fenton) and may be an alternative to apply in aquaculture systems before the aqueous effluent containing formaldehyde be released into environment. The AOPs are

particularly applied to remove higher formaldehyde concentrations (100 to 10000 mg/L) (Gonzalez-Gil et al. 1999; Guimaraes et al. 2012). These concentration levels are much higher than those found in aquaculture effluents, whereby these advanced treatments may present higher removal rates of formaldehyde from water containing lower concentrations of formaldehyde.

2.5 References

A.F.S.F.C.S. (2011). "Guide to Using Drugs, Biologics, and Other Chemicals in Aquaculture." American Fisheries Society Fish Culture Section Retrieved 20 Junho, 2014, from http://www.fws.gov/fisheries/aadap/AFS-FCS%20documents/GUIDE_FEB_2011.pdf.

Ahumada-Rudolph, R., V. Novoa, K. Saez, M. Martinez, A. Rudolph, C. Torres-Diaz and J. Becerra (2016). Marine fungi isolated from Chilean fjord sediments can degrade oxytetracycline. *Environmental Monitoring and Assessment* **188**(8).

AliAbadi, F. S. and J. D. MacNeil. (2002). "FAO FNP 41/14 Oxytetracycline." Retrieved June 03, 2016, from www.fao.org/fileadmin/user_upload/.../41-14-oxytetracycline.pdf.

Arias, M., M. S. Garcia-Falcon, L. Garcia-Rio, J. C. Mejuto, R. Rial-Otero and J. Simal-Gandara (2007). Binding constants of oxytetracycline to animal feed divalent cations. *Journal of Food Engineering* **78**(1): 69-73.

Barnabé, G. (1994). Ongrowing fish in intensive systems. *Aquaculture: biology and ecology of cultured species*. G. Barnabé, Ellis Horwood Limited**:** 349-370.

Bills, T. D., L. L. Marking and G. E. Howe (1993). Sensitivity of Juvenile Striped Bass to Chemicals Used in Aquaculture. Technical Report Series. Washington D.C., U.S. Fish and Wildlife Service**:** 17.

Bills, T. D., L. L. Marking and J. H. C. Jr. (1977). Formalin: its toxicity to nontarget aquatic organisms, persistence, and counteraction. Investigations in Fish Control 73**:** 7.

Bishop, Y., Ed. (2005). The Veterinaty Formulary. London, Pharmaceutical Press.

Blanco, S. L., A. Martinez, C. Porro and J. M. Vieites (2011). Dietary uptake of polybrominated diphenyl ethers (PBDEs), occurrence and profiles, in aquacultured turbots (Psetta maxima) from Galicia, Spain. *Chemosphere* **85**(3): 441-447.

Bly, J. E., S. M. A. Quiniou and L. W. Clem (1997). Environmental effects on fish immune mechanisms. *Fish Vaccinology*. R. Gudding, A. Lillehaug, P. Midtlyng and F. Brown. Basel, Karger. **90:** 33-43.

Boreen, A. L., W. A. Arnold and K. McNeill (2004). Photochemical fate of sulfa drugs in the aquatic environment: Sulfa drugs containing five-membered heterocyclic groups. *Environmental Science & Technology* **38**(14): 3933-3940.

Borghi, A. A. and M. A. Palma (2014). Tetracycline: production, waste treatment and environmental impact assessment. *Brazilian Journal of Pharmaceutical Sciences* **50**(1): 25-40.

Bowker, J. D., J. T. Trushenski, M. P. Gaikowski and D. L. Straus. (2014). "Guide to Using Drugs, Biologists, and other Chemicals in Aquaculture." American Fisheries Society Fish Culture Section. Retrieved January 06, 2016, from http://www.fws.gov/fisheries/aadap/PDF/GUIDE_June_2014b.pdf.

Boyd, C. and A. McNevin (2014). *Aquaculture, Resource Use, and the Environment*, John Wiley & Sons

Boyd, C. E. and L. Massaut (1999). Risks associated with the use of chemicals in pond aquaculture. *Aquacultural Engineering* **20**: 113–132.

Branson, E. (1993). Environmental Aspects of Aquaculture. *Aquaculture for veterinarians: fish husbandry and medicine*. L. Brown, Pergamon Press**:** 447.

Buchmann, K., J. Bresciani and C. Jappe (2004). Effects of formalin treatment on epithelial structure and mucous cell densities in rainbow trout, Oncorhynchus mykiss (Walbaum), skin. *Journal of Fish Diseases* **27**(2): 99-104.

Burridge, L., J. S. Weis, F. Cabello, J. Pizarro and K. Bostick (2010). Chemical use in salmon aquaculture: A review of current practices and possible environmental effects. *Aquaculture* **306**(1-4): 7-23.

Campos, J. L., J. M. Garrido, R. Mendez and J. M. Lema (2001). Effect of two broad-spectrum antibiotics on activity and stability of continuous nitrifying system. *Applied Biochemistry and Biotechnology* **95**(1): 1-10.

Cao, L., W. Wang, Y. Yang, C. Yang, Z. Yuan, S. Xiong and J. Diana (2007). Environmental impact of aquaculture and countermeasures to aquaculture pollution in China. *Environmental Science and Pollution Research* **14**(7): 452-462.

Carey, F. A. (2000). *Organic Chemistry*, McGraw-Hill Higher Education

Carlotti, B., A. Cesaretti and F. Elisei (2012). Complexes of tetracyclines with divalent metal cations investigated by stationary and femtosecond-pulsed techniques. *Physical Chemistry Chemical Physics* **14**(2): 823-834.

Carlucci, A. F. and D. Pramer (1960). An Evaluation of Factors Affecting the Survival of Escherichia coli in Sea Water. III. Antibiotics. *Applied Microbiology* **8**(4): 251-254.

Cenavisa. (2016). "Aquacen Oxitetraciclina Hidrocloruro 1000 mg/g." Retrieved February, 2016, from http://www.cenavisa.es/products/view/81/aquacen_oxitetraciclina_hidrocloruro_1000_mgg

ChemicalBook. (2016). "Oxytetracycline hydrochloride." Chemical Book Data Base, from http://www.chemicalbook.com/ChemicalProductProperty_EN_CB9311671.htm.

Chen, Y., H. Li, Z. P. Wang, T. Tao and C. Hu (2011). Photoproducts of tetracycline and oxytetracycline involving self-sensitized oxidation in aqueous solutions: Effects of Ca^{2+} and Mg^{2+}. *Journal of Environmental Sciences-China* **23**(10): 1634-1639.

Chinabut, S., C. Limsuwan, K. Tonguthai and T. Pungkachonboon (1988). Toxic and Sublethal effect of formalin on freshwater fishes, FAO**:** 15.

Chongcharoen, R., T. J. Smith, K. P. Flint and H. Dalton (2005). Adaptation and acclimatization to formaldehyde in methylotrophs capable of high-concentration formaldehyde detoxification. *Microbiology-Sgm* **151**: 2615-2622.

Clive, D. L. J. (1968). Chemistry of Tetracyclines. *Quarterly Reviews* **22**(4): 435-456.

Colt, J. and E. Cryer (2000). Ozone. Encyclopedia of Aquaculture. R. R. Stickney. New York, John Wiley & Sons, Inc.**:** 622-627.

Costello, M. J., A. Grant, I. M. Davies, S. Cecchini, S. Papoutsoglou, D. Quigley and M. Saroglia (2001). The control of chemicals used in aquaculture in Europe. *Journal of Applied Ichthyology* **17**: 173-180.

Daghrir, R. and P. Drogui (2013). Tetracycline antibiotics in the environment: a review. *Environmental Chemistry Letters* **11**(3): 209-227.

Dalmazio, I., M. O. Almeida, R. Augusti and T. M. A. Alves (2007). Monitoring the degradation of tetracycline by ozone in aqueous medium via atmospheric pressure ionization mass spectrometry. *Journal of the American Society for Mass Spectrometry* **18**(4): 679-687.

DGAV. (2015). "Medicamentos Veterinários autorizados." Retrieved May, 2016, from http://www.dgv.min-agricultura.pt/portal/page/portal/DGV/genericos?generico=17171&cboui=17171.

Dietze, J. E., E. A. Scribner, M. T. Meyer and D. W. Kolpin (2005). Occurrence of antibiotics in water from 13 fish hatcheries, 2001-2003. *International Journal of Environmental Analytical Chemistry* **85**(15): 1141-1152.

Dixon, B. A. (2000). Antibiotics. Encyclopedia of Aquaculture. R. R. Stickney. New York, John Wiley & Sons, Inc.: 38-44.

Dodder, N. G., B. Strandberg and R. A. Hites (2002). Concentrations and spatial variations of polybrominated diphenyl ethers and several organochlorine compounds in fishes from the northeastern United States. *Environmental Science & Technology* **36**(2): 146-151.

Doi, A. M. and M. K. Stoskopf (2000). The kinetics of oxytetracycline degradation in deionized water under varying temperature, pH, light, substrate, and organic matter. *Journal of Aquatic Animal Health* **12**(3): 246-253.

Drugs.com. (2016, April, 2016). "Terramycin 200 for Fish." Retrieved June, 2016, from https://www.drugs.com/vet/terramycin-200-for-fish.html.

Dzomba, P., J. Kugara and M. F. Zaranyika (2015). Characterization of microbial degradation of oxytetracycline in river water and sediment using reversed phase high performance liquid chromatography. *African Journal of Biotechnology* **14**(1): 1-9.

EHC162 (1994). *Brominated Diphenyl Ethers*. Geneva, WHO Library Cataloguing

EHC192 (1997). *Flame Retardants: A General Introduction*. Geneva, WHO Library Cataloguing

Eiroa, M., C. Kennes and M. C. Veiga (2004). Formaldehyde biodegradation and its inhibitory effect on nitrification. *Journal of Chemical Technology and Biotechnology* **79**(5): 499-504.

EMA. (1995). "Oxytetracycline, tetracycline, chlortetracycline: Summary report (3) - Committee for Veterinary Medicinal Products." Veterinary Medicines Retrieved June, 2016, from http://www.ema.europa.eu/ema/index.jsp?curl=pages/includes/document/document_detail.jsp?webContentId=WC500015378&mid=WC0b01ac058008d7ad.

EMA (1999). Antibiotic Resistance in the European Union Associated with Therapeutic Use of Veterinary Medicines. Report and Qualitative Risk Assessment by the Committee for Veterinary Medicinal Products. London, European Medicines Agency: 84.

EPA. (2006). "Polybrominated Diphenyl Ethers Project Plan." Retrieved 10 August, 2011, from http://www.epa.gov/oppt/pbde/pubs/proj-plan32906a.pdf.

FAO (2008). *Glossary of Aquaculture*. Rome, FAO Fisheries and Aquaculture

FAO. (n.d.). "Oxytetracycline." Retrieved June, 2016, from www.fao.org/fileadmin/user_upload/.../41-3-oxytetracycline.pdf.

FDA (1995). Environmental Impact Assessment for the Use of Formalin in the control of external parasites on fish. Environmental Assessments, Food and Drug Administration

FDA (2002). Formalin-F™. Freedom of information summary, Natchez Animal Supply Company**:** 18.

Fish, T. a. P. (2012). "Fish-Keeping and Oxygen." Retrieved January 07, 2016, from http://www.fishtanksandponds.co.uk/aquarium-science/oxygen.html.

Fox, C. H., F. B. Johnson, J. Whiting and P. P. Roller (1985). Formaldehyde fixation *Journal of Histochemistry & Cytochemistry* **33**(8): 845-853.

Francis-Floyd, R. (1996). "Use of formalin to control fish parasites " College of Veterinary Medicine Retrieved October, 24, 2014, from http://fisheries.tamu.edu/files/2013/09/Use-of-Formalin-to-Control-Fish-Parasites.pdf.

Fredricks, K. T. (2015). Literature Review of the Potential Effects of Formalin on Nitrogen Oxidation Efficiency of the Biofilters of Recirculating Aquaculture Systems (RAS) for Freshwater Finfish. Virginia, U.S. Geological Survey Open-File Report 2015-1097**:** 17.

Gearheart, J. M., A. L. Masters and J. Bebak-Williams (2006). Application of methods for the detoxification and neutralization of formalin in fish hatchery effluents. *North American Journal of Aquaculture* **68**(3): 256-263.

GESAMP (1997). Towards Safe and Effective Use of Chemicals in Coastal Aquaculture. *Reports and Studies No. 65*: 52.

Glaze, W. H. (1987). Drinking-water treatment with ozone. *Environmental Science & Technology* **21**(3): 224-230.

Goncalves, A. A. and G. A. Gagnon (2011). Ozone Application in Recirculating Aquaculture System: An Overview. *Ozone-Science & Engineering* **33**(5): 345-367.

Gonzalez-Gil, G., R. Kleerebezem, A. van Aelst, G. R. Zoutberg, A. I. Versprille and G. Lettinga (1999). Toxicity effects of formaldehyde on methanol degrading sludge and its anaerobic conversion in Biobed((R)) expanded granular sludge bed (EGSB) reactors. *Water Science and Technology* **40**(8): 195-202.

Guerra, W., P. P. Silva-Caldeira, H. Terenzi and E. C. Pereira-Maia (2016). Impact of metal coordination on the antibiotic and non-antibiotic activities of tetracycline-based drugs. *Coordination Chemistry Reviews* **327–328**: 188-199.

Guimaraes, J. R., C. R. T. Farah, M. G. Maniero and P. S. Fadini (2012). Degradation of formaldehyde by advanced oxidation processes. *Journal of Environmental Management* **107**: 96-101.

Halling-Sorensen, B. (2001). Inhibition of aerobic growth and nitrification of bacteria in sewage sludge by antibacterial agents. *Archives of Environmental Contamination and Toxicology* **40**(4): 451-460.

Halling-Sorensen, B., G. Sengelov and J. Tjornelund (2002). Toxicity of tetracyclines and tetracycline degradation products to environmentally relevant bacteria, including selected tetracycline-resistant bacteria. *Archives of Environmental Contamination and Toxicology* **42**(3): 263-271.

Hanaki, K., C. Wantawin and S. Ohgaki (1990). Nitrification at low levels of dissolved oxygen with and without organic loading in a suspended-growth reactor. *Water Research* **24**(3): 297-302.

Haya, K., L. E. Burridge and B. D. Chang (2001). Environmental impact of chemical wastes produced by the salmon aquaculture industry. *Ices Journal of Marine Science* **58**(2): 492-496.

He, J., D. Yang, C. Wang, W. Liu, J. Liao, T. Xu, C. Bai, J. Chen, K. Lin, C. Huang and Q. Dong (2011). Chronic zebrafish low dose decabrominated diphenyl ether (BDE-209) exposure affected parental gonad development and locomotion in F1 offspring. *Ecotoxicology* **20**: 1813-1822.

Homem, V. and L. Santos (2011). Degradation and removal methods of antibiotics from aqueous matrices - A review. *Journal of Environmental Management* **92**(10): 2304-2347.

Hu, Z., J. W. Lee, K. Chandran, S. Kim and S. K. Khanal (2012). Nitrous Oxide (N_2O) Emission from Aquaculture: A Review. *Environmental Science & Technology* **46**(12): 6470-6480.

Ingerslev, F., L. Toräng, M.-L. Loke, B. Halling-Sørensen and N. Nyholm (2001). Primary biodegradation of veterinary antibiotics in aerobic and anaerobic surface water simulation systems. *Chemosphere* **44**(4): 865-872.

Irwin, S. (2011) Comparison of the Use of Sodium Metabisulfite and Sodium Dithionite for Removing Rust Stains from Paper. *The Book and Paper Group Annual* **30**, 37-46.

IUPAC (2011). Compendium of Chemical Terminology Gold Book.

Jacobs, M. N., A. Covaci and P. Schepens (2002). Investigation of selected persistent organic pollutants in farmed Atlantic salmon (Salmo salar), salmon aquaculture feed, and fish oil components of the feed. *Environmental Science & Technology* **36**(13): 2797-2805.

Jiao, S. J., S. R. Meng, D. Q. Yin, L. H. Wang and L. Y. Chen (2008). Aqueous oxytetracycline degradation and the toxicity change of degradation compounds in photoirradiation process. *Journal of Environmental Sciences-China* **20**(7): 806-813.

Johnston, P. and D. Santillo. (2002). "Chemical Usage in Aquaculture: Implications for Residues in Market Products." Retrieved 22 Junho, 2014, from http://www.greenpeace.to/publications/technical_Note_06_02.pdf.

Jung, S. H., J. W. Kim, I. G. Jeon and Y. H. Lee (2001). Formaldehyde residues in formalin-treated olive flounder (Paralichthys olivaceus), black rockfish (Sebastes schlegeli), and seawater. *Aquaculture* **194**(3-4): 253-262.

Jung, S. H., D. S. Sim, M. S. Park, Q. T. Jo and Y. Kim (2003). Effects of formalin on haematological and blood chemistry in olive flounder, Paralichthys olivaceus (Temminck et Schlegel). *Aquaculture Research* **34**(14): 1269-1275.

Kamata, E. (1966). Aldehydes in lake and sea waters. *Bulletin of the Chemical Society of Japan* **39**(6): 1227-+.

Kaviraj, A., F. Bhunia and N. C. Saha (2004). Toxicity of methanol to fish, crustacean, oligochaete worm, and aquatic ecosystem. *International Journal of Toxicology* **23**(1): 55-63.

Keck, N. and G. Blanc (2002). Effects of formalin, chemotherapeutic treatments on biofilter efficiency in a marine recirculating fish farming system. *Aquatic Living Resources* **15**(6): 361-370.

Kitchens, J. F., R. E. Casner, G. S. Edwards, I. William E. Harvard and B. J. Macri (1976). Investigation of selected potential environmental contaminants: formaldehyde, U.S Environmental Protection Agency**:** 217.

Klaver, A. L. and R. A. Matthews (1994). Effects of oxytetracycline on nitrification in a modelm aquatic system. *Aquaculture* **123**(3-4): 237-247.

Kolodziejska, M., J. Maszkowska, A. Bialk-Bielinska, S. Steudte, J. Kumirska, P. Stepnowski and S. Stolte (2013). Aquatic toxicity of four veterinary drugs commonly applied in fish farming and animal husbandry. *Chemosphere* **92**(9): 1253-1259.

Kulshrestha, P., R. F. Giese and D. S. Aga (2004). Investigating the Molecular Interactions of Oxytetracycline in Clay and Organic Matter: Insights on Factors Affecting Its Mobility in Soil. *Environmental Science & Technology* **38**(15): 4097-4105.

Kummerer, K. (2009). Antibiotics in the aquatic environment - A review - Part I. *Chemosphere* **75**(4): 417-434.

Lalonde, B. A., W. Ernst and C. Garron (2015). Formaldehyde Concentration in Discharge from Land Based Aquaculture Facilities in Atlantic Canada. *Bulletin of Environmental Contamination and Toxicology* **94**(4): 444-447.

Lekang, O.-I. (2007). *Aquaculture Engineering*, Blackwell Publishing

Li, K. X., A. Yediler, M. Yang, S. Schulte-Hostede and M. H. Wong (2008). Ozonation of oxytetracycline and toxicological assessment of its oxidation by-products. *Chemosphere* **72**(3): 473-478.

Liteplo, R. G., R. Beauchamp, M. E. Meek and R. Chénier (2002). Formaldehyde. Concise International Chemical Assessment Document 40. Geneva, World Health Organization**:** 81.

Liu, J. G., Q. Y. Sun, C. Y. Zhang, H. Li, W. C. Song, N. Zhang and X. F. Jia (2016). Removal of typical antibiotics in the advanced treatment process of productive drinking water. *Desalination and Water Treatment* **57**(24): 11386-11391.

Loftin, K. A., C. D. Adams, M. T. Meyer and R. Surampalli (2008). Effects of ionic strength, temperature, and pH on degradation of selected antibiotics. *Journal of Environmental Quality* **37**(2): 378-386.

Lunestad, B. T. and J. Goksoyr (1990). Reduction in the bacterial effect of oxytetracycline in seawater by complex formation with magnesium and calcium. *Diseases of aquatic organisms* **9**: 67-72.

Lunestad, B. T., O. B. Samuelsen, S. Fjelde and A. Ervik (1995). Photostability of 8 antibacterial agents in seawater. *Aquaculture* **134**(3-4): 217-225.

Malvisi, J., G. dellaRocca, P. Anfossi and G. Giorgetti (1996). Tissue distribution and residue depletion of oxytetracycline in sea bream (Sparus aurata) and sea bass (Dicentrarchus labrax) after oral administration. *Aquaculture* **147**(3-4): 159-168.

Manahan, S. E. (2000). *Environmental Chemistry*, CRC Press LLC

Masters, A. L. (2004). A review of methods for detoxification and neutralization of formalin in water. *North American Journal of Aquaculture* **66**(4): 325-333.

Mayes, M. A. and M. G. Barron (1991). *Aquatic Toxicology and Risk Assessment: Fourteenth Volume*, ASTM International

Meinelt, T., M. Pietrock, K. Burnison and C. Steinberg (2005). Formaldehyde toxicity is altered by calcium and organic matter. *Journal of Applied Ichthyology* **21**(2): 121-124.

Migliore, L., M. Fiori, A. Spadoni and E. Galli (2012). Biodegradation of oxytetracycline by Pleurotus ostreatus mycelium: a mycoremediation technique. *Journal of Hazardous Materials* **215–216**: 227-232.

Muir, J. F. and R. J. Roberts (2012). *Recent Advances in Aquaculture*, Springer US

Namdari, R., S. Abedini and F. C. P. Law (1996). Tissue distribution and elimination of oxytetracycline in seawater chinook and coho salmon following medicated-feed treatment. *Aquaculture* **144**(1-3): 27-38.

NCBI. (2016). "Oxytetracycline hidrochloride." National Center for Biotecnology Information. PubChem Compound Database; CID=54680782, from https://pubchem.ncbi.nlm.nih.gov/compound/54680782.

Newman, E. C. and C. W. Frank (1976). Circular Dichroism Spectra of Tetracycline Complexes with Mg^{2+} and Ca^{2+}. *Journal of Pharmaceutical Sciences* **65**(12): 1728-1732.

Pedersen, L. F., P. B. Pedersen, J. L. Nielsen and P. H. Nielsen (2010). Long term/low dose formalin exposure to small-scale recirculation aquaculture systems. *Aquacultural Engineering* **42**(1): 1-7.

Pedersen, L. F., P. B. Pedersen and O. Sortkjaer (2007). Temperature-dependent and surface specific formaldehyde degradation in submerged biofilters. *Aquacultural Engineering* **36**(2): 127-136.

Pereira, A., L. J. G. Silva, L. M. Meisel and A. Pena (2015). Fluoroquinolones and Tetracycline Antibiotics in a Portuguese Aquaculture System and Aquatic Surroundings: Occurrence and Environmental Impact. *Journal of Toxicology and Environmental Health-Part a-Current Issues* **78**(15): 959-975.

Piedrahita, R. H. (2003). Reducing the potential environmental impact of tank aquaculture effluents through intensification and recirculation. *Aquaculture* **226**(1-4): 35-44.

Poirier, S. H., M. L. Knuth, C. D. Anderson-Buchou, L. T. Brooke, A. R. Lima and P. J. Shubat (1986). Comparative Toxicity of Methanol and N,N-Dimethylformamide to Freshwater Fish and Invertebrates. *Bulletin of Environmental Contamination and Toxicology* **37**: 615-621.

Rand, G. M. (1995). *Fundamentals Of Aquatic Toxicology: Effects, Environmental Fate And Risk Assessment*, CRC Press

Reimschuessel, R., L. Stewart, E. Squibb, K. Hirokawa, T. Brady, D. Brooks, B. Shaikh and C. Hodsdon (2005). Fish drug analysis—Phish-pharm: A searchable database of pharmacokinetics data in fish. *The AAPS Journal* **7**(2): E288-E327.

Reiser, S., S. Wuertz, J. P. Schroeder, W. Kloas and R. Hanel (2011). Risks of seawater ozonation in recirculation aquaculture - Effects of oxidative stress on animal welfare of juvenile turbot (Psetta maxima, L.). *Aquatic Toxicology* **105**(3-4): 508-517.

Rico, A., K. Satapornvanit, M. M. Haque, J. Min, P. T. Nguyen, T. C. Telfer and P. J. van den Brink (2012). Use of chemicals and biological products in Asian aquaculture and their potential environmental risks: a critical review. *Reviews in Aquaculture* **4**(2): 75-93.

Rigos, G., M. Alexis, A. Andriopoulou and I. Nengas (2002). Pharmacokinetics and tissue distribution of oxytetracycline in sea bass, Dicentrarchus labrax, at two water temperatures. *Aquaculture* **210**(1-4): 59-67.

Rigos, G., I. Nengas, M. Alexis and G. M. Troisi (2004). Potential drug (oxytetracycline and oxolinic acid) pollution from Mediterranean sparid fish farms. *Aquatic Toxicology* **69**: 281-288.

Rigos, G. and P. Smith (2015). A critical approach on pharmacokinetics, pharmacodynamics, dose optimisation and withdrawal times of oxytetracycline in aquaculture. *Reviews in Aquaculture* **7**(2): 77-106.

Rigos, G. and G. M. Troisi (2005). Antibacterial agents in mediterranean finfish farming: A synopsis of drug pharmacokinetics in important euryhaline fish species and possible environmental implications. *Reviews in Fish Biology and Fisheries* **15**(1-2): 53-73.

Rigos, G., Tyrpenou, I. Nengas, A. E. M. Alexis, F. Athanassopoulou and G. M. Troisi (2004). Poor bioavailability of oxytetracycline in sharpsnout sea bream Diplodus puntazzo. *Aquaculture* **235**(1-4): 489-497.

Rodgers, C. J. and M. D. Furones (2009). Antimicrobial agents in aquaculture: practice, needs and issues. The use of veterinary drugs and vaccines in Mediterranean aquaculture. C. Rogers and B. Basurco. Zaragoza, CIHEAM**:** 41 -59.

Romero, J., C. G. Feijoo and P. Navarrete (2012). Antibiotics in aquaculture - Use, abuse and alternatives. *Health and Environment in Aquaculture*. E. D. Carvalho, G. S. David and R. J. Silva.

Roose-Amsaleg, C. and A. M. Laverman (2016). Do antibiotics have environmental side-effects? Impact of synthetic antibiotics on biogeochemical processes. *Environmental Science and Pollution Research* **23**(5): 4000-4012.

Schmidt, L. J., M. P. Gaikowski, W. H. Gingerich, V. K. Dawson and T. M. Schreier (2007). An Environmental Assessment of the Proposed Use of Oxytetracycline-Medicated Feed in Freshwater Aquaculture. Wisconsin, U.S. Food and Drug Administration**:** 97.

Schmitt, M. O. and S. Schneider (2000). Spectroscopic investigation of complexation between various tetracyclines and Mg^{2+} or Ca^{2+}. *Physchemcomm* **3**(9): 42-55.

Scott, P. (1993). Therapy in Aquaculture. *Aquaculture for veterinarians: fish husbandry and medicine*. L. Brown, Pergamon Press**:** 447.

Sekkin, S. and C. Kum (2011). Antibacterial Drugs in Fish Farms: Application and Its Effects. *Recent Advances in Fish Farms*. F. Aral, InTech**:** 250.

Serrano, P. H. (2005). Responsible use of antibiotics in aquaculture. FAO Fisheries Technical Paper 469. Rome, FAO**:** 110.

Shao, Z. Z. J. (2001). Aquaculture pharmaceuticals and biologicals: current perspectives and future possibilities. *Advanced Drug Delivery Reviews* **50**(3): 229-243.

Shepherd, J. and N. Bromage (2001). *Intensive Fish Farming*. Oxford, Blackwell Science Ltd

Sigma-Aldrich. (2015). "Safety data sheet." Retrieved April, 10, 2016, from http://www.sigmaaldrich.com/catalog/product/sial/398160?lang=pt&region=PT.

Slana, M. and M. S. Dolenc (2013). Environmental Risk Assessment of antimicrobials applied in veterinary medicine-A field study and laboratory approach. *Environmental Toxicology and Pharmacology* **35**(1): 131-141.

Speare, D. J., G. Arsenault, N. MacNair and M. D. Powell (1997). Branchial lesions associated with intermittent formalin bath treatment of Atlantic salmon, Salmo salar L, and rainbow trout, Oncorhynchus mykiss (Walbaum). *Journal of Fish Diseases* **20**(1): 27-33.

Stapleton, H. M., M. Alaee, R. J. Letcher and J. E. Baker (2004). Debromination of the flame retardant decabromodiphenyl ether by juvenile carp (Cyprinus carpio) following dietary exposure. *Environmental Science & Technology* **38**(1): 112-119.

Stickney, R. R. and J. P. McVey (2002). *Responsible Marine Aquaculture*, CABI

Tongaree, S., D. R. Flanagan and R. I. Poust (1999). The interaction between oxytetracycline and divalent metal ions in aqueous and mixed solvent systems. *Pharmaceutical Development and Technology* **4**(4): 581-591.

Tucker, C. C. and E. H. Robinson (1990). *Channel Catfish Farming Handbook*, Springer

van Leeuwen, S. P. J., M. J. M. van Velzen, C. P. Swart, I. van der Veen, W. A. Traag and J. de Boer (2009). Halogenated Contaminants in Farmed Salmon, Trout, Tilapia, Pangasius, and Shrimp. *Environmental Science & Technology* **43**(11): 4009-4015.

Vonderheide, A. P. (2009). A review of the challenges in the chemical analysis of the polybrominated diphenyl ethers. *Microchemical Journal* **92**(1): 49-57.

Vonderheide, A. P., K. E. Mueller, J. Meija and G. Welsh (2008). Polybrominated diphenyl ethers: Causes for concern and knowledge gaps regarding environmental distribution, fate and toxicity. *Science of the Total Environment* **400**: 425-436.

WHO. (1989). "International Program on Chemical Safety, Environmental Health Criteria 89: Formaldehyde." Retrieved December 01, 2015, from http://www.inchem.org/documents/ehc/ehc/ehc89.htm.

Wienbeck, H. and H. Koops (1990). Decomposition of formaldehyde in recirculation fish-farmiong systems. *Archiv Fur Fischereiwissenschaft* **40**(1-2): 153-166.

Williams, H. A. and R. Wooten (1981). Some effects of the therapeutic levels of formalin and copper sulphate on blood parameters in rainbow trout. *Aquaculture* **24**: 341-353.

Xuan, R. C., L. Arisi, Q. Q. Wang, S. R. Yates and K. C. Biswas (2010). Hydrolysis and photolysis of oxytetracycline in aqueous solution. *Journal of Environmental Science and Health Part B-Pesticides Food Contaminants and Agricultural Wastes* **45**(1): 73-81.

Yalap, K. S. and I. A. Balcioglu (2009). Effects of Inorganic Anions and Humic Acid on the Photocatalytic and Ozone Oxidation of Oxytetracycline in Aqueous Solution. *Journal of Advanced Oxidation Technologies* **12**(1): 134-143.

Yildiz, H. Y. and M. B. Ergonul (2010). Is prophylactic formalin exposure a stress source for gilthead sea bream (Sparus aurata) and sea bass (Dicentrarchus labrax)? *Ankara Universitesi Veteriner Fakultesi Dergisi* **57**(2): 113-118.

Zhao, C., M. Pelaez, X. D. Duan, H. P. Deng, K. O'Shea, D. Fatta-Kassinos and D. D. Dionysiou (2013). Role of pH on photolytic and photocatalytic degradation of antibiotic

oxytetracycline in aqueous solution under visible/solar light: Kinetics and mechanism studies. *Applied Catalysis B-Environmental* **134**: 83-92.

Ziolkowska, A., M. Margas, H. Grajek, J. Wasilewski, B. Adomas, D. Michalczyk and A. I. Piotrowicz-Cieslak (2016). Comparison of UV-C irradiation, ozonation, and iron chelates treatments for degradation of tetracycline in water. *International Journal of Environmental Science and Technology* **13**(5): 1335-1346.

Zitko, V. (1999). Qualitative determination of 10,10 '-oxybisphenoxarsine and decabromodiphenyl ether in plastics. *Chemosphere* **38**(3): 629-632.

Chapter 3: Photo-degradation as a remediation process [2]

This chapter introduces the basic concepts of photo-degradation, referring the direct and the indirect photo-degradation. Within the scope of indirect photo-degradation, emphasis is given to natural components that can act as photosensitizers and also to synthetic TiO_2-based photo-catalysts.

Furthermore, this chapter compiles the state of art of the three contaminants (BDE-209, OTC and formalin) photo-degradation. With respect to OTC, the discussion is extended to the toxicity and biological activity of the by-products derived from its photo-degradation. In addition, a comparison between ozonation and photo-degradation processes is performed to understand the main advantages and limitations of each of them.

---

[2] The state of art relating to the OTC and formalin photo-degradation was also adapted from:

- **J.F. Leal**, E.B.H. Santos, V.I. Esteves. Oxytetracycline in intensive aquaculture: water quality during and after its administration, environmental fate, toxicity and bacterial resistance, *in preparation*.
- **J.F. Leal**, M.G.P.M.S. Neves, E.B.H. Santos, V.I. Esteves (2016). Use of formalin in intensive aquaculture: properties, application and effects on fish and water quality. *Reviews in aquaculture*, 0, 1-15.

3.1 Principles of photochemistry

In natural environments, namely in aquatic systems, the light from the sun reaches the surface water at various angles. One part of this sunlight is lost due to backscatter and reflection (about 10 %), and another part may be refracted at the air-water interface. Within the water column, the light is scattered and/or absorbed by suspended particles and absorbed by dissolved species such as natural organic matter (Schwarzenbach et al. 2003). Thus, only a portion of the sunlight that reaches surface water, whose wavelengths ranging from 290 to 800 nm (Challis et al. 2014), promotes several photochemical transformations, either by direct photolysis or photo-degradation, either by indirect photolysis (Vione et al. 2014). Sunlight provides enough energy to cause such transformations once its energy varies between 200 and 400 KJ/mol, which is the same order of magnitude of the covalent bonds energy of most organic compounds, namely C–C, C–H, C–O, C–Cl and C–Br (Christensen and Li 2014). However, it is important to note that intensity of solar radiation reaching Earth's surface is affected by several factors, such as season, location (latitude and altitude), time of day (incident angle of light), cloud coverage, temperature, among other (Kummerer 2009).

When a molecule (M) absorbs light ($h\upsilon$) from visible and ultraviolet region of the spectrum, it passes to an electronically excited state (**reaction 21**) (Pilling and Seakins 1995; Levine 2009).

$$M_0 + h\upsilon \rightarrow M^* \qquad \textbf{Reaction 21}$$

The excited state of a molecule is unstable and, therefore a molecule can lose its energy (previously absorbed) by different ways. As described by Jablonski diagram (**figure 7**), the excited molecule (M*) can transfer its extra vibrational energy to other molecules – vibrational relaxation (a) or may be deactivated to ground state (M_0) via fluorescence (b) or phosphorescence (c). Additionally, internal conversion (d) occurs when excited state transits between singlet states or triplet states, while intersystem crossing (e) happens when excited state transits between singlet and triplet states, or vice-versa (Pilling and Seakins 1995; Levine 2009; Christensen and Li 2014). To sum up, not all energy absorbed by molecule is used in chemical transformations. A measure of the photolysis efficiency is the determination of the reaction quantum yield. This is a parameter that will be discussed in *chapter 4*.

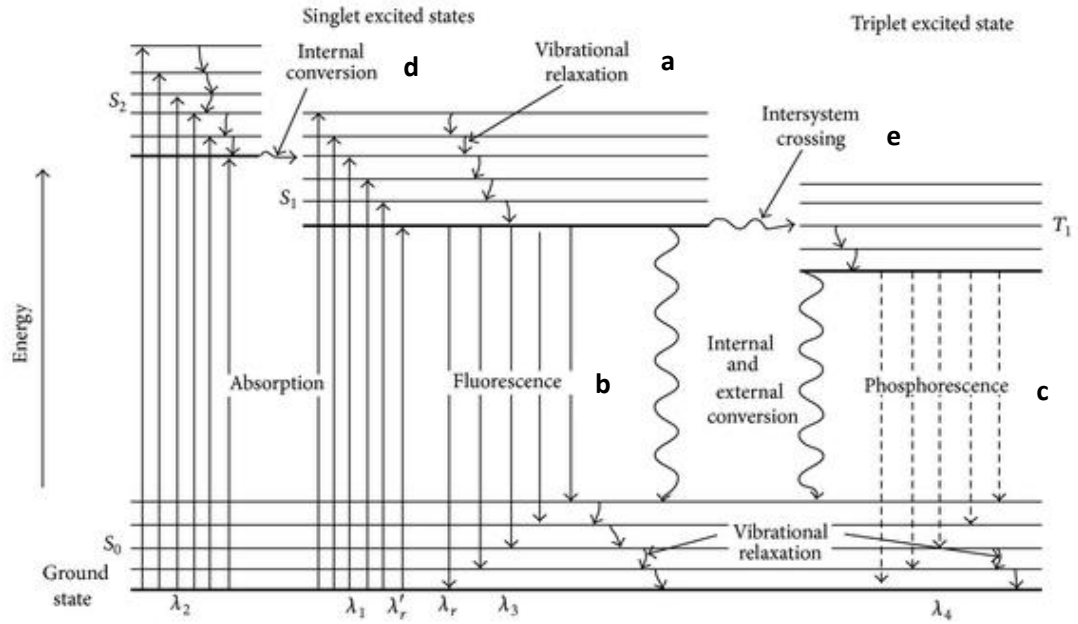

Figure 7 – Jablonski diagram: electronic levels of common organic molecules and possible transitions between different singlet and triplet states (Fereja et al. 2013)

3.1.1. Direct photo-degradation

Photolysis is the major process to remove several pharmaceuticals from aquatic environment (Challis et al. 2014). To occur direct photolysis or photo-degradation, molecules must be able to absorb the sunlight, absorbing directly photons (Cooper and Herr 1987).

The presence of certain groups or structures in molecules, such as aromatic rings and conjugated π systems, facilitates the direct absorption of solar radiation (Boreen et al. 2003). This is related to the reduced energy intervals between the ground (M_0) and the excited (M*) states. That difference is between the lowest unoccupied and the highest occupied molecular orbitals, commonly represented as $E_{LUMO} - E_{HOMO}$ (Christensen and Li 2014). One way to quantify the direct photolysis is determining experimentally the rate constant of the direct photolysis, under a given irradiation source (Challis et al. 2014). When only one compound exists in solution and suffers direct photolysis, its degradation by light commonly obeys a first-order reaction.

3.1.2 Indirect photo-degradation

Indirect or sensitized photolysis includes several types of reactions and starts with a non-target compound (Christensen and Li 2014). Those reactions may occur either with reactive molecules in ground or excited states, which are themselves products of primary photochemistry; or through photosensitized reactions in which the excited state species of some chromophores transfers its energy or an electron to compound (Cooper and Herr 1987). When other species or compounds are also involved in photo-degradation reaction, it may be appropriate to consider a second-order rate constant between compound and photosensitizer. Furthermore, when direct and indirect photolysis are involved, under same conditions, on a compound degradation, the kinetic rate constant experimentally determined (k_{total}) corresponds to the addition of the kinetic rate constants (**equation 1**) (Challis et al. 2014).

$$k_{total} = k_{direct} + k_{indirect} \qquad \textbf{(Eq.1)}$$

The likeness of indirect rate constant, which cannot be determined separately from other mechanisms, quantum yield is also difficult to determine in these conditions. There are ways to calculate the quantum yield of a photo-oxidant, but its identity and concentration must be well known (Schwarzenbach et al. 2003). However, in natural waters, it is very difficult to quantify a specific photo-oxidant by direct measurement, making also difficult the determination of overall quantum efficiency under those conditions.

Natural photosensitizers

In surface water, some important natural photosensitizers are known, namely, nitrate and nitrite anions and DOM (Vione et al. 2014). Among the mentioned photosensitizers, DOM will be highlighted as one of the main constituents of natural water. Moreover, the photochemical reactions initiated by the absorption of sunlight occur to a greater extent with DOM and to a lesser extent with inorganic compounds, such as nitrates and nitrites (De Mora et al. 2000). Such absorption by DOM, specifically by coloured or chromophore portion of DOM (CDOM), promotes several photochemical processes that begin with excitation of DOM by light (**reaction 22**).

$$DOM + h\upsilon \rightarrow {}^{3}DOM^{*} \qquad \textbf{(Reaction 22)}$$

Photochemical processes can be distinguished into two main categories. A first group of reactions regards to the intermediate or photo-transients produced upon excitation of DOM: the hydrated or solvated electrons (**reaction 23**). In the presence of oxygen, the hydrated electrons react quickly with it (**reaction 24**), leading to the formation of superoxide anions (O_2^-) and, then, to the formation of H_2O_2 by dismutation (**reaction 25**) (De Mora et al. 2000). Hydrogen peroxide (H_2O_2) is a good oxidant that can oxygenate some organic compounds, mainly, in alkaline solution. The oxygenation of amines and sulfides, the formation of peroxy acids from carboxylic acids or the hydroxylation of alkenes are some examples of the reactions promoted by the presence of H_2O_2 in solution (Blough and Zepp 1995). Additionally, H_2O_2 gives rise to the production of very reactive $HO^\bullet$ (**reaction 26**), also able to react with organic compounds.

$$^1DOM^* \rightarrow {}^1DOM^{\bullet+} + e^- \quad \textbf{(Reaction 23)}$$

$$e^- + O_2 \rightarrow O_2^- \quad \textbf{(Reaction 24)}$$

$$2O_2^- + 2H^+ \rightarrow H_2O_2 + O_2 \quad \textbf{(Reaction 25)}$$

$$H_2O_2 \rightarrow 2HO^\bullet \quad \textbf{(Reaction 26)}$$

A second group of photochemical reactions includes the main pathways of organic compounds photo-transformation. This type of reactions refers to energy, electron or hydrogen atom transfer reactions and is sub-grouped into two central types of reaction: the photo-sensitized oxygenations and the reactions of contaminants with the triplet state of DOM (Boule and Hutzinger 1999). The energy transfer between the triplet excited state of DOM and ground state molecular oxygen originates the formation of singlet oxygen (**reaction 27**), which is a very reactive specie able to react with organic compounds (Aguer et al. 1999; Boule and Hutzinger 1999; De Mora et al. 2000).

$$^3DOM^* + O_2 \rightarrow DOM + {}^1O_2^* \quad \textbf{(Reaction 27)}$$

Furthermore, excited triplet state of DOM can transfer its energy to ground state of an organic compound, represented by C, in **reaction 28**. This type of reaction is more probable to occur when the energy level of the triplet state of the acceptor is lower than that of DOM (Boule and Hutzinger 1999). Additionally, other reaction between excited triplet state of DOM and organic molecules may occur, by hydrogen transfer (**reaction 29**) (Aguer et al. 1999; Halladja et al. 2007).

$^3DOM^* + C \rightarrow DOM + {}^3C^*$ **(Reaction 28)**

$^3DOM^* + C \leftrightarrow DOM^\bullet + C^\bullet$ **(Reaction 29)**

Synthetic photo-catalysts/ photosensitizers

In addition to natural sensitizers, the use of photo-catalysts, non-toxic and easy to removal, can be interesting within the scope of organic contaminants photo-degradation in aquatic systems.

Photo-catalysts and photosensitizers are two terms sometimes difficult to distinguish, since they originate the degradation of a compound by absorption of radiation. According to IUPAC definition, a photo-catalyst is a "catalyst able to produce, upon absorption of light, chemical transformations of the reaction partners. The excited state of the photo-catalyst repeatedly interacts with the reaction partners forming reaction intermediates and regenerates itself after each cycle of such interactions." (IUPAC 2011). A photosensitizer is an entity able to absorb light and initiate photochemical or photo-physical alterations in the system, not being consumed therewith (IUPAC 2011; Marin et al. 2012). Thus, the photo-catalysis definition generally includes the photosensitization (Serpone and Pelizzetti 1989).

TiO_2 is recognized as an ideal catalyst because it presents a high oxidizing power, is chemically inert, stable, inexpensive and non-toxic. TiO_2 exists in three different crystalline modifications: anatase, brookite and rutile, being that anatase presents the highest overall photocatalytic activity (Castellote and Bengtsson 2011). Whenever possible, the immobilization of TiO_2 on a substrate has several advantages, namely, higher surface area, increased surface hydroxyl groups, reduced charge recombination and superior adsorption properties (Lazar et al. 2012). In addition to all these characteristics, a very important advantage of TiO_2 immobilization is its recuperation, avoiding its release into environment, and its possible reuse.

When TiO_2 is irradiated and absorbs photons ($h\upsilon$), electron-hole pairs are formed (**reaction 30**), promoting an electron (e^-) from the valence band (VB) to the conduction band (CB) and leaving a hole (h^+) behind in the valence band (**figure 8a**). However, this only happens when it is illuminated with energy equal or higher than band-gap energy (E_g) that, in the case of anatase-type TiO_2 is 3.2 eV (Castellote and Bengtsson 2011; Ramirez et al. 2015). To achieve this energy, UV radiation (wavelengths $\leq$ 400 nm) is necessary, which restricts the use of TiO_2 under visible light.

$$TiO_2 + h\upsilon \rightarrow e_{cb}^- + h_{vb}^+ \qquad \textbf{(Reaction 30)}$$

The solar spectrum comprises mostly visible light (about 50 %), while ultraviolet radiation accounts less than 4 % (Zhao et al. 2005; Chowdhury et al. 2012). To overcome the limitation of TiO_2 under visible light and take advantage of overall spectrum of sunlight radiation, some paths have been proposed (Zhao et al. 2005; Chowdhury et al. 2012; Ramirez et al. 2015), standing out the dye-sensitized TiO_2.

Dye sensitization (**figure 8b**) is a simple method that allows TiO_2 activation to wavelengths longer than those of its band gap (Chowdhury et al. 2012). Thus, the dye in the excited state (Dye^*) generally has lower redox potential than the corresponding ground state. When this occurs and the redox potential is lower than the CB of TiO_2, an electron may be injected from the excited state into the CB (Zhao et al. 2005).

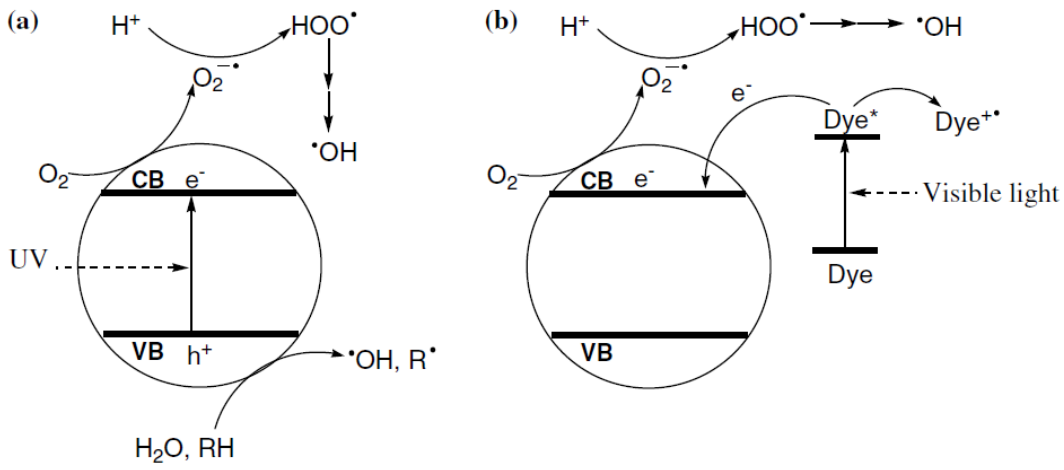

Figure 8 – Photocatalytic mechanism under UV (a) and visible light (b) illumination (Zhao et al. 2005)

The presence of oxygen on the TiO_2 surface not only prevents the recombination between e^- and h^+, but also scavenges the electrons to form several oxygen reactive species that will oxidize the compounds. **Reactions 31-35** describe the dye sensitization under visible light (**figure 8b**) (Zhao et al. 2005). Among the reactive species formed, $HO^\bullet$ is the most powerful oxidant in water, whereby its reaction with the organic compound (R-H) is described: **reaction 36** (Ramirez et al. 2015).

$$Dye + h\upsilon \rightarrow Dye^* \qquad \textbf{(Reaction 31)}$$

$$Dye^* + TiO_2 \rightarrow Dye^{+\bullet} + TiO_2(e) \qquad \textbf{(Reaction 32)}$$

$$TiO_2(e) + O_2 \rightarrow TiO_2 + O_2^{-\bullet} \quad \textbf{(Reaction 33)}$$

$$2O_2^{-\bullet} + 2H^+ \rightarrow {}^{\bullet}O_2 + H_2O_2 \quad \textbf{(Reaction 34)}$$

$$H_2O_2 + TiO_2(e) \rightarrow {}^{\bullet}OH + HO^- + TiO_2 \quad \textbf{(Reaction 35)}$$

$$R\text{-}H + {}^{\bullet}OH \rightarrow R^{\bullet} + H_2O \quad \textbf{(Reaction 36)}$$

Thus, dye sensitization involves mechanisms of photo-oxidation and photo-sensitizing under sunlight irradiation, meaning that TiO_2 acts as an electron mediator and the dye as a sensitizer (Ramirez et al. 2015).

Photoactive organic compounds, such as porphyrins, have been proposed for this type of dye sensitization (Marin et al. 2012; Higashino and Imahori 2015). Porphyrins present a core structure (**figure 9)** with four *meso*- and eight ß–positions. These positions allow to functionalize one or multiple linkers containing carboxylic acids or other substitutes as anchoring groups that attach to the TiO_2 surface. They have two main characteristics bands in the visible region: at 400–450 nm (Soret band) and at 500–650 nm (Q bands) (Li and Diau 2013).

In addition to photoactive organic compounds, graphene-based semiconductors (allotrope of carbon) have been pointed as a very efficient photo-catalyst (Xiang et al. 2012; Adán-Más and Wei 2013; Khalid et al. 2013). Graphene (GR) is a single layer of graphite with sp^2 carbon atoms (Adán-Más and Wei 2013). Besides its capability to extend the photo-catalysis in the visible region, acting as a dye, this allotrope of carbon has several good properties, including: high surface area of 2600 $m^2\ g^{-1}$, high electron mobility (15000 $m^2\ V^{-1}\ s^{-1}$ at room temperature) and conductivity, and good interfacial contact with adsorbents (Zhou et al. 2011; Xiang et al. 2012). Its surface properties allow chemical modifications that facilitate its use in composite materials, contributing to the effective photo-degradation of contaminants in the course of photo-catalysis (Khalid et al. 2013). Graphene oxide (GO) is the main derivative of graphene and can be directly synthetized from it. GO is composed by functional oxygen groups, like hydroxyl, epoxy, carbonyl and carboxyl, in sp^3 carbon (**figure 9**). The presence of these groups in GO is an advantage over graphene. During the electron transfer mechanism, TiO_2 particles have affinity for epoxy and carboxylate groups, where charge transfer occurs through the reduction of those compounds (Adán-Más and Wei (2013), and authors cited therein).

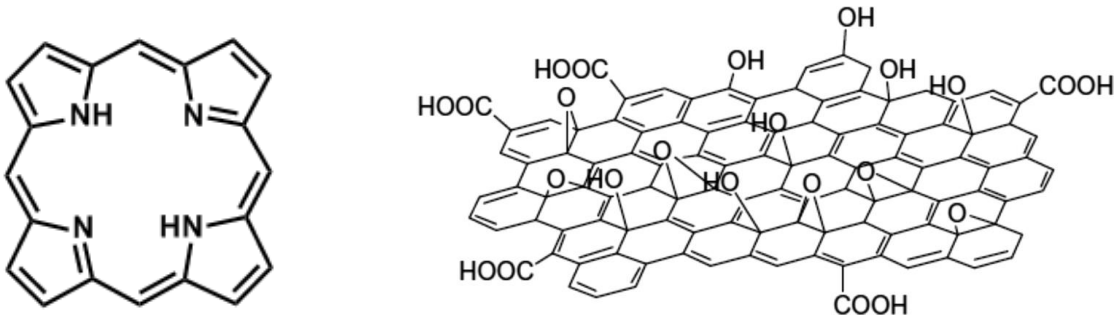

Figure 9 – Structures of porphyrin core (left) and graphene oxide (right).

3.2 Photo-degradation of BDE-209

3.2.1 State of art

Photo-degradation studies of BDE-209 in water, published in literature by other authors, are not known. The only known kinetic studies of BDE-209 photo-degradation in water (0.1% acetonitrile) were obtained during my master's thesis (Leal 2012). The kinetic rate constant and the half-life time determined were 0.0101 ± 0.0003 min^{-1} and 69 ± 2 min, respectively. The experiences developed during the master's thesis were further complemented by some experiments carried out at the beginning of this PhD, leading to the publication of an article (Leal et al. 2013).

In contrast, there are several studies of BDE-209 photo-degradation in different organic solvents, under different light conditions (Bezares-Cruz et al. 2004; Eriksson et al. 2004; Kuivikko et al. 2007; Shih and Wang 2009; Xie et al. 2009). Those studies indicate that the photo-degradation of BDE-209 in organic solvents occurs through a reductive dehalogenation. Additionally, its photo-degradation rate is largely related to the capacity of the solvent to give a hydrogen atom to the aryl radical formed by homolytic cleavage of a C-Br bond after molecular excitation by radiation. Indeed, in general, a greater ability of the solvent to give hydrogen promotes a higher rate of the photolytic process (Eriksson et al. 2004; Xie et al. 2009). The studies performed by Eriksson et al. (2004) showed that the BDE-209 photo-degradation was slower in methanol: water (80:20) than in methanol, in agreement with the lower tendency of water to give a hydrogen atom. The H-O bond dissociation energy in water is 119 kcal/mol, while the C-H bond dissociation energy in methanol is 96 kcal/ mol (Luo 2003). However, other reaction processes may occur. Other authors refer that hydrogen donating capacity of the solvent did not play a decisive role on the photolytic rate of BDE-209 because they observed a fast photo-degradation of BDE-209 in CCl_4 with a half-life only three times higher than that in THF (Xie et al. 2009).

3.3 Photo-degradation of OTC

3.3.1 State of art

It is known that photo-degradation is an important way of degradation of environmental contaminants. Considering the limitations of ozonation referred in *chapter 1*, namely in marine-based aquaculture, the photo-degradation could be a complementary method to adopt in aquaculture. There are several studies reporting the OTC photo-degradation in aqueous solutions, using different sources and conditions of irradiation (Lunestad et al. 1995; Pouliquen et al. 2007; Jiao et al. 2008; Lopez-Penalver et al. 2010; Xuan et al. 2010; Chen et al. 2011; Gomez-Pacheco et al. 2012; Zhao et al. 2013). Among these studies, only two of them use natural sunlight (Lunestad et al. 1995; Xuan et al. 2010), while other two studies applied irradiation conditions to simulate the sunlight in their experiments (Chen et al. 2011; Zhao et al. 2013).

Lunestad et al. (1995) evaluated the photo-stability of OTC (50 mg/L) in filtered (0.4 µm) seawater (33 ‰), illuminating the samples by daylight at sea level and submerged one meter in the sea. The experiments were performed under natural radiation, at latitude 60 ºN, in October and November, in Bergen (Norway). The authors concluded that after nine days of exposure, the OTC concentration decrease to 2 mg/L. In turn, Xuan et al. (2010) studied the photolysis of OTC (50 mM) in deionised water, under sunlight irradiation, in Riverside (California, USA) at 34.95 ºN and 117.40 ºW, and assessed the influence of Ca^{2+} (1 mM) on photolysis. They obtained a degradation rate constant of 3.61 ± 0.06 day^{-1} and reported a strong influence of Ca^{2+} on the enhancement of OTC photolysis, suggesting that OTC become more vulnerable to sunlight irradiation after chelating with Ca^{2+}. The differences of results observed in these two studies are probably attributed to the differences on initial OTC concentration and irradiation conditions, namely light intensity.

Chen et al. (2011) conducted photolysis studies of OTC (20 µM) in deionised water and in a natural water sample from Dongjiang river (in southern China), under simulated sunlight (150-W xenon short arc lamp). In addition, they studied the effect of Ca^{2+}, Mg^{2+} and pH variations on OTC photo-degradation. They observed that the rate constants obtained at pH 9.0 were higher than the rate constants obtained at pH 7.3. These results are more pronounced in the experiments performed in deionised water than in natural water, where the observed rate constants of the OTC photo-degradation are similar at

two pH values. At pH 7.3, the addition of Mg^{2+} (up to 1000 µM) slightly inhibited the OTC photo-degradation, while the presence of Ca^{2+} (up to 1000 µM) enhanced it.

Zhao et al. (2013) performed photochemical experiments under two 15W fluorescent lamps mounted with or without UV block filter to simulate visible or solar light, respectively. They also evaluated the effect of pH variation (2.0, 5.5, 8.5 and 11.0) on OTC photo-degradation and, similarity to observed by Chen et al. (2011), they also concluded that OTC photo-degradation is enhanced with the increase of pH. Their results indicate that, for the same OTC concentration (5 mg/L), its photolytic degradation is faster at high pH's values (8.5 and 11) under solar light than under visible light. Note that visible light is only a portion of solar light, which is also composed by ultraviolet and infrared light.

3.3.2 Ozonation vs. photo-degradation

Photo-degradation using sunlight is a simple and cheaper method than ozonation, once it uses a natural source of light and does not require so much care in handling by operators. Furthermore, contrarily to what happens in ozonation, OTC photo-degradation seems to be favoured in the presence of some sea-salts, such as calcium (Xuan et al. 2010). Nevertheless, photo-degradation is not a completely alternative method to ozonation, since the latter takes other functions (eg.: disinfection). Photo-degradation can be seen as a complementary method prior to ozonation, allowing reduce the ozone doses. The reduction of ozone levels will be beneficial for operators and aquatic species, which will be less exposed to dangerous levels of ozone and its sub-products, and also less expensive.

As the two methods do not mineralize completely OTC, it is important to know and evaluate the possible effects of its by-products in the environment, especially in aquatic systems. Since OTC is an antibiotic, it is worth not only know the toxicity of its by-products, but also their possible biological activity.

Toxicity of OTC and its by-products

There are several studies in literature reporting the toxicity of OTC for several aquatic species (Schmidt et al. 2007; Kolodziejska et al. 2013; Kolar et al. 2014). Most of the studies published in the literature were performed using bacteria and/or algae, but toxicity studies of OTC in fish can also be found (Murphy and Peters 1991; Bumguardner

and King 1996; Ambili et al. 2013; Botelho et al. 2015). However, among these studies, only two determined the values of $LC_{50.}$ This parameter is an indicator of acute toxicity (inversely correlated) and corresponds to the concentration able to kill 50 % of exposed organisms.

Murphy and Peters (1991) classified oxytetracycline hydrochloride as practically non-toxic to Rainbow Trout (*Oncorhynchus mykiss*), obtaining values of LC_{50} (96 hours) equal to 116 mg/L. Bumguardner and King (1996) studied the toxicity of OTC to juvenile Stripped Bass (*Morone saxatilis*) and determined LC_{50} (96 hours) = 597 mg/L for 6-h of chemical exposure. Considering these few studies (Murphy and Peters 1991; Bumguardner and King 1996) and the OTC concentrations typically administered in intensive aquaculture (**tables 4** and **5,** *subchapter 2.3.3*), acute toxicity of OTC to fish appears to be relatively low, but more studies are needed to deepen this topic. When talking about toxicity, it is also important not forget chronic toxicity. Although there are few studies on chronic toxicity of OTC, some authors highlighted the reproductive effects observed in the OTC concentration range from 5 to 50 mg/L. They referred a half maximal effective concentration (EC_{50}) value of 46.2 mg/L in a 21-days reproduction study on *Daphnia magna* (Wollenberger et al. 2000).

Equally or more important than to know the toxicity of the parent compound (OTC), it is to know the toxicity of the by-products. Since that the complete mineralization does not occur, either by ozonation, either by photo-degradation, it is imperative to evaluate the toxic effects that the by-products resulting from OTC degradation may have in aquatic systems.

With respect to ozonation, Li et al. (2008) applied the standardized bioluminescence assay with the marine bacteria *Vibrio fischeri*, before and after the ozone treatment (11 mg/L) to degrade OTC. The results obtained by them suggest that, after partial ozonation (5-30 min), the first OTC by-products were more toxic than the parent compound (Li et al. 2008). Khan et al. (2010), also evaluated the toxicities of samples before and during ozonation. These authors also used a bioluminescent assay and the bacteria *V. Fischeri*, but their studies were performed with tetracycline (TTC), which presents a similar structure to OTC. They concluded that the maximum removal of the relative toxicity was 40 % (approximately), after two hours of ozonation, at pH 7.0 and 2.2. Additionally, they observed that the by-products resulting of direct ozonation were more toxic than those generated through free radical (Khan et al. 2010).

Regarding to the photo-degradation, toxicity studies about OTC photo-products, under simulated or solar radiation are not known. There are in scientific literature two studies that evaluated the toxicity of OTC photoproducts, but under UV radiation (mercury lamp) (Jiao et al. 2008; Yuan et al. 2011). Jiao et al. (2008) assessed the toxicity of OTC and its photoproducts, using luminescence bacterium (*Photobacterium phosphoreum* T3). The authors observed that the luminescence inhibition rate of the initial solution containing 20 mg/L OTC was 47 %, after 240 minutes of irradiation. They proposed that the increase of toxicity during the irradiation process may be due to the combined toxicity of OTC and its photoproducts. Yuan et al. (2011) evaluated the toxicity of OTC (50 µM) and its oxidation by-products in ultrapure water. The OTC aqueous samples were exposed to UV direct photolysis and UV/H_2O_2 oxidation by different times. The standardized bioluminescent assay with *V. fischeri* revealed an increase of toxicity in UV photolysis, for the photoproducts that still preserved the structural characteristics of the parent compound, such as those identified by LC–MS/MS with m/z equal to 447.74, 475.50 and 414.69 (Yuan et al. 2011). Such photoproducts retain the core structure of 4 rings, with some of their substituent groups being altered. The authors refer that these changes result in a lower steric resistance and an easier penetration into the cell of the luminescent bacterium, leading to increased toxicity. When UV/H_2O_2 was applied, the authors reported the initial increase of toxicity and then, its decrease. They proposed the conversion of more toxic intermediate photoproducts into other non-toxic products, such as the propanedioic acid or the 1,4-Benzenedicarboxylic acid (identified by GC-MS).

To sum up, the formation of toxic or non-toxic products is unclear and appears to be strongly influenced by degradation mechanisms involved and, consequently, by the structure of the products formed.

Bacterial resistance

Antimicrobial resistance is the capability of microorganisms to resist to antimicrobial treatments (EuropeanComission 2016). In the specific case of treatments with antibiotics, antimicrobial resistance is designated as antibiotic resistance. This topic is of particular concern due to the possibility of horizontal transmission of bacterial resistant to other populations, namely to humans, decreasing the effectiveness of therapeutic action (Rigos and Troisi 2005).

The bacterial resistance to antibiotic may be intrinsic or acquired (Dixon 2000). Inherent or intrinsic resistance is an inherent physiological, biochemical or morphological

characteristic of cell that avoids the action of antibiotic, not depending on antibiotic exposure (Dixon 2000). This may be due to three main reasons: absence of the action site (target) in cell, nonexistence of affinity between the antibiotic and its target or even due to the incapability of the antibiotic to enter in bacteria cell and reach its target (Romero et al. 2012). In turn, acquired resistance is a resistance developed by an organism (Dixon 2000). This type of resistance may be developed either by mutation of a chromosomal gene, modifying the structure of the ribosomal target, either by acquisition of extrachromosomal elements like plasmids (Dixon 2000; Sekkin and Kum 2011). For the class of tetracyclines, the resistance mechanisms to antibiotics may be classified in three main groups: energy-dependent efflux pumps, ribosomal protection proteins (RPPs), or enzymatic inactivation (van Hoek et al. 2011).

Related to ozonation, some authors concluded that the increase of ozonation levels from 7.5 mg/L to 657 mg/L led to the disappearance of antibacterial activity to pathogenic bacterium *Staphylococcus aureus*. They suggest that ozonation products of OTC wastewater (WWTP) are not biologically active against the selected bacteria or that residual antibacterial activity of the ozonated effluent is totally attributed to OTC, which remained intact during the ozonation reaction (Zheng et al. 2010). Indeed, other study performed with TTC revealed that the reactions of ozone with it originate the loss of antibacterial activity of TTC ozonation products (Dodd et al. 2009). The authors also clarified that those observations are expected for other tetracyclines due to conservation of the fundamental structural system of tetracycline class.

With respect to photo-degradation, only two studies evaluating the biological activity of OTC photoproducts after its photo-degradation are known (Lunestad et al. 1995; Pereira et al. 2013). Lunestad et al. (1995) measured the antimicrobial activity in seawater, using the disk diffusion test and *Escherichia coli* (*E. coli*) B6 as test organism. They concluded that, after seven days, no inhibition zones were found when exposed to underwater light intensities, meaning that photoproducts do not retain the antibacterial activity of the parent compound. Pereira et al. (2013) followed the growth inhibition of *Escherichia coli* DSM1103 after solar TiO_2-assisted photocatalytic oxidation of OTC. They also reported that the remaining by-products do not show antibacterial activity.

3.4 Photo-degradation of formalin

3.4.1 State of art

Several authors have investigated the formaldehyde degradation by advanced oxidation processes – AOPs (Kajitvichyanukul et al. 2008; Liu et al. 2011; Guimaraes et al. 2012; Moussavi et al. 2012; MacDonald et al. 2014; Mendez et al. 2015) and some of them propose a possible combination between the AOPs and the biological treatments (Moussavi et al. 2012; Mendez et al. 2015).

Guimaraes et al. (2012) performed experiments of formaldehyde degradation in an aqueous solution (400 mg/L) using different processes: photolysis, peroxidation and AOPs (UV/H_2O_2, Fenton and Photo-Fenton). In accordance to what was expectable based on the discussion previously presented in sub*chapter 2.4*, the direct photolysis did not reduce the concentrations of formaldehyde in water. The authors concluded that, among the processes evaluated, the UV/H_2O_2 (**reaction 37**) and photo-Fenton (**reactions 38** and **39**) (Mendez et al. 2015) are in general the processes that present the highest degradation rate constants (Guimaraes et al. 2012). These three reactions have in common the formation of hydroxyl radicals, which react with formalin to form the hydrated formyl radical (**reaction 40**). Then, further reaction of this radical with molecular oxygen originates hydroperoxyl radical and formic acid (**reaction 41**) (McElroy and Waygood 1991). However, it is worth to remember that the formalin solution used in aquaculture contains 10-15 % of methanol and it may act as inhibitor on formaldehyde degradation, competing with it to consume hydroxyl radical in the oxidation reaction (**reaction 42**).

$$H_2O_2 + UV \longrightarrow 2HO^{\cdot} \qquad \textbf{(Reaction 37)}$$

$$Fe^{2+} + H_2O_2 \longrightarrow Fe^{3+} + HO^{-} + HO^{\cdot} \qquad \textbf{(Reaction 38)}$$

$$Fe^{3+} + UV + H_2O \longrightarrow Fe^{2+} + HO^{\cdot} + H^{+} \qquad \textbf{(Reaction 39)}$$

$$CH_2(OH)_2 + HO^{\cdot} \longrightarrow {}^{\cdot}CH(OH)_2 + H_2O \qquad \textbf{(Reaction 40)}$$

$${}^{\cdot}CH(OH)_2 + O_2 \longrightarrow HO_2^{\cdot} + HCOOH \qquad \textbf{(Reaction 41)}$$

$$CH_3OH + HO^{\cdot} \longrightarrow {}^{\cdot}CH_2OH + H_2O \qquad \textbf{(Reaction 42)}$$

So, there are several possibilities to minimize environmental exposure to formalin. Since that AOPs are relatively expensive, also due to the use of UV radiation, the focus on these advanced treatments should be, for example, towards to develop and/or adopt low-cost photo-catalysts, inert and reusable, preferring whenever possible the natural radiation as irradiation source. In this sense, some studies have proposed the visible light active TiO_2 photo-catalysts to remove organic compounds from water (Pelaez et al. 2012; Etacheri et al. 2015; Ramirez et al. 2015). Two studies referring the aqueous formaldehyde photo-degradation, using visible light active TiO_2-based composites, are already published in literature (Li et al. 2015; Lu and Chen 2015) and will be discussed in *Chapter 7*.

3.5 References

Adán-Más, A. and D. Wei (2013). Photoelectrochemical properties of graphene and its derivates. *Nanomaterials* **3**: 325-356.

Aguer, J. P., C. Richard and F. Andreux (1999). Effect of light on humic substances: Production of reactive species. *Analusis* **27**(5): 387-390.

Ambili, T. R., M. Saravanan, M. Ramesh, D. B. Abhijith and R. K. Poopal (2013). Toxicological Effects of the Antibiotic Oxytetracycline to an Indian Major Carp Labeo rohita. *Archives of Environmental Contamination and Toxicology* **64**(3): 494-503.

Bezares-Cruz, J., C. T. Jafvert and I. Hua (2004). Solar photodecomposition of decabromodiphenyl ether: Products and quantum yield. *Environmental Science & Technology* **38**(15): 4149-4156.

Blough, N. V. and R. G. Zepp (1995). Reactive Oxygen Species in natural waters. *Active oxygen in chemistry*. C. S. Foote, Chapman & Hall.

Boreen, A. L., W. A. Arnold and K. McNeill (2003). Photodegradation of pharmaceuticals in the aquatic environment: A review. *Aquatic Sciences* **65**(4): 320-341.

Botelho, R. G., C. A. Christofoletti, J. E. Correia, Y. Ansoar, R. A. Olinda and V. L. Tornisielo (2015). Genotoxic responses of juvenile tilapia (Oreochromis niloticus) exposed to florfenicol and oxytetracycline. *Chemosphere* **132**: 206-212.

Boule, P. and O. Hutzinger (1999). *Environmental Photochemistry*, Springer-Verlag

Bumguardner, B. W. and T. L. King (1996). Toxicity of Oxytetracycline and Calcein to Juvenile Striped Bass. *Transactions of the American Fisheries Society* **125**(1): 143-145.

Castellote, M. and N. Bengtsson (2011). Principles of TiO_2 Photocatalysis. *Applications of Titanium Dioxide Photocatalysis to Construction Materials: State-of-the-Art Report of the RILEM Technical Committee 194-TDP*. Y. Ohama and D. Van Gemert. Dordrecht, Springer Netherlands**:** 5-10.

Challis, J. K., M. L. Hanson, K. J. Friesen and C. S. Wong (2014). A critical assesment of the photodegradation of pharmaceuticals in aquatic environments: defining our current understanding and identifying knowledge gaps. *Environmental Science Processes & Impacts* **16**: 672-696.

Chen, Y., H. Li, Z. P. Wang, T. Tao and C. Hu (2011). Photoproducts of tetracycline and oxytetracycline involving self-sensitized oxidation in aqueous solutions: Effects of Ca^{2+} and Mg^{2+}. *Journal of Environmental Sciences-China* **23**(10): 1634-1639.

Chowdhury, P., J. Moreira, H. Gomaa and A. K. Ray (2012). Visible-Solar-Light-Driven Photocatalytic Degradation of Phenol with Dye-Sensitized TiO_2: Parametric and Kinetic Study. *Industrial & Engineering Chemistry Research* **51**(12): 4523-4532.

Christensen, E. R. and A. Li (2014). *Physical and Chemical Processes in the Aquatic Environment*, Wiley

Cooper, W. J. and F. L. Herr (1987). Introduction and Overview. Photochemistry of Environmental Aquatic Systems. R. G. Zika and W. J. Cooper. Washington, DC, American Chemical Society. **327**.

De Mora, S., S. Demers and M. Vernet (2000). *The Effects of UV Radiation in the Marine Environment*, Cambridge University Press

Dixon, B. A. (2000). Antibiotics. Encyclopedia of Aquaculture. R. R. Stickney. New York, John Wiley & Sons, Inc.**:** 38-44.

Dodd, M. C., H. P. E. Kohler and U. Von Gunten (2009). Oxidation of Antibacterial Compounds by Ozone and Hydroxyl Radical: Elimination of Biological Activity during Aqueous Ozonation Processes. *Environmental Science & Technology* **43**(7): 2498-2504.

Eriksson, J., N. Green, G. Marsh and A. Bergman (2004). Photochemical decomposition of 15 polybrominated diphenyl ether congeners in methanol/water. *Environmental Science &Technology* **38**(11): 3119-3125.

Etacheri, V., C. Di Valentin, J. Schneider, D. Bahnemann and S. C. Pillai (2015). Visible-light activation of TiO_2 photocatalysts: Advances in theory and experiments. *Journal of Photochemistry and Photobiology C-Photochemistry Reviews* **25**: 1-29.

EuropeanComission. (2016, 16-06-2016). "Antimicrobial Resistance." Health and Food Safety Retrieved July, 13, 2016, from http://ec.europa.eu/dgs/health_food-safety/amr/index_en.htm.

Fereja, T. H., A. Hymete and T. Gunasekaran (2013). A Recent Review on Chemiluminescence Reaction, Principle and Application on Pharmaceutical Analysis. *ISRN Spectroscopy* **2013**: 12.

Gomez-Pacheco, C. V., M. Sanchez-Polo, J. Rivera-Utrilla and J. J. Lopez-Penalver (2012). Tetracycline degradation in aqueous phase by ultraviolet radiation. *Chemical Engineering Journal* **187**: 89-95.

Guimaraes, J. R., C. R. T. Farah, M. G. Maniero and P. S. Fadini (2012). Degradation of formaldehyde by advanced oxidation processes. *Journal of Environmental Management* **107**: 96-101.

Halladja, S., A. T. Halle, J.-P. Aguer, A. Boulkamh and C. Richard (2007). Inhibition of Humic Substances Mediated Photooxygenation of Furfuryl Alcohol by 2,4,6-Trimethylphenol. Evidence for Reactivity of the Phenol with Humic Triplet Excited States. *Environmental Science & Technology* **41**: 6066-6073.

Higashino, T. and H. Imahori (2015). Porphyrins as excellent dyes for dye-sensitized solar cells: recent developments and insights. *Dalton Transactions* **44**(2): 448-463.

IUPAC (2011). Compendium of Chemical Terminology Gold Book.

Jiao, S. J., S. R. Meng, D. Q. Yin, L. H. Wang and L. Y. Chen (2008). Aqueous oxytetracycline degradation and the toxicity change of degradation compounds in photoirradiation process. *Journal of Environmental Sciences-China* **20**(7): 806-813.

Kajitvichyanukul, P., M. C. Lu and A. Jamroensan (2008). Formaldehyde degradation in the presence of methanol by photo-Fenton process. *Journal of Environmental Management* **86**(3): 545-553.

Khalid, N. R., E. Ahmed, Z. Hong, L. Sana and M. Ahmed (2013). Enhanced photocatalytic activity of graphene–TiO_2 composite under visible light irradiation. *Current Applied Physics* **13**(4): 659-663.

Khan, M. H., H. Bae and J. Y. Jung (2010). Tetracycline degradation by ozonation in the aqueous phase: Proposed degradation intermediates and pathway. *Journal of Hazardous Materials* **181**(1-3): 659-665.

Kolar, B., L. Arnus, B. Jeretin, A. Gutmaher, D. Drobne and M. K. Durjava (2014). The toxic effect of oxytetracycline and trimethoprim in the aquatic environment. *Chemosphere* **115**: 75-80.

Kolodziejska, M., J. Maszkowska, A. Bialk-Bielinska, S. Steudte, J. Kumirska, P. Stepnowski and S. Stolte (2013). Aquatic toxicity of four veterinary drugs commonly applied in fish farming and animal husbandry. *Chemosphere* **92**(9): 1253-1259.

Kuivikko, M., T. Kotiaho, K. Hartonen, A. Tanskanen and A. V. Vahatalo (2007). Modeled direct photolytic decomposition of Polybrominated diphenyl ethers in the Baltic sea and the Atlantic ocean. *Environmental Science & Technology* **41**(20): 7016-7021.

Kummerer, K. (2009). Antibiotics in the aquatic environment - A review - Part I. *Chemosphere* **75**(4): 417-434.

Lazar, M. A., S. Varghese and S. S. Nair (2012). Photocatalytic Water Treatment by Titanium Dioxide: Recent Updates. *Catalysts* **2**(4): 572-601.

Leal, J. F. (2012). Fotodegradação do retardador de chama BDE-209. Chemistry. Aveiro, University of Aveiro. **Master:** 91.

Leal, J. F., V. I. Esteves and E. B. H. Santos (2013). BDE-209: Kinetic Studies and Effect of Humic Substances on Photodegradation in Water. *Environmental Science & Technology* **47**: 14010-14017.

Levine, I. N. (2009). *Physical Chemistry*. New York, McGraw-Hill Higher Education

Li, H., W. Zhang, L.-x. Guan, F. Li and M.-m. Yao (2015). Visible light active TiO_2–ZnO composite films by cerium and fluorine codoping for photocatalytic decontamination. *Materials Science in Semiconductor Processing* **40**: 310-318.

Li, K. X., A. Yediler, M. Yang, S. Schulte-Hostede and M. H. Wong (2008). Ozonation of oxytetracycline and toxicological assessment of its oxidation by-products. *Chemosphere* **72**(3): 473-478.

Li, L. L. and E. W. G. Diau (2013). Porphyrin-sensitized solar cells. *Chemical Society Reviews* **42**(1): 291-304.

Liu, X. X., J. T. Liang and X. J. Wang (2011). Kinetics and Reaction Pathways of Formaldehyde Degradation Using the UV-Fenton Method. *Water Environment Research* **83**(5): 418-426.

Lopez-Penalver, J. J., M. Sanchez-Polo, C. V. Gomez-Pacheco and J. Rivera-Utrilla (2010). Photodegradation of tetracyclines in aqueous solution by using UV and UV/H_2O_2

oxidation processes. *Journal of Chemical Technology and Biotechnology* **85**(10): 1325-1333.

Lu, X. and H. Chen (2015). Graphite-based N-TiO_2 composites photocatalyst for removal of HCHO in water. *Desalination and Water Treatment* **56**(6): 1681-1688.

Lunestad, B. T., O. B. Samuelsen, S. Fjelde and A. Ervik (1995). Photostability of 8 antibacterial agents in seawater. *Aquaculture* **134**(3-4): 217-225.

Luo, Y.-R. (2003). *Handbook of Bond Dissociation Energies in Organic Compounds*, CRC Press

MacDonald, M. J., Z. J. Wu, J. Y. Ruzicka, V. Golovko, D. C. W. Tsang and A. C. K. Yip (2014). Catalytic consequences of charge-balancing cations in zeolite during photo-Fenton oxidation of formaldehyde in alkaline conditions. *Separation and Purification Technology* **125**: 269-274.

Marin, M. L., L. Santos-Juanes, A. Arques, A. M. Amat and M. A. Miranda (2012). Organic Photocatalysts for the Oxidation of Pollutants and Model Compounds. *Chemical Reviews* **112**(3): 1710-1750.

McElroy, W. J. and S. J. Waygood (1991). Oxidation of Formaldehyde by the Hydroxyl Radical in Aqueous Solution. *Journal of the Chemical Society, Faraday Transactions* **87**(10): 1513-1521.

Mendez, J. A. O., J. A. H. Melian, J. Arana, J. M. D. Rodriguez, O. G. Diaz and J. P. Pena (2015). Detoxification of waters contaminated with phenol, formaldehyde and phenol-formaldehyde mixtures using a combination of biological treatments and advanced oxidation techniques. *Applied Catalysis B-Environmental* **163**: 63-73.

Moussavi, G., A. Bagheri and A. Khavanin (2012). The investigation of degradation and mineralization of high concentrations of formaldehyde in an electro-Fenton process combined with the biodegradation. *Journal of Hazardous Materials* **237**: 147-152.

Murphy, D. and G. T. Peters (1991). Oxytetracycline hydrochloride: A 96-hour static acute toxicity test with the rainbow trout (*Oncorhynchus mykiss*). Laboratory study No.260A-103. New York, Prepared by Wildlife International Ltd, Submitted by Pfizer, Incorporated, EPA MRID No. 417832-02**:** 7.

Pelaez, M., N. T. Nolan, S. C. Pillai, M. K. Seery, P. Falaras, A. G. Kontos, P. S. M. Dunlop, J. W. J. Hamilton, J. A. Byrne, K. O'Shea, M. H. Entezari and D. D. Dionysiou (2012). A review on the visible light active titanium dioxide photocatalysts for environmental applications. *Applied Catalysis B: Environmental* **125**: 331-349.

Pereira, J., A. C. Reis, D. Queiros, O. C. Nunes, M. T. Borges, V. J. P. Vilar and R. A. R. Boaventura (2013). Insights into solar TiO_2-assisted photocatalytic oxidation of two antibiotics employed in aquatic animal production, oxolinic acid and oxytetracycline. *Science of the Total Environment* **463**: 274-283.

Pilling, M. J. and P. W. Seakins (1995). *Reaction Kinetics*. Oxford, Oxford Science Publications

Pouliquen, H., R. Delpepee, M. Larhantec-Verdier, M. L. Morvan and H. Le Bris (2007). Comparative hydrolysis and photolysis of four antibacterial agents (oxytetracycline oxolinic acid, flumequine and florfenicol) in deionised water, freshwater and seawater under ablotic conditions. *Aquaculture* **262**(1): 23-28.

Ramirez, R. J., C. A. P. Arellano, J. C. Varia and S. S. Martinez (2015). Visible Light-Induced Photocatalytic Elimination of Organic Pollutants by TiO_2: A Review. *Current Organic Chemistry* **19**(6): 540-555.

Rigos, G. and G. M. Troisi (2005). Antibacterial agents in mediterranean finfish farming: A synopsis of drug pharmacokinetics in important euryhaline fish species and possible environmental implications. *Reviews in Fish Biology and Fisheries* **15**(1-2): 53-73.

Romero, J., C. G. Feijoo and P. Navarrete (2012). Antibiotics in aquaculture - Use, abuse and alternatives. *Health and Environment in Aquaculture*. E. D. Carvalho, G. S. David and R. J. Silva.

Schmidt, L. J., M. P. Gaikowski, W. H. Gingerich, V. K. Dawson and T. M. Schreier (2007). An Environmental Assessment of the Proposed Use of Oxytetracycline-Medicated Feed in Freshwater Aquaculture. Wisconsin, U.S. Food and Drug Administration**:** 97.

Schwarzenbach, R. P., P. M. Gschwend and D. M. Imboden (2003). *Environmental Organic Chemistry*. New Jersey, John Wiley & Sons, Inc.

Sekkin, S. and C. Kum (2011). Antibacterial Drugs in Fish Farms: Application and Its Effects. *Recent Advances in Fish Farms*. F. Aral, InTech**:** 250.

Serpone, N. and E. Pelizzetti (1989). *Photocatalysis: fundamentals and applications*, Wiley

Shih, Y.-h. and C.-K. Wang (2009). Photolytical degradation of polybromodiphenyl ethers under UV-lamp and solar irradiations. *Journal of Hazardous Materials* **165**: 34-38.

van Hoek, A., D. Mevius, B. Guerra, P. Mullany, A. P. Roberts and H. J. M. Aarts (2011). Acquired antibiotic resistance genes: an overview. *Frontiers in Microbiology* **2**.

Vione, D., M. Minella, V. Maurino and C. Minero (2014). Indirect Photochemistry in Sunlit Surface Waters: Photoinduced Production of Reactive Transient Species. *Chemistry-a European Journal* **20**(34): 10590-10606.

Wollenberger, L., B. Halling-Sørensen and K. O. Kusk (2000). Acute and chronic toxicity of veterinary antibiotics to Daphnia magna. *Chemosphere* **40**(7): 723-730.

Xiang, Q. J., J. G. Yu and M. Jaroniec (2012). Graphene-based semiconductor photocatalysts. *Chemical Society Reviews* **41**(2): 782-796.

Xie, Q., J. Chen, J. Shao and C. e. Chen (2009). Important role of reaction field in photodegradation of deca-bromodiphenyl ether: Theoretical and experimental investigations of solvent effects. *Chemosphere* **76**: 1486-1490.

Xuan, R. C., L. Arisi, Q. Q. Wang, S. R. Yates and K. C. Biswas (2010). Hydrolysis and photolysis of oxytetracycline in aqueous solution. *Journal of Environmental Science and Health Part B-Pesticides Food Contaminants and Agricultural Wastes* **45**(1): 73-81.

Yuan, F., C. Hu, X. X. Hu, D. B. Wei, Y. Chen and J. H. Qu (2011). Photodegradation and toxicity changes of antibiotics in UV and UV/H_2O_2 process. *Journal of Hazardous Materials* **185**(2-3): 1256-1263.

Zhao, C., M. Pelaez, X. D. Duan, H. P. Deng, K. O'Shea, D. Fatta-Kassinos and D. D. Dionysiou (2013). Role of pH on photolytic and photocatalytic degradation of antibiotic oxytetracycline in aqueous solution under visible/solar light: Kinetics and mechanism studies. *Applied Catalysis B-Environmental* **134**: 83-92.

Zhao, J., C. Chen and W. Ma (2005). Photocatalytic Degradation of Organic Pollutants Under Visible Light Irradiation. *Topics in Catalysis* **35**(3): 269-278.

Zheng, S. K., C. C. Cui, Q. J. Liang, X. H. Xia and F. Yang (2010). Ozonation performance of WWTP secondary effluent of antibiotic manufacturing wastewater. *Chemosphere* **81**(9): 1159-1163.

Zhou, K., Y. Zhu, X. Yang, X. Jiang and C. Li (2011). Preparation of graphene-TiO_2 composites with enhanced photocatalytic activity. *New Journal of Chemistry* **35**(2): 353-359.

Chapter 4: Effect of humic substances on photo-degradation [3]

Humic substances (HS) are complex molecules able to sensitize or delay photo-degradation of contaminants. The retardation effect is frequently attributed to light-screening due to HS light absorption in a wide range of wavelengths; however, this may not be the unique or predominant pathway for retardation of photo-degradation.

In this chapter, the light-screening effect of different fractions of aquatic HS (humic acids, fulvic acids and XAD-4 fraction) is calculated and the expected retardation effect is compared with the experimentally observed for two very different contaminants: BDE-209 and OTC. The delay effect on OTC photo-degradation is predominantly justified by light-screening, but on BDE-209 photo-degradation, the light-screening has a minor effect and the association with HS seems to be the predominant effect.

In the present work, the quantum yields for BDE-209 ($\Phi_{290\text{-}350\ nm}$ = 0.010 ± 0.001) and OTC ($\Phi_{290\text{-}450\ nm}$ = 4.22 x10^{-4} ± 0.33 x10^{-4}) photo-degradation in water were also determined. This allowed estimate the outdoor half-life times (at sea level and 40º N) of OTC and BDE-209 in midsummer and midwinter days, in the absence and in the presence of HS.

---

[3] Adapted from:

- **J.F. Leal**, V.I. Esteves, E.B.H. Santos (2015). "Does light-screening by humic substances completely explain their retardation effect on contaminants photo-degradation?" *Journal of Environmental Chemical Engineering*, **3**: 3015-3019.
- **J.F. Leal**, V.I. Esteves, E.B.H. Santos (2013). BDE-209: Kinetic Studies and Effect of Humic Substances on Photodegradation in Water. *Environmental Science & Technology,* **47**(24): 14010-14017.

4.1 Contextualization

Humic substances (HS) are the main constituents of natural organic matter and assume an important role on the environmental fate and behaviour of organic compounds. Aquatic HS represent a high portion (40 – 60 %) of the dissolved organic carbon present in natural water (Thurman 1985). They are complex molecules with several structural components: aromatic rings, aliphatic carbon chains and many oxygen containing functional groups such as carboxyl, carbonyl and hydroxyls groups (Kordel et al. 1997). The prevalence of each type of functional group or structural moiety varies with aquatic system and is influenced by origin of HS (Thurman 1985; Esteves et al. 2009).

With respect to the role of HS on interactions of light with contaminants, two opposite effects must be considered: the photo-sensitisation and the retardation effects of HS. On one hand, the light absorption by HS can promote several photochemical processes (described in the previous chapter), increasing the environmental degradation of a contaminant. On the other hand, HS has a coloured or chromophore portion able to absorb solar radiation (Sulzberger and Durisch-Kaiser 2009) and modify the spectrum of radiation penetrating into the water column (Zepp et al. 2011). The retardation effect of HS on contaminants photo-degradation is frequently attributed to this light-screening (S_λ). But, does light-screening completely explain the delaying effect of HS on contaminants' photo-degradation? And, what is its contribution for the retardation on photo-degradation of different compounds?

The purpose of the present work was to evaluate how light-screening caused by natural HS affects the photo-degradation behaviour of the selected contaminants. For this study, two organic compounds found in aquaculture's water were considered: OTC and BDE-209. Additionally, hypotheses related with chemical structure and hydrophobicity of contaminants that can justify the retardation effect of natural HS on photo-degradation of OTC and BDE-209 are proposed. Moreover, the quantum yields and the outdoor half-life times for BDE-209 and OTC, for midsummer and midwinter days, are estimated for environmental conditions.

4.2 Material and methods

4.2.1 Chemicals

Oxytetracycline hydrochloride (OTC) and BDE-209 (bis(pentabromophenyl) ether) (98 %) were provided by Sigma Aldrich. For the preparation of all solutions, distilled water was used. The HS fractions – humic acids (HA), fulvic acids (FA) and XAD-4 fraction – were isolated from river Vouga water (Carvoeiro, Portugal) during September / October 1991, using two columns in tandem: one of Amberlit XAD-8 resin and the other of Amberlit XAD-4 resin (Santos 1994; Esteves et al. 1995). The relative abundance of each fraction in the sample was 10.3 %, 69.4 % and 20.3 % for HA, FA and XAD-4 fraction (Esteves et al. 1995), respectively. The humic substances were kept in an exsicator, protected from light.

4.2.2 Photo-degradation experiments

A 5 mg/L stock solution of BDE-209 in acetonitrile was made and used to prepare an aqueous working solution with a final concentration of 5 µg/L of BDE-209. In order to guarantee that acetonitrile does not affect the photo-degradation rates of BDE-209 in aqueous solution, the concentration of auxiliary solubilizing agent (acetonitrile) in aqueous solution was maintained much lower (0.1 %) than the value recommended by the OECD guideline TG316 (1 %) (OECD 2000). The working solution (5 µg/L) was transferred into quartz tubes (45 mL in each tube) to perform the irradiation experiments. The use of this low concentration required pre-concentration methodologies to analyse the compound by HPLC-UV. Those methodologies will not be presented in this work because they were developed during the author master's thesis and are described in detail in it (Leal 2012). Irradiation experiments with OTC were also performed in quartz tubes, using aqueous solutions of OTC (4 mg/L) prepared from OTC stock solution (10 mg/L) in distilled water. The pH was not adjusted, but for all solutions of OTC, the measured pH values varied between 4 and 5.

To study the effect of HS on OTC and BDE-209 photo-degradation, aqueous solutions of each compound with HS fractions (8 mg/L and 16 mg/L) were irradiated during 60 minutes. These HS concentrations may occur in the natural aquatic systems, namely in river water (Santos 1994; Esteves et al. 1995).

For each irradiation time, and each replicate, two tubes were introduced in the sunlight simulator: one was exposed to radiation and the other wrapped in aluminium foil to protect from light (dark control). Irradiated solutions and the respective dark controls

were maintained inside the solarbox during the same time and the degradation percentage was always calculated from the concentration difference between the exposed solution and respective dark control. For the kinetic studies, the OTC aqueous solutions were irradiated during 20, 40, 60, 90 and 120 min, while the BDE-209 aqueous solutions were irradiated during 30, 60, 90, 120 and 150 minutes. At least three non-simultaneous replicates of the photo-degradation experiments were made together with the respective dark controls, for each irradiation time.

Sunlight simulator

All irradiations were achieved using a sunlight simulator (**figure 10**) (Solarbox 1500 – Co.fo.me.gra, Italy) with an irradiance of 55 W/m^2 (290–400 nm), corresponding to 550 W/m^2 in all spectral range. This sunlight simulator is equipped with a 1500 W arc xenon lamp and outdoor UV filters that restrict the transmission of light of wavelengths below 290 nm (**figure 11**). To monitor irradiance and temperature of the experiments, a multimeter (Co.fo.me.gra, Italy), equipped with a UV 290-400 nm large band sensor and a black standard temperature sensor, was used. The device was refrigerated by an air-cooled system.

Figure 10 – Sunlight simulator (photo-reactor) – Solarbox 1500, Co.fo.me.gra

Although the solar simulator is not a perfect reproduction of the solar spectrum, it is considered a good approximation with some advantages for this type of kinetic studies. Sunlight simulators allow repeatability, predictability and enforcement of irradiation experiments continuously and at any time (Calisto 2011), because it does not depend on solar cycles (day/night) or weather conditions. Furthermore, knowing the spectra emitted by solar simulator, makes also possible to convert the experimental irradiation times in real outdoor half-life times, for different seasons and/or locations.

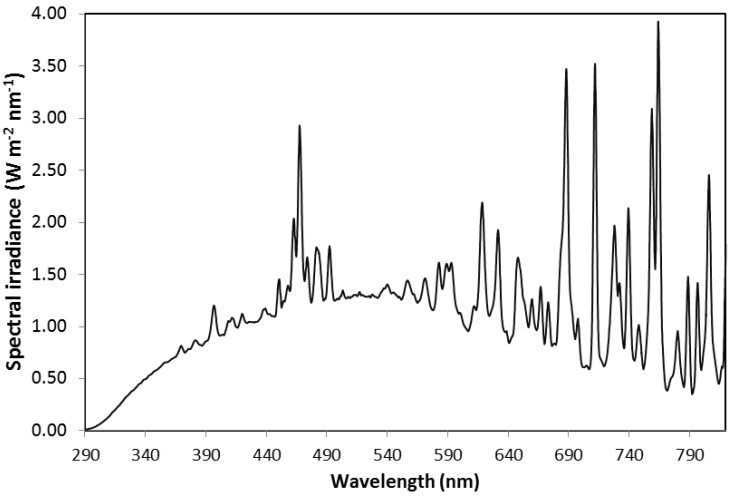

Figure 11 – Spectral irradiance of the 1500 W arc xenon lamp when using an outdoor UV filter, as given by the manufacturer (Solarbox 1500, Co.fo.me.gra, Italy). The spectrum is referred to a total irradiance of 550 Wm^{-2} between 290-800 nm.

4.2.3 Instrumentation

Quantitative analyses of OTC and BDE-209 were made by HPLC-UV, using a device which consists of a degasser DGU-20A5, a bomb LC-20AD, an UV-Vis detector SPD-20A and, a column oven CTO-10ASVP (T=25 ºC), all from Shimadzu. A New ACE® C18 column-PFP (5µm, 150 mm x 4.6 mm) and an injection loop of 20 µL were used. Cell temperature was maintained at 25 ºC. For quantification, the mobile phase used was 20 % acetonitrile and 80 % water acidified to pH 2 with formic acid for OTC and 100 % acetonitrile for BDE-209. The flow rate was 1.000 mL/min. The detection was done at 350 nm for OTC and at 230 nm for BDE-209.

A T90 + UV/VIS Spectrophotometer (**figure 12**) dual beam (PG Instruments Ltd), using a slit width of 2 nm, was used to acquire UV-Vis spectra of OTC and BDE-209 aqueous solutions. UV-Vis spectra of solutions were made in quartz cuvettes of 10 cm (rectangular cuvettes) and of 1 cm path length to the BDE-209 and OTC solutions, respectively.

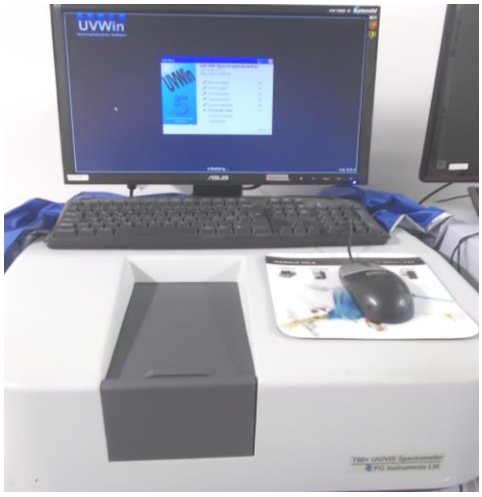

Figure 12 – T90 + UV/VIS Spectrophotometer dual beam

4.3 Results and discussion

4.3.1 Kinetic concepts

As referred in the previous chapter, when only one compound exists in solution and it suffers direct photolysis, its degradation by light obeys a first-order reaction. This is an integrated rate law described by **equations 2-6** (Atkins and De Paula 2006). *C* represents a compound; *t* is the time and *k* corresponds to the kinetic rate constant.

$$\frac{d[C]}{dt} = -k[C] \quad \textbf{(Eq.2)}$$

$$\frac{d[C]}{[C]} = -kdt \quad \textbf{(Eq.3)}$$

$$\int_{[C]_0}^{[C]} \frac{d[C]}{[C]} = -k\int_0^t dt \quad \textbf{(Eq.4)}$$

$$ln\left(\frac{[C]}{[C]_0}\right) = -kt \quad \textbf{(Eq.5)}$$

$$[C] = [C]_0 e^{-kt} \quad \textbf{(Eq.6)}$$

From these equations, one concludes that [C] decreases exponentially with time. Additionally, it is also possible to calculate the half-life time of reaction ($t_{1/2}$), according to **equations 7-8**. $t_{1/2}$ concerns the time taken for the concentration of a compound to decrease to half of its value and only depends on the kinetic rate constant (*k*) (Atkins and De Paula 2006).

$$kt_{1/2} = -ln\left(\frac{\frac{1}{2}[C]_0}{[C]_0}\right) = -ln\frac{1}{2} = \ln 2 \quad \textbf{(Eq.7)}$$

$$t_{1/2} = \frac{\ln 2}{k} \quad \textbf{(Eq.8)}$$

The values of half-life time and first-order kinetic rate constant are totally related to the specific experimental conditions adopted, namely to the total irradiance of the lamp.

4.3.2 Kinetics of BDE-209 photo-degradation in water

The degradation percentages for all irradiation times were calculated relatively to the dark controls (light protected solutions introduced inside the solar box together with the irradiated solutions); therefore, protected and exposed solutions were subjected to the same environmental conditions except exposition to radiation.

The kinetic results of BDE-209 photo-degradation in aqueous solution (5 µg/L) are presented in **figure 13** (Leal 2012), together with the curve $C/C_0 = e^{-kt}$, fitted to the data by non-linear regression using GraphPad Prism 6. In that equation, *k* is the rate constant, *t* is time and C_0 and *C* are the concentrations of BDE-209, when protected from light or exposed to it, respectively. The data for the variation of concentration of BDE-209, along irradiation time, were well fitted by the above mentioned equation (R^2 = 0.9687) showing that photo-degradation of BDE-209 in aqueous solution follows a pseudo first-order kinetics, with a rate constant of 0.0101 ± 0.0003 min^{-1}. The half-life time of BDE-209 in distilled water is 69 ± 2 minutes.

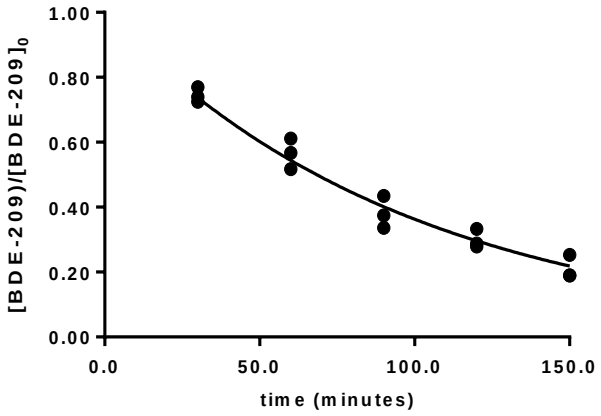

Figure 13 – Kinetics of BDE-209 photo-degradation in aqueous solution (three replicates)

4.3.3 Kinetics of OTC photo-degradation in water

The data acquired for kinetics of OTC photo-degradation were also well fitted (R^2=0.9755), by the non-linear regression, to the first-order equation (**Eq.6**). The results (**figure 14**) suggest that OTC photo-degradation in distilled water follows a pseudo first-order kinetics, whose first-order rate constant and the half-life time obtained were 0.0198 ± 0.0005 min^{-1} and 35.0 ± 0.9 minutes, respectively.

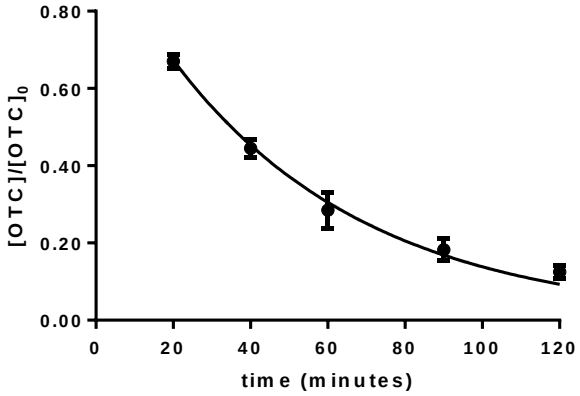

Figure 14 – Kinetics of OTC photo-degradation in distilled water. The vertical bars correspond to the standard deviation (n = 3)

4.3.4 Quantum yield for direct photo-degradation

The photo-degradation rate constant depends on the quantity of photons absorbed by each mole of compound per unit time (rate of light absorption) and also on the quantum yield (Challis et al. 2014).

Quantum yield (Φ) is a parameter of high relevance in photochemical studies that makes possible the comparison of results between different studies and may explain the differences in sunlight photo-degradation rates of compounds with similar spectral overlap (Calisto et al. 2011). However, this parameter is dependent on the type of light source (Challis et al. 2014). According to IUPAC, quantum yield is defined as the ratio between the amount of reactant consumed or product formed and the amount of photons absorbed (Braslavsky et al. 2011). It can be calculated from **equation 9**.

$$\Phi_{ave} = \frac{C_0 \times k}{\sum I^0_{\lambda_i} \times (1 - 10^{-\varepsilon_{\lambda_i} \times l \times C_0}) \times \Delta\lambda} \qquad \textbf{(Eq. 9)}$$

C_0 is the initial concentration of a contaminant in solution (mol.L^{-1}), k is the first-order rate constant (s^{-1}), ε is the molar absorptivity of a contaminant at λ_i (L.mol^{-1}.cm^{-1}), l is the path length inside the photo-reactor (≈ 1.4 cm) and $I^0_{\lambda_i}$ is the lamp irradiance at the wavelength λ_i (Ein.m^{-2}.s^{-1}.nm^{-1}), multiplied by the solution area exposed to light inside the container (m^2) and divided by the volume of solution (units of $I^0_{\lambda_i}$ = Ein.L^{-1}.s^{-1}.nm^{-1}). $\Delta\lambda$ corresponds to the wavelength interval of acquisition of the spectral irradiance of the lamp and λ_i is the central wavelength of that interval. The effective path length was approximated by the geometric average path length through the tube across its diameter. Thus, the effective path length (l) was calculated as the ratio between the solution volume and the cross-sectional area (diameter times height). For those calculations, and in all experiments, the quartz tubes were putted inside the photo-reactor in a leaning position and it was assumed that light came only from above (position of the lamp), as described in **figure 15**. Some uncertainty may be associated to this calculation because the tubes may also receive some radiation from below and the light incidence angle may be not perpendicular to the cross section (diameter times height).

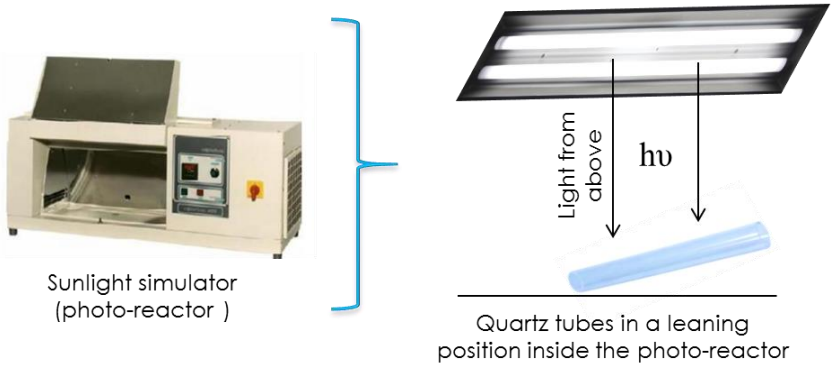

Figure 15 – Positions of quartz tubes and direction of light from sunlight simulator.

Quantum yield (Φ) commonly ranges between 0 and 1 and Φ is smaller the higher the degree of collisional deactivation and fluorescent of excited molecule (M*) (Levine 2009). In turn, Φ higher than 1 indicates the induction of chain reactions (Christensen and Li 2014). In the present work, all determinations of the average quantum yields were performed by radiometry, using **equation 9** (Chiron et al. 2006; Calisto et al. 2011).

For BDE-209, the quantum yield was determined for the range 290-350 nm, which corresponds to the maximum rate of light absorption of BDE-209 (**figure 16**) under the irradiation by simulated solar radiation in the solarbox. The quantum yield value obtained was 0.010 ± 0.001. The rate of light absorption at each wavelength was calculated using **equation 10,** where the symbols have the meaning previously described.

$$I_{\lambda_i}^{abs} = I_{\lambda_i}^{0} \times (1 - 10^{-\varepsilon_{\lambda_i} \times l \times C_0}) \qquad \textbf{(Eq.10)}$$

For OTC, the quantum yield was determined for the range between 290 and 450 nm, corresponding to its maximum of light absorption (**figure 17**). The quantum yield value obtained was 4.22 x10^{-4} ± 0.33 x10^{-4}. Other data for the quantum yield of OTC and BDE-209 in water using simulated sunlight are not known.

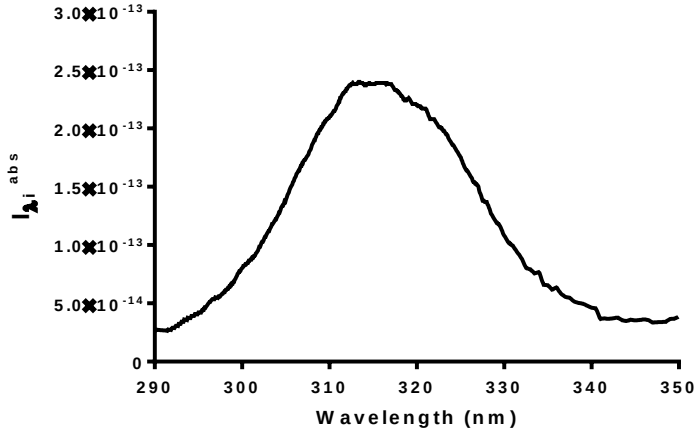

Figure 16 – Rate of light absorption of BDE-209 for each wavelength. The value of $I_{\lambda i}^{abs}$ has a maximum for λ = 313 nm.

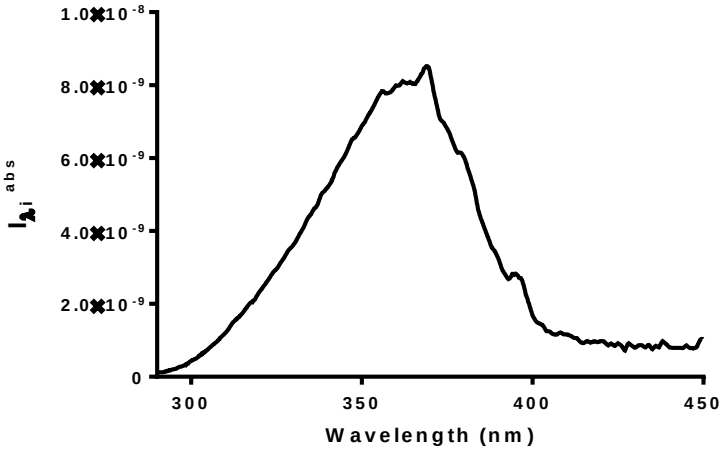

Figure 17 – Rate of light absorption versus wavelength for OTC in deionised water (pH 4.6). The value of $I_{\lambda i}^{abs}$ has a maximum for λ = 369 nm.

4.3.5 Outdoor half-life times

When the experiments are performed in laboratory, under simulated sunlight, it is useful to convert the experimental half-life times into the outdoor half-life times, to better simulate the real environmental conditions. The method used for this calculation requires the knowledge of the quantum yield calculated above and assumes that the sunlight radiation used in the laboratory experiments correctly simulates the solar spectrum (EPA 1998; Schwarzenbach et al. 2003). For that, the near surface specific rate of light absorption (k_a^0) needs to be firstly calculated, according to **equation 11** (Schwarzenbach et al. 2003).

$$k_a^0 = \sum_{\lambda}^{\lambda i} 2.3 \times Z(\lambda) \times \varepsilon_i(\lambda) \quad \textbf{(Eq.11)}$$

$Z(\lambda)$ corresponds to solar energy emitted by unit area and unit of time (millieinstein.cm^{-2}.s^{-1}) for midday (noon) at sea level, at 40º N latitude, for a midseason clear summer day, over a given wavelength range $\Delta\lambda$. The $Z(\lambda)$ values were obtained from Schwarzenbach et al. (2003). The $\varepsilon_i(\lambda)$ is the average molar extinction coefficient of the compound within each $\Delta\lambda$ range (290-350 nm for BDE-209 and 290-450 nm for OTC). The units of k_a^0 are millieinstein.cm^{-3}.dm^3.mol^{-1}.s^{-1} (= einstein.mol^{-1}.dm^3.s^{-1}).

Then, the near-surface first-order rate constant for direct photolysis (k_p^0) is determined using **equation 12** (Schwarzenbach et al. 2003). Lastly, the outdoor half-life time near aqueous surface may be determined as described in **equation 8**, only replacing the first-order rate constant (*k*) by the near-surface first-order rate constant (k_p^0).

$$k_p^0 = \Phi \times k_a^0 \quad \textbf{(Eq. 12)}$$

The predicted outdoor half-life times for a midsummer day, at 40"N Latitude (Sea Level) under clear skies are 3.5 h and 1.6 h for BDE-209 and OTC, respectively. For the two compounds, the diurnal fluctuations in sunlight intensity (24-hour averaged Z(λ)) were not considered because the outdoor half-life time calculated is lower than 24 hours.

BDE-209 photo-degradation studies in water are not known under natural or simulated sunlight radiation. In what concerns to OTC, the kinetic results attained are the same order of magnitude of other obtained by Xuan et al. (2010). These authors performed irradiation experiments under natural sunlight irradiation in a partially sunny day on June 28, 2005 in Riverside (34.95 ºN) and obtained a half-life time of 4.61 h for the

OTC concentration of 25 mg/L. Note that the experiments made by the authors were conducted in glass serum bottles, which restrict the radiation of absorption for low wavelengths. So, it is expected that, in experiments performed in quartz containers, as is the case of this work, the photolysis rate constant is higher (Xuan et al. 2010) and the half-life time lower than in glass containers, what is in agreement with results obtained in the present work.

4.3.6 Effect of HS on photo-degradation

In order to assess the effect of organic matter, represented by HS, on photo-degradation of the two compounds, new irradiation experiments in water were performed in the absence and in the presence of three fractions of aquatic HS – HA, FA and XAD-4 – with different concentrations (8 mg/L and 16 mg/L) during 60 min (time of irradiation). The results obtained for each compound are presented in **figure 18**, where one observes that any fraction of HS, at 8 mg/L and 16 mg/L significantly ($p < 0.001$) delays their photo-degradation.

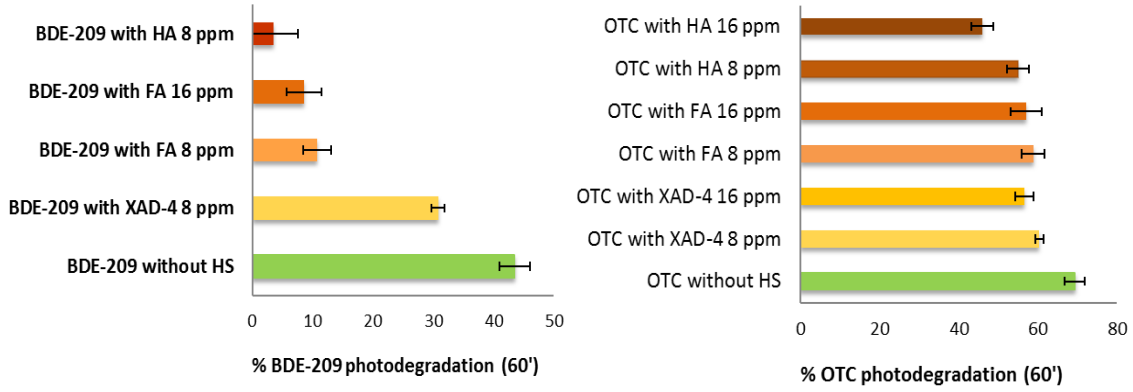

Figure 18 – Percentages of photo-degradation of BDE-209 (5 µg/L) and OTC (4 mg/L) in the absence and in the presence of different fraction of HS – humic acids, fulvic acids and XAD-4 fraction – at 8 mg/L and 16 mg/L.

The retardation effect caused by HS is frequently attributed to the light-screening. To verify this hypothesis, the overall screening factor ($S_{\Sigma\lambda}$) will be calculated for each fraction of HS. But, prior to calculate the $S_{\Sigma\lambda}$, it is important to understand what is effectively the screening effect.

In a water column (**figure 19**), the sunlight that reaches the surface water can be measured by the spectral photon fluence rate at sea level, represented by W(λ). This rate

is strongly dependent on weather conditions and geographic location. Within the water column, the light is scattered by suspended particles and absorbed by particles and dissolved species. This is the filtering or screening effect caused mainly by the coloured HS. Due to that effect, the sunlight photon fluence rate – W(λ) – that attains the contaminant at a depth Z is lower than the photon fluence rate at the surface: $W(\lambda, Z_{mix}) < W(\lambda)$.

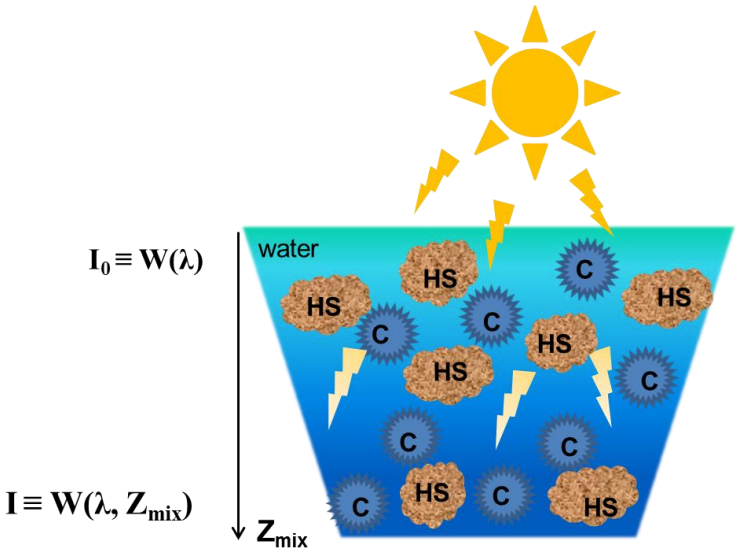

Figure 19 – Schematic representation of screening effect caused by HS to a compound in a water column.

According to the Lambert-Beer law, the two photon fluence rates are related by **equation 13**, where α(λ) represents the attenuation coefficient of water per unit path length and may be determined in a spectrophotometer for a non-turbid water. The optical path length (*l*) can be equal to the water column depth Z, but it commonly undergoes reflection in the suspended particles, implying that *l* be higher than depth Z. Therefore, *l* is obtained multiplying a distribution function D(λ), which is a correction factor, and the depth Z (**equation 14**) (Schwarzenbach et al. 2003).

$$-\log\left(\frac{W(\lambda,Z_{mix})}{W(\lambda)}\right) = \alpha(\lambda) \times l \qquad \textbf{(Eq.13)}$$

$$l = D(\lambda) \times Z_{mix} \qquad \textbf{(Eq.14)}$$

Thus, the amount of light absorbed, at given wavelength λ, by water column per unit surface area and time is described by **equation 15**. From this, the rate of light absorption per unit volume is determined as explained in **equation 16**.

Rate of light absorption by the water per unit surface area =

$$= W(\lambda) - W(Z_{mix}, \lambda) = W(\lambda) \times [1 - 10^{-\alpha_D(\lambda) \times Z_{mix}}] \quad \textbf{(Eq.15)}$$

Rate of light absorption by the water per unit volume =

$$= \frac{W(\lambda) \times [1 - 10^{-\alpha_D(\lambda) \times Z_{mix}}]}{Z_{mix}} \quad \textbf{(Eq.16)}$$

W(λ) is the spectral photon fluence rate (millieinstein.cm^{-2}.s^{-1}.nm^{-1}), $\alpha_D(\lambda)$ corresponds to apparent or diffuse attenuation coefficient (cm^{-1}) and is a measure of how much radiation is absorbed by the mixed water layer per unit vertical distance. Z_{mix} is the mean depth of the mixed water body (cm).

Considering now the presence of a compound, the fraction of radiation absorbed by it (F) relates the absorptivity and concentration of the contaminant and the absorbance of the water column per unit path length (**equation 17**). Thus, taking into account the rate of light absorption by the water per unit volume (**equation 16**) and the fraction of radiation absorbed by a contaminant (**equation 17**), the specific rates of light absorption of the contaminant in water column at depth Z_{mix} ($k_a(\lambda)$) and at near-surface ($k_a^0(\lambda)$) may be calculated using **equations 18** and **19**, respectively (Schwarzenbach et al. 2003).

$$F = \frac{\varepsilon_i \times C_i}{\alpha(\lambda)} \quad \textbf{(Eq.17)}$$

$$k_a = \frac{W(\lambda) \times \varepsilon_i(\lambda) \times [1 - 10^{-\alpha_D(\lambda).Z_{mix}}]}{Z_{mix} \times \alpha(\lambda)} \quad \textbf{(Eq.18)}$$

$$k_a^0(\lambda) = 2.3 \times W(\lambda) \times D^0(\lambda) \times \varepsilon_i(\lambda) = 2.3 \times Z(\lambda) \times \varepsilon_i(\lambda) \quad \textbf{(Eq.19)}$$

W(λ), α(λ), $\alpha_D(\lambda)$ and Z_{mix} have the meaning previously described, ε_i (λ) is the molar absorptivity of compound ($mol^{-1}.L^{-1}.cm^{-1}$), $D_0(\lambda)$ is a distribution function for shallow depths ($Z_{mix} \leq 50$ cm) and Z(λ) corresponds to solar energy emitted by unit area and unit of time ($millieinstein.cm^{-2}.s^{-1}$). W(λ) and Z(λ) are specific values for a determined geographic location, season and time of day. Tabulated values of W(λ) and Z(λ) for different conditions can be found in literature (Zepp and Cline 1977; Leifer 1988; EPA 1998; Schwarzenbach et al. 2003). α values are particularly affected between 300 and 600 nm and tend to decrease with enhancing wavelength (Schwarzenbach et al. 2003).The ratio between the two specific rates of light absorption at depth Z_{mix} ($k_a(\lambda)$) and at near-surface ($k_a^0(\lambda)$) allows to calculate the light screening factor caused by HS (**equation 20**).

$$S(\lambda) = \frac{W(\lambda)\times\varepsilon_i(\lambda)\times[1-10^{-\alpha_D(\lambda).Z_{mix}}]}{Z_{mix}\times\alpha(\lambda)\times 2.3\times W(\lambda)\times D^0(\lambda)\times\varepsilon_i(\lambda)} = \frac{1-10^{-\alpha_D(\lambda).Z_{mix}}}{2.3\times Z_{mix}\times\alpha_D^0(\lambda)} \qquad \textbf{(Eq. 20)}$$

$\alpha_D^0(\lambda)$ is the diffuse attenuation coefficient at the near surface and the others symbols have the meaning previously described. Note that $D^0(\lambda) = \alpha_D^0(\lambda)/\alpha(\lambda)$ (Schwarzenbach et al. 2003). A value of 1.0 for S(*λ*) means that the light is not significantly attenuated by dissolved humic substances (Miller and Chin 2002; Calisto et al. 2011).

When a contaminant absorbs light only relatively narrow wavelength range, a single value of $\alpha(\lambda)$ can be used instead of $\alpha_D(\lambda)$ value. A good estimate of the effect of light attenuation in the presence of HS can be achieved calculating *S*(*λ*) using the *α* value at the wavelength λ_m of the maximum specific rate of light absorption (Schwarzenbach et al. 2003). The wavelength λ_m corresponds to the maximum of the curve $I_{\lambda_i}^{abs}$ versus *λ*. For a given solution (laboratory conditions), the inside width of the cuvette – that may be presented as Z_{mix} – is equal to path length of the light, *l*(λ). Thus, the light screening factor can be expressed according to **equation 21**. Note that this equation is valid only in systems in which the attenuation due to the HS fractions is much higher than the attenuation of the contaminant, as is the case in the present work.

$$S_{\lambda_m} = \frac{(1-10^{-\alpha_\lambda\times l})}{2.3\times\alpha_\lambda\times l} \qquad \textbf{(Eq. 21)}$$

The value obtained to S(λ_m) represents the worst of the scenario of the attenuation of sunlight by the HS (Calisto et al. 2011). However, an integrated value of the screening factor ($S_{\Sigma\lambda}$) can also be determined, calculating the integrated area of a plot of S_λ versus wavelength and dividing by theoretical area of the plot if no inner filtering occurred (i.e. S_λ = 1.0 for all wavelengths) (Guerard et al. 2009). From the screening factor value, it is possible to estimate the kinetic rate constants of the compounds in the presence of these fractions, multiplying the value of screening by the first-order rate constant in water, in the absence of HS (**equation 22**) (Guerard et al. 2009).

$$k_{HS} = S \times k \qquad \textbf{(Eq.22)}$$

This rate in the presence of HS (k_{HS}) may be calculated separately for each fraction, or may consider a mixture $S_{\Sigma\lambda}$ once these three fractions are together in the environment. The mixture $S_{\Sigma\lambda}$ or $S_{\lambda m}$ is calculated using an α_λ (in **equation 21**), which is a weighted average of the α_λ (cm^{-1}) of each HS fraction, considering the relative abundances of each fraction on the water sample (relative abundances are presented in *subchapter 4.2.1*). Based on the kinetic rate constants obtained, the photo-degradation percentages for the respective solutions of BDE-209 and OTC with HS are also estimated. The $S_{\Sigma\lambda}$ values obtained for each HS fraction, for the two compounds, as well as the data determined from them are presented in **table 6** (A and B).

The results from **table 6** suggest that the light-screening is not the unique effect of retardation because the photo-degradation experimentally observed is lower than the photo-degradation estimated based on $S_{\Sigma\lambda}$ values. For OTC, the increase of HS concentrations (8 mg/L to 16 mg/L) only had a significant effect for the HA fraction (p = 0.008). For the FA and XAD-4 fractions, the increase of concentration did not significantly affect the retardation of OTC photo-degradation ($p > 0.05$).

The increase of FA concentration also did not significantly affect the retardation of BDE-209 photo-degradation. Comparing the photo-degradation percentages observed and estimated for BDE-209 in the presence of each HS fraction, one can observe a big difference between these two sets of values.

Table 6 (A and B) - Comparison of results obtained for aqueous solutions of OTC and BDE-209 in the presence of each fraction of HS (Humic Acids, Fulvic Acids and XAD-4 fraction), at 8 mg/L and 16 mg/L, for the same time of irradiation (60 min). S_λ is the screening effect caused by the presence of each HS in solution for the wavelength range of absorption of compounds (OTC: 290-450 nm; BDE-209: 290-350 nm)

6A	Aqueous solution of OTC			
	$S_{\lambda\ (290\text{-}450\ nm)}$	$k_{estimated}$ (min^{-1}) ± SD	% Photodegration estimated ± SD	% Photodegration observed ± SD
With HA 8 ppm	0,88	0.0175 ± 0.0004	65.0 ± 0.8	55.0 ± 2.8
With HA 16 ppm	0,79	0.0156 ± 0.0004	60.8 ± 0.9	45.9 ± 2.8
With FA 8 ppm	0,94	0.0187 ± 0.0004	67.4 ± 0.8	58.8 ± 2.9
With FA 16 ppm	0,89	0.0177 ± 0.0004	65.3 ± 0.8	57.0 ± 3.9
With XAD-4 8 ppm	0,97	0.0191 ± 0.0004	68.3 ± 0.8	60.3 ± 1.1
With XAD-4 16 ppm	0,93	0.0185 ± 0.0004	67.0 ± 0.8	56.6 ± 2.3

6B	Aqueous solution of BDE-209			
	$S_{\lambda(290\text{-}350\ nm)}$	$k_{estimated}$ (min^{-1}) ± SD	% Photodegration estimated ± SD	% Photodegration observed ± SD
With HA 8 ppm	0,82	0.0083 ± 0.0002	39.3 ± 0.6	3.6 ± 2.3
With HA 16 ppm	--	--	--	--
With FA 8 ppm	0,91	0.0092 ± 0.0003	42.5 ± 1.0	10.7 ± 3.9
With FA 16 ppm	0,81	0.0082 ± 0.0002	38.9 ± 0.6	8.6 ± 2.0
With XAD-4 8 ppm	0,94	0.0095 ± 0.0003	43.5 ± 1.0	30.8 ± 6.2
With XAD-4 16 ppm	--	--	--	--

Figure 20 shows the relation between the light-screening caused by the presence of HS and the compounds photo-degradation percentage (estimated and observed). When light-screening is the unique effect, there is a linear relation between the decrease of photo-degradation percentage and the decrease of $S_{\Sigma\lambda}$ values (graphically represented by "♦ estimated"). For the case of OTC, the observed photo-degradation values, although lower than the values estimated based on light-screening, follow the same graphic tendency, what suggest that, in this case, the light-screening effect caused by the presence of HS is the predominant delaying effect.

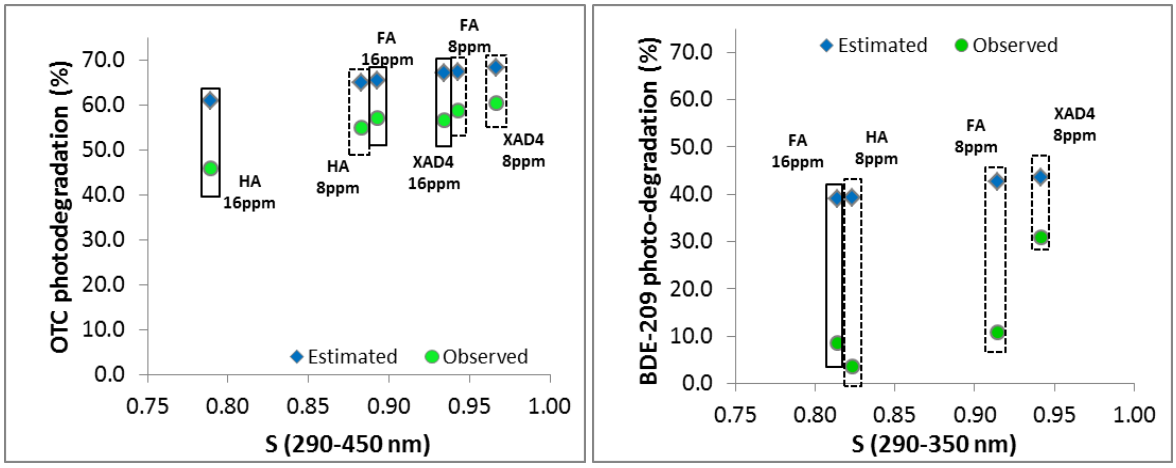

Figure 20 – Relation between the screening effect caused by the presence of HS (8 mg/L and 16 mg/L) and the compounds (OTC and BDE-209) photo-degradation percentages. The photo-degradation values estimated from screening values are represented by "♦ estimated" and the photo-degradation values observed experimentally are represented by "● observed". The set values inside ⬚ correspond to [HS] = 8 mg/L and the set values inside☐ correspond to [HS] = 16 mg/L.

Contrarily to what happens for OTC, the decrease of BDE-209 photo-degradation observed comparatively with photo-degradation estimated is high and does not follow the tendency that would be expected by the light-screening. The absorbance of FA and XAD-4 fractions are more similar between them than the absorbance of FA and HA fractions (**figure 21**), which is reflected in the values of the light screening factors obtained. However, one observes that HA and FA fractions delayed the BDE-209 photo-degradation in a similar way, while XAD-4 fraction did not have any effect on its photo-degradation. BDE-209 is a very hydrophobic compound, whereby its tendency to associate to the more hydrophobic fractions (HA and FA) is higher than to the hydrophilic fraction (XAD-4).

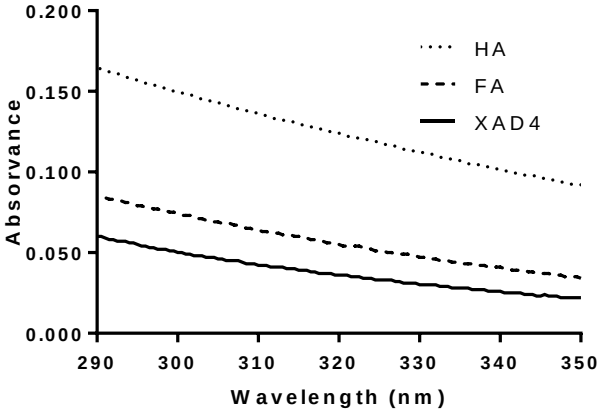

Figure 21 – UV spectra of HS (8 mg/L) in aqueous solution.

These results suggest that the delaying effect of humic substances cannot be attributed only to a light filtering effect. To assess the possible hydrophobic interaction of BDE-209 with each fraction of HS, some new experiments were made. Firstly, aqueous solutions of each fraction of HS with and without BDE-209 were prepared and analyzed by molecular fluorescence. For these experiments, aqueous solutions containing HS (16 ppm) were saturated with a large excess of BDE-209. All mixtures solution/solid BDE-209 were stirred (500 rpm) for a few hours, and during the same time. The solutions were filtered by 0.22 µm filters and their synchronous fluorescence spectra were registered. These spectra were obtained with excitation between 240 and 490 nm, excitation and emission slits of 5 nm and an offset of 60 nm. Three replicates of each experiment were performed. They are presented in **figures 22A-C**.

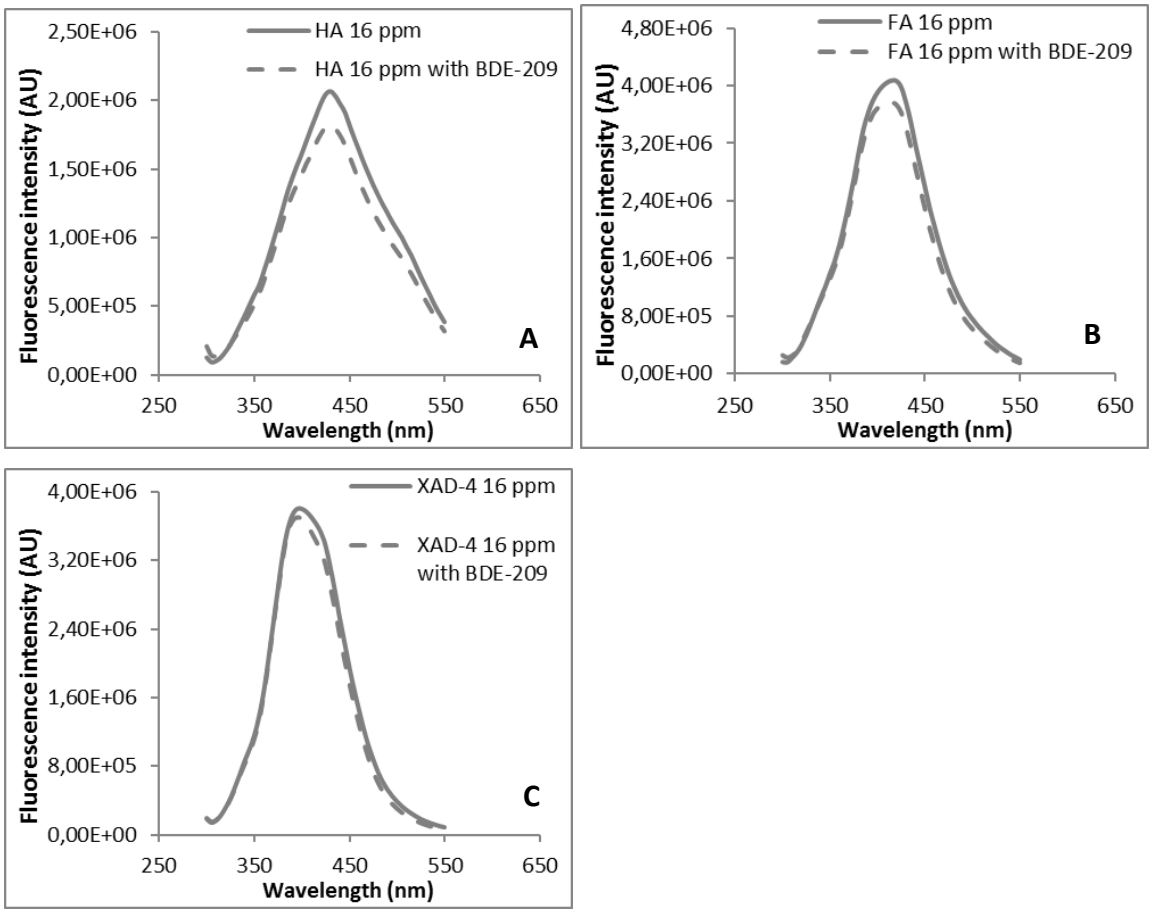

Figure 22 – Average fluorescence spectra of aqueous solutions of each HS (16 mg/L) and of aqueous solutions of each fraction of HS (16 mg/L) with BDE-209. Spectra presented are an average of three replicates.

The fluorescence intensities at the maximum of the fluorescence spectra of each HS fraction, in the absence and in the presence of BDE-209, were compared by one-way ANOVA. The results show that a significant decrease of HA fluorescence intensity occurs in the presence of BDE-209 (p=0.02) (**figure 22A**) and that there is not a significant effect caused by BDE-209 in XAD-4 fraction (p=0.40) (**figure 22C**). For the FA fraction, it seems that a fluorescence decrease occurs in presence of BDE-209 (**figure 22B**), but the statistical analysis is not conclusive (p=0.06). Thus, the hydrophobic associations between BDE-209 and HS seems to be dominant, which can protect the contaminants of photo-degradation (Clark et al. 2007) through the quenching or deactivation of the excited-state. On the other hand, the screening effect caused by the light absorption by HS seems to have only a small contribution, although both effects contribute to the inhibition of BDE-209 photo-degradation. In addition to these delaying effects, one should consider that HS can also produce reactive species that can induce the indirect photo-degradation of BDE-209 and, consequently, increase the degradation rate. Taking into consideration the results obtained, this effect is negligible or obscured by the delaying effects observed. This reduction of the photo-degradation rate of BDE-209 by HS can have important consequences on the half-life of BDE-209 in natural water.

For the case of OTC, the hydrophobic association with HS is not expectable due to the low hydrophobicity of the compound. However, another effect caused by HS can justify the delay on OTC photo-degradation beyond the delay caused by the light-screening. In addition to the direct photo-degradation, OTC is also able to self-photosensitize (Chen et al. 2011). In the presence of HS, a competition of HS by the reactive species produced by OTC, namely singlet oxygen, may occur. If HS react with $^1O_2$, one of the possible photo-degradation pathways – self-photosensitization – is inhibited and the photo-degradation delayed.

Similar to what was done above in the absence of HS, the outdoor half-life time of BDE-209 and OTC in the presence of HS can be calculated assuming that the radiation used correctly simulates sunlight. Considering **equation 23,** the first order rate constant for direct photolysis (k_p) can be calculated and, from obtained value, an outdoor half-life time of the compound can be predicted, as previously explained (Schwarzenbach et al. 2003; Guerard et al. 2009). The mixture of HS fractions (8 mg/L for BDE-209 and 16 mg/L for OTC) was considered to these calculations, taking into account the relative abundances of each fraction in river Vouga, used in this work.

$$k_p = S_{\Sigma\lambda} \, x \, k_p^{\,0} \qquad \textbf{(Eq. 23)}$$

The outdoor half-life times predicted in the presence of HS for BDE-209 and OTC, for a midsummer day, under clear sky, at sea level and 40 ºN, were 3.9 hours and 1.79 hours, respectively. These values are only slightly higher than the corresponding half-life times predicted in the absence of HS (3.5 hours and 1.60 hours, respectively). Nevertheless, the reduction caused by HS on the photo-degradation rate of BDE-209 and OTC can have important consequences on their half-life times in natural water. This effect will be probably more important in rivers than in the ocean, since in the ocean HS are less hydrophobic and HA represent a very small fraction of marine HS (Esteves et al. 2009).

4.4 Conclusions

To sum up, the light-screening does not completely explain the retardation effect of humic substances on the photo-degradation of OTC and BDE-209. These are two compounds with very different characteristics that seem to suffer different interactions with dissolved HS. On one hand, the screening effect seems to be the predominant delaying effect on OTC photo-degradation at sea level. One the other hand, for BDE-209, which is a very hydrophobic compound, the light screening caused by HS seems to have a minor contribution for the delaying effect observed. In this case, the association between BDE-209 and the HS, namely the most hydrophobic fractions (HA and FA) is proposed as the major delaying effect. Although the HS represent a large part of the natural dissolved organic carbon, they do not fully mimic the composition of natural water. In natural aquatic systems, several other factors must be considered, among them, the nature and composition of dissolved organic matter, the amount of suspended particulates or the presence of inorganic compounds.

Additionally, the work described in this chapter estimated, for the first time, with these irradiation conditions, the average quantum yield of BDE-209 and OTC photo-degradation in water (0.010 ± 0.001 and 4.22 $x10^{-4}$ ± 0.33 x 10^{-4}, respectively) and their outdoor half-life times in the absence and in the presence of HS, for midsummer days, at sea level and at 40º N of latitude.

With respect to BDE-209, although it is an indirect contaminant of aquaculture's water, further studies within this doctoral thesis were not made. There are several reasons for that, among which stand out the low solubility of the compound in water, the technical difficulty of implementing the methodology and the lower environmental relevance of this compound compared to other contaminants introduced directly into the aquaculture's water, as is the case of oxytetracycline.

4.5 References

Atkins, P. and J. De Paula (2006). *Atkins' Physical Chemistry*. New York, W. H. Freeman and Company

Braslavsky, S. E., A. M. Braun, A. E. Cassano, A. V. Emeline, M. I. Litter, L. Palmisano, V. N. Parmon, N. Serpone, O. M. Alfano, M. Anpo, V. Augugliaro, C. Bohne, S. Esplugas, E. Oliveros, C. von Sonntag, R. G. Weiss and M. Schiavello (2011). Glossary of terms used in photocatalysis and radiation catalysis (IUPAC Recommendations 2011). *Pure and Applied Chemistry* **83**(4): 931-1014.

Calisto, V., M. R. M. Domingues and V. I. Esteves (2011). Photodegradation of psychiatric pharmaceuticals in aquatic environments - Kinetics and photodegradation products. *Water Research* **45**(18): 6097-6106.

Calisto, V. M. A. (2011). Environmental occurence and fate of psychiatric pharmaceuticals. Department of Chemistry. Aveiro, University of Aveiro. **PhD:** 218.

Challis, J. K., M. L. Hanson, K. J. Friesen and C. S. Wong (2014). A critical assesment of the photodegradation of pharmaceuticals in aquatic environments: defining our current understanding and identifying knowledge gaps. *Environmental Science Processes & Impacts* **16**: 672-696.

Chen, Y., H. Li, Z. P. Wang, T. Tao and C. Hu (2011). Photoproducts of tetracycline and oxytetracycline involving self-sensitized oxidation in aqueous solutions: Effects of Ca^{2+} and Mg^{2+}. *Journal of Environmental Sciences-China* **23**(10): 1634-1639.

Chiron, S., C. Minero and D. Vione (2006). Photodegradation processes of the Antiepileptic drug carbamazepine, relevant to estuarine waters. *Environmental Science & Technology* **40**(19): 5977-5983.

Christensen, E. R. and A. Li (2014). *Physical and Chemical Processes in the Aquatic Environment*, Wiley

Clark, C. D., W. J. De Bruyn, J. Ting and W. Scholle (2007). Solution medium effects on the photochemical degradation of pyrene in water. *Journal of Photochemistry and Photobiology a-Chemistry* **186**(2-3): 342-348.

EPA (1998). Direct Photolysis Rate in Water By Sunlight. Fate, Transport and Transformation Test Guidelines. Washington, U. S. Environmental Protection Agency**:** 37.

Esteves, V. I., N. M. A. Cordeiro and A. D. Duarte (1995). Variation on the adsorption efficiency of Humic Substances from Estuarine waters using XAD resins. *Mar Chem* **51**(1): 61-66.

Esteves, V. I., M. Otero and A. C. Duarte (2009). Comparative characterization of humic substances from the open ocean, estuarine water and fresh water. *Organic Geochemistry* **40**(9): 942-950.

Guerard, J. J., P. L. Miller, T. D. Trouts and Y. P. Chin (2009). The role of fulvic acid composition in the photosensitized degradation of aquatic contaminants. *Aquatic Sciences* **71**(2): 160-169.

Kordel, W., M. Dassenakis, J. Lintelmann and S. Padberg (1997). The importance of natural organic material for environmental processes in waters and soils. *Pure & Appl. Chem* **69**(7): 1571-1600.

Leal, J. F. (2012). Fotodegradação do retardador de chama BDE-209. Chemistry. Aveiro, University of Aveiro. **Master:** 91.

Leifer, A. (1988). *The Kinetics of Environmental Aquatic Photochemistry*. Washington DC, American Chemical Society

Levine, I. N. (2009). *Physical Chemistry*. New York, McGraw-Hill Higher Education

Miller, P. L. and Y. P. Chin (2002). Photoinduced degradation of carbaryl in a wetland surface water. *Journal of Agricultural and Food Chemistry* **50**(23): 6758-6765.

OECD (2000). Phototransformation of Chemicals in Water - Direct and Indirect Photolysis. OECD Guideline for testing of chemicals Proposal for a new guideline**:** 60.

Santos, M. E. B. H. (1994). Extracção, caracterização e comportamento ácido-base de substâncias húmicas aquáticas. Aveiro, University of Aveiro. **Doctor**.

Schwarzenbach, R. P., P. M. Gschwend and D. M. Imboden (2003). *Environmental Organic Chemistry*. New Jersey, John Wiley & Sons, Inc.

Sulzberger, B. and E. Durisch-Kaiser (2009). Chemical characterization of dissolved organic matter (DOM): A prerequisite for understanding UV-induced changes of DOM absorption properties and bioavailability. *Aquat Sci* **71**(2): 104-126.

Thurman, E. M. (1985). *Organic Geochemistry of Natural Waters*, Kluwer Academic Publishers

Xuan, R. C., L. Arisi, Q. Q. Wang, S. R. Yates and K. C. Biswas (2010). Hydrolysis and photolysis of oxytetracycline in aqueous solution. *Journal of Environmental Science and Health Part B-Pesticides Food Contaminants and Agricultural Wastes* **45**(1): 73-81.

Zepp, R. G. and D. M. Cline (1977). Rates of direct photolysis in aquatic environment. *Environmental Science & Technology* **11**(4): 359-366.

Zepp, R. G., D. J. Erickson, N. D. Paul and B. Sulzberger (2011). Effects of solar UV radiation and climate change on biogeochemical cycling: interactions and feedbacks. *Photochemical & Photobiological Sciences* **10**(2): 261-279.

Chapter 5: Characterization of aquaculture's water [4]

The components of natural water can affect in different ways the photo-degradation of contaminants, contributing to their sensitization or inhibition. Since the photo-degradation studies will be performed using natural brackish aquaculture's water samples, they were previously characterized. The physical-chemical parameters considered were pH, salinity, total suspended solids (TSS), organic carbon and some inorganic ions (calcium, magnesium and iron). Additionally, water samples were characterized using molecular fluorescence and UV-Vis spectroscopies. Since the nature and composition of natural components may be affected by water treatment processes, water samples were collected at different locals of the water treatment circuit, from two different aquaculture companies (A and B).

The most significant differences between the two companies are the concentrations of TSS, DOC, particulate total carbon (TC_{part}) and calcium. In what concerns variations between sampling sites within each company, namely before and after ozonation, one observed that, in the two companies, ozonation did not induce significant changes of DOC. However, in one of companies, where DOC values are lower and a higher ozone dose is used, fluorescence and UV-visible spectroscopic characterization suggest a decrease of aromaticity and changes in nature of dissolved organic matter after ozonation.

---

[4] Adapted from:

- **J.F. Leal**, V.I. Esteves, E.B.H. Santos (2016). Use of sunlight to degrade oxytetracycline in marine aquaculture's waters. *Environmental Pollution*, **213**: 932-939.

5.1 Contextualization

The kinetics and mechanisms of contaminants photo-degradation depend on water composition, namely on inorganic compounds and type and content of dissolved organic matter (DOM) (Prabhakaran et al. 2009). In what concerns to DOM, its influence is dependent on its composition and concentration (Guerard et al. 2009), which can vary among different coastal water and be influenced by the fish production procedures in aquaculture. Besides, the composition and concentration of DOM may also vary along water treatment circuit of aquaculture systems. In addition to DOM, other components of natural matrices may influence the contaminants photo-degradation, namely suspended solids, which may scatter radiation, and inorganic compounds. For instance, among the several inorganic constituents present in aquaculture's water, calcium and magnesium have been proposed as affecting the OTC photo-degradation (Xuan et al. 2010; Chen et al. 2011). In fact, these are two of the main constituents of seawater (salinity ≈ 35 ‰). Some authors found concentrations of 1290 mg/L for magnesium and 412 mg/L for calcium, whereby their possible influence on OTC photo-degradation should not be neglected (Wright et al. 2013). Thus, a short characterization of samples collected at different points of the treatment circuits of the two aquaculture companies was performed.

5.2 Materials and methods

5.2.1 Planning and sampling

Natural water samples from two different aquaculture companies in the central region of Portugal (designated as company A and company B) of intensive production were collected twice (two independent samplings per each company). The first and second samplings were performed in April/May 2014 and in September/October 2014, respectively. These two companies have distinct water circuits, but have some common steps of water treatment. In the two companies (A and B), water samples were collected before entering in the production tanks (blank control, L0 – water intake), at the output of tanks (L1), after mechanical filter (L2) and after ozonation (L3). Additionally, in company B, water samples were collected after the biological filter (L2b). For each sampling site, three to six replicates were collected in each sampling. All water samples collected were characterized regarding to the following parameters: pH, salinity, total suspended solids (TSS), dissolved organic carbon (DOC), total and inorganic carbon of

suspended particles (TC_{part} and IC_{part}) and some dissolved metals (iron, calcium and magnesium). In addition, spectroscopic characteristics of water samples were analysed.

The water samples used to determine dissolved metals were collected in polypropylene flasks (100 mL). In laboratory, these samples were acidified with nitric acid 65 % (for analysis, Emsure®) at pH < 2 and stored in the refrigerator.

The material used for the total suspended solids and carbon determinations was previously washed with NaOH followed by ultrapure water to minimize the contamination with organic matter. The material used for determination of dissolved metals was previously washed with HNO_3 4M followed by water to prevent the contamination with metals ions.

5.2.2 Characterization methods of aquaculture's water

The characterization of water samples was performed according to the recommendations of Standard Methods For the Examination of Water & Wastewater (Eaton et al. 2005) and the procedures are thoroughly described below.

Total suspended solids (TSS)

- ✓Weight the glass microfiber filter 1.2 µm (diameter 47 mm, GF/C, Whatman®)
- ✓Wet / rinse the filter before passing the sample.
- ✓Stir the sample and filter it (1L).
- ✓Carefully, remove the filter containing the suspended solids and place it on a support of aluminium.
- ✓Repeat the previous four steps for each replicate of each sampling place.
- ✓Dry in oven all samples at 105 °C during 1 hour.
- ✓Cool in desiccator.
- ✓Weight the filter + suspended solids in the analytical balance.
- ✓Repeat the last three steps until obtaining a constant weight.

Dissolved organic carbon (DOC)

- ✓For calibration curve, prepare standards of potassium hydrogen phthalate ($KHC_8H_4O_4$) and analyse.

✓Acidify each sample previously filtered (glass fibre filter) with 2 % (v/v) of HCl 2M.

✓Purge with nitrogen each sample during 10 minutes.

✓Cover with Parafilm® and analyse using a total organic carbon analyser TOC-VCPH.

Total carbon in suspended solids (TC_{part})

✓For calibration, weight different masses of glucose, introduce them in a small ceramic boat, in the oven of the accessory for solids of the total carbon analyser TOC-VPH, and analyse by combustion at 900 ºC.

✓Put each glass microfiber filter containing the suspended solids of each water sample inside the above mentioned support, and determine the total carbon content.

Inorganic carbon in suspended solids (IC_{part})

✓For calibration, introduce known quantities of Na_2CO_3 in a small ceramic boat inside oven, add 4 mL of phosphoric acid (one part of undiluted acid 85 % to two parts of water) and analyse by combustion at 200 ºC.

✓Put each glass microfiber filter containing suspended solids of each water sample on ceramic boat, add 4 mL of phosphoric acid and determine the carbon dioxide produced by heating in the oven.

Dissolved metals

✓Wash the membrane filter (0.2 µm, NL16 Whatman®) with deionised water.

✓Filter all samples of each sampling site.

✓Acidify all samples with nitric acid 65 % (for analysis, Emsure®) to pH ≤ 2 (add 150 µL HNO_3 65 % to 100 mL of sample).

✓Refrigerate the samples until the analysis by flame atomic absorption (direct air-acetylene flame method). The samples should reach room temperature before the analysis.

According to the instruction of equipment and due to the possibility of ionization, KCl 0.25% was added to the samples and standard solutions for the calcium and

magnesium determinations. 0.5 mL of KCl 25 % were added to 50 mL of solution (samples and standard solutions) to have a final concentration of 0.25%.

5.2.3 3D molecular fluorescence – spectra correction

All excitation-emission matrix (EEM) spectra acquired for each aqueous solution were corrected. For that, the inner filter effects were firstly corrected according to **equation 24**, using a quartz cell of 1 cm with right-angle geometry (Mendonça et al. 2013).

$$I_{corr} = I \times 10^{\left[\left(A_{\lambda_{exc}} + A_{\lambda_{em}}\right)/2\right]} \quad \textbf{(Eq.24)}$$

I_{corr} corresponds to the fluorescence intensity corrected with respect to the inner filter effect, I is fluorescence intensity attenuated by the inner filter effect, $A_{\lambda exc}$ and $A_{\lambda em}$ are the absorbances at excitation and emission wavelengths, respectively, for an optical path length of 1 cm. Secondly, the 3D-spectrum of Milli-Q water made in each day of analysis was subtracted to the 3D spectrum of each sample. Lastly, to eliminate the Rayleigh scattering from the spectra, only the range of emission wavelengths (λ_{em}) comprised between λ_{exc} +10 nm and 2*λ_{exc} –10 nm was considered.

5.2.4 Instrumentation

To quantify the carbon in liquid and solids samples, a Total Organic Carbon Analyser (**figure 23**) Shimadzu (liquid and solid sample modules: TOC-VcPH and SSM-5000A, respectively) was used. In the solid sample module, the temperatures of total carbon furnace and inorganic carbon furnace are 900 ºC and 200 ºC, respectively. To determine the pH, a pH meter (Eutech Instruments, EcoScan pH 5) was used. The salinity was measured using a salinity meter (WTW-Cond 330i). An atomic absorption spectrophotometer Perkin Elmer, Analyst 100 (**figure 24**) was used to determine calcium, magnesium and iron by flame atomic absorption spectroscopy (air-acetylene).

Figure 23 – Total Organic Carbon Analyser Shimadzu (TOC-VcPH and SSM-5000A)

Figure 24 – Atomic absorption spectrophotometer Perkin Elmer, Analyst 100

For the characterization of the filtered water samples by spectroscopy, UV-Vis spectra were obtained using a T90 + UV/VIS Spectrophotometer (PG Instruments Ltd), with a slit width of 2 nm. UV-Vis spectra of aqueous solutions were made in quartz cuvettes of 1 cm path length, acquired with 1 nm of interval in the range 200-600 nm. The excitation-emission matrix (EEM) spectra were acquired with a spectrofluorometer FluoroMax-4 (Horiba Jobin Yvon) (**figure 25**). The excitation and emission wavelengths ranged from 245 to 350 nm and from 290 to 600 nm, respectively. Excitation and emission slits of 10 nm and an increment of 5 nm were chosen to acquire the spectra. A quartz 1 cm-cell was used as sample container.

Figure 25 – Spectrofluorometer FluoroMax-4 (Horiba Jobin Yvon)

In the aquaculture's companies, Wedeco Effizon® ozone generators are used to produce ozone from oxygen (feed gas), in normal conditions of temperature and pressure (NTP). In company A, the ozone concentration is about 78 mg/L (ozone generator GSO 50). In company B, the ozone concentration produced from the ozone system (SMO 200, EFFIZON® HP) is approximately 52 mg/L.

5.3 Results and discussion

5.3.1 Analytical methods – calibration

For quantification of dissolved organic carbon (DOC) in filtered aquaculture's water samples, six standards of potassium hydrogen phthalate in Milli-Q water (0.502 – 10.037 mg C/L) were prepared. The determination coefficient (R^2) of the calibration and the detection limits (LOD) obtained were 0.9989 and 0.408 mg C/L, respectively. LOD was calculated as $(3S_{y/x})/m$, where m is the slope of the regression line and $S_{y/x}$ is the statistical parameter that estimates the random errors in the y axis. To confirm the stability of calibration curve, control standards were prepared and analyzed every day of analysis. Control standards correspond to the fresh solutions of potassium hydrogen phthalate in Milli-Q water (0.5 mg C/L and 10.0 mg C/L). The concentrations determined did not differ more than 2 % compared to the real concentrations.

For the analysis of the total and inorganic carbon (TC and IC), in suspended particles, six standards of glucose (2.500 – 75.00 mg) and Na_2CO_3 (4.000 – 88.00 mg) were made, respectively. The percentages of TC_{part} and IC_{part} in the standards of glucose and Na_2CO_3 are 40.0 % and 11.3 %, respectively. The calibration curves, which were made considering the areas of signal versus the mass of carbon, ranged between 1.000 – 30.00 mg C and 0.453 – 9.970 mg C for TC_{part} and IC_{part}, respectively. The determination coefficients (R^2) and LOD obtained for TC_{part} were 0.9991 and 1.09 mg, respectively, and for IC_{part} were 1.000 and 0.01 mg, respectively. Several blanks of filters were made to demonstrate that the filters do not interfere with combustion of the sample and with determination of the particulate carbon. They were subjected to the same procedure as the samples and no carbon was detected. The organic carbon in suspended particles was estimated by the difference between the total and the inorganic carbon, for each sample.

For the determination of total suspended solids (TSS, mg/L), four to six replicates of each sampling local were performed in each sampling event. The variations between weight measurements of the replicates were lower than 5 %. Blanks of the glass

microfiber filters were also performed to ensure that changes of mass of the filters during the drying processes are not source of errors in the determination of suspended particles mass. For that, three independent experiments were made and the TSS determined in the blanks were 0.00 mg/L.

To quantify the dissolved calcium, magnesium and iron by the flame atomic absorption method, calibration curves were made for each element. Five or six standards were prepared in Milli-Q water. The obtained values of R^2 and LOD are summarized in **table 7**. For the quantification of calcium and magnesium by atomic absorption, water samples were diluted 100 and 2000 times, respectively.

Table 7 – Calibration details for determination of calcium, magnesium and iron by atomic absorption (air-acetylene)

	Concentration range (mg/L)	R^2	LOD (mg/L)
Calcium	1.0 – 5.0	0.9992 – 0.9999	0.07 – 0.16
Magnesium	0.10 – 0.60	0.9991 – 0.9999	0.006 – 0.02
Iron	0.10 – 1.0	0.9988 – 0.9992	0.03– 0.04

5.3.2 Physical-chemical characterization of aquaculture's waters

Figure 26 (A to F) shows the results of the physical-chemical characterization of aquaculture's water samples collected in the two samplings and for the two companies. The values of pH and salinity ranged from 7.0 to 7.5 and from 20 ‰ to 22 ‰, respectively, in all water samples.

The concentrations of TSS (A), DOC (B), TC_{part} (C) and calcium (E) are the main differences between water collected in these two companies. TSS are much related to the density of fish production. The particles in suspension may have different origins, namely the faeces of fish, the uneaten feed and/or also particles suspended in air that are deposited in water. Associated to this higher concentration of TSS in company B, TC_{part} is also higher for this company than for company A. Its highest value in company B appears after the bio-filter, which is probably associated to the presence of microorganisms. In all determinations, the particulate inorganic carbon (IC_{part}) is residual comparatively to the particulate total carbon (TC_{part}), whereby TC_{part} is a good approximation of OC_{part}.

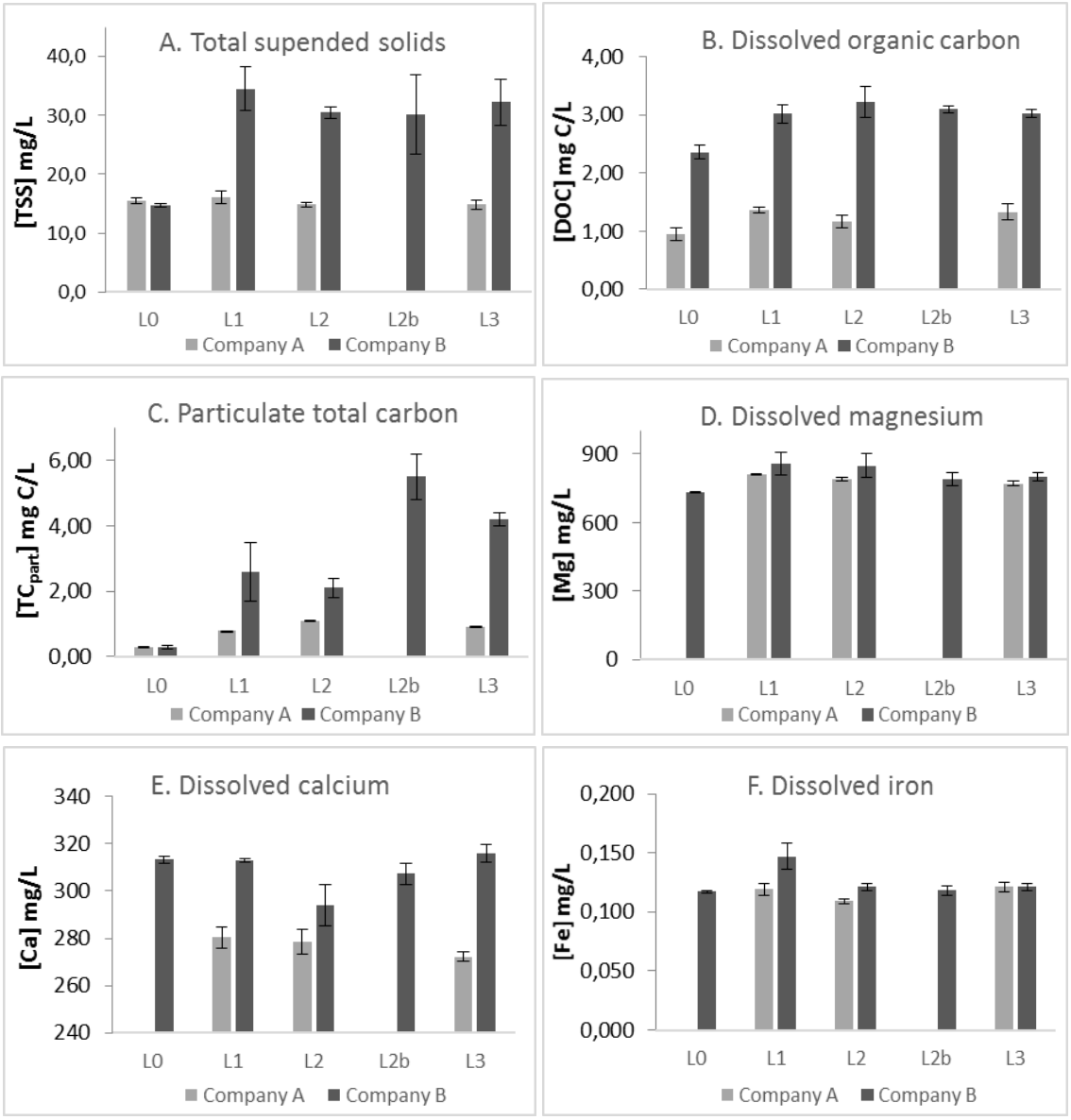

Figure 26 – Results of water characterization for the two companies and different sampling locals. A – TSS: Total suspended solids (mg/L), B – DOC: Dissolved organic carbon (mg C/L), C – Particulate total carbon (approximately equal to particulate organic carbon – OC_{part}) (mg C/L), D – dissolved magnesium (mg/L), E – dissolved calcium (mg/L) and F – dissolved iron (mg/L). The vertical bars of each column correspond to the standard deviations. L0 – water intake, blank control; L1 – at the output of tanks; L2 – after mechanical filter; L2b – after biological filter; L3 – after ozonation.

Significant statistical differences ($p < 0.03$) for TC_{part} are observed in water samples collected before and after ozonation. In the two companies, there is a decrease of TC_{part} concentration after ozonation, suggesting that ozone promotes the oxidation of particulate carbon. However, DOC differences between water samples collected before and after ozonation were not significant ($p > 0.09$) in the two companies. These data

suggest that ozonation is not efficient on mineralization of dissolved organic matter (DOM) or that the oxidation caused by ozone transforms the particulate organic carbon into DOC, eventually compensating a partial mineralization of DOC which may occur.

In what concerns to the dissolved metals, typical values of iron, calcium and magnesium for seawater (salinity 35 ‰) are 0.0034, 411 and 1290 mg/L (Anthoni 2006). The concentrations of calcium (272–315 mg/L) and magnesium (770–862 mg/L) are large and in the same order of magnitude for the two companies. The differences between the determined values in aquaculture's waters and the above reported values for seawater (35 ‰) can be related to the differences of salinity (21±1 ‰ *vs.* 35 ‰), once calcium and magnesium concentrations in water generally increase with the increasing salinity (Lucas and Southgate 2012). Regarding to the dissolved iron quantified in aquaculture's water samples (0.108–0.147 mg/L), which is a potentially toxic metal (Gerber et al. 2016), the values are much higher than those reported for a salinity of 35 (0.0034 mg Fe/L, Anthoni 2006). In water equilibrated with atmosphere, at these pH values (pH > 7), the iron will be predominantly in the oxidation state +3 (Fe^{3+}) and can form iron oxides and/or iron hydroxides that precipitate in the tanks.

5.3.3 Spectroscopic characterization of aquaculture's waters

Although ozonation is not able to promote a significant decrease of DOC at these conditions, it may promote the transformation of dissolved organic matter (DOM) into compounds with different structural characteristics. Therefore, studies using UV-Vis spectroscopy were performed with water samples collected before and after ozonation to evaluate the existence of differences on the composition of DOM. UV-vis spectra of DOM are characterized by the absence of well-defined bands (**figure 27**), but several parameters, which may be calculated from those spectra, have been correlated to some structural characteristics of DOM. In this case, the specific UV absorbance at 254 nm ($SUVA_{254}$) was used. It is a measure of DOC aromaticity and is calculated as the ratio between the absorbance at 254 nm, for the path length of 1 m, and the DOC concentration (Weishaar et al. 2003). **Table 8** summarizes the results obtained for the two companies. The decrease of $SUVA_{254}$ values after ozonation, in company A, indicates an alteration of DOM composition, suggesting a decrease of aromaticity after ozonation (differences in company B are not significant).

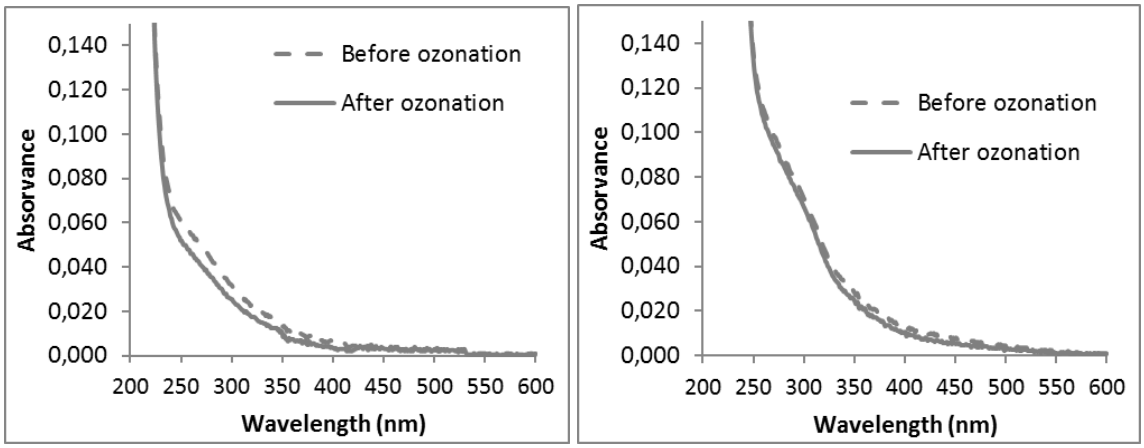

Figure 27 – UV-Vis spectra of aquaculture's water from company A (left) and company B (right).

Table 8 – Values (average ± SD, n ≥ 3) of absorbance at 254 nm, DOC and $SUVA_{254}$ for water samples collected before and after ozonation, in companies A and B.

	Company A		Company B	
	Before Ozonation	After ozonation	Before Ozonation	After ozonation
A(254 nm)	0.058 ± 0.001	0.050 ± 0.001	0.123 ± 0.002	0.119 ± 0.004
DOC (mg/L)	1.17 ± 0.11	1.33 ± 0.14	3.17 ± 0.13	3.00 ± 0.07
$SUVA_{254}$ (L mg^{-1} m^{-1})	5.0 ± 0.4	3.8 ± 0.3	3.9 ± 0.1	4.0 ± 0.1

Structural changes of DOM were also assessed by 3D-molecular fluorescence spectroscopy. The excitation-emission matrix (EEM) spectra of aquaculture's water samples collected before and after ozonation are shown in **figure 28** (company A) and **figure 29** (company B). All spectra were recorded at room temperature (around 20.0 ± 1.0) and were corrected as explained in *subchapter 5.2.3*. Analysing the spectra before ozonation, in the two companies, one observes a maximum intensity band centred at $\lambda_{exc/em}$ ≈ 250/440 nm. This band is often reported in literature as a characteristic band of aquatic humic substances (Swietlik and Sikorska 2004; Rodriguez et al. 2014). Additionally, a lower intensity band centred at $\lambda_{exc/em}$ ≈ 270/340 nm is also observed on spectra. It is characteristic of protein-like organic matter and is associated to the presence of aromatic amino acids (Swietlik and Sikorska 2004).

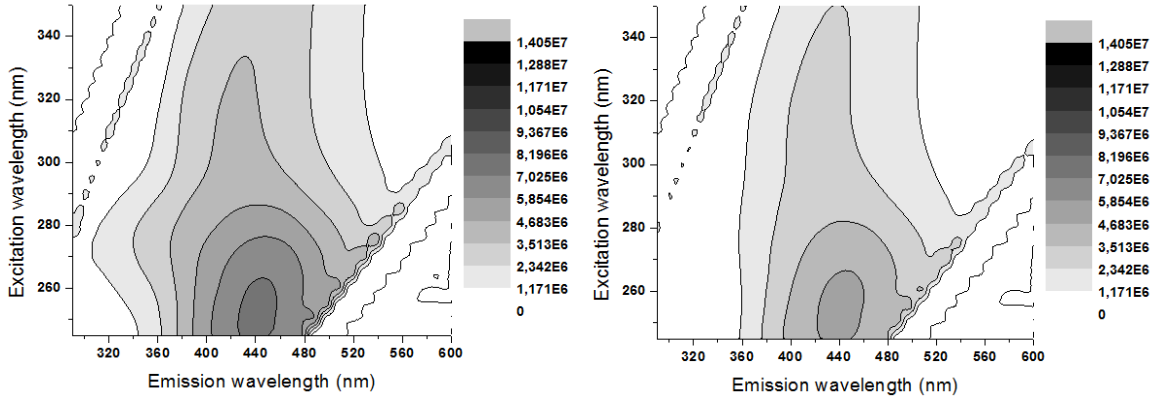

Figure 28 – Excitation-emission spectra (n ≥ 2) of filtered aquaculture's water samples (contour maps) collected before (left) and after (right) ozonation, in company A.

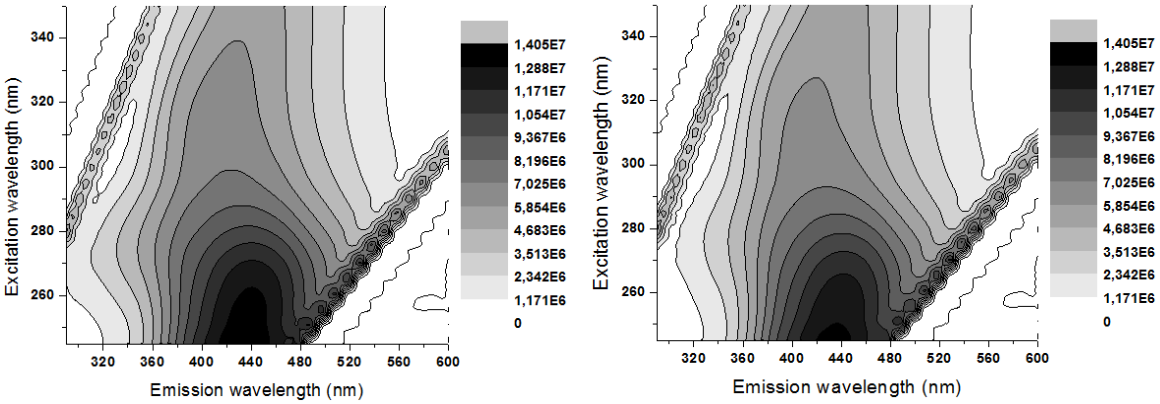

Figure 29 – Excitation-emission spectra (n ≥ 2) of filtered aquaculture's water samples (contour maps) collected before (left) and after (right) ozonation, in company B.

Comparing the spectra of water samples collected in company A, before and after ozonation, a significant decrease on the fluorescence intensity is observed after ozonation (**figure 28**). However, that decrease is not the same for all wavelengths. Making the ratio of fluorescence intensities for each band above referred, before and after ozonation, one concludes that there is a change in nature of the fluorescent organic matter since the ratios for bands at $\lambda_{exc/em}$ ≈ 250/440 nm and at $\lambda_{exc/em}$ ≈ 270/340 nm are 1.48 and 3.24, respectively. This means that the characteristic band of protein-like organic matter (at $\lambda_{exc/em}$ ≈ 270/340 nm) is the most affected by ozonation. In company B, the decrease on fluorescence intensity after ozonation (**figure 29**) is almost negligible and only the protein-like band is slightly affected (the ratios for bands at $\lambda_{exc/em}$ ≈ 250/440 nm and at $\lambda_{exc/em}$ ≈ 270/340 nm are 1.05 and 1.40, respectively). Changes in nature of fluorescent organic matter are, thus, much less than those observed in company A. This is

probably attributed to the lower ozone dose (≈ 52 mg/L) and higher DOC concentration in company B, comparatively to the higher ozone dose (≈ 78 mg/L) and lower DOC concentration in company A.

5.4 Conclusions

This chapter presents the characterization of aquaculture's waters collected from two aquaculture companies. The obtained results revealed that the most significant differences between the two companies are the concentrations of TSS, DOC, OC_{part} and calcium, which are higher in company B than in company A. The remaining physical-chemical parameters assessed (pH, salinity, magnesium and iron) did not differ much between companies.

Throughout the water treatment circuit (L2, L2b and L3 sampling sites), the analyzed parameters did not show a large variation. The most obvious example is the absence of significant degradation or mineralization of dissolved organic carbon after the ozonation process. Using UV-Vis and 3D molecular fluorescence spectroscopies, one also concluded that very significant changes on the structure of the organic matter after ozonation did not occur, namely in company B, where DOC before treatment is higher and the ozone dose is lower than in company A.

The results obtained in this chapter corroborate the low efficiency of ozonation to degrade organic matter, in saltwater, putting into evidence the need to combine it with another treatment process, in order to improve the efficiency of water treatment.

5.5 References

Anthoni, J. F. (2006). "The chemical composition of seawater." Retrieved April, 2014, from http://www.seafriends.org.nz/oceano/seawater.htm.

Chen, Y., H. Li, Z. P. Wang, T. Tao and C. Hu (2011). Photoproducts of tetracycline and oxytetracycline involving self-sensitized oxidation in aqueous solutions: Effects of Ca^{2+} and Mg^{2+}. *Journal of Environmental Sciences-China* **23**(10): 1634-1639.

Eaton, A. D., L. S. Clesceri, E. W. Rice and A. E. Greenberg (2005). *Standard Methods For the Examination of Water & Wastewater* Washington, Centennial Edition

Gerber, M. D., A. S. Varela Junior, J. S. Caldas, C. D. Corcini, T. Lucia Jr, L. B. Corrêa and É. K. Corrêa (2016). Toxicity evaluation of parboiled rice effluent using sperm quality of zebrafish as bioindicator. *Ecological Indicators* **61, Part 2**: 214-218.

Guerard, J. J., P. L. Miller, T. D. Trouts and Y. P. Chin (2009). The role of fulvic acid composition in the photosensitized degradation of aquatic contaminants. *Aquatic Sciences* **71**(2): 160-169.

Lucas, J. S. and P. C. Southgate (2012). *Aquaculture Farming Aquatic Animals and Plants*. UK, Wiley-Blackwell

Mendonça, A., A. C. Rocha, A. C. Duarte and E. B. H. Santos (2013). The inner filter effects and their correction in fluorescence spectra of salt marsh humic matter. *Analytica Chimica Acta* **788**: 99-107.

Prabhakaran, D., P. Sukul, M. Lamshoft, M. A. Maheswari, S. Zuhlke and M. Spiteller (2009). Photolysis of difloxacin and sarafloxacin in aqueous systems. *Chemosphere* **77**(6): 739-746.

Rodriguez, F. J., P. Schlenger and M. Garcia-Valverde (2014). A comprehensive structural evaluation of humic substances using several fluorescence techniques before and after ozonation. Part I: Structural characterization of humic substances. *Science of the Total Environment* **476**: 718-730.

Swietlik, J. and E. Sikorska (2004). Application of fluorescence spectroscopy in the studies of natural organic matter fractions reactivity with chlorine dioxide and ozone. *Water Research* **38**(17): 3791-3799.

Weishaar, J. L., G. R. Aiken, B. A. Bergamaschi, M. S. Fram, R. Fujii and K. Mopper (2003). Evaluation of Specific Ultraviolet Absorbance as an Indicator of the Chemical Composition and Reactivity of Dissolved Organic Carbon. *Environmental Science & Technology* **37**: 4702-4708.

Wright, J. M., A. Colling and G. Bearman (2013). *Seawater: Its Composition, Properties and Behaviour: Prepared by an Open University Course Team*, Elsevier Science

Xuan, R. C., L. Arisi, Q. Q. Wang, S. R. Yates and K. C. Biswas (2010). Hydrolysis and photolysis of oxytetracycline in aqueous solution. *Journal of Environmental Science and Health Part B-Pesticides Food Contaminants and Agricultural Wastes* **45**(1): 73-81.

Chapter 6: Photo-degradation of oxytetracycline (OTC) [5]

[5] Adapted from:

- **J.F. Leal**, V.I. Esteves, E.B.H. Santos (2016). Use of sunlight to degrade oxytetracycline in marine aquaculture's waters. *Environmental Pollution*, **213**: 932-939.
- **J.F. Leal**, V.I. Esteves, E.B.H. Santos. Ca^{2+} and Mg^{2+} binding to oxytetracycline in brackish aquaculture's water: effects on photo-degradation kinetics and on by-products formation, *submitted*.
- **J.F. Leal**, I. S. Henriques, A. Correia, E. B. H. Santos, V. I. Esteves (2017). Antibacterial activity of oxytetracycline photoproducts in marine aquaculture's water. *Environmental Pollution*, **220**: 644-649.

Chapter 6A:

Kinetics of OTC photo-degradation in marine aquaculture's water

OTC photo-degradation has been widely studied in synthetic aqueous solutions, sometimes resorting to expensive methods (e.g. UV radiation with TiO_2) and without proven effectiveness in natural water, mainly in saltwater. Thus, the possibility to apply the solar photo-degradation for the removal of OTC from marine aquaculture's water was studied. For that, the samples were spiked with OTC and irradiated using simulated sunlight to evaluate the matrix effects on OTC photo-degradation. From kinetic results, the apparent quantum yields and the outdoor half-life times, at 40ºN for midsummer and midwinter days were estimated by the first time for these conditions. For a midsummer day, at sea level, the outdoor half-life time predicted for OTC in these aquaculture's water ranged between 21 and 26 min. Additionally, the pH and salinity effects on the OTC photo-degradation were evaluated and it has been shown that typical pH values of saltwater (generally higher than in freshwater) and the presence of sea-salts increase the OTC photo-degradation rate in brackish aquaculture's water, compared to results in deionised water.

6A.1 Contextualization

Photo-degradation of OTC under UV or visible light has been studied by several authors (Jiao et al. 2008; Lopez-Penalver et al. 2010; Xuan et al. 2010; Pereira et al. 2013; Zhao et al. 2013). Most of these studies used UV with TiO_2, which is a procedure that, besides requiring considerable energetic costs, has been demonstrated to loss efficiency in the presence of chloride ions (Pereira et al. 2013); thus is less adequate for salt water. The main advantages of the photo-degradation using sunlight are the use of a free natural source of light and the low cost of its implementation, comparatively with UV radiation. There are some studies that report the photo-degradation of OTC using simulated or natural sunlight (Lunestad et al. 1995; Pouliquen et al. 2007; Chen et al. 2008; Xuan et al. 2010; Leal et al. 2015). Among them, only Lunestad et al. (1995) and Pouliquen et al. (2007) used natural and artificial saltwater, respectively. Must be highlighted that the kinetics and mechanisms of contaminants photo-degradation could be dependent on water composition, which can also vary along water treatment circuit of aquaculture systems.

Thus, in this sub-chapter, the possibility of applying solar photo-degradation for removal of OTC in marine aquaculture's water was studied. Additionally, the effects of pH and salinity on OTC photo-degradation kinetics were also studied in order to explain their contribution in these aquatic systems.

6A.2 Material and methods

6A.2.1 Chemicals

Oxytetracycline hydrochloride (98 %) was provided from Sigma Aldrich. The stock solution of phosphate buffer 0.1 M was prepared in ultrapure water, from a mixture of 0.05 mol of sodium dihydrogen phosphate dehydrate – $NaH_2PO_4.2H_2O$ (Fluka, Biochemika, ultra ≥ 99 %) and 0.05 mol of di-sodium hydrogen phosphate dihydrate – $Na_2HPO_4.2H_2O$ (Fluka, Biochemika) for each litre of buffer. The buffer pH was adjusted to 7.3 with a NaOH solution. Ultrapure water was obtained from a milli-Q Millipore system.

To prepare the synthetic saltwater solutions (21 ‰), "Tropic Marin Pro Reef Sea Salt" (Tropical Marine Centre Limited- TMC) was dissolved in phosphate buffer solution (0.001 M) and the pH was also adjusted to 7.3. Tropic Marin Pro Reef Sea Salt is free from synthetic additives and contains no nitrates, phosphates or silicates (MarineDepot 2015).

The aquaculture's water samples were collected from two different companies of fish production in brackish water, as described in *chapter 5*.

6A.2.2 Photo-degradation experiments

Water samples collected in the two aquaculture companies after mechanical filter (L2) and ozonation (L3) and, in company B, also after bio-filter (L2b) were spiked with OTC 4 mg/L (8 x 10^{-6} M) and submitted to artificial solar irradiation. Photo-degradation experiments were performed with filtered and non-filtered samples. Solutions of OTC 4mg/L in phosphate buffer 0.001 M at different salinities (0 and 21 ‰) were also prepared and irradiated for comparison. The temperature of the experiments ranged between 30 and 35 ºC. Quartz tubes (internal diameter × height = 1.8 × 20 cm) were used for the irradiation experiments (15 mL of solution per tube).

For all OTC photo-degradation experiments, one dark control (quartz tube wrapped in aluminium foil to protect from light) per kinetics was maintained inside the sunlight simulator during the longer irradiation time of the respective experiment. The concentration of OTC in the dark control after that time did not change comparatively to the initial concentration. Three to six non-simultaneous replicates of the photo-degradation experiments were made. To perform the kinetic studies, OTC aqueous solutions were irradiated during five different times (2 to 20 minutes) per kinetics.

All irradiations were achieved in a sunlight simulator, using an irradiance of 55 W/m^2 (290–400 nm), which corresponds to 550 W/m^2 in all spectral range. The characteristics of this sunlight simulator are presented in *chapter 4*.

6A.2.3 Instrumentation

Analyses of OTC were performed by HPLC-DAD (SPD-M20A, 200–600 nm, Shimadzu – **figure 30**), using an ACE5 – C18 column (250 mm x 4.6 mm) with particle and pore size of 5 µm and 100 Å, respectively. The mobile phase, at a flow rate of 0.900 mL/min, was composed of 15 % acetonitrile and 85 % water acidified to pH 2 with formic acid. The quantification of OTC was done at 350 nm.

UV-Vis spectra of OTC aqueous solutions were obtained using the same equipment described in *chapter 5*.

Figure 30 – HPLC equipment

6A.2.4 Data analysis

The data of OTC photo-degradation in aquaculture's water and in phosphate buffer solutions at different salinities were fitted by non-linear regression to the first order kinetics equation: $C/C_0 = e^{-kt}$. The non-linear curve fitting was made using GraphPad Prism 6. The experimental half-life times were calculated using **equation 8** (*subchapter 4.3.1*).

The mean values of the rate constants in the aquaculture's water were compared by two factor analysis of variance (ANOVA 2D) with replicates, at 95 % confidence level. The two factors considered were: filtration and sampling site. The Kolmogorov-Smirnov test was previously done, confirming the normal distribution of the data. Whenever ANOVA revealed the existence of significant differences, multiple pairwise comparisons were made by the Bonferroni's t test (Field 2009). Comparisons between two means were made by *t*-test. The statistical tests referred were made using Microsoft Excel 2013 and SPSS Statistics 22.

6A.3 Results and discussion

6A.3.1 Calibration for OTC determination

To quantify OTC by HPLC-DAD along the kinetic studies of photo-degradation, calibration standards of OTC were made using the aquaculture´s water samples (spiked with OTC, obtaining 0.5 to 4.0 mg/L final concentrations). The determination coefficients (R^2) calculated from these calibrations curves ranged between 0.9988 and 1.000 and the detection limits ranged from 0.03 to 0.17 mg/L.

Calibrations curves (0.5 to 4.0 mg/L) were also done in aqueous solutions of phosphate buffer (0.001 M) in the absence and presence of synthetic sea-salts (21 ‰). The determination coefficients (R^2) and detection limits (LOD) for these phosphate buffer solutions (0 and 21 ‰) ranged between 0.9992 and 0.9999 and from 0.06 to 0.14 mg/L, respectively.

6A.3.2 Photo-degradation in aquaculture's waters

OTC photo-degradation experiments were performed in filtered and non-filtered samples from the different sampling sites, as described in the experimental section. The natural aquaculture's samples were previously analysed before their fortification with the antibiotic and OTC was not detected. The decrease of OTC concentration along time of irradiation followed a pseudo – first order kinetics in all the samples (**figure 31**). The values of the pseudo-first order rate constants (*k*) and the corresponding values of the coefficient of determination (R^2) are presented in **table 9**.

Table 9 – Kinetics results of OTC photo-degradation in aquaculture's waters. OTC was spiked to each non-filtered (NF) and filtered (F) aquaculture's water sample collected in companies A and B. *n* – Number of irradiation experiments, *k* – kinetic rate constants, R^2 - determination coefficients of the non-linear adjustment, $t_{1/2}$ – experimental half-life time. SD: standard deviation; L2: after mechanical filter; L2b: after biological treatment; L3: after ozonation.

OTC photo-degradation experiment	n	k (min^{-1}) ± SD	R^2	$t_{1/2}$ (min) ± SD
Company A – L2 (NF)	3	0.076 ± 0.002	0.9912	9.1 ± 0.2
Company A – L2 (F)	3	0.077 ± 0.002	0.9799	9.1 ± 0.2
Company A – L3 (NF)	3	0.080 ± 0.003	0.9706	8.6 ± 0.3
Company A – L3 (F)	6	0.082 ± 0.001	0.9847	8.5 ± 0.1
Company B – L2 (NF)	3	0.078 ± 0.002	0.9738	8.9 ± 0.3
Company B – L2 (F)	3	0.087 ± 0.002	0.9775	8.0 ± 0.2
Company B– L2b (NF)	3	0.087 ± 0.002	0.9762	8.0 ± 0.2
Company B– L2b (F)	6	0.091 ± 0.002	0.9827	7.6 ± 0.1
Company B – L3 (NF)	3	0.084 ± 0.002	0.9785	8.3 ± 0.2
Company B – L3 (F)	6	0.092 ± 0.001	0.9873	7.6 ± 0.1

To determine whether filtration and/or site of water sample collection influenced the OTC photo-degradation rate, two-way ANOVA with replicates (three replicates) was used to compare the mean values of the kinetic rate constants from the first sampling event. Data for each company were analysed separately (**tables 10** and **11**).

Table 10 – Two-way ANOVA with replicates for company A (L2 and L3)

Source of variation	*SS*	*df*	*MSS*	*F*	*P- value*	F_{critic}
Inter-samples (filtration)	1,64E-06	1	1,64E-06	0,062793	0,80845	5,317655
Inter-treatments	2,71E-05	1	2,71E-05	1,036618	0,338409	5,317655
Interactions (filtration x treatment)	3,31E-06	1	3,31E-06	0,126423	0,731363	5,317655
Residual	0,000209	8	2,62E-05			
Total	0,000241	11				

Table 11 – Two-way ANOVA with replicates for company B (L2, L2b and L3)

Source of variation	*SS*	*df*	*MSS*	F_{calc}	*P- value*	F_{critic}
Inter-samples (filtration)	0,000371	1	0,000371	44,94039	2,18E-05	4,747225
Inter-treatments	0,000248	2	0,000124	15,00346	0,000543	3,885294
Interactions (filtration x treatment)	1,4E-05	2	7E-06	0,847556	0,452579	3,885294
Residual	9,91E-05	12	8,26E-06			
Total	0,000732	17				

No interaction between the two factors considered (filtration and sampling site) was observed ($F_{interaction} < F_{critic.}$). For company A, the mean values of the kinetic rate constants of OTC photo-degradation did not differ between filtered and non-filtered samples, or between samples from different sampling sites ($p > 0.3$). However, for company B, the *k* mean values were influenced by filtration ($p = 2.2 \times 10^{-5}$) and sampling site ($p < 0.0006$).

The results obtained from Bonferroni's test indicate that the mean values of the kinetic rate constants are not significantly different between water samples collected in L2b (after biological treatment and before ozonation) and L3 (after ozonation) ($p = 1.000$) but are significantly different between these two locals (L2b and L3) and L2 (after mechanical filtration) ($p < 0.003$). Regarding to the effect of filtration in company B, it was observed that the kinetic rate constant values for the non-filtered samples are lower than the corresponding values for the filtered samples (**table 9**). This may be related to the ability of suspended particles to scatter and attenuate the light that reaches the compound, contributing to the decrease of OTC photo-degradation rate. This effect of suspended particles is only observed in company B, which presents higher contents of TSS.

Based on the results of the OTC photo-degradation in aquaculture's water collected in the first sampling, additional photo-degradation experiments (three replicates) were performed using only the filtered (2 µm) aquaculture's water samples (second sampling event). The criteria to choose the sites was the higher value of the kinetic rate constants (*k*) obtained in the first sampling for each company. Thus, the locals L3 for company A and L2b and L3 for company B were chosen. The kinetic constants of OTC photo-degradation in filtered aquaculture's water do not differ significantly between first and second sampling events, for the same company and the same sampling site (*t*-test, $p > 0.08$). The rate constants of OTC photo-degradation are significantly different between the two companies for samples from the same sites of the treatment circuit (*t*-test, $p < 0.0001$). As shown in **table 9,** the rate constant of OTC photo-degradation in all aquaculture's water samples is higher, at least 3.9 times, than the OTC photo-degradation kinetic constant in deionised water ($k = 0.0198 \pm 0.0005$ min^{-1}). This increase suggests that the physical-chemical characteristics of the aquaculture's water are influencing the kinetics of OTC photo-degradation.

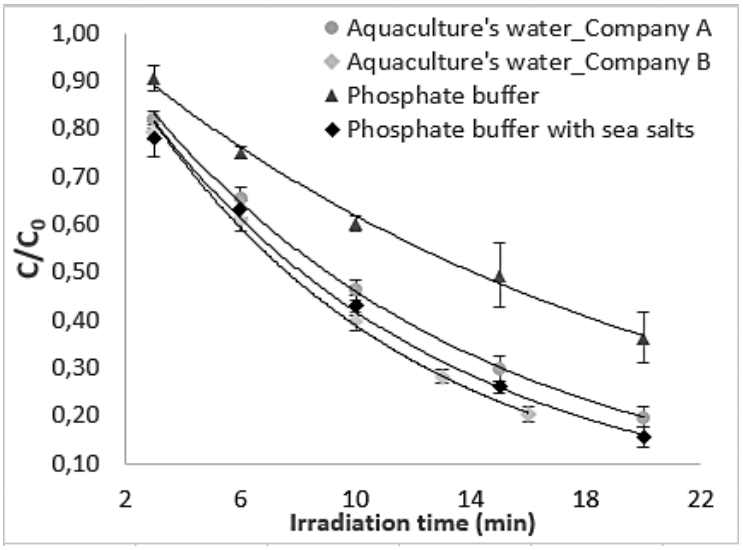

Figure 31 – First-order kinetics of OTC 4 mg/L photo-degradation in filtered aquaculture's water, in 0.001M phosphate buffer without and with synthetic sea salts (21 ‰). The vertical bars correspond to the standard deviations (n ≥ 3).

6A.3.3 Effect of pH on the OTC photo-degradation kinetics

It is known that pH variations cause alterations on OTC structure. At pH 4.6, OTC is predominantly in neutral form while between pH 7 and 8, its ionization state ranges between the neutral and negative form (Jiao et al. 2008). These pH variations modify the

absorption spectrum of OTC. Several authors have reported a strong relation between the kinetics of OTC photo-degradation and the increase of pH (Pouliquen et al. 2007; Jiao et al. 2008; Zhao et al. 2013). Zhao et al. (2013) observed a red shift on the light absorption of OTC with the increase of pH, suggesting that a greater amount of photons is absorbed at high pH values, which promotes the direct photo-degradation. Furthermore, OTC molecules predominantly in negative form (at high pH values) may imply an increase of electrical density on the ring system (Jiao et al. 2008).

Thus, to evaluate the effect of pH on OTC photo-degradation kinetics, buffered solutions of OTC (OTC in phosphate buffer 0.001 M) were irradiated. These solutions had approximately the same pH of aquaculture's water (pH 7.3). The pH did not significantly change after 20 minutes of irradiation. From the non-linear fitting to the first-order kinetic equation (R^2 = 0.9727), the pseudo-first order rate constant (*k*) and the half-life time obtained were 0.051 ± 0.002 min^{-1} and 13.6 ± 0.5 min, respectively.

Based on the kinetic constants obtained for the photo-degradation of OTC in different matrices (deionised water, aquaculture's waters and 0.001 M phosphate buffer solution), the pH seems to be responsible for 43-55 % of increase of the OTC photo-degradation rate in aquaculture's water. Nevertheless, the photo-degradation is even greater in brackish aquaculture's water than in buffered aqueous solution at pH 7.3, suggesting that other factors besides pH are contributing to increase the photo-degradation rate in aquaculture's water.

6A.3.4 Effect of sea-salts on the OTC photo-degradation

For evaluating the salinity effect, the photo-degradation of OTC was also studied in buffer solutions containing synthetic sea-salts (artificial seawater with the same pH and salinity as aquaculture's water). The non-linear kinetic adjustment (R^2 = 0.9866) originates a kinetic rate constant and a half-life time corresponding to 0.085 ± 0.002 min^{-1} and 8.1 ± 0.2 min, respectively. These values are within the range of the results obtained in aquaculture's water, suggesting that pH conjugated with salinity are the major factors contributing to a higher photo-degradation rate of OTC in these waters comparatively to deionised water.

The presence of sea-salts in phosphate buffer solution enhances c.a. 1.7 times the kinetic rate constant of the OTC photo-degradation, comparatively to the phosphate buffer solution without sea salts. An increase of pH and ionic strength may favour some highly charged form (negatively) of the molecule, which cause a higher circulation of

electrons in the structure and a consequent deviation of light absorption to higher wavelengths.

Indeed, UV-Vis spectra of OTC in synthetic saltwater present a deviation to higher wavelengths, comparatively to the OTC spectra in phosphate buffer solution without sea-salts (**figure 32**). This gives rise to a higher overlap between the spectrum of OTC solution and the spectrum of the artificial solar light, justifying, at least in part, the increase observed on the OTC photo-degradation rate in synthetic saltwater. This deviation for higher wavelengths was also observed by other authors as result of complexation of OTC with Ca^{2+} or Mg^{2+} (Schmitt and Schneider 2000). Thus, the salinity effect may be due to the presence of some ions that may interact with OTC, changing its speciation and its spectrum in solution and/or can be attributed to the ionic strength, which can affect the acidity equilibrium constants.

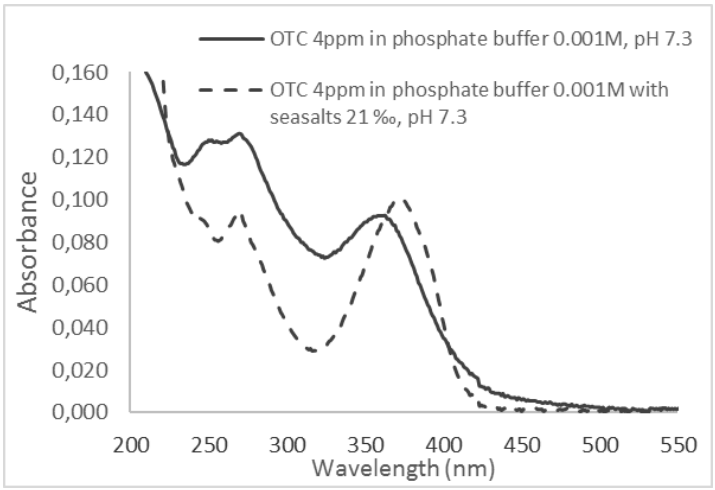

Figure 32 – UV-Vis spectra of OTC 4 mg/L in solutions of phosphate buffer 0.001 M without and with synthetic sea-salts (0 and 21 ‰, respectively)

6A.3.5 Estimative of apparent quantum yields and outdoor half-life times

As previously introduced, the photo-degradation rate constant depends on the quantity of photons absorbed by each mole of OTC per unit time and on the quantum yield. Thus, considering the spectral distribution of the irradiance of the solar light simulator (**figure 10**) and the absorption spectra of the OTC solutions, the initial rate of

light absorption by OTC solutions in the solar simulator was calculated for each wavelength using the following **equation 25**, which is an adaptation of **equation 10**:

$$I_{\lambda_i}^{abs} = I_{\lambda_i}^{0} \times (1 - 10^{-A_{\lambda_i} \times l}) \qquad \textbf{(Eq. 25)}$$

$I_{\lambda_i}^{0}$ is the quantity of photons of wavelength λ_i which are received per second per liter of solution, while $I_{\lambda_i}^{abs}$ is the quantity of photons of the same wavelength which are absorbed by OTC per second per litre of solution; A_{λ_i} is the initial absorbance of OTC in solution per unit path-length (absorbance of the solution minus absorbance of the solution matrix) and *l* is the light path-length inside the photo-reactor. The units of $I_{\lambda_i}^{0}$ and $I_{\lambda_i}^{abs}$ are Ein s^{-1} L^{-1} nm^{-1}. The irradiance values of the lamp were taken at intervals of 0.08 nm from the spectrum of the lamp supplied by the manufacturer. The absorbance values of the samples were acquired at intervals of 1 nm and the programme Matlab R2007b was used for the interpolation at intervals of 0.08 nm, in order to obtain the A_{λ_i} values. The plots of the rate of light absorption versus wavelength for each OTC solution are presented in **figure 33**. This figure clearly shows that the rate of light absorption is considerably higher for OTC in the solutions containing sea-salts than in the solutions without sea-salts. It is also clear that the rate of light absorption of OTC in aquaculture's water is similar (overlapped) to that of OTC solution in phosphate buffer containing synthetic sea-salts, suggesting a similar speciation of OTC in the buffer solution with sea-salt and in aquaculture's water. The effect of salinity, conjugated with pH, completely explains the higher values of the rate of light absorption observed in aquaculture's water.

The increase of the rate of light absorption by OTC causes an increase of the photolysis rate constant. However, as previously referred, the rate constants depend not only on the rate of light absorption but also on the photo-reactivity of the compound (quantum yield). Changes in the speciation of OTC not only change the UV-visible spectrum of OTC in solution, but may also change the OTC photo-reactivity. Thus, the apparent quantum yield of OTC in different solutions was calculated. This quantum yield should be referred as apparent since OTC is present in different forms in solution (neutral, ionized, or complexed with metal ions such as Ca^{2+} or Mg^{2+}) and those different species may have different quantum yields due to different electronic distributions. Besides, indirect photo-degradation can also be involved. Photolysis of OTC includes some self-sensitization, through the production of singlet oxygen (Zhao et al. 2013), and when

dissolved organic matter is present, it can also contribute to the production of singlet oxygen and other reactive species, promoting indirect photolysis of OTC.

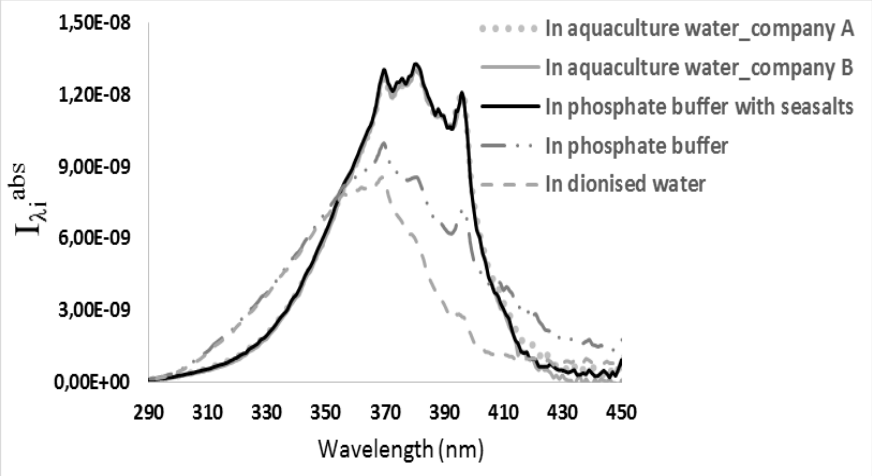

Figure 33 – Rate of light absorption versus wavelength for OTC in each solution: deionised water (pH 4.6), 0.001 M phosphate buffer solution without and with synthetic sea-salts (pH 7.3) and aquaculture's water from company A and B (pH 7.0-7.5). The plots for all brackish water (synthetic and natural) are overlapped.

The apparent quantum yield was calculated from **equation 9**, but replacing its denominator by the integration of the rate of light absorption, for the interval of wavelengths between 290 and 450 nm, calculated from **equation 25**. The apparent quantum yields are presented in **table 12**.

It is worth to notice that the apparent quantum yield is higher for OTC in artificial or aquaculture's brackish waters than in the solutions without sea-salts. Thus, the increase of the OTC photo-degradation rate constant in artificial seawater at pH 7.3, relatively to deionised water or to phosphate buffer (pH 7.3) without sea-salt, is due not only to an increase of the quantity of photons absorbed, but also to a higher apparent quantum yield. That suggests that the OTC species which are present in seawater at pH 7.3, probably complexes with Ca^{2+} or Mg^{2+}, have a higher photo-reactivity (higher quantum yield) than free OTC species, ionized (OTC^{-}) or neutral (OTC^{0}). No significant differences were observed between the quantum yields in artificial brackish water and aquaculture's water from L2 site of company A ($p > 0.5$). However, the apparent quantum yields for the photolysis of OTC in aquaculture's water from L2b or L3 sites of company B is higher than in company A or artificial brackish water ($p < 0.003$). Since the rate of light absorption by

OTC species is the same in all the brackish waters studied, suggesting a similar speciation of OTC, this difference is not due to differences in direct photo-degradation of OTC, but may be attributed to a contribution of indirect photo-degradation in company B, due to differences of the concentrations of photo-sensitizers such as DOM. Indeed, Jiao et al. (2008) referred that low concentrations of commercial humic acids do accelerate OTC photo-degradation (in ultra-pure water). However, as the HA concentration increased to values higher than 7.5 mg/L, an opposite effect was observed by the authors, due to the possibility of HA acting as a radiation filter and a sink of oxygen reactive species more than a source. These results are also in agreement with the inhibitory effect previously observed (*chapter 4*) on OTC photo-degradation, in distilled water for the different fractions of HS isolated from river water, at concentrations higher than 8 mg/L. Furthermore, it is important to note that these quantum yields were calculated discounting the absorbance of matrix and, consequently, the filter effect caused by it was also discounted, meaning that only the photosensitizing effect is being observed.

Table 12 – Estimative of apparent quantum yields and outdoor half-life times in filtered solutions of OTC: aquaculture's waters, phosphate buffer solution 0.001 M containing or not synthetic sea salts (21 ‰). *Φ* – (apparent) quantum yield (290 – 450 nm) and outdoor half-life times for a midsummer and midwinter day at 40 degrees north of latitude, at sea level. L2b: after biological treatment; L3: after ozonation.

OTC photo-degradation experiment	Φ (x 10^{-3})	Outdoor $t_{1/2}$ midsummer day (min^{-1})	Outdoor $t_{1/2}$ midwinter day (min^{-1})
Company A – L3	1.23 ± 0.08	24.4 ± 1.5	54.0 ± 3.3
Company B– L2b	1.44 ± 0.04	21.9 ± 0.7	48.9 ± 1.5
Company B – L3	1.43 ± 0.07	22.1 ± 1.1	49.2 ± 2.5
In phosphate buffer with sea salts (21 ‰)	1.26 ± 0.05	23.9 ± 0.9	53.0 ± 1.9
In phosphate buffer (0 ‰)	0.80 ± 0.02	36.5 ± 0.7	81.1 ± 1.6
In deionised water	0.42 ± 0.03	95.8 ± 7.6	220 ± 17

The outdoor half-life times estimated for the OTC photo-degradation in aquaculture's water at 40º N latitude (Sea level) under clear skies, for midsummer and midwinter days are also presented in **table 12**. In literature, there are only two published photo-degradation studies of OTC in saltwater (Lunestad et al. 1995; Pouliquen et al. 2007):

- Lunestad et al. (1995) studied the photo-stability of eight antibacterial agents, including OTC (50 mg/L) in seawater. Field experiments were made in October and

November in Bergen (Norway), at latitude 60 ºN, at sea level, under natural radiation. Their results pointed to 96 % of degradation (50 mg/L to 2 mg/L) after nine days of natural exposure (Lunestad et al. 1995). Since the authors give no data about the solar energy received by the samples or data concerning quantum yields, the comparison of such results with those of the present study is difficult. Based on the results estimated in the present work, the time required for 96% of degradation in aquaculture's water at 40ºN latitude in clear sky midwinter days should be 230 minutes (approximately). The higher degradation time obtained by Lunestad et al. (1995) may be due to lower irradiance in Bergen, at 60ºN and during winter. Besides, there is no information about climacteric conditions or daytime in the authors' experiments. The much higher initial concentration of OTC used by the authors relatively to the one used in the present work (50 mg/L vs. 4 mg/L) may also contribute to a lower photo-degradation rate. According to several studies, a higher initial concentration of OTC decreases the kinetics of OTC photo-degradation (Jiao et al. 2008; Lopez-Penalver et al. 2010; Zhao et al. 2013).

- Pouliquen et al. (2007) performed photolysis experiments of OTC (1 mg/L) in deionised water, natural freshwater and artificial seawater, all of them in abiotic conditions. The light was provided by a Biolux® neon tube at intensity of 1400 lux that, according to the authors, is near the one of daylight in the first 20 cm of the aquatic column (Pouliquen et al. 2007). However, the authors do not refer whether the spectrum of the lamp is similar to the one of solar light. As in the present work, the authors observed a higher photo-degradation rate of OTC in seawater than in deionised water. However, they did not observe significant differences between OTC photo-degradation rates in freshwater and seawater and concluded that there was no close connection between OTC photolysis and OTC binding to cations or organic matter. Their results do not seem to agree with those obtained in this work. The results of the present work suggest a significant influence of the ions from sea-water and that is in agreement with results published in literature (Werner et al. 2006; Xuan et al. 2010). For instance, Werner et al. (2006) demonstrated that changes in the concentrations of Mg^{2+} and Ca^{2+} within values relevant to natural conditions can induce differences up to one order of magnitude in the pseudo-first order rate constant for the photolysis of TTC (Werner et al. 2006).

6A.3.6 Possibility of application of the methodology *in situ*

The present work shows that brackish aquaculture's waters have chemical characteristics (namely pH and salinity) which are favourable to a fast photo-degradation of OTC by solar radiation. The short outdoor half-life times estimated for OTC in marine aquaculture's water, namely for midsummer days (21 to 26 minutes, approximately), are promising indicators for the application of photo-degradation using sunlight as a low-cost method to degrade OTC from these waters. The time of solar exposure needed to guarantee a 90 % degradation of OTC ranges between 70 and 180 minutes, for midsummer and midwinter days at 40ºN. So, for the application of this remediation procedure, any tank or system to be included in the circuit of the effluents of aquaculture tanks should have a reduced depth (≤ 50 cm) for light penetration and an extension and water flow adjusted to ensure the enough time of solar exposure. As the presence of suspended particles in water affects the rate of OTC photoreaction due to the scattering of light, the extension of the circuit may also be adjusted in function of suspended particles concentration. Thus, the tank for photo-degradation may also be used as particle settling tank, containing a canvas at the bottom to facilitate the removal of particles.

6A.4 Conclusions

The present work proposes a very simple and low-cost methodology to quickly degrade OTC from marine aquaculture's water. The kinetic results of the irradiation experiments performed using filtered and non-filtered aquaculture's water, collected at different points of water treatment, suggest that suspended matter scatters radiation and decreases the photolysis rate of OTC. The outdoor half-life times for midsummer days in filtered marine aquaculture's waters ranged between 21 and 26 minutes, which makes possible the application of methodology by aquaculture companies. The solar photo-degradation of OTC in brackish aquaculture's water is at least 3.9 times higher than in deionized water. The experiments with synthetic aqueous solutions revealed that this enhance is almost completely justified by the conjugation of two factors: pH and salinity.

6A.5 References

Chen, Y., C. Hu, J. H. Qu and M. Yang (2008). Photodegradation of tetracycline and formation of reactive oxygen species in aqueous tetracycline solution under simulated sunlight irradiation. *Journal of Photochemistry and Photobiology a-Chemistry* **197**(1): 81-87.

Field, A. (2009). *Discovering Statistics using SPSS*, SAGE

Jiao, S. J., S. R. Meng, D. Q. Yin, L. H. Wang and L. Y. Chen (2008). Aqueous oxytetracycline degradation and the toxicity change of degradation compounds in photoirradiation process. *Journal of Environmental Sciences-China* **20**(7): 806-813.

Leal, J. F., V. I. Esteves and E. B. H. Santos (2015). Does light-screening by humic substances completely explain their retardation effect on contaminants photo-degradation? *Journal of Environmental Chemical Engineering* **3**: 3015-3019.

Lopez-Penalver, J. J., M. Sanchez-Polo, C. V. Gomez-Pacheco and J. Rivera-Utrilla (2010). Photodegradation of tetracyclines in aqueous solution by using UV and UV/H_2O_2 oxidation processes. *Journal of Chemical Technology and Biotechnology* **85**(10): 1325-1333.

Lunestad, B. T., O. B. Samuelsen, S. Fjelde and A. Ervik (1995). Photostability of 8 antibacterial agents in seawater. *Aquaculture* **134**(3-4): 217-225.

MarineDepot. (2015). "Tropic Marin Pro Reef Sea Salt." Retrieved February, 2015, from http://www.marinedepot.com/Tropic_Marin_Pro_Reef_Sea_Salt_Salt_Mix_for_Aquarium_Water-Tropic_Marin-TP1113-FISM-vi.html.

Pereira, J., A. C. Reis, D. Queiros, O. C. Nunes, M. T. Borges, V. J. P. Vilar and R. A. R. Boaventura (2013). Insights into solar TiO_2-assisted photocatalytic oxidation of two antibiotics employed in aquatic animal production, oxolinic acid and oxytetracycline. *Science of the Total Environment* **463**: 274-283.

Pouliquen, H., R. Delpepee, M. Larhantec-Verdier, M. L. Morvan and H. Le Bris (2007). Comparative hydrolysis and photolysis of four antibacterial agents (oxytetracycline oxolinic acid, flumequine and florfenicol) in deionised water, freshwater and seawater under ablotic conditions. *Aquaculture* **262**(1): 23-28.

Schmitt, M. O. and S. Schneider (2000). Spectroscopic investigation of complexation between various tetracyclines and Mg^{2+} or Ca^{2+}. *Physchemcomm* **3**(9): 42-55.

Werner, J. J., W. A. Arnold and K. McNeill (2006). Water hardness as a photochemical parameter: Tetracycline photolysis as a function of calcium concentration, magnesium concentration, and pH. *Environmental Science & Technology* **40**(23): 7236-7241.

Xuan, R. C., L. Arisi, Q. Q. Wang, S. R. Yates and K. C. Biswas (2010). Hydrolysis and photolysis of oxytetracycline in aqueous solution. *Journal of Environmental Science and Health Part B-Pesticides Food Contaminants and Agricultural Wastes* **45**(1): 73-81.

Zhao, C., M. Pelaez, X. D. Duan, H. P. Deng, K. O'Shea, D. Fatta-Kassinos and D. D. Dionysiou (2013). Role of pH on photolytic and photocatalytic degradation of antibiotic oxytetracycline in aqueous solution under visible/solar light: Kinetics and mechanism studies. *Applied Catalysis B-Environmental* **134**: 83-92.

Chapter 6B:

Ca^{2+} and Mg^{2+} binding to OTC – effects on photo-degradation kinetics and by-products formation

OTC can complex with the major metal ions existing in brackish water. The present study evaluated the effect of Ca^{2+} and Mg^{2+} on the kinetics of the OTC photo-degradation and the role of OTC complexation on the by-products formation. Experiments were made in brackish aquaculture's waters and in synthetic solutions with the same salinity (NaCl 21 g/L) and Ca^{2+} and Mg^{2+} concentrations, buffered at the same pH (7.3). At these experimental conditions, complexes 1:1 with Ca^{2+} and both 1:1 and 1:2 with Mg^{2+} are proposed based on studies of molecular fluorescence and UV-Vis spectroscopy.

The presence of Ca^{2+} increases about 65 % the OTC photo-degradation, while Mg^{2+} seems not have a significant influence on its photo-degradation kinetics in a phosphate buffer solution containing NaCl. In turn, the Ca^{2+} addition to brackish aquaculture's water increased about 21 % the OTC photo-degradation.

The presence of Mg^{2+} in the OTC solution had a predominant effect on by-products formation. This work demonstrates for the first time the formation of, at least, two new photoproducts only in the presence of Mg^{2+}, in addition to the inhibition of some photoproducts formed in its absence. The appearance of different by-products when different aqueous matrices are considered suggests different mechanisms in the presence of different cations. Furthermore, those different mechanisms seem also to affect the kinetics of formation/degradation of some photoproducts.

6B.1 Contextualization

The use of OTC in marine or brackish aquaculture raises some concern due to its poor bioavailability and absorption caused by chelation with ions from saltwater, namely the divalent cations calcium and magnesium (Schmidt et al. 2007). While in freshwater the higher fraction of OTC is in the non-complexed form (Serrano 2005), some authors (Lunestad and Goksoyr 1990), who performed theirs experiments with OTC concentrations ranging from 0.5 to 100 mg/L, refer that in seawater about 95% of OTC is bound to magnesium and calcium ions. This implies that the minimum inhibitory concentration (MIC) of OTC can be much higher in saltwater or hard fresh water than in soft fresh water (Rodgers and Furones 2009). The need to use higher concentrations of OTC raises concerns about its environmental fate. Photo-degradation is one of the main degradation pathways of OTC in surface water, but it is also affected by the complexation with metal ions, namely Ca^{2+} and Mg^{2+} (Xuan et al. 2010; Chen et al. 2011).

The pH has an important role on OTC complexation with the typical ions present in saltwater (Lunestad and Goksoyr 1990). The OTC cation is usually considered a triprotic acid. The macroscopic pk_a values reported in the literature for OTC are 3.2 to 3.6 for pk_{a1}, 7.3 to 7.5 for pk_{a2} and 8.9 to 9.9 for pk_{a3} (Kulshrestha et al. 2004; Jiao et al. 2008; Zhao et al. 2013). Thus, four ionization states of OTC may be defined: H_3L^+ – H_2L^0 – HL^- – L^{2-} (Kulshrestha et al. 2004; Jiao et al. 2008; Zhao et al. 2013). The neutral form in aqueous solution is a zwitterionic species and it results from the loss of a proton from OH3 in the tricarbonyl system (system i in **figure 34**) (Bhatt and Jee 1985). Regarding to the other protons, their loss at pka_2 and pka_3 is commonly attributed to phenolic diketone (OH12) and dimethyl-ammonium groups, respectively (Kulshrestha et al. 2004; Jiao et al. 2008; Zhao et al. 2013). However, other authors (Bhatt and Jee 1985) reported very similar microscopic constants for the deprotonation of the phenolic diketone (pk 7.85) and dimethyl-ammonium (pk 7.48) groups of OTC, in aqueous solutions (ionic strength 0.1 M). Thus, it is difficult to match the macroscopic pk_a values to different groups when their intrinsic acidity is close.

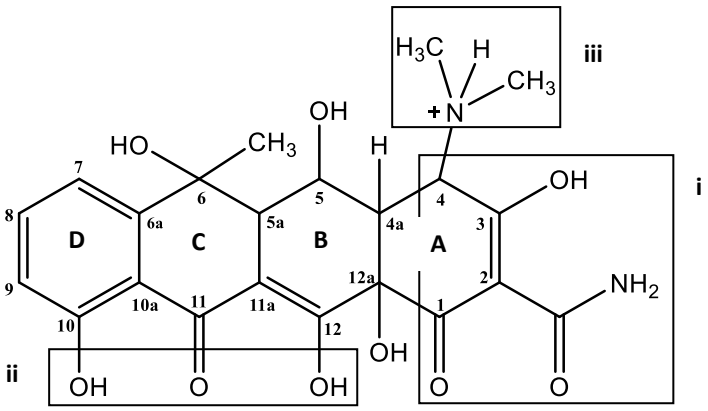

Figure 34 – Molecular structure of oxytetracycline cation: i – tricarbonyl system (pka_1); ii – phenolic diketone (pka_2); iii – dimethyl-ammonium group (pka_3) (Kulshrestha et al. 2004; Zhao et al. 2013)**.**

Although there are several studies referring the complexation between OTC and the cations Ca^{2+} and Mg^{2+} (Lunestad and Goksoyr 1990; Tongaree et al. 1999; Schmitt and Schneider 2000; Serrano 2005; Arias et al. 2007; Schmidt et al. 2007), few are the published studies referring the effect of these complexes formation on OTC photo-degradation (Xuan et al. 2010; Chen et al. 2011). Xuan et al. (2010) observed that OTC photolysis under sunlight irradiation was accelerated in the presence of Ca^{2+}, and attributed that effect to the increase of OTC absorbance after chelating with Ca^{2+}, turning it more vulnerable to sunlight irradiation. The same effect should then be expected for Mg^{2+}, since its complexation with OTC causes an even higher increase of OTC absorbance (Schmitt and Schneider 2000). However, Chen et al. (2011) concluded that, at pH 7.3, the addition of Mg^{2+} slightly inhibited the photolysis of OTC, while the addition of Ca^{2+} enhanced it. The authors attributed the different effects of these two cations to distinct modes of coordination of OTC with each of them, but there are contradictions in the literature relatively to the Mg^{2+} or Ca^{2+} binding sites in OTC. Besides, the type of complexes formed (1:2, 1:1, 2:1) and the OTC sites to which the metal cations are bound are strongly dependent on pH and on the proportion between the total concentrations of metal ion and ligand (Schmitt and Schneider 2000; Carlotti et al. 2012; Guerra et al. 2016).

The two studies referred above (Xuan et al. 2010; Chen et al. 2011) were performed at different conditions from those in brackish or marine aquaculture's water, namely, Ca^{2+} and Mg^{2+} concentrations, ionic strength and/or pH, whereby their conclusions cannot be extrapolated to the natural conditions found in marine or brackish aquaculture. Thus, one of the aims of this work was to study the individual and combined effect of Ca^{2+} and Mg^{2+} on the kinetics of the OTC photo-degradation, at experimental conditions relevant for

brackish water. Additionally, this work intends to assess the consequences arising from the formation of these OTC complexes in the formation of by-products.

6B. 2 Material and methods

6B.2.1 Chemicals

To prepare saline solutions containing calcium and/or magnesium, NaCl (99.5 %, JMGS), $CaCl_2.2H_2O$ (p.a., Merck) and $MgCl_2.6H_2O$ (Riedel-de Haën® p.a.) were used. All these solutions were prepared in phosphate buffer solution (0.001 M) and adjusted to pH 7.3 with a NaOH solution. The stock solution of phosphate buffer 0.1 M was prepared as described in *subchapter 6A.2.1*.

6B.2.2 UV-Vis and fluorescence spectra

UV-Vis and fluorescence spectra of OTC aqueous solutions were obtained using the same equipments and conditions described in *chapter 5*. All excitation-emission matrix (EEM) spectra acquired, for each aqueous solution, were corrected as explained in *subchapter 5.2.3*.

6B.2.3 Photo-degradation experiments

Irradiation experiments of aqueous solutions of OTC 4 mg/L (8×10^{-6} M) were performed using quartz tubes (15 mL of solution per tube). All irradiations were achieved using the same sunlight simulator described in *subchapter 4.2.2*, with an irradiance of 550 W/m^2. To perform the kinetic studies, OTC aqueous solutions were irradiated (three non-simultaneous replicates) during five different times (2 to 20 minutes). For all OTC photo-degradation experiments, one dark control was maintained inside the Solarbox during the longer irradiation time of each experiment.

Quantitative analyses of OTC were performed by HPLC-DAD, using the same equipment and method previously described in *subchapter 6A.2.3*. Additionally, to detect the products resulting of OTC photo-degradation, a fluorescence detector was also used (RF-$20A_{XS}$, Shimadzu).

6B.3 Results and discussion

6B.3.1 Absorption and fluorescence properties

It has been reported that the kinetics and quantum yields of tetracyclines photolysis may be affected by speciation (Werner et al. 2006; Xuan et al. 2010; Chen et al. 2011), specifically by the complexation with Ca^{2+} and Mg^{2+}. A variety of stoichiometries and different binding sites of Ca^{2+} and Mg^{2+} to tetracyclines have been proposed, giving rise to complexes with different spectral characteristics (Schmitt and Schneider 2000; Werner et al. 2006; Guerra et al. 2016). Thus, before proceeding with the OTC photo-degradation studies, absorption and fluorescence properties of the OTC aqueous solutions were studied. The following five OTC ($8.0x10^{-6}$ M) solutions containing phosphate buffer 0.001 M and NaCl (21 g/L) were considered: (1) without the divalent cations, (2) with Ca^{2+} $7.5x10^{-3}$ M (300 mg/L), (3) with Mg^{2+} $7.5x10^{-3}$ M, (4) with Mg^{2+} $3.3x10^{-2}$ M (800 mg/L), (5) with Ca^{2+} $7.5x10^{-3}$ M together with Mg^{2+} $3.3x10^{-2}$ M. The Ca^{2+} and Mg^{2+} concentrations of solutions (2), (4) and (5) were chosen since they correspond to the average concentrations detected in aquaculture's water previously characterized (*chapter 5*). The Mg^{2+} concentration of solution (3) was included to compare the spectra of solutions containing the same molar concentrations of Ca^{2+} and Mg^{2+}. The UV-vis spectra of the OTC solutions are presented in **figure 35**.

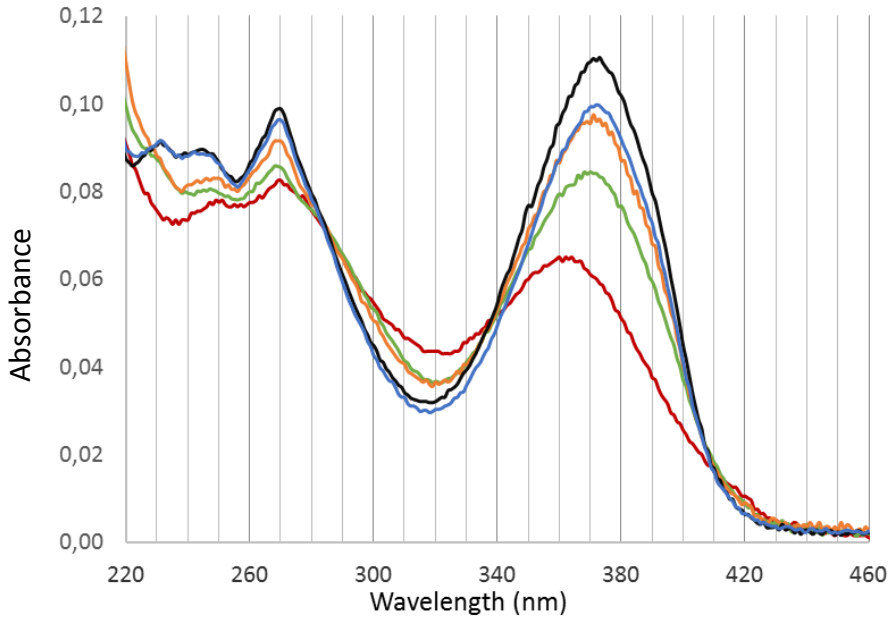

Figure 35 – UV-vis spectra of OTC 4 mg/L (8.0×10^{-6} M) in phosphate buffer solutions 0.001 M, at pH 7.3, and NaCl 21 g/L: without cations (red), with Ca^{2+} 7.5×10^{-3} M (green), with Mg^{2+} 7.5×10^{-3} M (orange), with Mg^{2+} 3.3×10^{-2} M (black), with Ca^{2+} 7.5×10^{-3} M and Mg^{2+} 3.3×10^{-2} M (blue).

Absorption spectra of OTC (**figure 35**) are characterised by two main bands centred at *ca.* 270 nm and 360-380 nm. The first band is attributed to the A chromophore, while the second band is related to the BCD ring system (**figure 34**) (Mitscher et al. 1972; Sompolinsky and Samra 1972; Carlotti et al. 2012). However, according to some authors (Sompolinsky and Samra 1972) the system BCD also contributes to the absorbance at lower wavelengths.

As shown in **figure 35**, an increase of absorbance, a bathochromic shift of the absorption band at 360-380 nm and a decrease in the absorption tail above 400 nm are observed in the OTC solutions after addition of Ca^{2+} or Mg^{2+} $7.5x10^{-3}$ M. When Mg^{2+} concentration is increased to $3.3x10^{-2}$ M, the narrowing of band above 400 nm is higher, the position of the band at 360-380 nm is approximately maintained and only an intensification of that band is observed. Additionally, at higher Mg^{2+} concentrations, an intensification of the band at 270 nm is observed and bands at 230 nm and 245-250 nm are evidenced.

In the present work, since the solutions contain a large excess of metal ions, only the possibility of complexes formation 1:1 and 2:1 (metal: ligand) is considered (not 1:2). Schmitt and Schneider (2000) determined the conditional binding constants for the consecutive formation of complexes 1:1 and 2:1 (M^{2+}: ligand) and obtained similar values for complexes with TTC and OTC. Using those constants, the authors calculated the speciation of TTC (percentages of free ligand, ligand in 1:1 complexes, and ligand in 2:1 complexes) for different total concentrations of metal cation in solution. In this work, the OTC concentration is 8.0×10^{-6} M and the metal concentrations used, $7.5x10^{-3}$ M and $3.3x10^{-2}$ M, correspond to a metal concentration 937 and 4125 times higher than the OTC concentration, respectively. According to the graphic presented by Schmitt and Schneider (2000) (**figure 36**) for the distribution of species of TTC 3×10^{-5} M, at pH 7.0, for a concentration of metal cation 937 times higher than the TTC concentration ($[M^{2+}]$ = 2.8×10^{-2} M), the ligand is mainly present in the form of 1:1 complexes and the formation of complexes 2:1 is negligible (less than 20%). However, for a metal cation concentration 4125 times higher than TTC concentration ($[M^{2+}]$ = 1.2×10^{-1} M), the percentage of TTC in 2:1 complexes increases to about 45%.

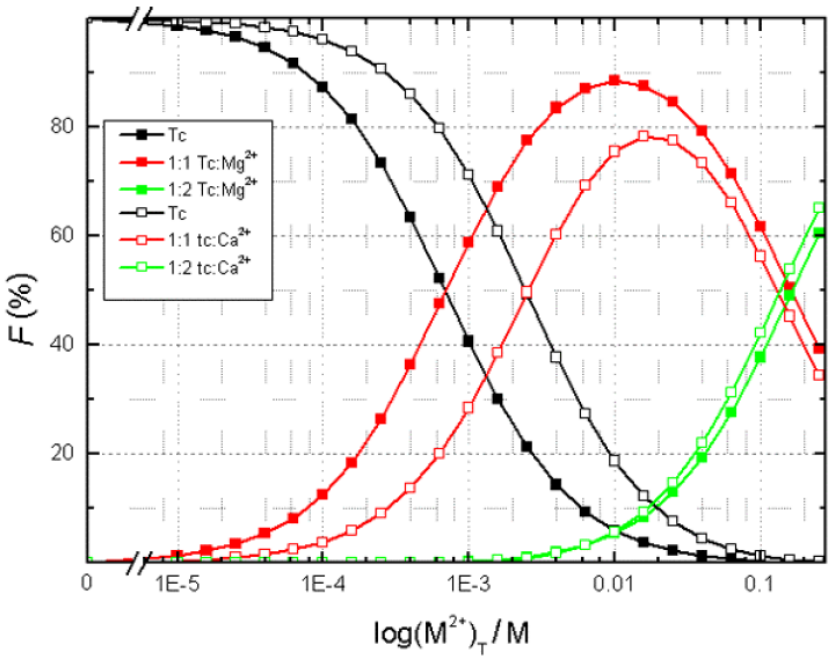

Figure 36 – Fraction (%) of the individual species for the complexes formed between tetracycline (TTC) and Mg^{2+} or Ca^{2+}, at pH 7.0 in aqueous Tris buffer (Schmitt and Schneider 2000).

Thus, in the present work one assumes that, for the lowest concentration of cation studied ($7.5x10^{-3}$ M), the complexes formed are mainly 1:1, while for the highest Mg^{2+} concentration the second step of complexation occurred, and both 1:1 and 2:1 complexes (M^{2+}: ligand) are present in similar concentrations. Werner et al. (2006) have also studied the complexation of TTC with Ca^{2+} and Mg^{2+} by UV-visible spectroscopy, in the pH range 5.5-8.5. They concluded that only complexes 1:1 were formed for a TTC concentration of $1.5–2.5×10^{-5}$ M and concentrations of Mg^{2+} up to 3 mM (200 times higher than TTC concentration) and Ca^{2+} up to 32 mM (2133 times higher than TTC concentration). That agrees with our assumption that for the lowest cation concentration used in the present work, the complexes formed are mainly, or only, 1:1 (at least for Ca^{2+}). However, according to Werner et al. (2006), in the pH range 5.5-8.5, two types of complexes 1:1 can be formed with Ca^{2+}, namely complexes $CaHL^{+}$ and CaL^{0}, which involve the mono-anion and the di-anion of the ligand, respectively. The authors concluded that Mg^{2+} did not form MgL^{0} complexes in the pH range considered. The spectra obtained in the present work for the solutions of OTC containing Ca^{2+} or Mg^{2+} 7.5 x 10^{-3} M are consistent with the spectra presented by Werner et al. (2006) for MHL^{+} complexes of TTC, as can be seen by comparison of spectra shown in **figure 35** with the spectra of complexes MHL^{+} and ML^{0}, shown in **figure 37**.

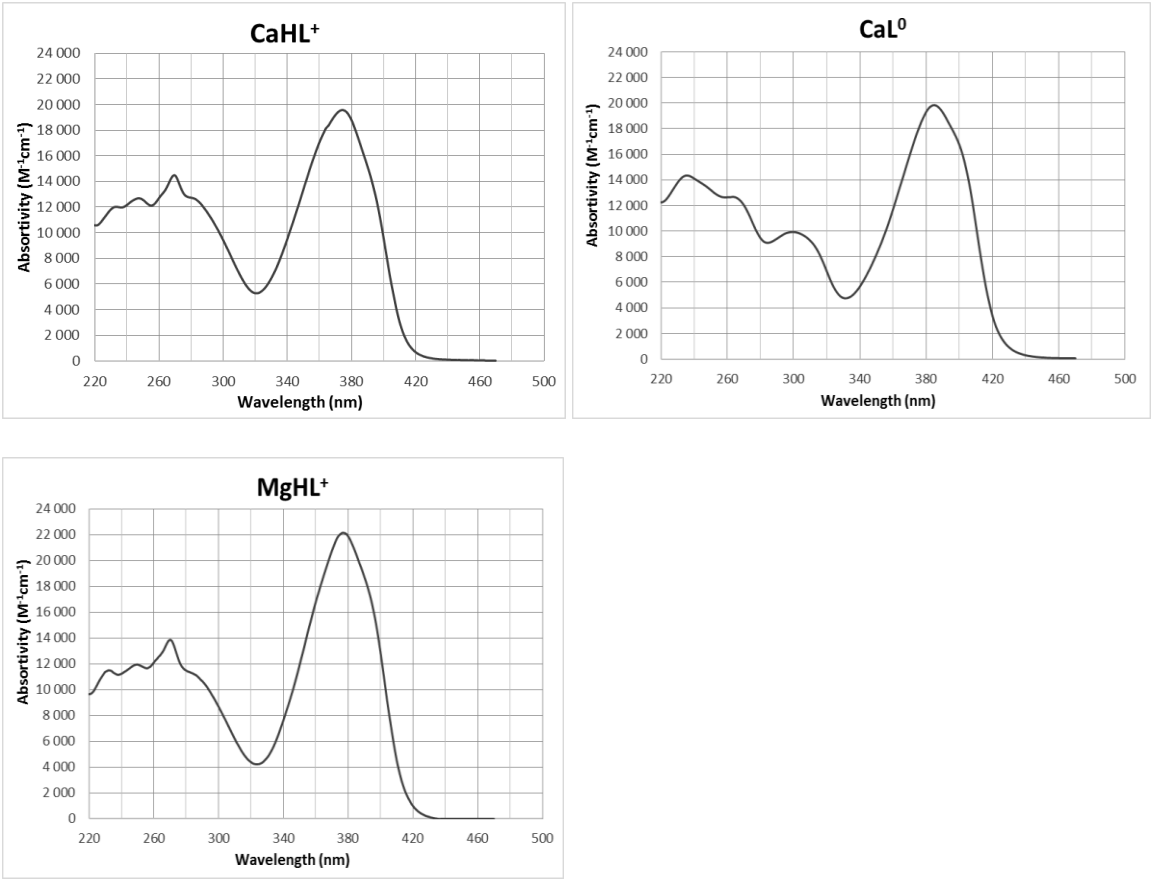

Figure 37 – Spectra of complexes MHL^+ and ML^0, obtained using the spreadsheet of the supplementary material provided by Werner et al. (2006).

In what concerns to the binding sites on TTC or OTC for Ca^{2+} and Mg^{2+} cations, there are contradictory conclusions in the literature. **Table 13** presents the type of complex and the proposed binding sites for tetracycline (TTC) and oxytetracycline (OTC) complexation with Ca^{2+} and Mg^{2+}, at different pH values.

During the titration at pH 7.0, a bathochromic deviation and an increase of the intensity of the long wavelength absorbance band was observed by Schmitt and Schneider (2000) during formation of complexes 1:1, suggesting binding of the first M^{2+} ion to the BCD chromophore. Carlotti et al. (2012) refer that a decrease of the tail above 400 nm and a more pronounced maximum at 270 nm are also evidence of binding at the BCD rings. The same spectral changes were observed in the present work by addition of Ca^{2+} or Mg^{2+} $7.3x10^{-3}$ M.

Table 13 – Proposed binding sites for TTC and OTC complexation with Ca^{2+} and Mg^{2+}.

L	Type of complex (M^{2+}: L)	M = Ca^{2+}	Type of complex (M^{2+}: L)	M = Mg^{2+}	pH	Reference
TTC	2: 1	(O10-O11), (O12-O1)	1: 1	(O11-O12)	7.4	(Newman and Frank 1976)
TTC	2: 1	(N4-O12a), (O12-O1)	2: 1	(N4-O3), (O10-O12)	> 8	(Lambs et al. 1988)
TTC	2: 1	(O10-O11), (O12-O1)	2: 1	(N4-O3), (O11-O12)	8.02	(Wessels et al. 1998)
TTC	1: 1	A ring	1: 1	A ring	2.3, 5.0	(Carlotti et al. 2012)
TTC	2: 1	A ring, BCD rings	2: 1	A ring, BCD rings	5.0	(Carlotti et al. 2012)
TTC	1: 1	BCD rings	1: 1	BCD rings	9.0	(Carlotti et al. 2012)
TTC	2: 1	BCD rings, A ring	2: 1	BCD rings, A ring	9.0	(Carlotti et al. 2012)
OTC	1: 1	(N4-O12a)	1: 1	(O5-O12a)	>7.5	(Mitscher et al. 1972)
OTC	1: 1	(O12-O1)	---	---	> 8	(Lambs et al. 1988)
OTC	2: 1	(O12-O1), (N4-O12a)	---	---	> 8	(Lambs et al. 1988)
OTC	1: 1	(O11-O12)	1: 1	(O11-O12)	7.0	(Schmitt and Schneider 2000)
OTC	2: 1	(O11-O12), (N4-O3)	2: 1	(O11-O12), (N4-O3)	7.0	(Schmitt and Schneider 2000)
OTC	1: 1	(O12-O1)	1: 1	(O11-O12)	8.5	(Schmitt and Schneider 2000)
OTC	2: 1	(O12-O1), (O10-O11)	2: 1	(O11-O12), (N4-O3)	8.5	(Schmitt and Schneider 2000)
OTC	---	---	1: 1	A ring	2.3, 5.0, 9.0, 11	(Carlotti et al. 2012)
OTC	---	---	2: 1	A ring, BCD rings	5.0, 9.0, 11	(Carlotti et al. 2012)

The spectra presented by Schmitt and Schneider (2000), for the titrations at pH 7.0, also show that the second step of complexation has only a small effect on the position of the long wavelength band and induces a slight increase of the intensity of that band, but the most important changes are observed in the lower wavelength region. Thus, the second step of complexation gives rise to a sharp band at 270 nm, and a well-defined minimum between this band and the band at *ca.* 245 nm, whose intensity also increases, indicating the involvement of the A chromophore in the coordination. Carlotti et al. (2012) also refer the appearance of a shoulder at 240 nm and a pronounced minimum between that band and the band at 270 nm as indicative of binding to the A

chromophore. These spectral changes are similar to those observed in the present work, when the Mg^{2+} concentration increases from $7.5x10^{-3}$ M to $3.3x10^{-2}$ M (**figure 35**).

According to Schmitt and Schneider (2000), the similarity of the spectra for complexes with Ca^{2+} and Mg^{2+}, also observed in the present work, suggests that Ca^{2+} and Mg^{2+} binding follow the same pattern. These authors proposed that, at pH 7.0, TTC and OTC bind the first metal cation M^{2+} (Ca^{2+} or Mg^{2+}) via C11-O{M}O-C12 and the second via C4-Me_2N{M}O-C3. The binding of the first cation displaces the proton at C11-O{H}O-C12, giving rise to complexes MHL^+. In fact, the spectra of the complexes 1:1 obtained in this work and by Schmitt and Schneider (2000) are similar to those provided by Werner et al. (2006) for this type of complex (MHL^+) with tetracycline (**figure 37**).

Wessels et al. (1998) considered that Mg^{2+} coordinated via C4-Me_2N{M}O-C3 in complexes 1:1 at pH 8.02, despite observing a bathochromic deviation of the longer wavelength band. The authors attributed this to an increased acidity of O10-O11-O12 moieties due to complexation at N4-O3.

Carlotti et al. (2012) studied the complexation of TTC with Ca^{2+} and Mg^{2+}, at pH's 2.3, 5.0, 9.0 and 11.0, and refer that for the two lowest pH's the first cation binding involves the A ring and the second the BCD ring system, while at pH's 9 and 11, the order is reversed: first binding site at BCD rings and second at A ring. However, the authors refer that, for OTC, Mg^{2+} coordinates first at the A ring at all pH values studied. This is not consistent with the coincidence of spectral changes for TTC and OTC during titrations with these cations, observed by Schmitt and Schneider (2000). According to the authors (Schmitt and Schneider 2000), binding of the first cation via C11-O{M}O-C12 is corroborated by the strong variation of the conditional Mg^{2+}-binding constant with pH in the range 7.0-8.5, indicating binding to the group with a pK_a in that range (pK_{a2}). However, this reasoning assumes that pK_{a2} corresponds to the loss of a proton from group ii (**figure 34**), and that is not clear, since, as previously referred, the microscopic constants for proton losses at ii and iii groups are similar (Bhatt and Jee 1985). Indeed, recently, other authors (Jin et al. 2017) have shown that OTC absorption spectra changed smoothly from pH 5.5 to 12, not allowing to distinguish the transformation of $H_2L^{\pm} \rightarrow HL^-$ and $HL^- \rightarrow L^{2-}$. According to the authors, this indicates that the proton loss occurs continuously and simultaneously from OH12 (at ii in **figure 34**) and N4 (at iii in **figure 34**). Nevertheless, the bathochromic deviation of the long wavelength absorption band is usually considered as an indication of interaction with the BCD ring system (Wessels et al. 1998; Schmitt and Schneider 2000; Carlotti et al. 2012).

Further evidences for the binding sites involved can be obtained from fluorescence spectra. Fluorescence spectra of OTC complexes exhibit maxima at λ_{em} = 500-530 nm and with two excitation maxima, being one of them at λ_{exc} ≈ 270 nm (**figure 38**). High increases of the fluorescence quantum yield caused by complexation of Ca^{2+} or Mg^{2+} cations have been associated to the involvement of the BCD fluorophore in the complexation (Wessels et al. 1998; Schmitt and Schneider 2000; Carlotti et al. 2012). At *ca.* 270 nm, the absorbance does not vary much between OTC solutions containing or not Ca^{2+} and/or Mg^{2+} (variations lower than 20 %), but the fluorescence at this λ_{exc} is much higher in the presence of those cations. This means that the complexes 1:1 with Ca^{2+} or Mg^{2+} exhibit a higher fluorescence quantum yield than the unbound OTC, suggesting an interaction with the BCD ring system, as previously proposed. Additionally, one verifies that the increase of Mg^{2+} concentration to $3.3x10^{-2}$ M (when 2:1 complexes are formed) leads to a small increase on fluorescence quantum yield, evidencing interactions between the second Mg^{2+} cation and the A ring (Carlotti et al. 2012).

In short, the proposed binding site for 1:1 complexes of Mg^{2+}: OTC and Ca^{2+}: OTC is O11-O12. Regarding to the second binding site, for 2: 1 complexes of Mg^{2+}: OTC, there are evidences of the coordination in the A ring, being the site N4-O3 the most favourable for binding.

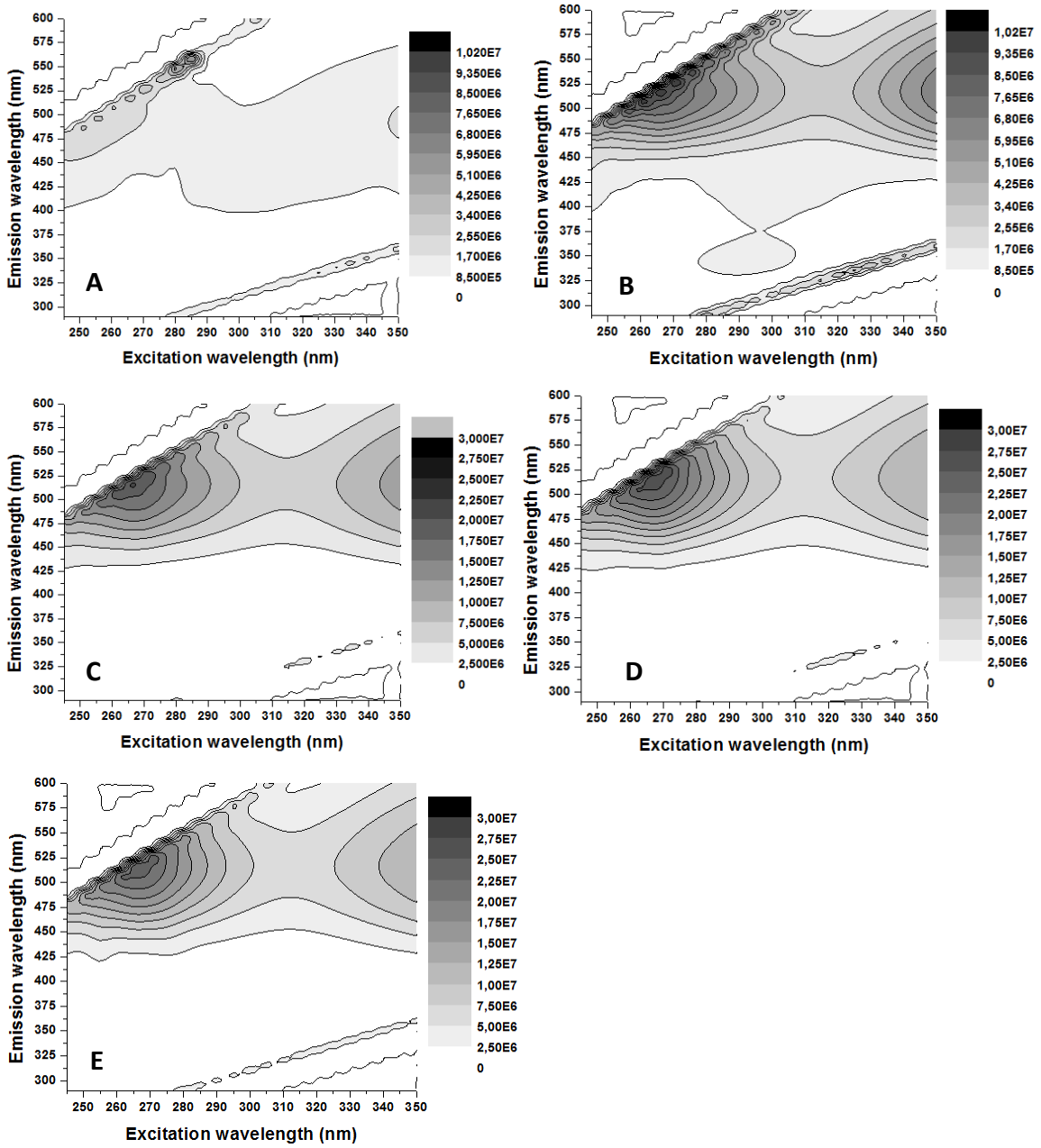

Figure 38 – 3D fluorescence spectra (contour maps) of the aqueous solutions of OTC $8.0x10^{-6}$ M in phosphate buffer (0.001 M) with NaCl (21 g/L): without cations (A), with calcium $7.5x10^{-3}$ M (B), with magnesium $7.5x10^{-3}$ M (C), with magnesium $3.3x10^{-2}$ M (D), with calcium $7.5x10^{-3}$ M together with magnesium $3.3x10^{-2}$ M (E).

6B.3.2 Photo-degradation kinetics studies

In the previous subchapter (6A), one concluded that the sea-salts in aquaculture's water strongly enhanced the OTC photo-degradation comparatively with aqueous solutions not containing those sea-salts. Since calcium and magnesium are two of the main cations of seawater, several experiments to evaluate the effect of these two cations on OTC photo-degradation (at pH 7.3) were performed, at concentration levels found in brackish aquaculture's water. The data of all these experiments were fitted by non-linear regression to the first order kinetics equation and the experimental half-life times were calculated as ln(2)/*k*. Non-linear curve fitting was made using GraphPad Prism 6. The results are summarized in **table 14**.

Table 14 – Kinetic results of OTC photo-degradation in phosphate buffer aqueous solutions (0.001 M) containing NaCl (21 g/L), calcium (7.5 x 10^{-3} M) and/or magnesium (3.3 x 10^{-2} M). k – Kinetic rate constant; SD – standard deviation; R^2 – determination coefficient; $t_{1/2}$ – experimental half-life time.

OTC photo-degradation experiment	k (min^{-1}) ± SD	R^2	$t_{1/2}$ (min) ± SD
NaCl without cations added	0.082 ± 0.003	0.9639	8.4 ± 0.3
NaCl with [Ca^{2+}] = 7.5x10^{-3} M	0.135 ± 0.003	0.9865	5.1 ± 0.1
NaCl with [Mg^{2+}] = 3.3x10^{-2} M	0.079 ± 0.001	0.9926	8.8 ± 0.1
NaCl with [Ca^{2+}] = 7.5x10^{-3} M and [Mg^{2+}] = 3.3x10^{-2} M	0.077 ± 0.003	0.9801	9.0 ± 0.4

From this table, one concludes that Ca^{2+} in the solution significantly enhances the OTC photo-degradation (about 65 %) when compared with the OTC photo-degradation in NaCl, in the absence of Ca^{2+} or Mg^{2+}. Contrarily, the kinetic rate constants of OTC photo-degradation containing Mg^{2+}, or Ca^{2+} and Mg^{2+}, did not differ significantly ($p > 0.13$) from those obtained only in NaCl, without addition of the cations. These results suggest that, at these levels of concentrations and proportions, the Mg^{2+} not only did not affect the kinetics of OTC photo-degradation as also seems to inhibit the sensitizing effect promoted by the presence of Ca^{2+} in solution.

The inhibition of the calcium effect in the presence of magnesium can be attributed to a competition of magnesium by the binding sites of OTC. This possible competition is justified either by the higher magnesium concentration in solution, either by the higher affinity of magnesium to complex with OTC, comparatively with calcium. Indeed, several authors determined the conditional binding constants for OTC: Mg^{2+} and OTC: Ca^{2+}, at

different pHs (4.0-8.5) and ionic strengths, obtaining higher values for complexes with Mg^{2+} (Lunestad and Goksoyr 1990; Schmitt and Schneider 2000; Arias et al. 2007).

An increase of the absorbance of the OTC solution at 360-380 nm, in the presence of Ca^{2+} and Mg^{2+} was observed in the present work (**figure 35)**. The samples were exposed to radiation with wavelengths higher than 290 nm in a sunlight simulator, with higher intensity above 350 nm. This means that these cations cause a higher rate of light absorption, since there is a higher superposition of light intensity and absorbance at each wavelength. Thus, the different effects of Ca^{2+} and Mg^{2+} are not explained by differences in the rate of light absorption of those complexes, since the absorbance of Mg^{2+}: OTC complexes is even higher than the absorbance of Ca^{2+}: OTC and only Ca^{2+} enhances the OTC photo-degradation.

As previously referred, Chen et al. (2011) attributed the distinct effects of these cations to their different binding patterns. The authors verified that the addition of sodium azide, which is a quencher of singlet oxygen, to the solution did not affect the OTC photo-degradation in the presence of magnesium 10 mM (at pH 7.3 and 9.0), but markedly inhibited the OTC photo-degradation in the presence of calcium 10 mM, at pH 7.3. From extrapolation of results obtained by Wessels et al. (1998), who performed their studies at a different pH value (pH 8.02), Chen at al. (2011) suggested that Ca^{2+} coordinates at O10-O11 and O12-O1 sites, favouring the attack of $^1O_2$ on the dimethylamine group and the self-sensitizing oxidation. Chen et al. (2011) also assumed that the magnesium complexation occurred at N4-O3 site, which decreased the availability of N-electrons and inhibited the self-sensitized oxidation.

The availability of dimethylamine group and the self-OTC sensitized oxidation could be an explanation for the results obtained in the present work. Indeed, when Mg^{2+} is in solution with the above referred concentration (**table 14**), it coordinates at O11-O12 and N4-O3, effectively decreasing the availability of N-electrons and inhibiting the possible OTC self-sensitized oxidation. Since the spectral evidence presented in *subchapter 6B.3.1* suggests a similar coordination of the two cations in 1:1 complexes, it would be expected an acceleration of OTC photo-degradation in presence of Mg^{2+} at lower concentration.

To confirm whether the availability of N4 is directly related to the OTC photo-degradation rate, new kinetic experiments (three replicates) were performed, considering $[Mg^{2+}] = 7.5 \times 10^{-3}$ M. Based on the kinetic constant obtained with the highest concentration of Mg^{2+} (3.3×10^{-2} M), the predicted degradation after 10 minutes of irradiation would be 54.6 %. The degradation obtained with the lowest Mg^{2+}

concentration (7.5 x 10^{-3} M), also after 10 minutes, was similar (51.6 %). Thus, the effect of Mg^{2+} is different from the effect of Ca^{2+}, even when they at the same concentration. This may suggest two different things: Ca^{2+} and Mg^{2+} are coordinating at different binding sites or the self-sensitizing effect is not the main reason for the acceleration of its photo-degradation rate in the presence of Ca^{2+}.

Chen et al. (2011) also observed different effects of these cations in experimental conditions with low excess of cation in solution. The authors have a maximum molar excess of cation (≤ 1000 µM) of 50 times in relation to OTC (20 µM), meaning that 2:1 (M^{2+}: L) complexes are not formed at their conditions. Based on the work of Wessels et al. (1998), the authors (Chen et al. 2011) assumed that Mg^{2+} binds first to N4-O3 (in complexes 1:1) while the second cation binds at O12-O11 (in complexes 2:1). It must be noticed that Wessels et al. (1998) observed a bathochromic shift of the long wavelength absorption band for 1:1 complexes with Mg^{2+}, as in the case of Ca^{2+}. Despite the general assumption that this bathochromic shift is associated to an interaction with the BCD ring system, in this particular case, the authors (Wessels et al. 1998) attributed this spectral change to an increase of acidity of the O10-O11-O12 moieties when Mg^{2+} is bound to N4. The same authors obtained different spectra for Ca^{2+} and Mg^{2+} complexes at pH 8.02, that were in agreement with different binding patterns for these two cations.

Schmitt and Schneider (2000) observed that Ca^{2+} coordination changes when pH changes from 7.0 to 8.5. Thus, Ca^{2+} and Mg^{2+} present the same binding patterns at pH 7.0, while at pH 8.5, Ca^{2+} coordination involves different binding sites. Besides, the spectral evidences presented previously corroborate the same binding pattern for the two cations, at pH 7.3. So, a different coordination of these cations and the involvement of N4 in the case of Mg^{2+}, with a consequent decrease of self-sensitized oxidation does not seem to be the explanation of the different effects of Mg^{2+} and Ca^{2+}.

Werner et al. (2006) calculated the quantum yields for direct photolysis (not considering self-sensitizing effects) and verified that, for species MHL^{+} (1:1 complexes), the direct photolysis quantum yield for the complex with calcium ($CaHL^{+}$) is higher than for the complex with magnesium ($MgHL^{+}$). In turn, the quantum yields of the complex with magnesium and of the unbound ligand (HL^{-}) are very close. The authors did not provide explanations for the differences in quantum yields and obtained similar spectra for the complexes 1:1 MHL^{+} with these two cations. The spectra of complexes 1:1 obtained in the present work or by Schmitt and Schneider (2000), at pH 7.0, do not allow to attribute different binding patterns for these cations. So, further studies are needed to explain their different effects on photo-degradation.

6B.3.3 Photo-degradation in real aquaculture's water

Similar changes (e.g.: higher intensity, bathochromic shift) to those obtained in the OTC solutions containing Ca^{2+} and Mg^{2+} were previously observed in the spectra of the OTC solutions containing sea-salts (21 ‰) – natural (from aquaculture) and synthetic. This may indicate that these cations may be primarily responsible for changing the spectra of the OTC solutions containing sea-salts.

Since that calcium seems to act as a sensitizer of the OTC photo-degradation, additional experiments were performed in real aquaculture's water. For those experiments 500 mg/L of calcium were added to the filtered aquaculture's water samples previously collected. As the aquaculture's water sample already contained about 300 mg/L of dissolved calcium, the total concentration of calcium in the aqueous sample was about 800 mg/L (2.0×10^{-2} M). This concentration was chosen in order to obtain a concentration of calcium similar to the magnesium in the solution. Thus, two independent replicates were performed using marine aquaculture's water (21 ‰) and the data were fitted to first-order kinetics ($R^2 = 0.967$). Comparing to the kinetic rate constant of OTC photo-degradation obtained in aquaculture's water sample ($k = 0.082 \pm 0.001$ min^{-1}), an increase of about 21 % was observed with the addition of calcium 500 mg/L to the aquaculture´s water ($k = 0.099 \pm 0.004$ min^{-1}). A similar experiment was tentatively made adding 800 mg/L of calcium and 800 mg/L of magnesium to the OTC solution in phosphate buffer and NaCl (21 g/L). However, contrarily to what happened using marine aquaculture's water, this synthetic solution stayed completely saturated, suggesting that in the real brackish aquaculture's water there are other constituents helping the total dissolution of a higher calcium concentration.

6B.3.4 Photoproducts formation

Along the irradiation of OTC in the several aqueous solutions, one observed the formation of different products in each aqueous matrix: aqueous solution of phosphate buffer 0.001 M and NaCl (21 g/L) with calcium 7.5×10^{-3} M (solution 1), with magnesium 3.3×10^{-2} M (solution 2) and with calcium 7.5×10^{-3} M together with magnesium 3.3×10^{-2} M (solution 3). Thus, to better compare the products formation in different aqueous matrices, each solution was irradiated during the time necessary to reduce the OTC concentration to 75 % (t1) and 25 % (t2) of its initial value and a dark control was maintained the longer time of irradiation in the sunlight simulator (t2).

OTC analyses were performed using HPLC-DAD, at 275 nm and the corresponding chromatograms are presented in **figure 39-B, -C, -E, -G**. In those chromatograms, there is a compound (ii) always present in all chromatograms concerning the OTC solutions irradiated in the presence or absence of the divalent cations. Additionally, the compound (i) was formed in the OTC solution irradiated in the absence of magnesium and in the presence of calcium, but disappears when OTC is irradiated in the presence of magnesium. The compound (iii) was formed only when OTC is irradiated in the presence of magnesium (**figure 39-E** and **-G**).

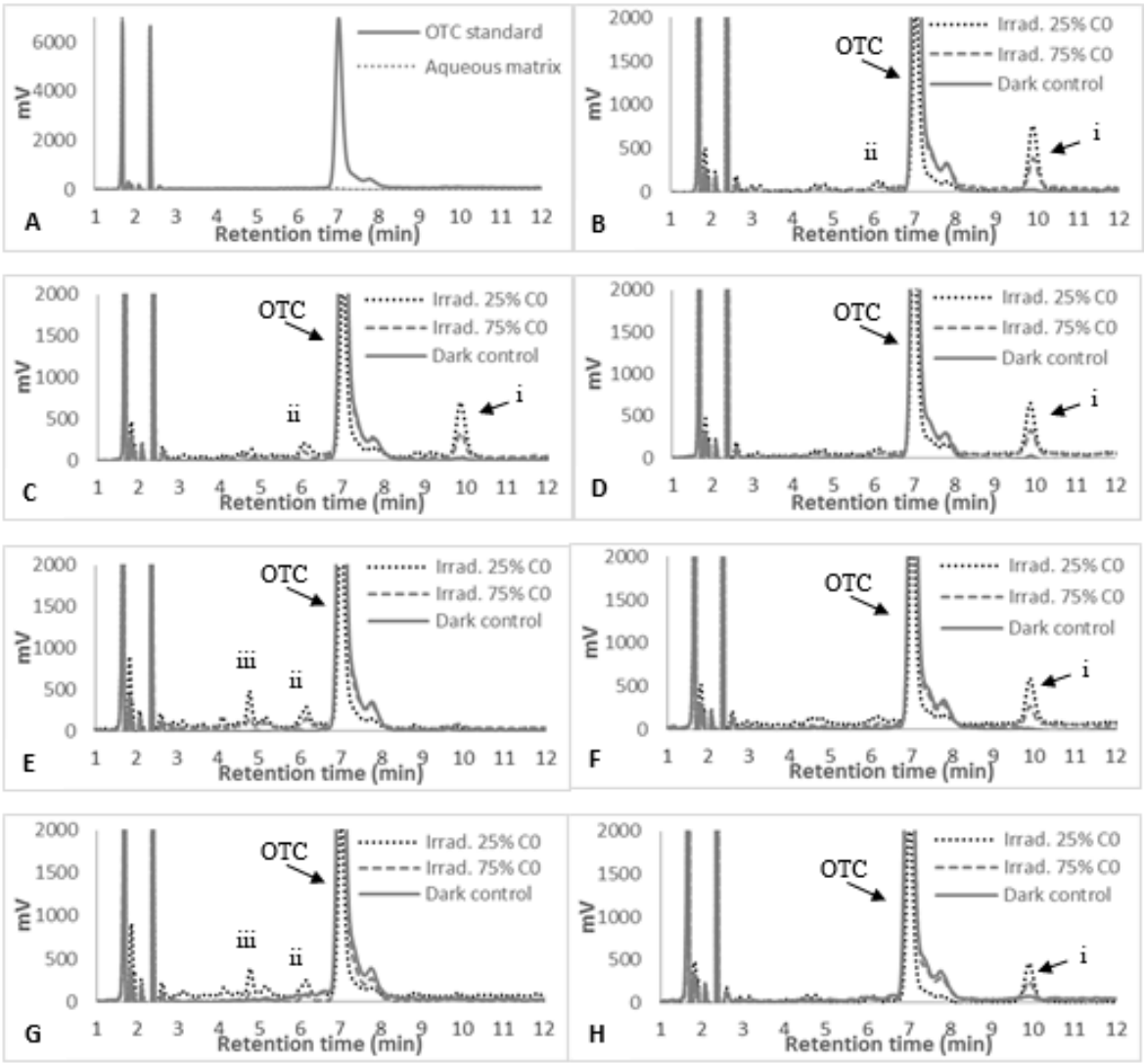

Figure 39 – Chromatograms (detection by HPLC-UV, at 275 nm) of OTC (8.0 x 10^{-6} M) aqueous solutions in phosphate buffer (0.001 M) with NaCl 21 g/L (A and B) before and after OTC photo-degradation without addition of cations. C and D – with addition of calcium (7.5 x 10^{-3} M) before and after photo-degradation, respectively. E and F – with addition of magnesium (3.3 x 10^{-2} M) before and after photo-degradation, respectively. G and H – with addition of calcium (7.5 x 10^{-3} M) and magnesium (3.3 x 10^{-2} M) before and after photo-degradation, respectively. C0 corresponds to the initial OTC concentration.

In addition to the chromatograms obtained with a DAD detector at 275 nm, the chromatograms of the same irradiated solutions were also acquired with detection by fluorescence, at excitation and emission wavelengths of 260 nm and 470 nm, respectively (**figure 40**). Analysing **figure 40-B, -C**, -**E** and -**G**, one observes the formation of other compounds identified as (II), (III) and (IV), which were not detected by UV at 275 nm. Based on the retention time, the compound (I) identified in **figure 40** corresponds to the compound (ii) identified in **figure 39**. The compounds (I), (II) and (III) appeared in all OTC solutions irradiated in the absence or presence of Ca^{2+} and/or Mg^{2+}. The compound (IV) only appears in the chromatograms corresponding to the OTC solutions irradiated in the presence of magnesium (solutions with Mg^{2+} or with Mg^{2+} + Ca^{2+}).

In order to clarify whether differences in the chromatograms are due to differences in the degradation products formed or to the complexation with those products, additional experiments were performed. For that, calcium $7.5x10^{-3}$ M (solution 1), magnesium $3.3x10^{-2}$ M (solution 2) and calcium $7.5x10^{-3}$ M together with magnesium $3.3x10^{-2}$ M (solution 3) were added to the solutions of OTC in phosphate buffer 0.001 M with NaCl (21 g/L) after irradiation in the absence of these cations. The chromatograms regarding to these experiments are presented in **figure 39-D**, **-F**, **-H** (detection by UV, at 275 nm) and in **figure 40-D**, **-F**, **-H** (detection by fluorescence: λ_{ex}= 260 nm, λ_{em}= 470 nm).

Comparing all chromatograms of the OTC solutions acquired with detection at 275 nm, one observes the presence of compound (i) in all aqueous matrices containing Ca^{2+} or/and Mg^{2+} added after OTC photo-degradation (**figure 39-D**, **-F**, **- H**), and in the OTC aqueous buffered solutions containing only NaCl (**figure 39-B**). This compound (i) also appears in the OTC solution irradiated in the presence of Ca^{2+}, but it is absent when the solution was irradiated in the presence of Mg^{2+}. Those results suggest that the compound (i) is a photoproduct from OTC and that, while Ca^{2+} did not affect its formation during irradiation, Mg^{2+} seems to inhibit it.

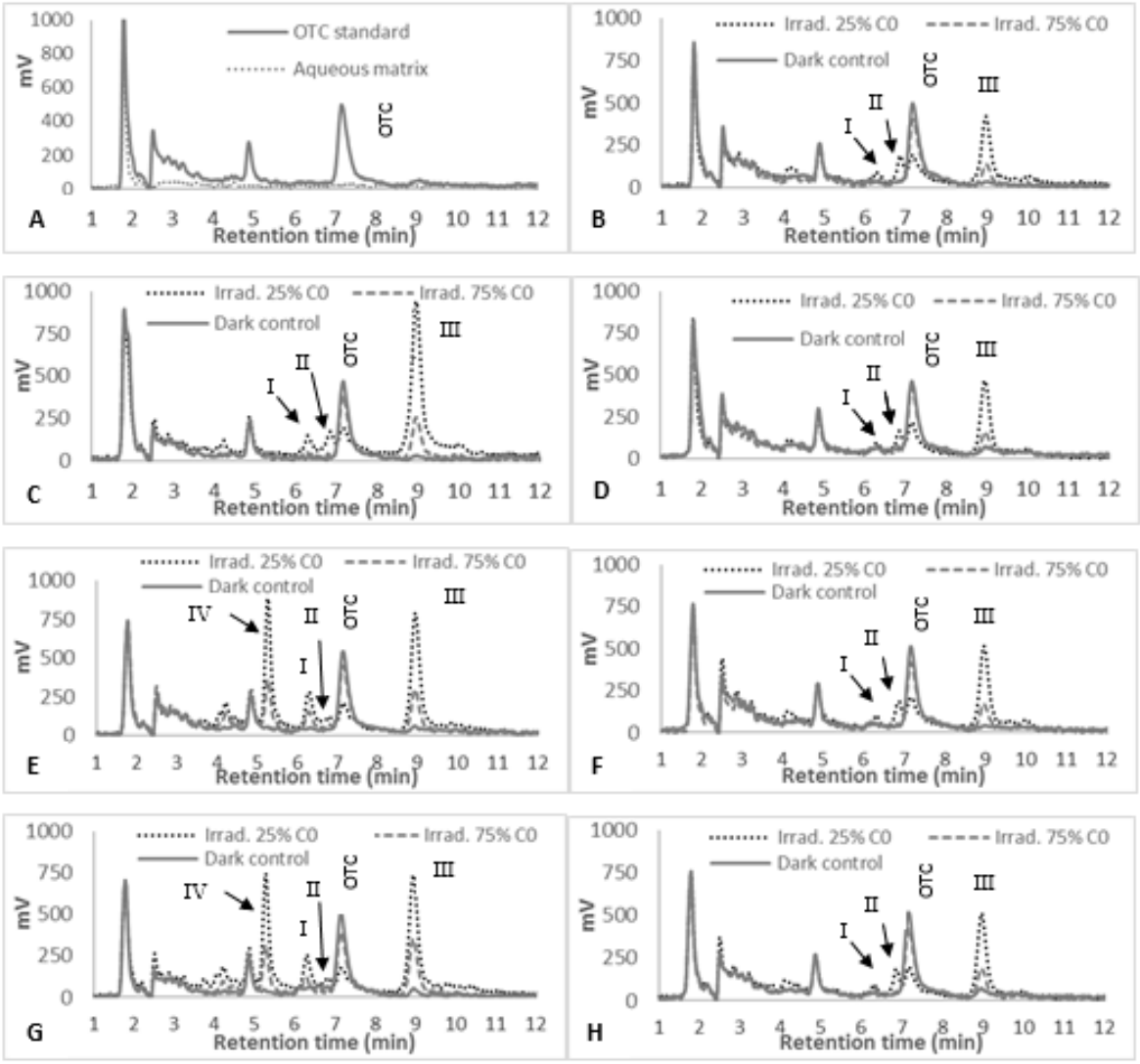

Figure 40 – Chromatograms (detection by fluorescence: λ_{em} = 470 nm; λ_{ex} = 260 nm) of OTC (8.0 x 10^{-6} M) aqueous solutions in phosphate buffer (0.001 M) with NaCl 21 g/L before and after OTC photo-degradation (A and B) without addition of cations. C and D – with addition of calcium (7.5 x 10^{-3} M) before and after photo-degradation, respectively. E and F – with addition of magnesium (3.3 x 10^{-2} M) before and after photo-degradation, respectively. G and H – with addition of calcium (7.5 x 10^{-3} M) and magnesium (3.3 x 10^{-2} M) before and after photo-degradation, respectively. C0 corresponds to the initial OTC concentration.

Analysing now the chromatograms with detection by fluorescence (**figure 40**), one concludes that, among the four products previously referred (I to IV), only the compound IV was not detected in the aqueous matrices where the addition of Mg^{2+} was done after irradiation of OTC solutions. Thus, these results indicate that the compound IV can be an OTC photoproduct induced by the presence of Mg^{2+} during irradiation, while the products I, II and III are OTC photoproducts which are formed in all the studied matrices. However,

for the same percentage of OTC photo-degradation, the concentration of these products (peak area) differs when the OTC solutions are irradiated in the absence or presence of the divalent cations. For example, for a reduction of the OTC concentration to 25% of its initial value, the concentration of the product III is higher when OTC is irradiated in the presence of Ca^{2+} or/and Mg^{2+}, and the concentration of peak I is higher when the irradiation of OTC is performed in the presence of Mg^{2+}. The results obtained suggest that these cations, particularly Mg^{2+}, induce different mechanisms of OTC photo-degradation. These possible different mechanisms seem to affect the kinetics of formation/degradation of some photoproducts.

The formation of different products in the presence or absence of cations is corroborated by studies of 3-D molecular fluorescence. The corrected 3D spectra of OTC solutions are presented in **figures 41-43** and they are different for solutions containing cations added before or after irradiation. One can observe differences in the fluorescence intensity and in the position of the fluorescence peaks. There was a shift to lower $\lambda_{ex/em}$ (nm) with the increase of the irradiation time when Ca^{2+} or/and Mg^{2+} were added prior to OTC irradiation. These results suggest that new fluorescence photoproducts were formed from OTC photo-degradation in the presence of these cations. However, the deviation to lower $\lambda_{ex/em}$ (nm) was much more pronounced in the presence of Mg^{2+} than when only Ca^{2+} was dissolved. Besides, the photoproduct induced by Mg^{2+} (peak b) presents the highest fluorescence intensity, even when the two cations are dissolved in the OTC solutions prior their irradiation. Comparing these results with the chromatograms of OTC solutions detected by fluorescence (λ_{ex} = 260 nm, λ_{em} = 470 nm), the photoproduct IV is proposed as the product induced by the presence of Mg^{2+}, whose maximum $\lambda_{ex/em}$ is at 260/465 nm (peak b). Based on high fluorescence intensity of the OTC photoproducts formed in the presence of magnesium, some authors (Granados et al. 2005) proposed a post-column derivatization with Mg^{2+} as fluorimetric detection method to analyze low tetracyclines concentrations in water samples, using column liquid chromatography.

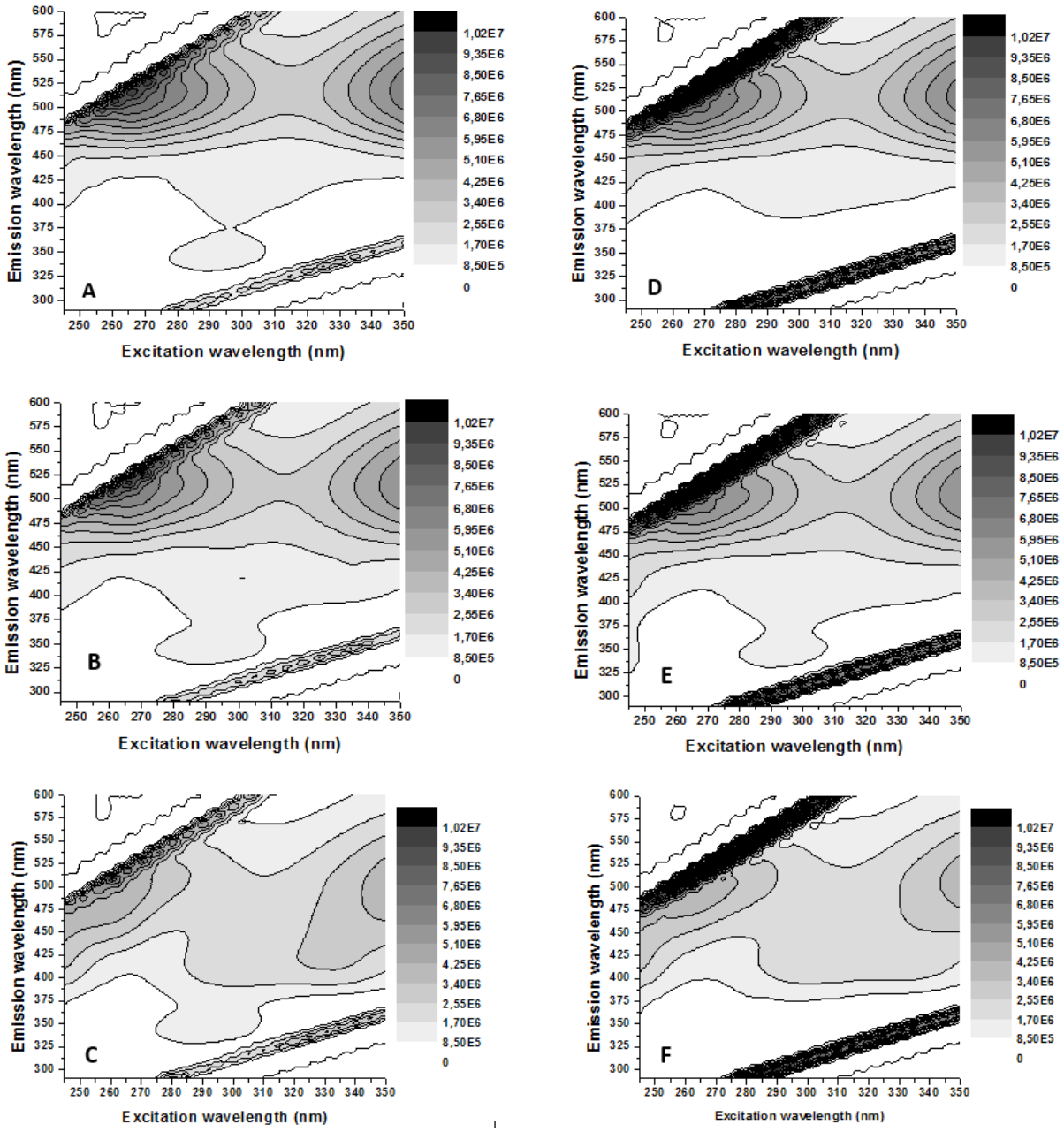

Figure 41 – 3D fluorescence spectra (contour maps) of the aqueous solutions of OTC 4 mg/L in phosphate buffer (0.001 M) with NaCl (21 g/L) and calcium (7.5×10^{-3} M) added before the OTC photo-degradation (A, B and C) or after the OTC photo-degradation (D, E and F). A and D correspond to the dark controls of the OTC aqueous solution; B and E show the irradiated solutions at times corresponding to about 75 % of the initial OTC concentration; C and F show the irradiated solutions at times corresponding to about 25 % of the initial OTC concentration.

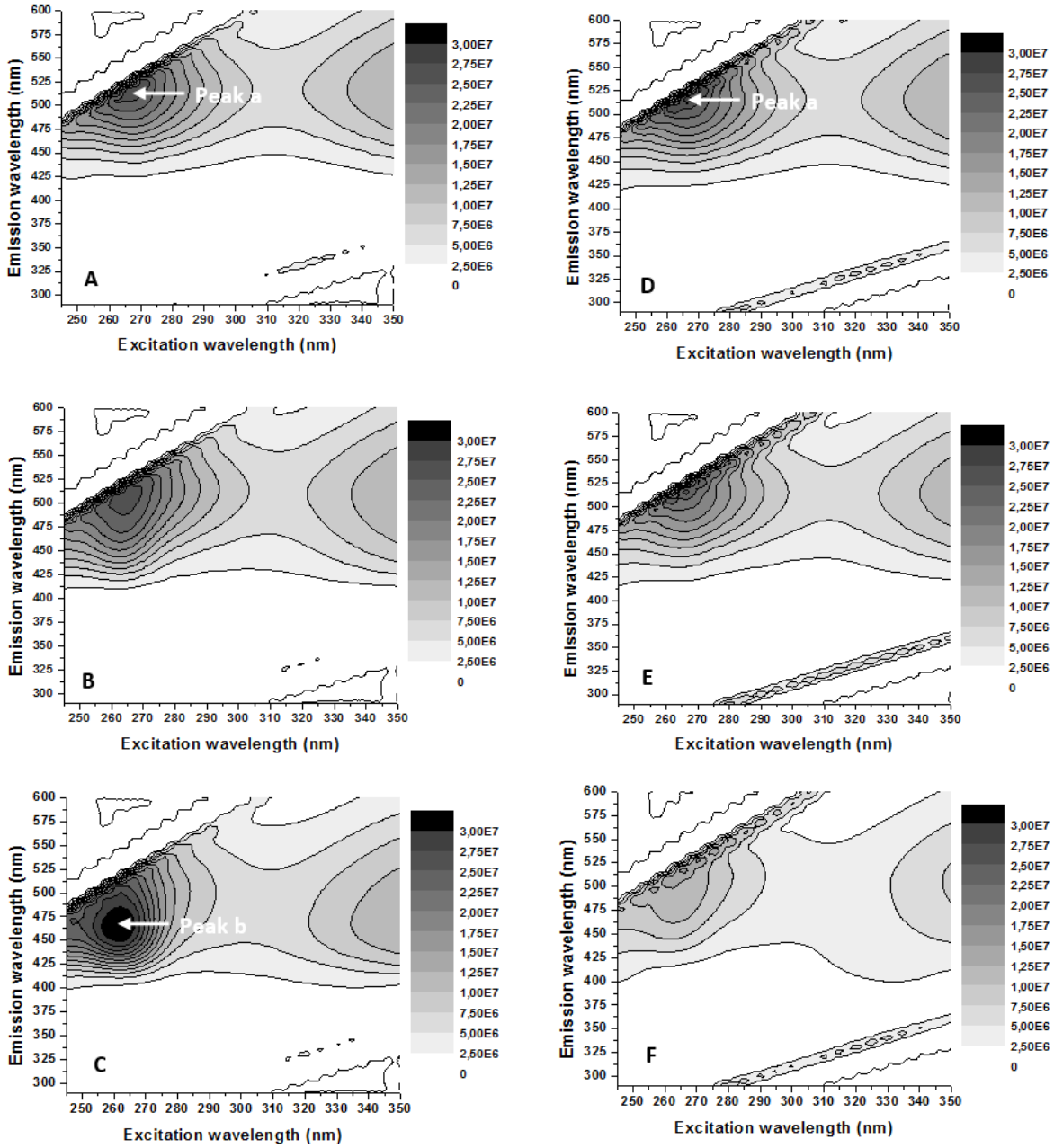

Figure 42 – 3D fluorescence spectra (contour maps) of the aqueous solutions of OTC 4 mg/L in phosphate buffer (0.001 M) with NaCl (21 g/L) and magnesium (3.3 x 10^{-2} M) added before the OTC photo-degradation (A, B and C) or after the OTC photo-degradation (D, E and F). A and D correspond to the dark controls of the OTC aqueous solution; B and E show the irradiated solutions at times corresponding to about 75 % of the initial OTC concentration; C and F show the irradiated solutions at times corresponding to about 25 % of the initial OTC concentration.

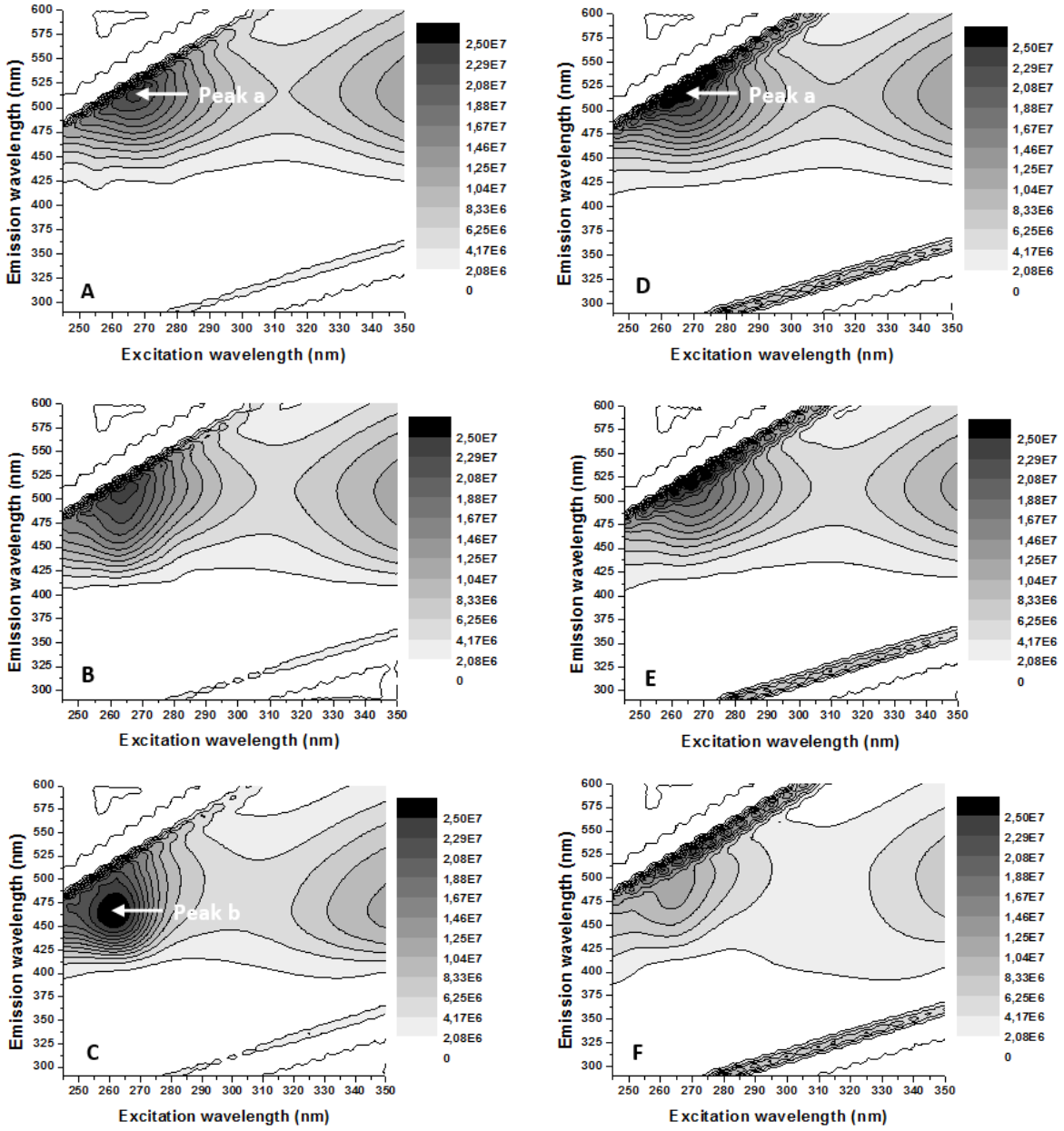

Figure 43 – 3D fluorescence spectra (contour maps) of the aqueous solutions of OTC 4 mg/L in phosphate buffer (0.001 M) with NaCl (21 g/L), calcium (7.5 x 10^{-3} M) and magnesium (3.3 x 10^{-2} M) added before the OTC photo-degradation (A, B and C) or after the OTC photo-degradation (D, E and F). A and D correspond to the dark controls of the OTC aqueous solution; B and E show the irradiated solutions at times corresponding to about 75 % of the initial OTC concentration; C and F show the irradiated solutions at times corresponding to about 25 % of the initial OTC concentration.

6B.4 Conclusions

This subchapter presents the effects of Ca^{2+} and Mg^{2+} on the OTC photo-degradation, using concentrations of those cations, as well as salinity and pH values, typical of marine-based aquacultures. The complexes formed between cations (Ca^{2+} or Mg^{2+}) and OTC are mainly 1:1, for a cation excess of 937 times, and both 1:1 and 2:1 (M^{2+}: ligand), for a Mg^{2+} excess of 4125 times. The spectral evidences (by UV-Vis spectroscopy and molecular fluorescence) suggest the same binding pattern of Ca^{2+} and Mg^{2+}, at pH 7.3. Regarding the kinetic results, the presence of calcium in solution significantly enhances the OTC photo-degradation. However, when magnesium is also present (at concentrations typical of marine-based aquaculture´s water), it inhibits the accelerating effect of calcium on OTC photo-degradation. Comparing these two divalent cations, while calcium seems to affect primarily the OTC kinetics, magnesium had a predominant influence on by-products formation. Thus, the formation of certain products is inhibited by magnesium. Furthermore, it has been demonstrated for the first time in this work that the presence of magnesium during irradiation induces the formation of at least two new products, not detected when irradiation is made in its absence.

So, it is important to be prudent when the conclusions about the identification of the OTC by-products, formed in synthetic matrices, and/or their possible biological activity or toxicity are extrapolated to environmental matrices with different compositions. Some studies in the literature refer conclusions that may not correspond to what happens in natural water since they are mainly developed in deionized water or in synthetic aqueous solutions. Thus, more studies should be developed considering water samples with environmental relevance.

6B.5 References

Arias, M., M. S. Garcia-Falcon, L. Garcia-Rio, J. C. Mejuto, R. Rial-Otero and J. Simal-Gandara (2007). Binding constants of oxytetracycline to animal feed divalent cations. *Journal of Food Engineering* **78**(1): 69-73.

Bhatt, V. K. and R. D. Jee (1985). Micro-ionization acidity constants for tetracyclines from fluorescence measurements. *Analytica Chimica Acta* **167**: 233-240.

Carlotti, B., A. Cesaretti and F. Elisei (2012). Complexes of tetracyclines with divalent metal cations investigated by stationary and femtosecond-pulsed techniques. *Physical Chemistry Chemical Physics* **14**(2): 823-834.

Chen, Y., H. Li, Z. P. Wang, T. Tao and C. Hu (2011). Photoproducts of tetracycline and oxytetracycline involving self-sensitized oxidation in aqueous solutions: Effects of Ca^{2+} and Mg^{2+}. *Journal of Environmental Sciences-China* **23**(10): 1634-1639.

Granados, M., M. Encabo, R. Companó and M. D. Prat (2005). Determination of Tetracyclines in Water Samples Using Liquid Chromatography with Fluorimetric Detection. *Chromatographia* **61**: 471-477.

Guerra, W., P. P. Silva-Caldeira, H. Terenzi and E. C. Pereira-Maia (2016). Impact of metal coordination on the antibiotic and non-antibiotic activities of tetracycline-based drugs. *Coordination Chemistry Reviews* **327–328**: 188-199.

Jiao, S. J., S. R. Meng, D. Q. Yin, L. H. Wang and L. Y. Chen (2008). Aqueous oxytetracycline degradation and the toxicity change of degradation compounds in photoirradiation process. *Journal of Environmental Sciences-China* **20**(7): 806-813.

Jin, X., H. Xu, S. Qiu, M. Jia, F. Wang, A. Zhang and X. Jiang (2017). Direct photolysis of oxytetracycline: Influence of initial concentration, pH and temperature. *Journal of Photochemistry and Photobiology A: Chemistry* **332**: 224-231.

Kulshrestha, P., R. F. Giese and D. S. Aga (2004). Investigating the Molecular Interactions of Oxytetracycline in Clay and Organic Matter: Insights on Factors Affecting Its Mobility in Soil. *Environmental Science & Technology* **38**(15): 4097-4105.

Lambs, L., B. Decock-Le Reverend, H. Kozlowski and G. Berthon (1988). Metal ion-tetracycline interactions in biological fluids. 9. Circular dichroism spectra of calcium and magnesium complexes with tetracycline, oxytetracycline, doxycycline, and chlortetracycline and discussion of their binding modes. *Inorganic Chemistry* **27**(17): 3001-3012.

Lunestad, B. T. and J. Goksoyr (1990). Reduction in the bacterial effect of oxytetracycline in seawater by complex formation with magnesium and calcium. *Diseases of aquatic organisms* **9**: 67-72.

Mitscher, L. A., B. Slater-Eng and T. D. Sokoloski (1972). Circular Dichroism Measurements of the Tetracyclines IV. 5-Hydroxylated Derivatives. *Antimicrobial Agents and Chemotherapy* **2**(2): 66-72.

Newman, E. C. and C. W. Frank (1976). Circular Dichroism Spectra of Tetracycline Complexes with Mg^{2+} and Ca^{2+}. *Journal of Pharmaceutical Sciences* **65**(12): 1728-1732.

Rodgers, C. J. and M. D. Furones (2009). Antimicrobial agents in aquaculture: practice, needs and issues. The use of veterinary drugs and vaccines in Mediterranean aquaculture. C. Rogers and B. Basurco. Zaragoza, CIHEAM**:** 41 -59.

Schmidt, L. J., M. P. Gaikowski, W. H. Gingerich, V. K. Dawson and T. M. Schreier (2007). An Environmental Assessment of the Proposed Use of Oxytetracycline-Medicated Feed in Freshwater Aquaculture. Wisconsin, U.S. Food and Drug Administration**:** 97.

Schmitt, M. O. and S. Schneider (2000). Spectroscopic investigation of complexation between various tetracyclines and Mg^{2+} or Ca^{2+}. *Physchemcomm* **3**(9): 42-55.

Serrano, P. H. (2005). Responsible use of antibiotics in aquaculture. FAO Fisheries Technical Paper 469. Rome, FAO**:** 110.

Sompolinsky, D. and Z. Samra (1972). Influence of Magnesium and Manganese on Some Biological and Physical Properties of Tetracycline. *Journal of Bacteriology* **110**(2): 468-476.

Tongaree, S., D. R. Flanagan and R. I. Poust (1999). The interaction between oxytetracycline and divalent metal ions in aqueous and mixed solvent systems. *Pharmaceutical Development and Technology* **4**(4): 581-591.

Werner, J. J., W. A. Arnold and K. McNeill (2006). Water hardness as a photochemical parameter: Tetracycline photolysis as a function of calcium concentration, magnesium concentration, and pH. *Environmental Science & Technology* **40**(23): 7236-7241.

Wessels, J. M., W. E. Ford, W. Szymczak and S. Schneider (1998). The complexation of tetracycline and anhydrotetracycline with Mg^{2+} and Ca^{2+}: A spectroscopic study. *Journal of Physical Chemistry B* **102**(46): 9323-9331.

Xuan, R. C., L. Arisi, Q. Q. Wang, S. R. Yates and K. C. Biswas (2010). Hydrolysis and photolysis of oxytetracycline in aqueous solution. *Journal of Environmental Science and Health Part B-Pesticides Food Contaminants and Agricultural Wastes* **45**(1): 73-81.

Zhao, C., M. Pelaez, X. D. Duan, H. P. Deng, K. O'Shea, D. Fatta-Kassinos and D. D. Dionysiou (2013). Role of pH on photolytic and photocatalytic degradation of antibiotic oxytetracycline in aqueous solution under visible/solar light: Kinetics and mechanism studies. *Applied Catalysis B-Environmental* **134**: 83-92.

Chapter 6C:

Antibacterial activity of OTC photoproducts in brackish aquaculture's water and in synthetic aqueous solutions

The main concern related to the use of OTC in aquaculture is the bacterial resistance, when ineffective treatments are applied for its removal or inactivation. OTC photo-degradation has been suggested as an efficient complementary process to conventional methods used in intensive fish production (e.g.: ozonation). Despite this, and knowing that the complete mineralization of OTC is difficult, few studies have examined the antibacterial activity of OTC photoproducts. Thus, the main aim of this work is to assess whether the OTC photoproducts retain the antibacterial activity of its parent compound (OTC) after its irradiation, using simulated sunlight. For that, three Gram-negative bacteria (Escherichia coli, Vibrio sp. *and Aeromonas* sp.*) and different synthetic and natural aqueous matrices (phosphate buffered solutions at different salinities, 0 and 21 ‰, and three different samples from marine aquaculture industries) were tested. The microbiological assays were made using the well-diffusion method before and after OTC has been exposed to sunlight. The results revealed a clear effect of simulated sunlight, resulting on the decrease or elimination of the antibacterial activity for all strains and in all aqueous matrices due to OTC photo-degradation. For E. coli, it was also observed that the antibacterial activity of OTC is lower in the presence of sea-salts, as demonstrated by comparison of halos in aqueous matrices containing or not sea-salts.*

6C.1 Contextualization

The main concern related to the use of antibiotics, like OTC, is the emergence of bacterial resistance (Levy et al. 1976; FAO/OIE/WHO 2006; Cabello et al. 2013). Some authors refer that about 70-80 % of antibiotics used in fish feed in aquaculture are excreted in water (Serrano 2005; Romero et al. 2012; Cabello et al. 2013; Gastalho et al. 2014). This contributes to contamination of aquatic systems, which can act as a reservoir of resistant genes (Baquero et al. 2008; Tacão et al. 2012). Dissemination in aquatic systems, including aquaculture environment, can occur by horizontal gene transfer and subsequently resistance can reach humans through transfer of drug-resistant pathogens from the aquatic environment (Heuer et al. 2009; Marshall and Levy 2011). To evaluate whether the antibacterial activity of OTC remains after irradiation, i.e, whether the photoproducts also have antibacterial activity, is an important aspect to consolidate the OTC degradation method because if its photoproducts retain the antibacterial activity of the parent compound, the degradation method is not so good.

Only two works, which compared the antibacterial activity of OTC before and after its photo-degradation, are known in literature (Lunestad et al. 1995; Pereira et al. 2013), but they only considered *Escherichia coli* as test organism, leaving out phylogenetic groups causing disease in fish in aquaculture, such as *Aeromonas* spp. and *Vibrio* spp. (Menezes 2000). Furthermore, the physical-chemical characteristics of water used in these studies are different from those used in the present study, which may influence the results. Thus, the main aim of this work is to assess whether the photoproducts of OTC have antibacterial activity in marine aquaculture's water and in synthetic aquatic systems, simulating the natural conditions. For that, antibacterial assays were performed considering three Gram-negative strains identified as *Escherichia coli*, *Aeromonas* sp. and *Vibrio* sp.

6C.2 Materials and methods

6C.2.1 Chemicals

The reagents used to prepare the OTC aqueous solutions in phosphate buffer (0.001 M) without or with synthetic sea-salts (21 ‰) are the same described previously in *subchapter 6A.2.1*.

6C.2.2 Sampling of aquaculture's water

Water samples from two different intensive aquaculture companies in Portugal (company A and company B) were collected again, in September/October and November 2015. Seven replicates were collected at each sampling site, three for the kinetic studies and four for biological tests. The sampling sites were chosen based on the kinetic results previously obtained and were the following: L2b – after the biological treatment (only in company B) and L3 – after ozonation (in the two companies). The pH and salinity of the water samples are around 7.0–7.5 and 21 ± 1 ‰, respectively. The total organic carbon content in these samples was analysed as described in *subchapter 5.2.2*.

6C.2.3 Photo-degradation experiments

The aquaculture's water samples were previously filtered (glass microfiber filter of 1.2 µm, 47 mm, GF/C Whatman®), spiked with OTC 40 mg/L (8.0×10^{-5} M) and submitted to simulated solar radiation in quartz tubes. Solutions of OTC 40 mg/L in phosphate buffer 0.001 M at different salinities (0 and 21 ‰) were also prepared and irradiated for comparison.

To assess if the sunlight removes the antibacterial activity of OTC, i.e., if OTC by-products, at the concentrations produced, have antibacterial activity, two different times per aqueous solution were chosen based on the corresponding kinetic rate constants. Thus, each OTC solution was irradiated the time necessary to decrease OTC concentration to about 50% of its initial value (t1) and the time needed to reduce it to a residual value lower than 7% of the initial OTC concentration (t2). Additionally, all aqueous matrices without OTC (M) were irradiated during the longer irradiation time of the respective experiment. Each irradiation was performed together with the dark controls for t1 (Ct1), for t2 (Ct2) and for matrix (Mc). After irradiation, all aqueous matrices (containing or not

OTC) were sterilized using syringe filters of cellulose acetate (Sterile-R, 0.22 µm, Frilabo), which were previously conditioned with the corresponding aqueous matrix. Then, the aqueous samples were stored in sterile tubes (culture tubes, 17 x 95 mm, Simport Scientific) in the refrigerator, protected from light for a maximum time period of four hours until their application to the petri dishes to perform the antibacterial assays.

All irradiations (three to five replicates together with the respective dark controls) were performed with the sunlight simulator (using an irradiance of 550 W/m^2 in all spectral range) described previously, in *subchapter 4.2.2*.

The analyses of OTC in aqueous solutions were performed by HPLC–DAD (SPD-M20A, 200–600 nm) and fluorescence detector (RF-20A$_{XS}$). The fluorescent photoproducts were detected at the excitation and emission wavelengths of 260 nm and 470 nm, respectively. The conditions of analysis, as well as, the characteristics of C18 column were the same described above, in *subchapter 6A.2.3*.

6C.2.4 Antimicrobial assays

Antibacterial activity was determined by well-diffusion method against *Escherichia coli* ATCC 25922, *Vibrio* sp. C7 and *Aeromonas* sp. B48. *Vibrio* and *Aeromonas* strains were previously isolated from environmental samples and identified by biochemical tests and by sequencing the 16S rRNA gene (Henriques et al. 2016). *E. coli* was chosen as representative of faecal contamination, while strains identified as *Vibrio* sp. and *Aeromonas* sp. were chosen to represent two of the main pathogens causing diseases in fish (Menezes 2000). The strains were stored at -80 ºC in LB broth (Fisher BioReagents^{TM}, Belgium) supplemented with 20% glycerol until use. When needed, cultures were inoculated in LB broth or Mueller Hinton agar (MHA, Oxoid, England) media and incubated overnight at the optimum growth temperatures (37 ºC for *E. coli* and 30 ºC for *Vibrio* sp. and *Aeromonas* sp.).

To determine the antibacterial activity, several colonies were transferred from fresh plates to LB broth and incubated until cultures reached 0.5 OD (optical density) at 580 nm. Five hundred microliters of this inoculum were mixed with 350 mL of molten MHA, homogenized to ensure the distribution of bacteria, and poured immediately onto square petri dishes (≈ 70 mL per petri dish). The plates were left to solidify for 10 min. Using a sterile cork borer, 12 or 18 round wells (Ø = 8 mm) were made into each plate. The wells were filled with 100 µL of the aqueous solutions (containing or not the antibiotic). Plates

were incubated at the optimum growth temperature for 16 h. All procedures were performed under strict aseptic conditions.

The diameter of the inhibition areas around the wells was measured and expressed in millimetres (mm). The zone of inhibition of bacterial growth (Ø), which is indicative of antibacterial activity, corresponds to the difference between the total diameter ($Ø_{total}$) and the diameter of halo ($Ø_{halo}$ = 8 mm), as illustrated in **figure 44**.

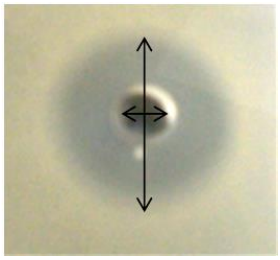

Figure 44 – Inhibition zone of the bacterial growth. The horizontal line corresponds to diameter of halo, while the vertical line corresponds to total diameter ($Ø_{total}$) (diameter of halo plus inhibition zone), in millimetres.

The experiments were carried out in two groups. The first group concerns the experiments with the two synthetic aqueous samples – phosphate buffer 0.001 M at different salinities – 0 and 21 ‰ – 12 wells per petri dish: 6 wells per aqueous matrix (M, t1, t2, Mc, Ct1, Ct2). The second group of experiments was done using marine aquaculture water samples – 18 wells per petri dish: 6 wells per aqueous matrix, three matrices (corresponding to two sampling points from company B and one from company A). The assays performed in each petri dish were replicated independently four to five times, meaning that each well, which count as n = 1, was replicated in different petri dishes four to five times.

6C.3 Results and discussion

6C.3.1 Kinetics of OTC (40 mg/L) photo-degradation

To detect the photoproducts in all aqueous matrices and to determine their antibacterial activity, the OTC concentration had to be increased to 40 mg/L. Calibration standards of OTC ranging between 1 and 40 mg/L were prepared in all aqueous matrices, including aquaculture's water. The R^2 values ranged between 0.9998 and 1.000 and the LOD values varied from 0.28 to 0.67 mg/L.

The kinetics at this OTC concentration (40 mg/L) was studied to choose the times t1 and t2 to make biological assays. Previous studies carried out by other authors (Lopez-Penalver et al. 2010; Zhao et al. 2013) reported the effect of the initial OTC concentration on its photo-degradation kinetics. Similar to what was observed in the previous subchapters, the data of C/C_0 (y-axis) versus the irradiation time (x-axis) were well-fitted to the first order kinetics equation by non-linear regression. The kinetic data for the OTC photo-degradation are presented in **table 15.** In agreement with the results obtained at [OTC] = 4 ppm, the kinetic rate constants of OTC 40 ppm in marine aquaculture's water or artificial brackish water are higher than the corresponding rate constants in phosphate buffer solutions (0 ‰), which may be attributed to the effect of sea-salts already discussed in this work. In contrast, the average pseudo-first order rate constants obtained at [OTC] = 40 ppm (0.047 min^{-1} in phosphate buffer without sea-salts and 0.060-0.078 min^{-1} in saline solutions) were similar or lower than those obtained at [OTC] = 4 ppm (0.051 min^{-1} in phosphate buffer without sea-salts and 0.082-0.092 min^{-1} in saline solutions).

Table 15 – Kinetic results of OTC photo-degradation (40 mg/L) in different aqueous matrices: in marine aquaculture's water (OTC was spiked to each filtered aquaculture's water sample collected in companies A and B), in 0.001 M phosphate buffer solution without (0 ‰) and with synthetic sea salts (21 ‰). k – Kinetic rate constants (min^{-1}), R^2 – determination coefficients of the non-linear adjustment, $t_{1/2}$ – experimental half-life time (min), Φ – apparent quantum yield (290-450 nm). SD: standard deviation; L2b: after biological treatment; L3: after ozonation.

Aqueous matrix	k (min^{-1}) ± SD	R^2	$t_{1/2}$ ± SD	$\Phi_{(290-450\ nm)}$ x10^{-3}
Company A – L3	0.067 ± 0.005	0.9414	10.5 ± 0.8	2.03 ± 0.14
Company B– L2b	0.060 ± 0.005	0.9211	11.6 ± 1.1	1.85 ± 0.06
Company B – L3	0.070 ± 0.006	0.9379	10.0 ± 0.8	2.14 ± 0.24
In phosphate buffer with synthetic sea salts (21 ‰)	0.078 ± 0.007	0.9392	8.9 ± 0.8	2.28 ± 0.29
In phosphate buffer (0 ‰)	0.047 ± 0.002	0.9959	14.9 ± 0.5	1.12 ± 0.08

The increase of OTC concentration (one order of magnitude) would increase the amount of light blocked by OTC to other OTC molecules in solution. To clarify this aspect and normalize the two sets of results (4 mg/L vs. 40 mg/L), the apparent quantum yields – $\Phi_{290-450nm}$ – of reactions using OTC 40 mg/L were calculated using the same methodology explained above (*subchapter 6A.3.5*). This parameter considers the effective rate of light absorption by the compound (discounting the absorbance of matrix). The values of the

apparent quantum yields obtained using OTC 40 ppm (**table 15**) are higher than those previously obtained at OTC concentrations of 4 ppm. This may be attributed to a higher self-sensitizing effect observed at higher OTC concentrations (Zhao et al. 2013). However, due to the opposite self-screening effects, the kinetic rate constants obtained at OTC 40 ppm are lower (natural water) or not significantly different (synthetic matrices) relatively to those determined at OTC 4 ppm.

6C.3.2 Determination of antibacterial activity of OTC and its photoproducts

The antibacterial activity was determined before and after irradiation of the OTC aqueous solutions, using the bacterial strains *Escherichia coli* ATCC25922, *Vibrio* sp. C7 and *Aeromonas* sp. B48. For these experiments, synthetic and natural water samples were considered, as explained in *subchapter 6C.2.4*. The chromatograms of the irradiated solutions of OTC revealed the presence of new peaks, not present in the chromatograms of the original OTC solution (**figures 45 and 46**). Those peaks can be attributed to degradation products and they are more clearly seen with fluorescence detection (**figure 46**). The irradiation times resulting in the intermediate and residual OTC concentration were chosen, because the intermediate photoproducts formed at irradiation time corresponding to OTC half-concentration (t1) almost disappeared at the final irradiation time (t2). All aqueous matrices were considered for these experiments since the comparison of the retention times of the peaks in the chromatograms suggests that different photoproducts of OTC are formed in different aqueous matrices (**figures 45** and **46**).

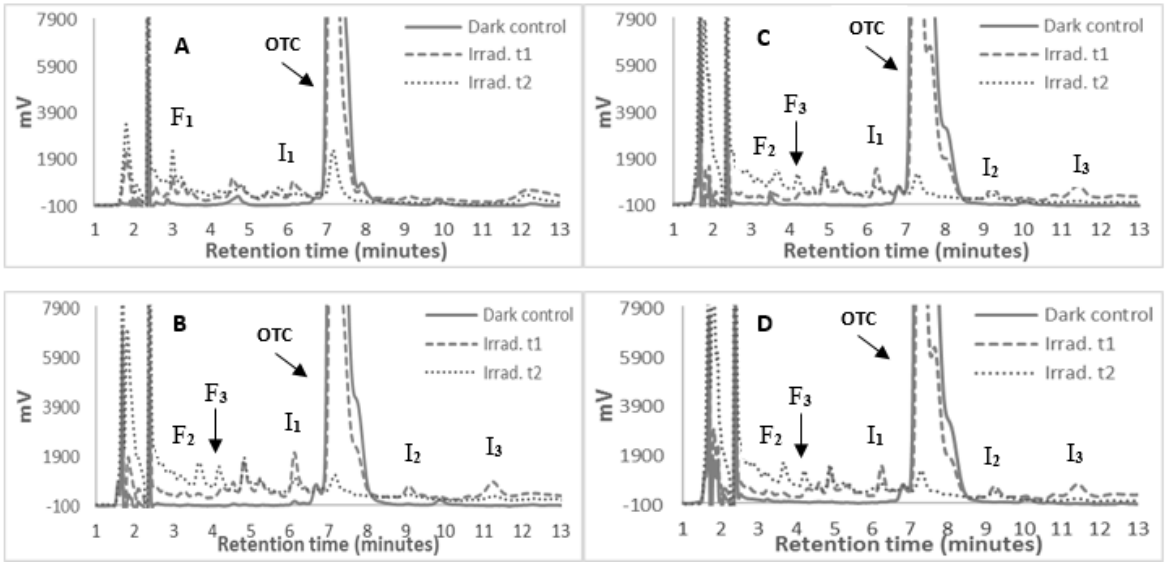

Figure 45 – Chromatograms obtained by HPLC-UV (λ = 275 nm) in the different aqueous matrices: in phosphate buffer 0.001 M without sea-salts (A) and with synthetic sea-salts (B), in brackish aquaculture's water from company A (C) and in brackish aquaculture's water from company B (D). t1: irradiation time corresponding to about 50 % of $[OTC]_0$; t2: irradiation time corresponding to a residual $[OTC]_0$. I_1, I_2, I_3 – intermediate photoproducts; F_1, F_2, F_3 – final photoproducts.

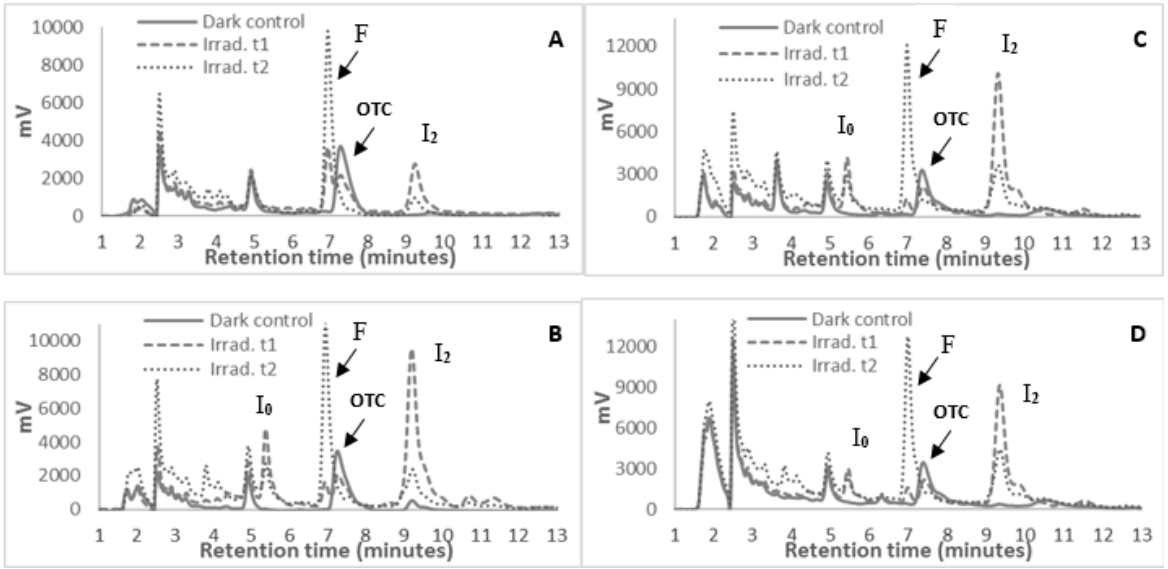

Figure 46 – Chromatograms obtained by HPLC-fluorescence ($\lambda_{exc.}$: 260 nm, $\lambda_{em.}$: 470 nm) in the different aqueous matrices: in phosphate buffer 0.001 M without sea-salts (A) and with synthetic sea-salts (B), in brackish aquaculture's water from company A (C) and in brackish aquaculture's water from company B (D). t1: irradiation time corresponding to about 50 % of $[OTC]_0$; t2: irradiation time corresponding to a residual $[OTC]_0$. I_0, I_1, I_2 – intermediate photoproducts; F – final photoproduct.

The main differences on formation of OTC photo-products are visible between the synthetic aqueous solutions containing or not sea-salts (21%). In the OTC solution containing synthetic sea-salts (**figures 45-B** and **46-B**) one observes the formation of intermediate and final photo-products that do not seem to be formed in the OTC solution of phosphate buffer without sea-salts (**figures 45-A** and **46-A**). Among the brackish water samples (synthetic and natural), the differences on formation of OTC photoproducts are less evident, but also exist. Differences on formation of photoproducts in company B, between water samples collected at different sites of water treatment, were not observed. Thus, the antibacterial assays were performed for all aqueous matrices, containing or not OTC. The assays made with all aqueous matrices without addition of OTC did not reveal zones of inhibition of bacterial growth around the well, confirming the inexistence of antibacterial activity in any of the irradiated matrices. The overall results obtained from antibacterial assays are presented in **table 16**. **Figure 47** illustrates the typical results obtained in antibacterial assays performed in synthetic and natural water.

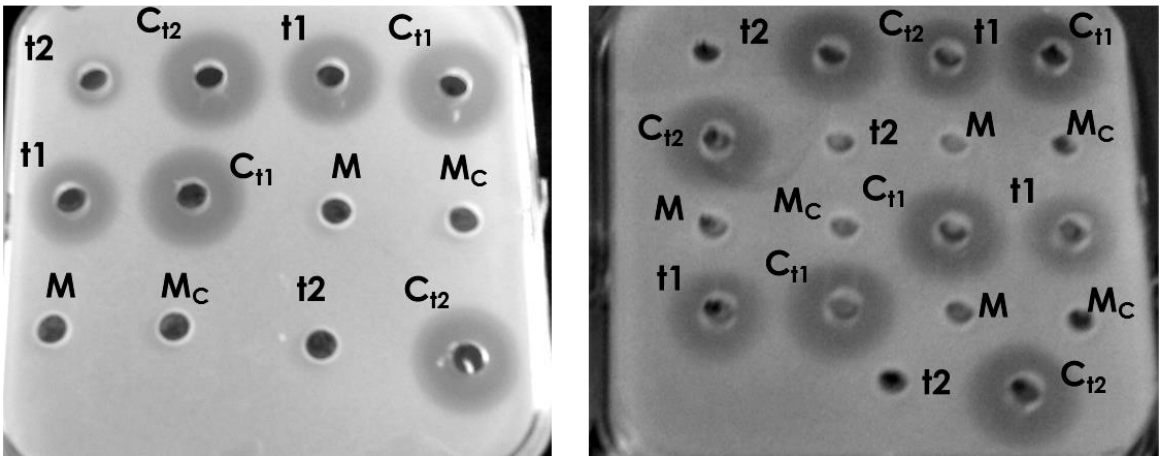

Figure 47 – Results of antibacterial assays performed with *Vibrio* sp. in synthetic (left) and natural (right) water samples. C – dark control; M – aqueous matrix; t1 – irradiated solution at time (min) corresponding to about 50 % of the initial concentration of OTC; t2 – irradiated solution at time (min) corresponding to a residual OTC concentration (2 – 7 %).

Several important conclusions may be taken from the analysis of **table 16**. First of all, the observed susceptibility pattern is strain-dependent. For each matrix, comparing the diameters of halos (in millimetres) of the dark controls between the three bacterial strains, one observes that *Vibrio* and *Aeromonas* strains present higher susceptibility to OTC than the tested *E. coli* strain for all aqueous matrices. The data of **table 16** also

indicate that there are differences in halos of dark controls between the five aqueous matrices for *E. coli* strain. These differences have been confirmed by statistical analysis (ANOVA 1D, $p << 0.001$). In order to assess which matrices differ between them, multiple pairwise comparisons were made by the Bonferroni's test, using SPSS Statistics 24. The statistical data indicate that all averages of halos in different aqueous matrices differ from each other ($p < 0.029$), except the averages for the locals L2b and L3 of company B ($p = 1.0$). This puts into evidence that the nature (natural or synthetic) and composition of the different aqueous matrices affect the susceptibility of *E. coli.* It is observed that the presence of sea-salts in the buffer solution causes a decrease of the halos (very significant difference between buffer solutions with and without sea-salts: $p << 0.001$). Furthermore, the average halos in aquaculture's water are also lower than the halos in buffer without sea-salts ($p < 0.001$) but are higher than the halos in buffer with sea-salts ($p < 0.001$). Thus, the reduction of OTC antibacterial activity observed in the presence of sea-salts seems to be attenuated by the presence of several components existing in aquaculture's water samples. Possible causes may be related to the differences in the composition of sea-salts (synthetic vs. natural) or to the presence of organic matter in aquaculture's water. This latter hypothesis is raised once the attenuation of the effect of sea-salts seems to be more pronounced in water samples collected in company B, which presents a higher DOC content comparatively to company A (1.19 ± 0.05 mg C/L in water collected in company A; 3.40 ± 0.02 mg C/L and 3.42 ± 0.06 mg C/L in the sites L2b and L3, respectively, of company B).

Table 16 – Results (mean diameter of the inhibition zone ± standard deviation) of antibacterial assays performed for OTC and its photoproducts in different water samples: in marine aquaculture water (companies A and B), in phosphate buffer solution 0.001 M without (0 ‰) and with synthetic sea salts (21 ‰). L2b: after biological treatment; L3: after ozonation. Ø – Diameter of the inhibition zone (mm): Ø = $Ø_{total}$ – $Ø_{halo}$. t1 and t2 – times of irradiation necessary to achieve the intermediate OTC concentration (≈ 50 % of its initial concentration) and a residual OTC concentration, respectively.

		Phosphate buffer		Synthetic sea-salts 21‰		Company A_L3		Company B_L3		Company B_L2b	
Bacteria	Irradiation	**Ø (mm)**	[OTC] ppm	**Ø (mm)**	[OTC] ppm	**Ø (mm)**	[OTC] ppm	**Ø (mm)**	[OTC] ppm	**Ø (mm)**	[OTC] ppm
E. coli	Control – t1	**8.6 ± 1.1**	39.4 ± 0.5	**3.8 ± 0.8**	39.0 ± 0.5	**5.5 ± 0.6**	39.6 ± 1.8	**6.8 ± 1.0**	39.8 ± 2.7	**6.8 ± 0.5**	39.7 ± 1.1
	Irradiated – t1	**5.0 ± 0.7**	19.8 ± 3.4	**2.4 ± 0.9**	20.2 ± 4.5	**3.0 ± 0.0**	19.6 ± 1.4	**3.0 ± 0.0**	20.0 ± 1.9	**3.0 ± 0.0**	19.7 ± 0.7
Reduction (%)	---	**41.9 ± 3.0**	---	**37.3 ± 12.8**	---	**45.0 ± 5.8**	---	**54.9 ± 6.1**	---	**55.4 ± 3.6**	---
E. coli	Control – t2	**8.2 ± 1.1**	39.5 ± 0.7	**3.4 ± 0.9**	38.8 ± 0.6	**5.3 ± 0.5**	39.7 ± 1.8	**6.5 ± 0.6**	40.0 ± 2.6	**6.8 ± 0.5**	39.7 ± 1.2
	Irradiated – t2	**0**	2.2 ± 0.3	**0**	0.8 ± 0.2	**0**	1.1 ± 0.2	**0**	0.9 ± 0.1	**0**	0.7 ± 0.2
Reduction (%)	---	**100 ± 0.0**	---	**100 ± 0.0**	---	**100 ± 0.0**	---	**100 ± 0.0**	---	**100 ± 0.0**	---
***Vibrio* sp.**	Control – t1	**17.2 ± 1.1**	38.2 ± 0.8	**16.8 ± 0.8**	39.6 ± 0.7	**16.3 ± 0.5**	39.6 ± 1.8	**18.0 ± 0.8**	39.8 ± 2.7	**18.0 ± 0.8**	39.7 ± 1.1
	Irradiated – t1	**15.4 ± 1.1**	21.3 ± 1.4	**14.0 ± 0.7**	22.5 ± 1.0	**14.0 ± 0.8**	19.6 ± 1.4	**14.0 ± 0.8**	20.0 ± 1.9	**14.8 ± 1.0**	19.7 ± 0.7
Reduction (%)	---	**10.3 ± 6.4**	---	**16.6 ± 2.4**	---	**13.9 ± 3.3**	---	**22.3 ± 1.0**	---	**18.1 ± 2.9**	---
***Vibrio* sp.**	Control – t2	**17.6 ± 0.9**	38.4 ± 0.6	**16.6 ± 0.9**	39.4 ± 1.0	**16.3 ± 0.5**	39.7 ± 1.8	**18.0 ± 0.8**	40.0 ± 2.6	**17.3 ± 0.5**	39.7 ± 1.2
	Irradiated – t2	**4.4 ± 0.9**	2.9 ± 0.3	**0**	1.7 ± 0.4	**0**	1.1 ± 0.2	**0**	0.9 ± 0.1	**0**	0.7 ± 0.2
Reduction (%)	---	**75.1 ± 3.8**	---	**100 ± 0.0**	---	**100 ± 0.0**	---	**100 ± 0.0**	---	**100 ± 0.0**	---
***Aeromonas* sp.**	Control – t1	**19.2 ± 0.8**	38.2 ± 0.8	**18.2 ± 0.4**	39.6 ± 0.7	**17.0 ± 0.8**	39.6 ± 1.8	**18.5 ± 1.3**	39.8 ± 2.7	**18.8 ± 1.0**	39.7 ± 1.1
	Irradiated – t1	**16.4 ± 0.9**	21.3 ± 1.4	**15.0 ± 0.7**	22.5 ± 1.0	**13.3 ± 1.0**	19.6 ± 1.3	**14.5 ± 1.3**	20.0 ± 1.9	**14.5 ± 1.0**	19.7 ± 0.7
Reduction (%)	---	**14.6 ± 2.4**	---	**17.6 ± 2.6**	---	**22.1 ± 3.2**	---	**21.7 ± 1.5**	---	**22.7 ± 2.6**	---
***Aeromonas* sp.**	Control – t2	**19.0 ± 0.7**	38.4 ± 0.6	**18.2 ± 0.4**	39.4 ± 1.0	**17.0 ± 0.8**	39.7 ± 1.8	**18.5 ± 1.3**	40.0 ± 2.6	**18.0 ± 0.0**	39.7 ± 1.2
	Irradiated – t2	**6.0 ± 0.0**	2.9 ± 0.3	**0**	1.7 ± 0.4	**0**	1.1 ± 0.2	**0**	0.9 ± 0.1	**0**	0.7 ± 0.2
Reduction (%)	---	**68.4 ± 1.2**	---	**100 ± 0.0**	---	**100 ± 0.0**	---	**100 ± 0.0**	---	**100 ± 0.0**	---

The decrease of the halos, for *E.coli*, in the presence of sea-salts is in agreement with the reduction of antibacterial activity of OTC in saltwater reported in literature (Lunestad and Goksoyr 1990; Serrano 2005). These authors attributed the strong reduction of the antibacterial effect of OTC in seawater to the formation of complexes of OTC with calcium and magnesium. Thus, on the one hand, a greater concern is associated to the antibacterial activity in freshwater once the most fraction of OTC probably remains in an un-complexed form (Serrano 2005), depending on the water hardness. On the other hand, the amount of OTC that will be necessary to obtain a similar effect of the antibiotic in saltwater will be probably higher (Lunestad and Goksoyr 1990).

However, contrary to what was observed for *E. coli*, in the case of *Vibrio* and *Aeromonas* strains, the average diameters of halos in phosphate buffer solution containing sea-salts did not differ significantly ($p > 0.05$) from those determined in buffer without sea-salts. Similar behaviour was observed for aquaculture water comparatively to buffers without sea-salts.

Regarding the effect of solar radiation on the antibacterial effect of OTC solutions, one observes that, for each strain and in each matrix, the diameters of the halos for the irradiated solutions are lower than those for the dark controls, even for irradiation time t1 (*t*-test, 95 % confidence level). In what concerns *E. coli*, a reduction of the inhibition zone between 37.3±12.8 % in synthetic sea-salts and 55.4±3.6 % in company B_L3 was obtained at approximately the half-life time of OTC. With respect to *Vibrio* and *Aeromonas* strains, the average reduction of inhibition zone (antibacterial activity) at OTC half-life time is lower when compared to the values obtained for *E. coli*., ranging between 10.3±6.4 % in phosphate buffer and 22.3±1.0 % in company B_L2 for *Vibrio* and between 14.6±2.4 % in phosphate buffer and 22.7±2.6 % in company B_L2b for *Aeromonas*. It is expectable that the antibacterial activity existing at half-life time be mainly due to the antibiotic OTC, but a possible contribution of the intermediate photo-products should not be discarded. At the second time of OTC irradiation (t2), no zones of inhibition around the well were detected in any saltwater aqueous matrices for the three strains of bacteria. For *E. coli*, which one verified to be less susceptible to OTC than the other tested strains, antibacterial activity was also not detected in phosphate buffer solution without sea-salts. For the two other strains – *Vibrio* and *Aeromonas* – a reduction of 75.1±3.8 % and 68.4±1.2 % was obtained in the buffer without sea-salts, respectively. These results may be associated to the differences between the final average OTC concentration in solutions containing sea-salts (0.7 – 1.7 ppm) or not containing them (2.9 ppm). However, those differences in the OTC final concentration, namely between synthetic solutions (1.7

versus 2.9 ppm), are not so high that may justify the total inhibition of the antibacterial activity of OTC in the presence of sea-salts or only its reduction in the absence of sea-salts, for the strains *Vibrio* and *Aeromonas*. This residual activity observed in the buffer solutions, without sea-salts, may also result of by-products with antibacterial activity that are not formed in the other matrices. Indeed, in **figure 45**, one can observe the final product F1, which is not present in the saline samples after irradiation (t2). Furthermore, the possibility of formation of other products not detected cannot be discarded.

Although the extension of the radiation effect depends on the strains and aqueous matrices, there was always an extensive decrease of the antibacterial activity after photo-degradation. The same type of effect was also observed by other authors using other irradiation conditions, aqueous matrices and/or different strains. Pereira et al. (2013) performed TiO_2-assisted photocatalytic degradation of OTC (40 mg/L) in deionized water, using a solar pilot plant and followed the growth inhibition of *Escherichia coli* DSM 1103. The authors observed that, after complete removal of the antibiotic, the remaining photoproducts no longer showed antibacterial activity (Pereira et al. 2013). Lunestad et al. (1995), who exposed OTC (50 mg/L) to underwater light intensities, measured the antibacterial activity of OTC in seawater (33 ‰), using the disk diffusion technique. The authors used *Escherichia coli* B_6 and did not detect biological activity in solutions of OTC after their irradiation to the final OTC concentration of 2 mg/L (Lunestad et al. 1995). Wammer et al. (2011) carried out the photolysis of TTC in different natural and artificial water samples, using simulated sunlight, and performed microbiological assays with *Escherichia coli* DH5α and *Vibrio fischeri* to determine the antibacterial activity. They concluded that in all evaluated conditions, the photoproducts retain no significant antibacterial activity (Wammer et al. 2011).

6C.4 Conclusions

This study is a contribution for seeking effective methods able to reduce the persistence of antibiotics and with potentiality of application to real aquatic environments, once the mitigation of resistance dissemination is crucial in these systems. The results obtained suggest an acceleration of OTC photo-degradation in the presence of sea-salts and the formation of different photoproducts in different aqueous matrices. Physical-chemical characteristics of aqueous matrices affect the photo-degradation and the antibacterial activity of OTC. The photoproducts do not maintain the antibacterial

activity (*E. coli*, *Vibrio* sp. and *Aeromonas* sp.) in saltwater after irradiation, thus minimizing the bacterial resistance.

6C.5 References

Baquero, F., J. Martinez and R. Cantón (2008). Antibiotics and antibiotic resistance in water environments. *Current Opinion in Biotechnology* **19**: 260-265.

Cabello, F. C., H. P. Godfrey, A. Tomova, L. Ivanova, H. Dolz, A. Millanao and A. H. Buschmann (2013). Antimicrobial use in aquaculture re-examined: its relevance to antimicrobial resistance and to animal and human health. *Environmental Microbiology* **15**(7): 1917-1942.

FAO/OIE/WHO (2006). Antimicrobial use in aquaculture and antimicrobial resistance. Seoul, Republic of Korea**:** 107.

Gastalho, S., G. J. daSilva and F. Ramos (2014). Uso de antibióticos em aquacultura e resistência bacteriana: Impacto em saúde pública (Antibiotics in aquaculture and bacterial resistance: Health care impact). *Acta Farmacêutica Portuguesa* **3**(1): 29-45.

Henriques, I., M. Tacão, L. Leite, C. Fidalgo, S. Araújo, C. Oliveira and A. Alves (2016). Coselection of antibiotic and metal(loid) resistance in gram-negative epiphytic bacteria from contaminated salt marshes. *Marine Pollution Bulletin* **109**(1): 427-434.

Heuer, O. E., H. Kruse, K. Grave, P. Collignon, I. Karunasagar and F. J. Angulo (2009). Human Health Consequences of Use of Antimicrobial Agents in Aquaculture. *Clinical Infectious Diseases* **49**(8): 1248-1253.

Levy, S. B., G. B. Fitzgerald and B. Macone (1976). Changes in Intestinal Flora of Farm Personnel after Introduction of a Tetracycline-Supplemented Feed on a Farm *New England Journal of Medicine* **295**(11): 583-588.

Lopez-Penalver, J. J., M. Sanchez-Polo, C. V. Gomez-Pacheco and J. Rivera-Utrilla (2010). Photodegradation of tetracyclines in aqueous solution by using UV and UV/H_2O_2 oxidation processes. *Journal of Chemical Technology and Biotechnology* **85**(10): 1325-1333.

Lunestad, B. T. and J. Goksoyr (1990). Reduction in the bacterial effect of oxytetracycline in seawater by complex formation with magnesium and calcium. *Diseases of aquatic organisms* **9**: 67-72.

Lunestad, B. T., O. B. Samuelsen, S. Fjelde and A. Ervik (1995). Photostability of 8 antibacterial agents in seawater. *Aquaculture* **134**(3-4): 217-225.

Marshall, B. M. and S. B. Levy (2011). Food Animals and Antimicrobials: Impacts on Human Health. *Clinical Microbiology Reviews* **24**(4): 718-733.

Menezes, J. (2000). *Manual sobre doenças de peixes ósseos (Manual on finfish diseases)*, IPIMAR

Pereira, J., A. C. Reis, D. Queiros, O. C. Nunes, M. T. Borges, V. J. P. Vilar and R. A. R. Boaventura (2013). Insights into solar TiO_2-assisted photocatalytic oxidation of two antibiotics employed in aquatic animal production, oxolinic acid and oxytetracycline. *Science of the Total Environment* **463**: 274-283.

Romero, J., C. G. Feijoo and P. Navarrete (2012). Antibiotics in aquaculture - Use, abuse and alternatives. *Health and Environment in Aquaculture*. E. D. Carvalho, G. S. David and R. J. Silva.

Serrano, P. H. (2005). Responsible use of antibiotics in aquaculture. FAO Fisheries Technical Paper 469. Rome, FAO**:** 110.

Tacão, M., A. Correia and I. Henriques (2012). Resistance to broad-spectrum antibiotics in aquatic systems: anthropogenic activities modulate the dissemination of blaCTX-M-like genes. *Applied and Environmental Microbiology* **78**: 4134-4140.

Wammer, K. H., M. T. Slattery, A. M. Stemig and J. L. Ditty (2011). Tetracycline photolysis in natural waters: Loss of antibacterial activity. *Chemosphere* **85**(9): 1505-1510.

Zhao, C., M. Pelaez, X. D. Duan, H. P. Deng, K. O'Shea, D. Fatta-Kassinos and D. D. Dionysiou (2013). Role of pH on photolytic and photocatalytic degradation of antibiotic oxytetracycline in aqueous solution under visible/solar light: Kinetics and mechanism studies. *Applied Catalysis B-Environmental* **134**: 83-92.

Chapter 7: Photo-degradation of formalin

Formalin (aqueous solution of formaldehyde) is one of the most common disinfectants applied in aquaculture. After its use, it is commonly diluted and released into aquatic environment, without a specific treatment. It does not suffer direct photo-degradation, whereby its removal from water is sometimes achieved using photo-catalysts with UV light, which is more expensive radiation source comparative to visible or natural light.

In the present chapter, the efficiency of neat TiO_2 and two visible light active TiO_2 catalysts (TiO_2–Tetra-phenyl porphyrin and TiO_2–Graphene oxide) on aqueous formaldehyde degradation was evaluated. Synthetic seawater and brackish aquaculture's waters samples were considered for this study. The degradation efficiency using the photo-catalysts was lower in brackish aquaculture´s water than in aqueous matrix without synthetic sea-salts and organic matter, probably due to the competition of those species for $HO^{\bullet}$. The photo-catalyst TiO_2–GO proved to be more effective in removing formaldehyde from water, increasing the photo-degradation reaction rate and promoting some mineralization.

7.1 Contextualization

After the application of the disinfectant formalin (aqueous formaldehyde) in aquaculture establishments, it is generally discharged in environment after dilution. In semi-closed circuits, when bio-filter is before ozonation, water containing formalin should not pass through the circuit due to the reasons presented in *chapter 2*. Moreover, not all aquaculture production systems have ozonation, whereby methodologies to optimize the degradation/ removal of formaldehyde (FM) from water are necessary.

Direct photo-degradation of formalin is not possible since it does not absorb solar radiation. Based on literature, a possible mechanism to degrade FM is via $HO^{\bullet}$ (McElroy and Waygood 1991; Guimaraes et al. 2012). Some AOPs (e.g. UV/H_2O_2 and Photo-Fenton) have been proposed for indirect photo-degradation of formaldehyde in water (Kajitvichyanukul et al. 2006; Kowalik 2011; MacDonald et al. 2014). Additionally, the use of TiO_2 photo-catalyst has also been suggested (Mendez et al. 2015). Indeed, TiO_2 is recognized as an ideal catalyst due to its high oxidizing power, stability, relative low-cost and non-toxicity (Castellote and Bengtsson 2011). However, the processes above mentioned imply the use of UV radiation ($\lambda < 400$ nm), which is a radiation much more expensive and less available than visible radiation.

To use sunlight as irradiation source, new approaches to the photo-degradation of formaldehyde in water were tested and will be presented in this chapter. There are two recent works using visible-light active TiO_2 applied to formaldehyde removal from water (Li et al. 2015; Lu and Chen 2015). Li et al. (2015) tested the catalytic activities of a visible-light active Ce/F co-doped TiO_2-ZnO film in organic pollutants solutions, including formaldehyde. Lu and Chen (2015) investigated the photo-degradation of formaldehyde aqueous solution, using N-TiO_2/graphite as photo-catalyst. In these studies, only deionized water was used and the performance of these catalysts in natural water is unknown. Furthermore, in one of the studies (Lu and Chen, 2015), the pH used in the experiments (pH 3.5) is not even representative of common pH values found in natural water.

Thus, one of the goals of this work was to evaluate the efficiency of two visible light active TiO_2 catalysts (TiO_2–Tetra-phenyl porphyrin and TiO_2–Graphene oxide) on photocatalytic degradation of formaldehyde in water, under simulated sunlight. For the first time with these photo-catalysts, a natural water matrix (brackish aquaculture's water) was considered in the experiments. Additionally, aqueous solutions of phosphate buffer (simulating the pH of aquaculture's water) were prepared and used to compare the

performance of the photo-catalysts in the two aqueous matrices (natural and synthetic). The aqueous buffer solutions were also used to optimize the FM photo-degradation conditions. Knowing that 3.5 to 8 % of solar spectrum corresponds to UV radiation (Chowdhury et al. 2012), neat TiO_2 was also considered for the irradiation experiments to assess its contribution on the FM photo-degradation.

7.2 Material and methods

7.2.1 Chemicals

Formalin (ACS reagent) or formaldehyde (37 % wt.) aqueous solution containing 10–15 % methanol was provided by Sigma Aldrich. The stock solution of formaldehyde (5000 mg/L) was prepared mixing 0.248 mL of formalin solution in ultrapure water (final volume: 20 mL). The stock solution was divided into three vials, sealed with Parafilm® and protected from light. The stock solution of phosphate buffer 0.1 M was also prepared in ultrapure water, as explained in the previous chapter. The pH of buffered solution was adjusted to 7.3 with a diluted NaOH solution. Aquaculture's (brackish) water was collected at the output of tanks (L1) in company A. The FA fraction was isolated from Praia da Vagueira (Aveiro) water samples, using one column of Amberlit XAD-8 resin (Esteves et al. 1995). The TiO_2 photo-catalyst (P25–Aeroxide) was provided by Evonik Industries and its specific surface area is 50 ± 15 m^2/g. It consists of aggregated primary particles with a mean diameter of 21 nm and a density of 4 g/cm^3. The weight ratio of anatase and rutile crystalline structures is approximately 80/20 (Evonik 2015).

To detect formaldehyde (FM) in aqueous solutions, Nash's reagent (0.5 L) was prepared mixing 75 g of ammonium acetate (pro analysis, Merck), 1.5 mL of acetic acid 100 % (VWR Chemicals) and 1 mL of acetyl-acetone (p.a., Fluka) (Nash 1953).

7.2.2 Preparation of visible light active TiO_2-based composites

To prepare the photo-catalyst TiO_2-Tetraphenyl porphyrin (TiO_2-TPP), the tetra-phenyl porphyrin (TPP) was immobilized on TiO_2 P25. To achieve this immobilization, TPP (12 µmol) was dissolved in 30 mL of CH_2Cl_2 and 2 g of TiO_2 P25 were added to this solution. The suspension was magnetically stirred at room temperature during 10 h. Then, the solvent was removed under vacuum and the photo-catalyst was dried at 60 ºC during 12 h (Zhou et al. 2012). The TPP concentration in TiO_2 is 7.50 x 10^{-5} mol/g. This photo-

catalyst was synthesized and provided by the organic chemistry group (QOPNA), from University of Aveiro, through the collaboration with Prof. Dra Graça P. M. S. Neves.

To synthetize the nanocomposites TiO_2-Graphene oxide (TiO_2-GO), TiO_2 nanoparticles and graphite flakes (99.99 %) were used. Graphene oxide (GO) was obtained as described in Almeida et al. (2016). A GO suspension 4 mg/mL (pH 7) was obtained following that procedure. To prepare the TiO_2-GO nanocomposites with different percentages of GO (1 and 5 % wt.), the one-step hydrothermal method (Zhang et al. 2010) was adopted. After the hydrothermal treatment, a reduction of GO occurs (Wang et al. 2013), meaning that several oxygen functional groups are lost, although not completely (Almeida et al. 2016). Briefly, 62.5 µL (1 % GO) and 312.5 µL (5 % GO) of the GO aqueous dispersion (4 mg/mL) were dispersed in a mixture of deionized water (10 mL) and ethanol 96 % (5 mL) and magnetically stirred during 30 minutes, at 500 rpm. Then, 25 mg of TiO_2 P25 were added and the suspension was magnetically stirred (also at 500 rpm), during 30 minutes. At last, 15 mL of this suspension was transferred into a 20-mL Teflon lined autoclave, sealed and kept at 120 ºC during 3 h. The resultant nanocomposite was freeze-dried to avoid the particles agglomeration (Almeida et al. 2016). The GO suspension was provided by the Nanoengineering Research Group (NRG), from TEMA (University of Aveiro). The photo-catalysts were synthesized in collaboration with Dra Paula A. A. P. Marques.

7.2.3 Photo-degradation experiments

Before FM photo-degradation, 3.5 mg of the photo-catalyst (TiO_2-TPP, TiO_2-GO or neat TiO_2) were dispersed in the aqueous solutions (20 mL) of FM and stirred during 30 minutes (Lu and Chen 2015), to reach the adsorption-desorption equilibrium. Then, irradiation experiments of FM 40 mg/L in phosphate buffer (0.001 M) without sea-salts and in brackish aquaculture's waters were performed. In the case of aquaculture's water, FM was added in the laboratory to the filtered (1.2 µm) water samples. This FM concentration corresponds to 108 mg/L (approximately) of commercial formalin solution and it is within the range of concentrations applied in aquaculture. The aqueous suspensions containing FM were irradiated in quartz tubes during 2 hours, under simulated sunlight. Some aqueous suspensions containing FM were stirred (at 200 rpm) during the irradiation time to assess the stirring contribution on the FM photo-degradation. At least three independent replicates of the FM photo-degradation experiments were made together with the respective dark controls, for each aqueous

matrix. The irradiation conditions and the equipment are the same described in the previous chapters for BDE-209 and OTC. After irradiation, the aqueous suspensions were filtered to glass vials, using 25 mm syringe filters (PVDF, 0.22 µm, Simple pure) and sterile syringes of 5 mL (4606051v, Braun).

7.2.4 Formalin quantification – derivatization reaction

To quantify the decrease of the FM concentration in function of irradiation time, the following procedure was considered: 1 mL of irradiated FM solution (initial concentration of 40 mg/L) was mixed with 2 mL of Nash's reagent and adjusted to the final volume (10 mL) with ultrapure water. Then, samples were heated in a water bath at 50 ºC (Jones et al. 1999), during 30 min. This reaction time was chosen because, after this time, the derivatization reaction attains the equilibrium and the solution absorbance reaches its maximum value, as one can see in **figure 48**.

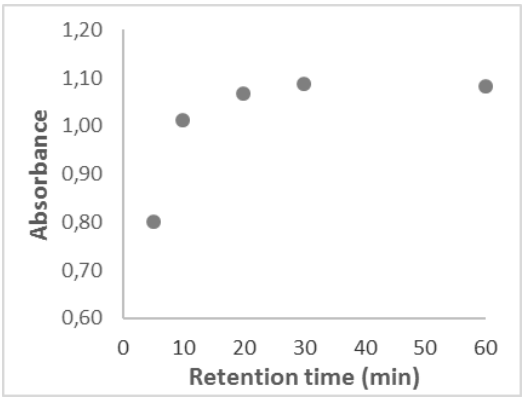

Figure 48 – Stabilization curve of the derivatization reaction of FM in function of reaction time

During this process, a condensation reaction of ammonia and acetyl-acetone (2,4-pentanedione) in Nash's reagent with formaldehyde occurs, originating 3,5-diacetyl-1,4-dihydrolutidine (DDL) (**reaction 43**). DDL presents a yellow-green colour and its maximum absorbance occurs at 412 nm (Jones et al. 1999).

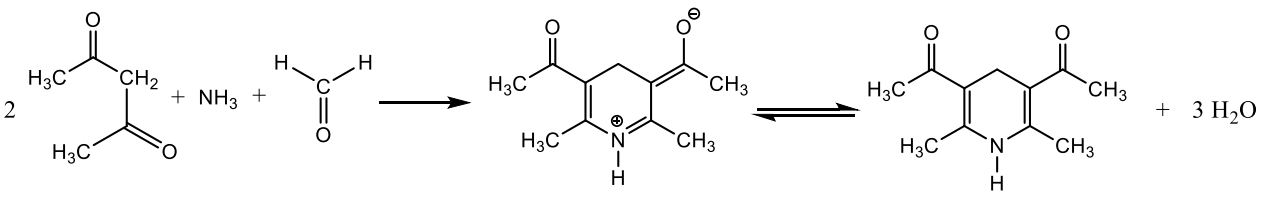

(Reaction 43)

7.2.5 Instrumentation

The absorbance measures were made using the UV-Vis spectrophotometer described in the previous chapters. As FM is the limiting reagent, the decrease in absorption intensity at 412 nm corresponds to the decrease of the FM concentration.

Another UV-Vis spectrophotometer (V-560 Jasco) was used to perform the UV-Vis diffuse reflectance spectra (DRS) of the photo-catalysts, in the solid phase, under the following conditions: slow response, band width of 5.0 nm and scanning speed of 100 nm/min.

The dissolved organic carbon (DOC) in the samples was determined using the Total Organic Carbon Analyser (Shimadzu) described in *chapter 5*.

Samples morphology was evaluated by scanning electron microscopy (SEM), using a Phenom ProX desktop microscope (**figure 49**). It is composed by an electron source of lanthanum hexaboride and a silicon drift detector (PhenomWorld 2015).

Figure 49 – Desktop scanning electron microscope (PhenomWorld 2015)

7.3 Results and discussion

7.3.1 Calibration for formaldehyde determinations

To quantify FM by UV-Vis spectroscopy, calibration curves were prepared in each day of analysis, with FM concentrations ranging from 0.5 mg/L to 4.0 mg/L (five standards). These standards were prepared in phosphate buffer solution 0.001 M and were subjected to the same derivatization reaction described above. The R^2 and LOD

values calculated from these calibrations curves ranged from 0.9993 to 1.000 and from 0.01 to 0.13 mg/L, respectively.

For the direct quantification of DOC in filtered (0.22 µm) water samples, the NPOC (non-purgeable organic carbon) method was used. Briefly, 2 % (v/v) of an HCl solution 2M was mixed in the diluted aqueous samples, followed by the purge of the samples during 3 minutes (within the equipment) with nitrogen. To perform the calibration curve, six standards of potassium hydrogen phthalate in milli-Q water (0.500 – 10.000 mg C/L) were prepared. The R^2 and LOD values obtained were 0.9999 and 0.126 mg C/L, respectively. To confirm the stability of calibration curve, control standards were prepared as described in *subchapter 5.3.1* and analyzed every day of analysis.

7.3.2 Formalin photo-degradation

As previously mentioned, the direct FM photo-degradation is not possible because it does not absorb sunlight. In turn, the photo-sensitizing effect of DOM on degradation of organic contaminants (topic already discussed in *subchapter 3.1.2*) is known. Thus, the first hypothesis was to assess whether the organic matter dissolved in the aquaculture's water would be able to photo-sensitize the FM degradation, under sunlight. For that, photo-degradation experiments were performed, using the aquaculture's water collected at the exit of tanks (company A_L1), but no FM photo-degradation was observed. The non-sensitization of the FM photo-degradation by DOM could be attributed to its low concentration and/or the presence of sea-salts, which may be affecting the indirect FM photo-degradation. To evaluate this hypothesis, an aqueous solution of FM without sea-salts and containing 20 mg/L of FA (major fraction representative of HS sample) was prepared, but after 12 hours of irradiation, there was not any FM photo-degradation.

Thus, to degrade and remove FM from water, synthetic photo-catalysts were tested in alternative to natural photo-sensitizers. The first results regarding to the irradiation (during 2 h) of the FM aqueous solutions, using two different types of visible-light active TiO_2 photo-catalysts (≈ 0.18 g/L), TiO_2-TPP and TiO_2-GO 1%, are presented in **figure 50**. The results obtained in synthetic and aquaculture's waters are presented in that figure. As one can see, the FM photo-degradation percentage in phosphate buffer aqueous solutions, ranging from 35.5±3.6 % to 44.5±1.2 %, is much higher than the corresponding percentage obtained in aquaculture's water, from 10.1±1.5 % to 14.6±1.4 %, for the two catalysts.

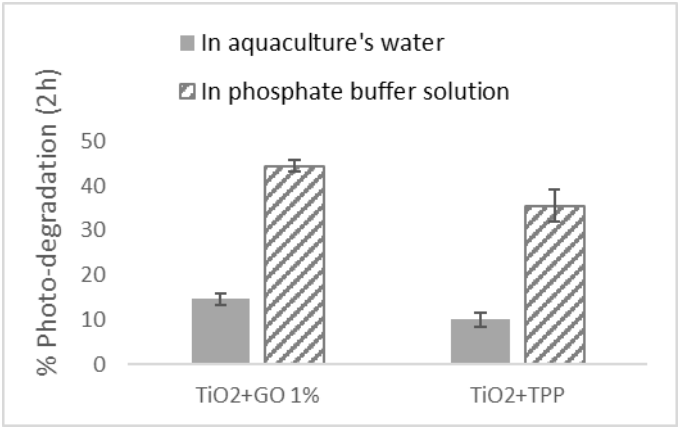

Figure 50 – FM photo-degradation percentages, after 2h of irradiation, in the presence of TiO_2–TPP and TiO_2–GO 1%, in aquaculture's water and aqueous phosphate buffer solution.

The lower efficiency of FM photo-degradation catalysed by TiO_2-based composites in brackish aquaculture's water may be attributed to two main factors. On the one hand, DOM can consume $HO^{\bullet}$ produced during photo-catalysis, which means that there will be less $HO^{\bullet}$ available to attack FM. On the other hand, it has been reported that inorganic ions present in natural waters, such as CO_3^{2-}/HCO_3^-, NH_4^+, SO_4^{2-}, NO_3^- or Cl^-, may inhibit the photocatalytic oxidation of organic compounds (Guillard et al. 2005; Yang et al. 2005). This inhibition is mainly due to the effect of $HO^{\bullet}$ scavenging and the competitive adsorption between inorganic ions and the contaminant on the TiO_2 surface, then acting as photo-generated holes (h^+) scavengers or directly reacting with $HO^{\bullet}$ (Chen et al. 1997; Carbajo et al. 2016).

In agreement with these results, some authors (Calza et al. 2016) reported a strong dependence of the efficiency of TiO_2-GO catalyst on the constitution of the irradiated media. They observed a decrease of risperidone photo-degradation in the following order: distilled water > tap water > river water > lake water. The authors attributed this to the increased organic carbon content (0.00 mg/L in distilled water, 13.0 mg/L in lake water) and to the presence of some species, like Cl^- and HCO_3^-/CO_3^{2-}, able to compete for $HO^{\bullet}$ and photo-catalyst surface sites. Other authors (Pastrana-Martínez et al. 2015) also verified a decrease of the photocatalytic efficiency of TiO_2–GO on photo-degradation of diphenhydramine and methyl orange, in simulated brackish water (with NaCl) comparatively to distilled water. They proposed that Cl^- existing in brackish water could generate less reactive species, such as chlorine radicals ($Cl^{\bullet}$) and dichloride radical anions ($Cl_2^{-\bullet}$), decreasing the degradation rate.

Comparing now the efficiency of the two photo-catalysts (TiO_2–TPP and TiO_2–GO 1%), TiO_2–GO 1% induces a faster FM photo-degradation than TiO_2–TPP, in the two aqueous matrices. In order to understand the differences in the photocatalytic activity of these composites, their optical properties were studied by UV-Vis diffuse reflectance spectroscopy. Those spectra are shown in **figure 51**. The band between 300 and 350 nm is characteristic of TiO_2. The other bands observed in the case of TiO_2–TPP are characteristics of the porphyrin: Soret band, at 400–450 nm and Q bands, at 500–650 nm (Li and Diau 2013).

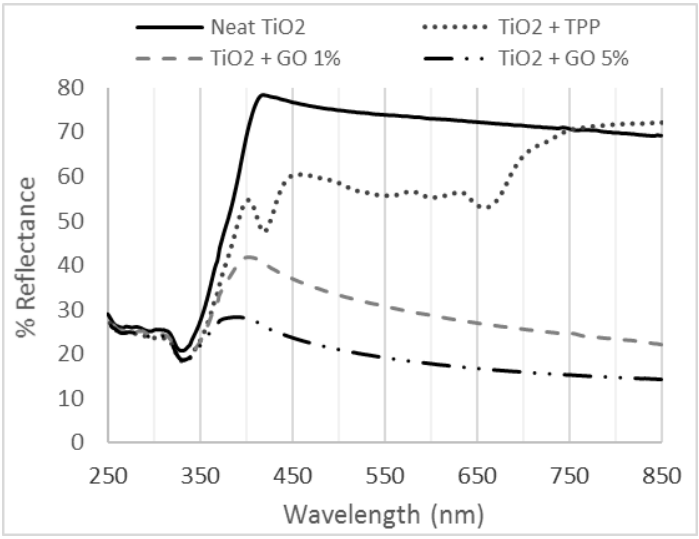

Figure 51 – UV-Vis diffuse reflectance spectra (DRS) of the photo-catalysts (in solid phase).

Figure 51 evidences the lower reflectance of TiO_2–TPP and TiO_2–GO 1 % comparatively to neat TiO_2 in the visible range. Comparing now the visible light active TiO_2 photo-catalysts, TiO_2–GO 1% presents lower reflectance in the visible range (20 to 40 %) than TiO_2–TPP (50 to 80 %). This means that TiO_2–GO 1% displays a great absorbance in the visible range, justifying its higher efficiency on FM photo-degradation comparatively to TiO_2–TPP.

Aiming to assess whether mineralization (conversion to CO_2 and H_2O) occurred during the photo-catalysis or if there is the formation of intermediate organic products, DOC was quantified in the aqueous samples. The results of these experiments, in aquaculture's water and phosphate buffer solution, are presented in **figures 52** and **53**, respectively.

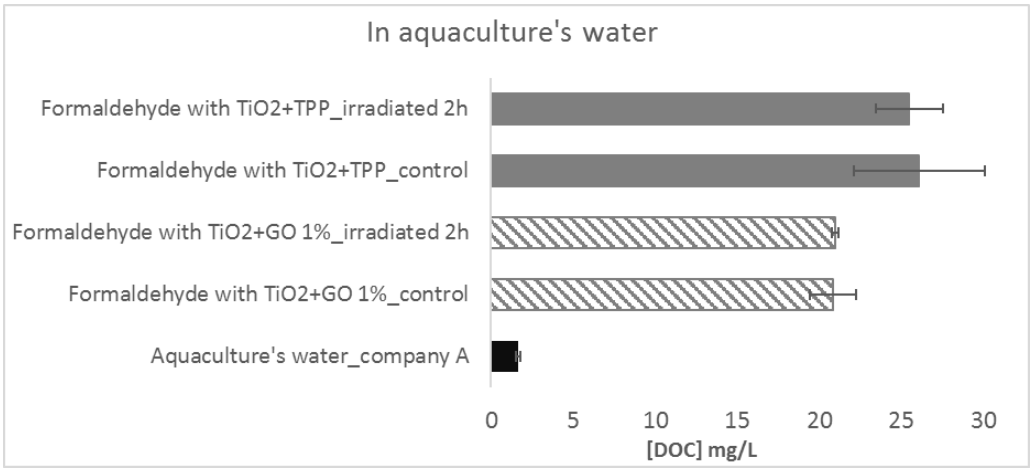

Figure 52 – Dissolved organic carbon (mg/L) in brackish aquaculture's water containing FM and TiO_2-based composites.

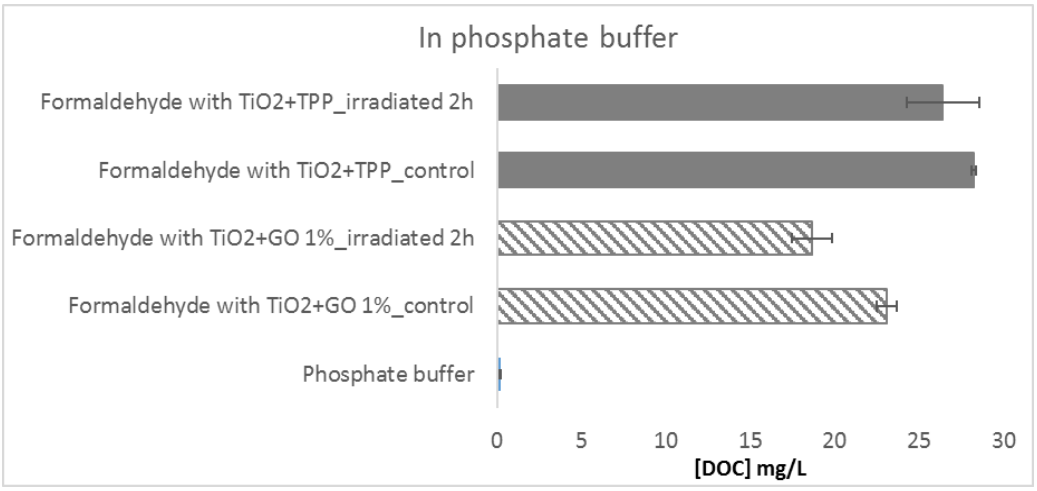

Figure 53 – Dissolved organic carbon (mg/L) in aqueous solution of phosphate buffer (0.001 M) containing FM and TiO_2-based composites.

As shown in the above figures, no mineralization occurs in any matrices using the photo-catalyst TiO_2–TPP. A similar result was obtained in the samples of brackish aquaculture's waters (**figure 52**) using the photo-catalyst TiO_2–GO 1%. However, a significant (one-tailed *t*-test, $p < 0.005$) decrease on DOC concentration is observed using the photo-catalyst TiO_2–GO 1% in phosphate buffer solutions. The average mineralization was about 19 %. Since the percentage of mineralization is lower than the FM photo-degradation percentage (44.5 ± 1.2 %), the results suggest that not all photo-degraded FM was converted to CO_2 and H_2O. Indeed, some authors (McElroy and Waygood 1991) have proposed the formation of formic acid by loss of an hydrogen atom to form

hydrated formyl radical (**reaction 44**) and, then, by addition of molecular oxygen and rearrangement (**reaction 45**).

$$H_2C(OH)_2 + HO^{\bullet} \rightarrow HC(OH)_2^{\bullet} + H_2O \quad \textbf{(Reaction 44)}$$

$$HC(OH)_2^{\bullet} + O_2 \rightarrow HOO^{\bullet} + HCOOH \quad \textbf{(Reaction 45)}$$

Another aspect that should be highlighted from analysis of **figures 52** and **53** is the higher DOC concentration observed in the presence of TiO_2–TPP comparatively to TiO_2–GO 1%. Based on the composition of commercial formalin (37 % of formaldehyde and 15 % of methanol) used to prepare the solutions for irradiation, containing 40 mg/L of FM, the DOC concentration in these solutions is about 22 mg/L. The higher DOC values observed in the presence of TiO_2–TPP may be attributed to TPP release into solution.

Comparing the two visible light active photo-catalysts, TiO_2–GO 1% is more efficient than TiO_2–TPP, either by the higher percentage of FM photo-degradation, either by the mineralization obtained. Therefore, only the photo-catalyst TiO_2–GO will be considered for the FM photo-degradation method optimization.

Thus, additional experiments were done considering a higher proportion of GO on TiO_2 (TiO_2-GO 5 %). This percentage was chosen due to lower reflectance in the visible range comparatively to TiO_2-GO 1 % (**figure 51**). As the sunlight includes some UV radiation, FM solutions containing neat TiO_2 were also irradiated to evaluate its contribution to FM photo-degradation rate. In addition to initial stirring (before irradiation), this second set of experiments was made with stirring during all the irradiation time, aiming to promote a higher contact between the contaminant and the photo-catalyst. The results of those experiments are presented in **figure 54**.

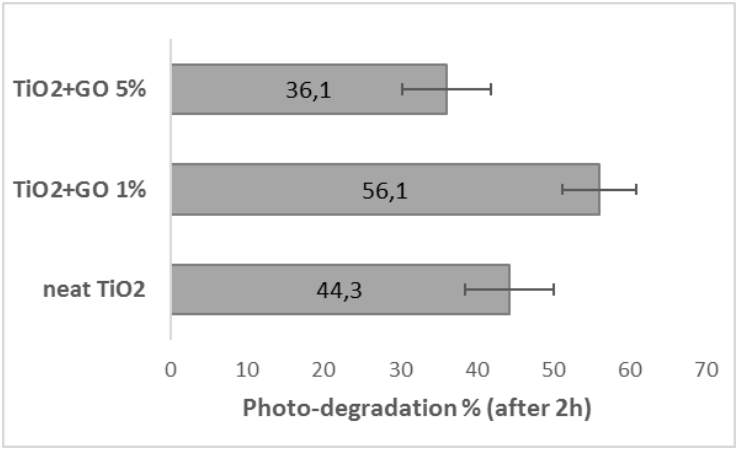

Figure 54 – FM photo-degradation percentages in aqueous phosphate buffer solutions, after 2h of irradiation, with different ratios of GO in TiO_2. Stirring before and during irradiation.

Three main conclusions can be drawn from the analysis of **figure 54,** for the same time of irradiation (two hours), using simulated sunlight (290-800 nm):

(1) Neat TiO_2 is the main responsible by the FM photo-degradation (44.3 ± 5.8 %). Its maximum absorbance is around 330 nm (UV region), suggesting that the low percentage of UV radiation existing in the solar spectra is the main responsible by aqueous FM photo-degradation. Calza et al. (2016) performed their irradiation studies under simulated sunlight (λ > 290 nm) and visible light (λ > 430 nm). They obtained rate constants to the risperidone photo-degradation with TiO_2 much lower using visible light than using simulated sunlight, corroborating the contribution of UV radiation (in simulated sunlight) to photocatalytic degradation using neat TiO_2.

(2) The addition of GO 1 % to TiO_2 caused an increase of the FM photo-degradation to 56.1 ± 4.8 %. In addition to the more favourable optical properties of TiO_2-GO 1 % comparatively to neat TiO_2 (**figure 51**), in the visible range, GO can inhibit the electron/hole (e^-/h^+) pairs recombination. This occurs because the excited electrons of TiO_2 can quickly transfer from the conduction band (CB) of TiO_2 to GO. Thus, more charge carriers will be available to form highly reactive species that promote the oxidation/degradation (Jiang et al. 2011; Adamu et al. 2016; Almeida et al. 2016). Moreover, the addition of GO in TiO_2 can improve its adsorption capability, contributing to the enhancement of the photocatalytic activity of composite. This was demonstrated by some authors (Jiang et al. 2011) who measured the adsorption dynamics of methyl orange onto TiO_2 and GO/TiO_2 composites and verified that GO/TiO_2 presented higher adsorption capacity than neat TiO_2. Comparing the FM photo-degradation percentages without (**figure 50**) and with stirring (**figure 54**) during the irradiation, one observes an

average increase of 11.6 % in the photocatalytic degradation when stirring (at 200 rpm) is maintained during irradiation.

(3) The addition of GO 5 % to TiO_2 caused a decrease of the FM photo-degradation to 36.1 ± 5.8 %, an average value lower than the corresponding value using only neat TiO_2 as photo-catalyst. Three main factors may be pointed to justify the decrease of FM photo-degradation using TiO_2–GO 5%: hydrophobicity, screening effect and surface area. The high hydrophobicity of this composite inhibits its potential action in aqueous solutions (a thin layer of the photo-catalyst was observed on the top of solutions during the irradiation experiments, even with stirring). The photocatalytic efficiency generally increases with increasing GO content, but until it reaches a saturation/opacity point. Several authors (Jiang et al. 2011; Wang and Zhang 2011; Wang et al. 2013; Adamu et al. 2016) have reported that, for weight percentages equal to or greater than 5 % GO in TiO_2, the screening effect overlaps the photo-absorption, justifying the decrease of photo-degradation. On the other hand, the increase of the GO concentration promotes the formation of larger agglomerates, decreasing the exposed surface area available to react. **Figure 55** shows the SEM photographs of TiO_2 nanoparticles agglomerate (**figure 55a**) and TiO_2–GO composites (**figure 55b-d**). For the TiO_2-GO 1% nanocomposites, in addition to dispersed TiO_2 nanoparticles, a large agglomeration of the TiO_2 nanoparticles covering the GO sheets (e.g. highlighted sheets 1 and 2) is observed (**figure 55b**), confirming the contact between these two components. In some cases, there seems to be some winding of GO sheets (e.g. highlighted sheet 3). At higher GO concentration (**figure 55c-d**), the agglomeration and winding of GO sheet is higher, reducing the available surface area to react.

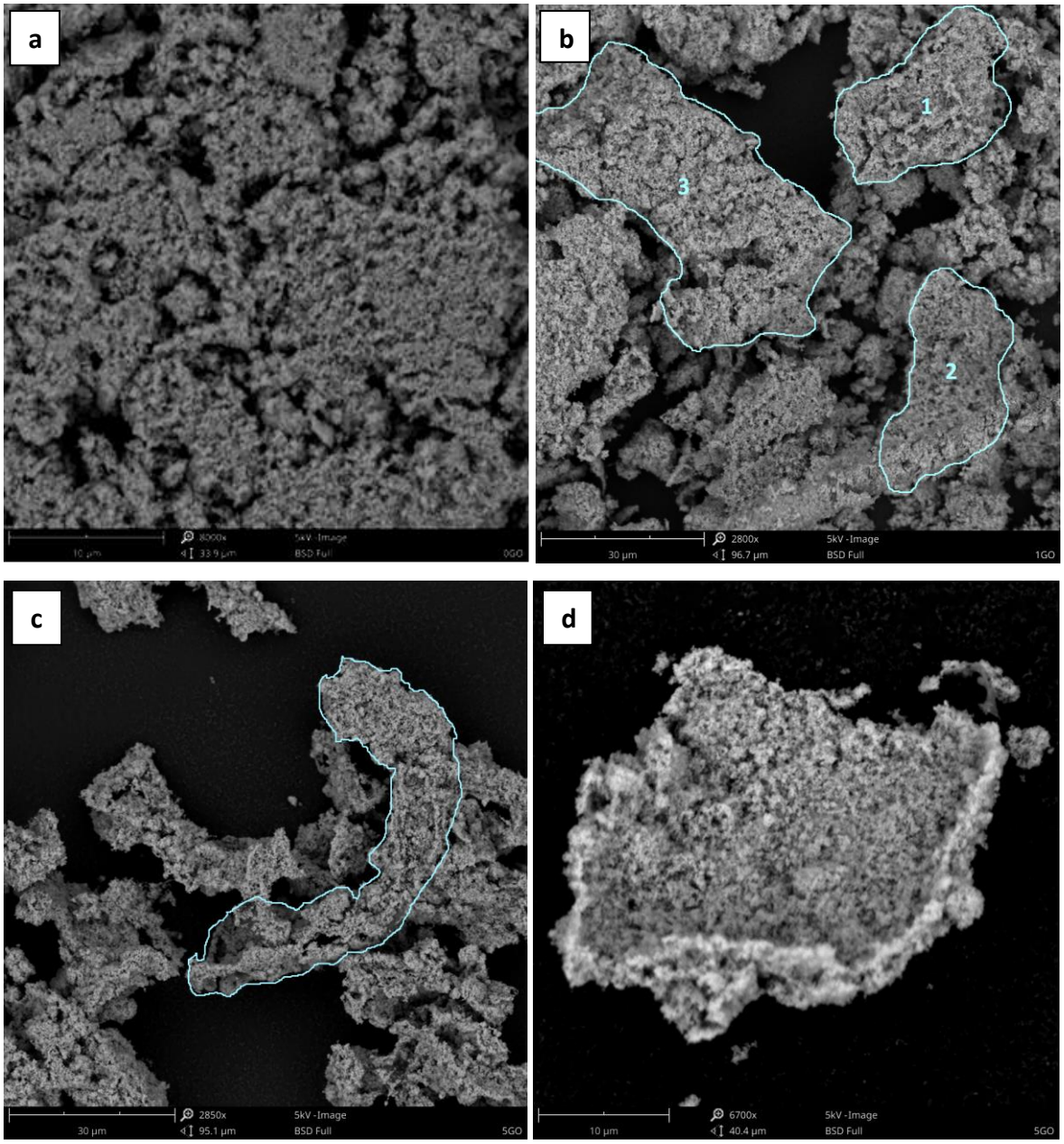

Figure 55 – SEM photographs of neat TiO_2 nanoparticles (a), TiO_2 with GO 1% (b), TiO_2 with GO 5 % (c, d).

There are two recent studies in literature that refer the FM photo-degradation in aqueous solution, using visible-light active TiO_2 (Li et al. 2015; Lu and Chen 2015). They were made in deionised water and their results will be used to compare with results obtained in the present work using phosphate buffer solutions (pH 7.3).

Li et al. (2015) performed the irradiation experiments of FM (5 mg/L) aqueous solutions in the presence of TiO_2 film, TiO_2-ZnO film and Ce/F co-doped TiO_2-ZnO film. They concluded that the FM photo-degradation is faster in the presence of Ce/F co-doped TiO_2-ZnO film, obtaining 82 % of FM degradation after 200 min (3h20min) of irradiation

under visible light (40 $mW.cm^{-2}$ = 400 $W.m^{-2}$). In turn, Lu and Chen (2015) studied the FM degradation photo-catalysed by N-TiO_2/graphite (2 g/L). After 4 hours, under natural light in summer, the authors obtained a degradation rate of 92.45 %, at pH 3.5, using an initial FM concentration of 10 mg/L.

Given the effect that a much smaller amount (≈ 0.18 g/L) of catalyst (TiO_2-GO) had on photo-degradation of a higher FM concentration (40 mg/L) after a shorter time of irradiation, in relation to the above mentioned studies, the results obtained so far suggest a great application potential of photo-catalysts tested in this work for the FM degradation. Nonetheless, more studies will be developed to optimize the process efficiency.

7.4 Conclusions

The removal of formalin (37 % of formaldehyde and 10-15 % of methanol) after its use in aquaculture establishments is a concern for aquaculture producers, not only by the effects that it causes into the system production, but also by the consequences of its release into environment. Since formalin does not absorb light, its photo-degradation must be catalysed. The photo-catalyst TiO_2–GO 1% proved to be more effective than TiO_2–TPP in removing FM from water, increasing the photo-degradation reaction rate and promoting some mineralization. The increase of GO content (1 to 5 %) in TiO_2 did not contribute to the acceleration of the FM photo-degradation. On the contrary, the FM photo-degradation was slower with TiO_2–GO 5% than with neat TiO_2. The results demonstrate that the efficiency of the photo-catalysts tested is decreased in brackish aquaculture's water, which is probably attributed to the interaction of its natural constituents in the photo-catalysis process.

7.5 References

Adamu, H., P. Dubey and J. A. Anderson (2016). Probing the role of thermally reduced graphene oxide in enhancing performance of TiO_2 in photocatalytic phenol removal from aqueous environments. *Chemical Engineering Journal* **284**: 380-388.

Almeida, N. A., P. M. Martins, S. Teixeira, J. A. L. d. Silva, V. Sencadas, K. Kühn, G. Cuniberti, S. Lanceros-Mendez and P. A. A. P. Marques (2016). TiO_2/graphene oxide immobilized in P(VDF-TrFE) electrospun membranes with enhanced visible-light-induced photocatalytic performance. *Journal of Materials Science* **51**(14): 6974-6986.

Calza, P., C. Hadjicostas, V. A. Sakkas, M. Sarro, C. Minero, C. Medana and T. A. Albanisb (2016). Photocatalytic transformation of the antipsychotic drug risperidone in aqueous media on reduced graphene oxide-TiO_2 composites. *Applied Catalysis B: Environmental* **183**: 96-106.

Carbajo, J., M. Jiménez, S. Miralles, S. Malato, M. Faraldos and A. Bahamonde (2016). Study of application of titania catalysts on solar photocatalysis: Influence of type of pollutants and water matrices. *Chemical Engineering Journal* **291**: 64-73.

Castellote, M. and N. Bengtsson (2011). Principles of TiO_2 Photocatalysis. *Applications of Titanium Dioxide Photocatalysis to Construction Materials: State-of-the-Art Report of the RILEM Technical Committee 194-TDP*. Y. Ohama and D. Van Gemert. Dordrecht, Springer Netherlands**:** 5-10.

Chen, H. Y., O. Zahraa and M. Bouchy (1997). Inhibition of the adsorption and photocatalytic degradation of an organic contaminant in an aqueous suspension of TiO_2 by inorganic ions. *Journal of Photochemistry and Photobiology A: Chemistry* **108**(1): 37-44.

Chowdhury, P., J. Moreira, H. Gomaa and A. K. Ray (2012). Visible-Solar-Light-Driven Photocatalytic Degradation of Phenol with Dye-Sensitized TiO_2: Parametric and Kinetic Study. *Industrial & Engineering Chemistry Research* **51**(12): 4523-4532.

Esteves, V. I., N. M. A. Cordeiro and A. D. Duarte (1995). Variation on the adsorption efficiency of Humic Substances from Estuarine waters using XAD resins. *Mar Chem* **51**(1): 61-66.

Evonik. (2015). "AEROXIDE®, AERODISP® and AEROPERL®, Titanium Dioxide as Photocatalyst." Technical Information 1243 Retrieved December, 2016, from https://www.aerosil.com/sites/lists/RE/DocumentsSI/TI-1243-Titanium-Dioxide-as-Photocatalyst-EN.pdf.

Guillard, C., E. Puzenat, H. Lachheb, A. Houas and J.-M. Herrmann (2005). Why inorganic salts decrease the TiO_2 photocatalytic efficiency. *International Journal of Photoenergy* **7**(1): 1-9.

Guimaraes, J. R., C. R. T. Farah, M. G. Maniero and P. S. Fadini (2012). Degradation of formaldehyde by advanced oxidation processes. *Journal of Environmental Management* **107**: 96-101.

Jiang, G., Z. Lin, C. Chen, L. Zhu, Q. Chang, N. Wang, W. Wei and H. Tang (2011). TiO_2 nanoparticles assembled on graphene oxide nanosheets with high photocatalytic activity for removal of pollutants. *Carbon* **49**(8): 2693-2701.

Jones, S. B., C. M. Terry, T. E. Lister and D. C. Johnson (1999). Determination of Submicromolar Concentrations of Formaldehyde by Liquid Chromatography. *Analytical Chemistry* **71**(18): 4030-4033.

Kajitvichyanukul, P., M. C. Lu, C. H. Liao, W. Wirojanagud and T. Koottatep (2006). Degradation and detoxification of formaline wastewater by advanced oxidation processes. *Journal of Hazardous Materials* **135**(1-3): 337-343.

Kowalik, P. (2011). Chemical pretreatment of formaldehyde wastewater by selected Advanced Oxidation Processes (AOPs). *Challenges of Modern Technology* **2**(4): 42-48.

Li, H., W. Zhang, L.-x. Guan, F. Li and M.-m. Yao (2015). Visible light active TiO_2–ZnO composite films by cerium and fluorine codoping for photocatalytic decontamination. *Materials Science in Semiconductor Processing* **40**: 310-318.

Li, L. L. and E. W. G. Diau (2013). Porphyrin-sensitized solar cells. *Chemical Society Reviews* **42**(1): 291-304.

Lu, X. and H. Chen (2015). Graphite-based N-TiO_2 composites photocatalyst for removal of HCHO in water. *Desalination and Water Treatment* **56**(6): 1681-1688.

MacDonald, M. J., Z. J. Wu, J. Y. Ruzicka, V. Golovko, D. C. W. Tsang and A. C. K. Yip (2014). Catalytic consequences of charge-balancing cations in zeolite during photo-Fenton oxidation of formaldehyde in alkaline conditions. *Separation and Purification Technology* **125**: 269-274.

McElroy, W. J. and S. J. Waygood (1991). Oxidation of Formaldehyde by the Hydroxyl Radical in Aqueous Solution. *Journal of the Chemical Society, Faraday Transactions* **87**(10): 1513-1521.

Mendez, J. A. O., J. A. H. Melian, J. Arana, J. M. D. Rodriguez, O. G. Diaz and J. P. Pena (2015). Detoxification of waters contaminated with phenol, formaldehyde and phenol-formaldehyde mixtures using a combination of biological treatments and advanced oxidation techniques. *Applied Catalysis B-Environmental* **163**: 63-73.

Nash, T. (1953). The colorimetric estimation of formaldehyde by means of the Hantzsch reaction. *Biochemical Journal* **55**(3): 416-421.

Pastrana-Martínez, L. M., S. Morales-Torres, J. L. Figueiredo, J. L. Faria and A. M. T. Silva (2015). Graphene oxide based ultrafiltration membranes for photocatalytic degradation of organic pollutants in salty water. *Water Research* **77**: 179-190.

PhenomWorld. (2015). "Specification Sheet Phemon ProX " Retrieved September, 2016, from https://www.phenom-world.com/downloads/specification_sheets/Product-SpecSheet_PROX_LR.pdf.

Wang, F. and K. Zhang (2011). Reduced graphene oxide–TiO_2 nanocomposite with high photocatalystic activity for the degradation of rhodamine B. *Journal of Molecular Catalysis A: Chemical* **345**: 101-107.

Wang, P., J. Wang, X. Wang, H. Yu, J. Yu, M. Lei and Y. Wang (2013). One-step synthesis of easy-recycling TiO_2-rGO nanocomposite photocatalysts with enhanced photocatalytic activity. *Applied Catalysis B: Environmental* **132–133**: 452-459.

Yang, S. Y., Y. X. Chen, L. P. Lou and X. N. Wu (2005). Involvement of chloride anion in photocatalytic process. *Journal of Environmental Sciences* **17**(5): 761-765.

Zhang, H., X. Lv, Y. Li, Y. Wang and J. Li (2010). P25-Graphene Composite as a High Performance Photocatalyst. *ACS Nano* **4**(1): 380-386.

Zhou, X.-T., H.-B. Ji and X.-J. Huang (2012). Photocatalytic Degradation of Methyl Orange over Metalloporphyrins Supported on TiO_2 Degussa P25. *Molecules* **17**(2): 1149.

Chapter 8: Concluding remarks

8.1 General conclusions

Can sunlight photo-degradation be used as a method to remediate organic contaminants from aquaculture's water? The answer to this question, which is also the primary purpose of this doctoral thesis, is "*yes*", despite its efficiency depends on the contaminant and matrix.

This PhD thesis brings together a set of results that allows to take several conclusions:

✓The light-screening does not completely explain the retardation effect of HS on the photo-degradation of OTC and BDE-209.

✓The screening effect seems to be the predominant delaying effect on OTC photo-degradation at sea level, while the association between BDE-209 and the most hydrophobic fractions of HS is proposed as the major delaying effect

✓The outdoor half-life time of BDE-209 photo-degradation in water, in the presence of HS, for midsummer days is 1.79 h, at sea level and at 40º N of latitude.

✓In water samples collected after ozonation, significant degradation or mineralization of DOC was not observed, revealing the low efficiency of ozonation in saltwater. However, for the company with lower DOC concentration and higher ozone dose, changes in nature of dissolved organic matter after ozonation were observed.

✓The outdoor half-life times, for midsummer days, of OTC photo-degradation in filtered marine aquaculture's water ranged between 21 and 26 minutes, at sea level and at 40º N of latitude.

✓The solar photo-degradation of OTC in brackish aquaculture's water is at least 3.9 times higher than in deionized water; this enhance is almost completely justified by the conjugation of two factors: pH and salinity.

✓Calcium significantly enhances the OTC photo-degradation in synthetic saltwater (about 65 %), but the presence of magnesium in the same solution inhibits the accelerating effect of calcium on the OTC photo-degradation.

✓Magnesium has a predominant influence on by-products formation: the formation of certain products is inhibited while others are promoted in its presence.

✓The OTC photoproducts do not maintain the antibacterial activity in any saltwater evaluated (synthetic and from aquaculture), using the following strains: *E. coli*, *Vibrio* sp. and *Aeromonas* sp..

✓The photo-catalyst TiO_2-GO 1 % promotes a faster FM degradation in aqueous solutions, under simulated sunlight, than TiO_2-TPP.

✓The increase of GO concentration in TiO_2 (from 1 to 5% wt.) does not cause a faster FM photo-degradation; contrarily, its photo-degradation in the presence of TiO_2-GO 5 % is slower than when it is catalysed only by neat TiO_2.

8.2 Future perspectives and potentialities

Since the work developed during this PhD thesis originates a set of research articles, we think there is a great potential for the development of future studies. Despite the developed studies are directed to the aquaculture sector, some of the results and proposals presented may cover other areas. Thus, among the various possibilities for further studies, three topics, highlighted below, can be considered as priority:

- Identification of the OTC photoproducts in the different aqueous matrices, containing or not sea-salts, avoiding wrong extrapolations between different aqueous matrices.
- Evaluation of the OTC by-products toxicity for aquatic species after irradiation, using sunlight.
- Optimization of the formalin photo-degradation conditions, making possible its adaptation to real aquaculture's water.